

**SYNTHESIS AND CATALYTIC STUDIES ON  
METAL PHTHALOCYANINES**

**A Thesis submitted to Goa University for the award of the degree of  
DOCTOR OF PHILOSOPHY**

**IN  
CHEMISTRY**

**By**

**Ms. PUZY ATHMARAM PAVASKAR**

547  
PAV/Syn

**Research Guide  
Prof. A. V. Salker.**

**GOA UNIVERSITY**

**Taleigao Goa**

**2012**

T-564

# DECLARATION

I hereby declared that the work incorporated in the thesis entitled "**Synthesis and catalytic studies on metal Phthalocyanines**" is the result of investigation carried out by me under the guidance of Prof. A. V. Salker and it has not previously formed basis for any other titles.

In keeping with the general practice of reporting scientific observations, due acknowledgement has been made wherever the work described is based on the findings of other investigators.



**Ms. Puzy A. Pavaskar**

Research student

Department of Chemistry

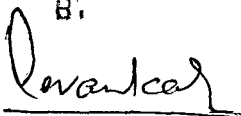
Goa University

Goa 403206, India

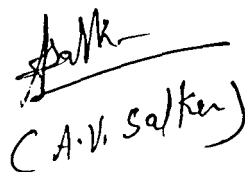
January 2012

EXAM

B.



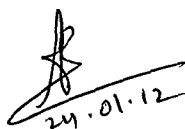
(Prof. V. K. Revankar)



(A. V. Salker)

# CERTIFICATE

As required under the University ordinance, I certify that the thesis entitled "**Synthesis and catalytic studies on metal Phthalocyanines**" submitted by Ms. Puzy A. Pavaskar, for the award of Doctor of Philosophy in Chemistry is a record of research done by the candidate during the period of study under my guidance and that it has not previously formed the basis for the award to the candidate of any degree, diploma, associateship, fellowship or other similar titles.



24.01.12

**Prof A. V. Salker**

Research guide,

Department of Chemistry

Goa University

Goa 403206, India

January 2012

# ACKNOWLEDGEMENT

First and foremost, I would like to express my sincere gratitude to my advisor Prof. A. V. Salker for the continuous support through out my research, for his patience, motivation, enthusiasm, and immense knowledge. I could not have imagined having a better advisor and mentor for my Ph.D study. I would like to express my feelings as “**Guru Devo Namaha**”.

I offer my sincere thanks to the Vice-chancellor of Goa University for allowing me to work in this institute. I am very much grateful to Prof. S. G. Tilve (Head, Department of Chemistry), Prof. Desa (Dean), Prof. J. B. Fernandes (Ex-Head and Ex-Dean), Prof. S. P. Kamat (Ex-Head) and Prof. K. S. Rane (Ex-Dean) for providing all the necessary facilities to carry out my research work.

I am also grateful to Dr. V. M. S. Verenkar, Prof. B. R. Srinivasan, Prof. Nadkarni, Prof. I. Furtado and Prof. S. K. Paknikar for their constant encouragement and useful advises.

I am grateful to all the teaching and non-teaching staff of the Department of Chemistry who has helped me directly or indirectly during my research work. I acknowledge the Librarian and the staff members of Library of Goa University for their constant help.

I am grateful to Dr. Solima, Dr. Lizette and Mr. Rajesh of NIO-Goa. I am also grateful to IIT SAIF Mumbai for analysis.

My sincere thanks to the authorities of Goa University for providing me all the necessary facilities to carry out my research work.

I am thankful to all my friends for their help and support during the entire period of my thesis work. Notably among these are Jose, Sulaksha, Satish, Prachi, Rohan, Shrikant, Santosh, Vinod, Prakash, Mahesh, Rupesh, Rajesh, Shambhu, Chinmaya, Umesh, Priyanka, Kashinath, Hari, Sandesh, Reshma, Siddhali, Lactina, Sonia, Kiran, Rajashree, Sifali, Divya, Ratan, Ashish, Milind, Savia, Sagar, Prajesh, Deeptesh, Madhavi and Sushma. Their untiring company, suggestions and constant encouragement always boosted my morale enabling me to give my investigation the present shape and making my stay

enjoyable over here. I am also very much grateful to my best friends Sunita, Vrushali, Pratija, Sudesh and Brijesh, for their constant motivation.

I am very grateful to ratio Pharm Pvt. Ltd. and Vergo research Laboratory where I was employed during my research work and my Seniors specially Mr. Candet Castelo, Haresh, Sufala, Shambo, Gaurish, Swati, Roshan, Premanand Dr Borker, Dr. Gawas and colleagues Pinky, Alpa, Leena, Yogita, Shivanand, Sanjana and Kiran.

I am very grateful to the people of Amsar, Indore and Medule (Cipla) specially Dr. Chaya Bhatt, Mr Ashok, Mr. Gupta, Mrs Swati, Mr Anand Kulkarni and Mr. Satish for motivating me constantly at work place.

It gives me immense pleasure to express my deep sense of gratitude to all the people who have directly or indirectly helped me in various capacities in the successful completion of the thesis.

I am greatly indebted to my parents Smt Shobha and late Atmaram Dattu Pavaskar. I am also obliged to my husband Mr. Mahadev Shashikant Shirodker, my little prince Dhruv and my mother in law Smt Satyabhama for morale support, encouragement, valuable suggestions, great affection and selfless sacrifice. Without their constant support and inspiration, it would have been impossible for me to be where I am at present.

I close with thanks giving to the Almighty for the showers of blessing during the hours of trial.

**Ms. Puzy Pavaskar**

# CONTENTS

## CHAPTER 1

### 1. INTRODUCTION

<b>1.1 Phthalocyanine and Porphyrins</b>	1
<b>1.2 The Structure of Phthalocyanines and Porphyrins</b>	2
<b>1.3 Phthalocyanines: General applications</b>	4

## CHAPTER 2

### 2. LITERATURE REVIEW

<b>2.1 The Discovery of Phthalocyanines</b>	10
<b>2.2 Synthesis of phthalocyanine</b>	
2.2.1 Synthesis of nonsubstituted metal free Phthalocyanine	11
2.2.2 Synthesis of non substituted metal phthalocyanine	12
<b>2.3 Synthesis of Substitute Phthalocyanine</b>	
2.3.1 Tetra-substituted Phthalocyanines	13
2.3.2 Octa-substituted Phthalocyanines	18
2.3.3 Axial substituted phthalocyanine	18
2.3.4 Synthesis of phthalocyanine having macrocycle	19
<b>2.4 Synthesis of Sub phthalocyanine (SubPc)</b>	19
<b>2.5 Synthesis of SuperPc</b>	20
<b>2.6 Related Synthetic strategies</b>	21
<b>2.7 Synthesis of water soluble Phthalocyanines</b>	22
<b>2.8 Different tools for the characterization of phthalocyanine</b>	23
2.8.1 Magnetic susceptibility studies	23
2.8.2 UV-Visible spectroscopy studies	24
2.8.3 TG-DSC/DTA studies	25
2.8.4 Fluorimetry	26
2.8.5 X-ray studies	26
<b>2.9 Catalysis</b>	
2.9.1 Catalytic Degradation	26
2.9.2 Mechanism of photocatalysis	29

2.9.3 Catalytic Oxidation	30
2.9.4 Catalytic reduction	31
2.9.5 Catalytic Oxidation of benzyl to benzoine	31
2.9.6 Catalytic Oxidation of 2-hydroxy Naphthol to Lawson	32
<b>2.10 Applications of Phthalocyanine</b>	
2.10.1 High temperature Lubrication	36
2.10.2 Electro oxidation	36
2.10.3 Oxidation of sulphur containing compound	36
2.10.4 Thin Film	37
2.10.5 PDT	38
2.10.6 Photoluminescence	40
2.10.7 Antimicrobial activity	41

## CHAPTER 3

### 3. EXPERIMENTAL

<b>3.1 Synthesis of Phthalocyanine</b>	43
3.1.1 Synthesis of non substituted Phthalocyanines	43
3.1.2 Synthesis of substituted Phthalocyanines	44
<b>3.2 Characterization</b>	49
3.2.1 Vibrational spectroscopy (IR spectroscopy)	49
3.2.2 UV-Visible spectroscopy	49
3.2.3 X-ray powder diffraction technique	50
3.2.4 Elemental analysis	50
3.2.5 UV-visible reflectance study	50
3.2.6 B.E.T. method (surface area measurement)	51
3.2.7 Magnetic Susceptibility Measurements	51
3.2.8 Thermal studies	53
3.2.9 Electron spin resonance spectroscopy (ESR)	53
3.2.10 Proton magnetic resonance spectroscopy:	54
<b>3.3 Photoluminescent studies</b>	54
3.3.1. Photoluminescence	55
3.3.2 Upconversion luminescence	58
3.3.3. Set up of Photoluminescence	58

<b>3.4 Scanning Electron Microscopy</b>	59
<b>3.5 Photocatalytic Studies</b>	60
<b>3.6 Catalytic Oxidation</b>	60
<b>3.7 Antimicrobial Activity</b>	61

## **CHAPTER 4**

### **4. CHARACTERIZATION AND SPECTROSCOPIC STUDIES**

<b>4.1 FTIR Spectroscopy</b>	63
<b>4.2 UV-Visible spectroscopy</b>	74
<b>4.3 X-ray diffraction</b>	80
<b>4.4 Elemental Analysis</b>	87
<b>4.5 TG-DSC</b>	88
<b>4.6 Magnetic Susceptibility</b>	98
<b>4.7 Diffuse Reflectance UV- visible Spectroscopy (DRS)</b>	100
<b>4.8 Electron spin resonance</b>	103
<b>4.9 NMR spectroscopy</b>	107
<b>4.10 Photoluminescent studies</b>	108
<b>4.11 Scanning Electron Microscopy</b>	113

## **CHAPTER 5**

### **5. CATALYTIC AND ANTIMICROBIAL STUDIES**

<b>5.1 BET Surface area measurement</b>	116
<b>5.2 Photocatalytic degradation of Amido Black 10B</b>	117
<b>5.3 Photocatalytic degradation of Auramine O</b>	124
<b>5.4 Photocatalytic degradation of Methylene blue</b>	128
<b>5.5 Mechanism for photocatalytic reaction</b>	133
<b>5.6 Catalytic oxidation of 2-hydroxynaphthalene</b>	134
5.6.1 Procedure for the oxidation of 2-hydroxynaphthalene to 2-hydroxy-1,4-Naphthoquinone	135
5.6.2 Effect of amount of 2-Hydroxy naphthalene on the rate of reaction	140
5.6.3 Effect of amount of Catalyst on the rate of reaction	141
5.6.4 Effect of amount of NaOH the rate of reaction	143



5.6.5 Effect of amount of H <sub>2</sub> O <sub>2</sub> on the rate of reaction	146
<b>5.7 Catalytic oxidation of benzoin to benzil</b>	<b>153</b>
<b>5.8 Effect of Phthalocyanines on Microbial cultures</b>	<b>157</b>
5.8.1 Antimicrobial activity on water soluble Pcs	157
5.8.2 Effect of solvent on the antimicrobial activity of TCCoPc and TCMnPc	160
5.8.3 Antimicrobial activity on non substituted MPcs	163
<b>CHAPTER 6</b>	
<b>6. SUMMARY AND CONCLUSIONS</b>	<b>167</b>
<b>REFERENCES</b>	<b>173</b>
<b>APPENDIX-I</b>	<b>186</b>

## LIST OF ABBRIVATIONS

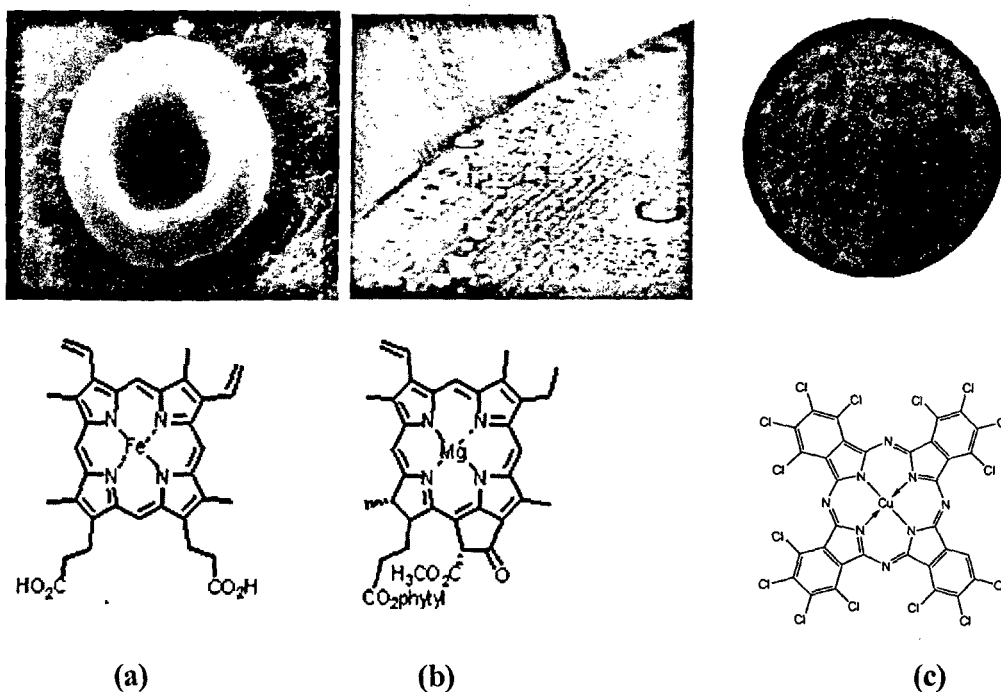
AC <sub>2</sub> O	Acetic Anhydride
BE	Binding energy
BET	Brunauer-Emmett-Teller
DMSO	Dimethyl sulphoxide
DMF	Dimethyl formamide
DRS	Diffuse reflectance spectroscopy
ESR	Electron spin resonance spectroscopy
FTIR	Fourier transform infrared
MPc	Metal Phthalocyanine
MeOH	Methanol
NMR	Nuclear magnetic resonance
Pc	Phthalocyanine
Pcs	Phthalocyanines
PL	Photoluminescence
SEM	Scanning electron microscopy
TAMPc	Tetra amino metal phthalocyanine
TCMPc	Tetra(N-Carbonylacrylic)amine metal Phthalocyanine
TNMPc	Tetra nitro metal phthalocyanine
TG/DTA	Thermogravimetry/Differential thermal analysis
UV	Ultraviolet
UV-Vis	Ultraviolet- Visible
XRD	X-ray diffraction

# **CHAPTER 1**

## *INTRODUCTION*

## 1.1 Phthalocyanine and Porphyrins

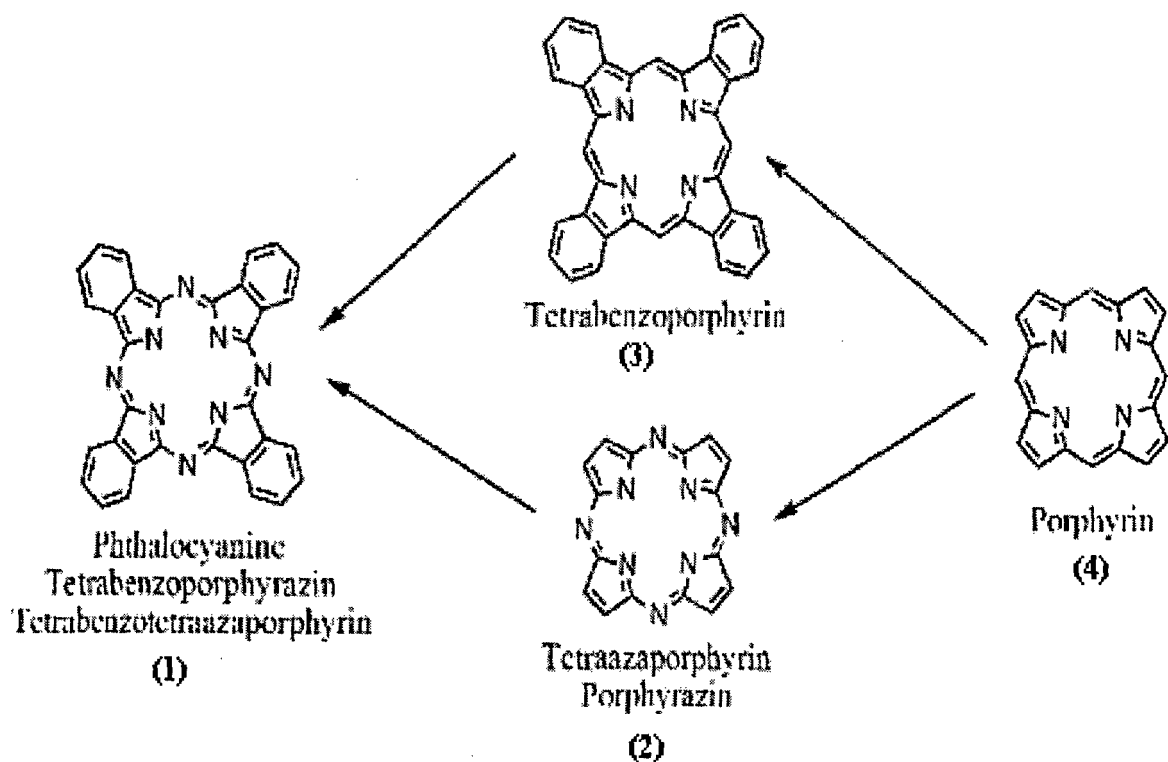
Porphyrins have been often called the ‘colours of life’. These are much more than mere colour, but are the “master rings” at the center of producing energy, transporting oxygen and generally sustaining life<sup>1</sup>. Photosynthetic properties of plants are because of chlorophyll molecule and oxygen transport of blood is because of hemoglobin molecule (Fig. 1.1). The name porphyrin comes from the Greek word *Porphura* meaning purple<sup>2</sup>. Phthalocyanines (Pcs) are synthetic analogues of porphyrins and are structurally related. Like porphyrins, they are strongly coloured ranging from dark blue to green. They are robust molecules, with stability to higher temperatures, UV light and are insoluble in most solvents except in strong acids or when functionalized with sulfonate groups. Despite of their low solubility, Pcs are one of the most important pigments produced, for the use in paints and dyes accounting 25% of all pigments synthesized world wide<sup>3</sup>.



**Fig. 1.1 (a) Hemoglobin, (b) Chlorophyll and (c) Phthalocyanine**

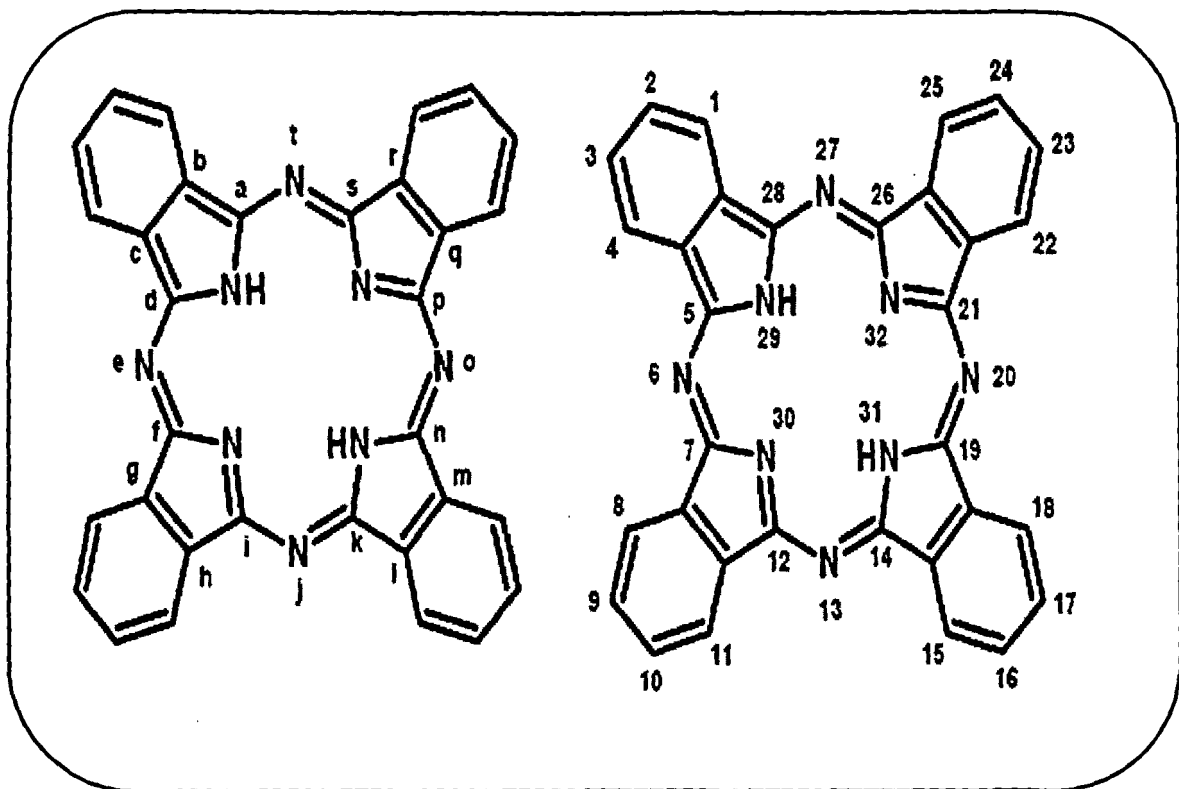
## 1.2 The Structure of Phthalocyanines and Porphyrins

Fig. 1.2 belong to a class of compounds known as tetrapyrrolic macrocycles which includes tetraazaporphyrins also known as Phthalocyanines (1), porphyrans (2), tetrabenzoporphyrins (3) and porphyrins (4). The macrocycles are structurally similar except (1) and (2) have imino nitrogen atoms at each of the four *meso* positions, commonly known as azamethine bridges, while (3) and (4) have methane bridges. The type of bridges connecting the iminoisoindoline units determines the size of the cavity, thus macrocycles with azamethine bridges are known to have smaller inner cavities than macrocycles with methane bridges<sup>4,5</sup>. Macrocycles (1) and (3) additionally have four benzo-subunits which allow for addition of functional groups onto their respective framework. The annulation of the Pcs greatly affects their electronic spectra and therefore they tend to have much stronger absorbance at longer wavelengths than do porphyrins.



**Fig. 1.2 Tetrapyrrolic macrocycles**

The four iminoisoindoline units make up the structure of a phthalocyanine, a symmetrical macrocycle with a conjugated system of 18  $\pi$  electrons that exhibits exceptional good stability of the compound. The extended conjugation is responsible for the blue green colour of these macrocycles. Pcs are considered as fused porphyrin analogues and by using the known International Union of Pure and Applied Chemistry (IUPAC) nomenclature of tetrapyrroles<sup>6</sup> These are formally known as tetrabenzob[*b,g,l,q*][5,10,15,20]tetraazaporphyrins as seen in Fig. 1.3.



**Fig. 1.3 Tetrabenzob[b,g,l,q][5,10,15,20]tetraazaporphyrins**

There are 16 possible sites of substitution onto the fused benzene rings (red), i.e. peripheral substitution (carbon number 2, 3, 9, 10, 16, 17, 23, 24) and non peripheral substitution (carbon number 1, 4, 8, 11, 15, 18, 22, 25). Change in the central metal ion or substitution onto the fused benzene rings results in modification in the properties of the molecule, e.g. colour, crystal structure, solubility, electronic and catalytic properties.

### 1.3 Phthalocyanines: General Applications

Phthalocyanines are versatile system in which the two central hydrogen atoms can be substituted by elements shaded with blue and those highlighted in red form

phthalocyanine nanoporous crystals (PNCs). Those highlighted in blue have been investigated but have not produced a PNC till date. The others have not yet been investigated<sup>7</sup>, as shown in Fig. 1.4. Due to its ability to get substituted with different elements and substitution possible at different peripheral and non peripheral positions, Pcs have shown wide applications right from dyeing of clothes to that in electronics. A major application of phthalocyanine pigment is in the production of cyano printing inks used for printing paper and packaging materials. Nowadays, both metal-containing pigments and metal-free phthalocyanine pigments are commercially available and compete with one another. Copper phthalocyanine (CuPc) dye is produced by introducing solubilizing groups, such as one or more sulfonic acid functionalities in CuPc structure. These dyes find extensive use in various areas of textile dyeing (Direct dyes for cotton), for spin dyeing and in the paper industry. Direct blue 86 is the sodium salt of CuPc - sulfonic acid whereas direct blue 199 is the ammonium salt of the CuPc - sulfonic acid<sup>3,8-11</sup>. Phthalocyanine has high resonating structure, which is responsible for its high thermal stability and therefore makes its application possible as a lubricant at high temperature<sup>12-</sup>



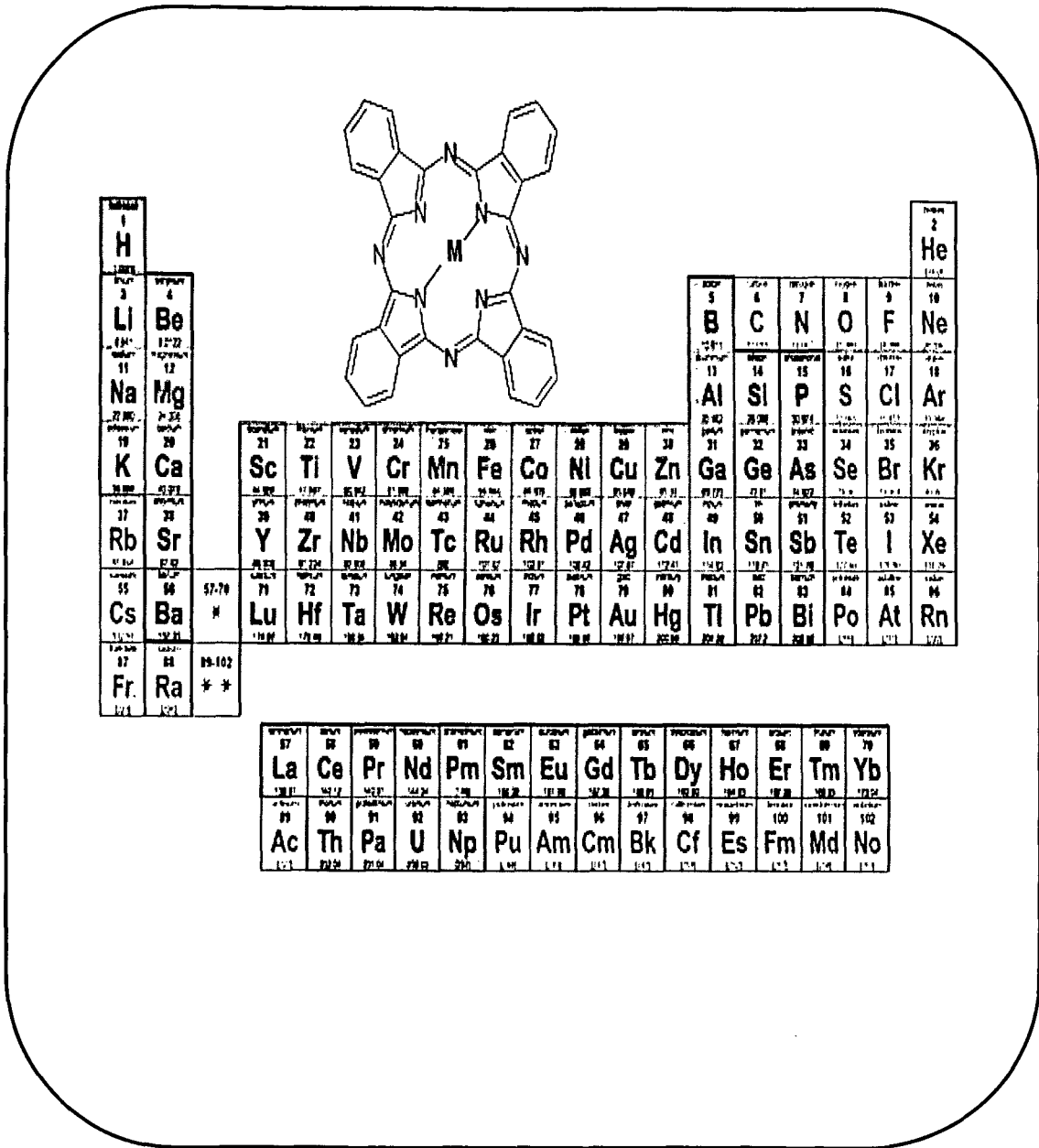


Fig. 1.4 Phthalocyanine relationships with elements in periodic table

Metallophthalocyanines (MPcs) and related compounds hold considerable promise for the development of nonlinear optical devices because of their large third-order nonlinearity, fast response times, unique electronic absorption characteristics, high thermal and environmental stability<sup>16-17</sup>. The large nonlinearity originates from their extensively delocalized  $\pi$ -electron distribution. They are highly stable and versatile compounds, capable of including more than 70 different metallic and non-metallic ions in the ring cavity. These properties along with the semiconducting nature, makes them very good photoconductors and sensors<sup>18-20</sup>. Apart from high spectral properties and thermal stability their application are limited due to low solubility. The current work focuses on the attempt to synthesize water soluble Pcs and study their various applications.

### **Highlights of the Thesis**

- 1) Preparation of metal phthalocyanine using different techniques such as refluxing in Nitro benzene, melt method and Microwave method was carried out. Phthalocyanines containing Zn, Ni, Mn, Co, Cu, Ni, Al and Fe, as central metal atoms were synthesized.
- 2) 4-Nitrophthalimide was synthesized from phthalimide using nitrating mixture. This nitrophthalimide was used for the synthesis of tetra Nitro metal phthalocyanines (TNMPcs) using melt and microwave method, containing Zn, Ni, Mn, Co, Cu, Ni and Fe, as central metal atom.
- 3) The above synthesized TNMPcs were used for the synthesis of series of tetraamino phthalocyanine(TAMPc) by reducing the nitro group using either  $\text{SnCl}_2$  or  $\text{Na}_2\text{S}$  containing Zn, Ni, Mn, Co, Cu, Ni and Fe, as central metal atoms.

- 4) Water soluble Pcs were prepared by reacting TAMPCs with maleic anhydride to form tetra (N-Carbonylacrylic) amine metal Phthalocyanine (TCMPcs) having Zn, Mn, Co, Cu and Ni, as central metal atoms.
- 5) The above synthesized Phthalocyanine were characterized using FTIR, UV-Visible spectroscopy, X-ray powder diffraction (XRD) and Elemental analysis.
- 6) Studies such as Thermal Analysis, Magnetic Susceptibility, Diffused reflectance spectroscopy (DRS), Surface area measurement using BET technique, SEM and photoluminescence were undertaken.
- 7) Photocatalytic degradation of azo dyes such as Amido Black 10B, Auramine and Methylene Blue.
- 8) Catalytic oxidation of Benzoin to benzil in presence of TCMPc at different experimental condition, i.e. at different temperatures and in different solvents was carried out.
- 9) Catalytic oxidation of  $\beta$ -naphthol to 2-hydroxy 1,4-Napthaquinone in presence of specific catalyst such as CuPc and TACuPc, using different experimental condition was performed.
- 10) The synthesized Pcs were tested for their antimicrobial activity.

**Thesis under present investigation will be divided into following six chapters.**

**Chapter- I** deals with the brief introduction, aim and objective of the research work is being spelt out in this chapter.

**Chapter- II** describes the literature studies pertaining to the synthesis of different types of Phthalocyanines and their various applications.

**Chapter- III** highlights the different methods of preparation and characterization of the compounds by employing different instrumental tools.

**Chapter- IV** describes characterization and the spectroscopic studies.

**Chapter- V** discusses and evaluate the catalytic activity towards the degradation of dyes, oxidation of alcohols and antimicrobial studies.

**Chapter- VI** summarizes the overall results and conclusions.

# CHAPTER 2

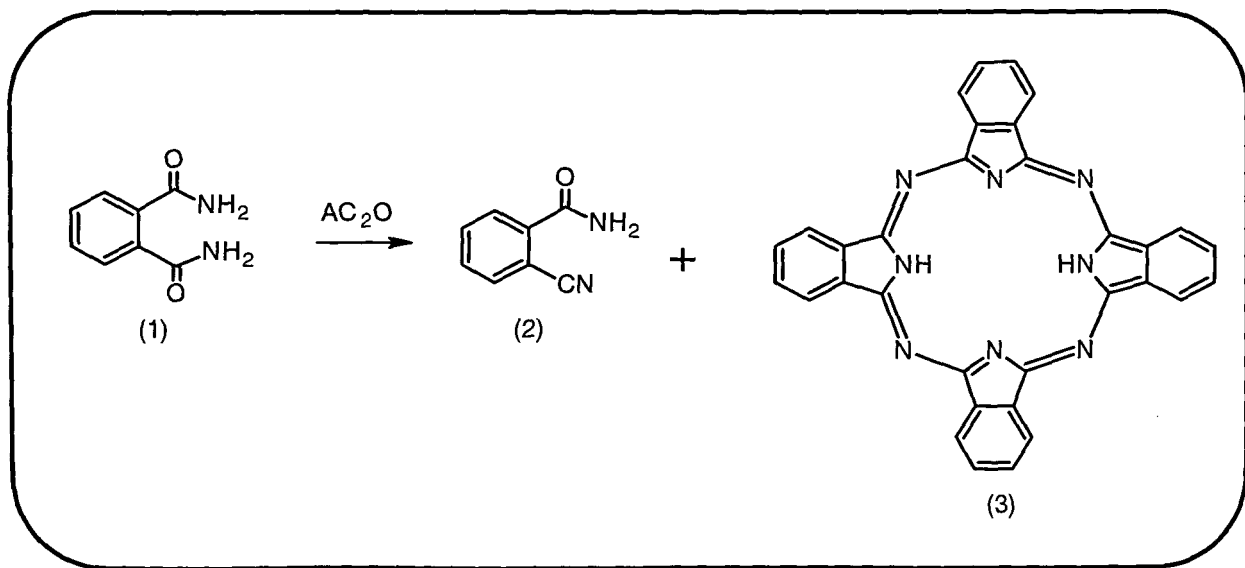
## *LITERATURE REVIEW*

## Introduction

This chapter deals with the literature survey on the discovery of phthalocyanine, different types of phthalocyanine, various synthetic strategies, different tools of characterization, its various applications in the field of catalysis, PDT, Lubricant, sensors and antimicrobial activity.

### 2.1 The Discovery of Phthalocyanines

The wonderful existence of phthalocyanine (Pc) is the one that was purely accidental. In 1907, Braun and Tscherniac accidentally discovered the first sample of a highly coloured phthalocyanine (Pc). The bright bluish compound, later known as metal-free phthalocyanine (3) as seen in Scheme 2.1, was obtained as a by-product during an attempted synthesis of *o*-cyanobenzamide (2) from phthalamide (1). However this discovery was of no special interest at that time.



Scheme 2.1

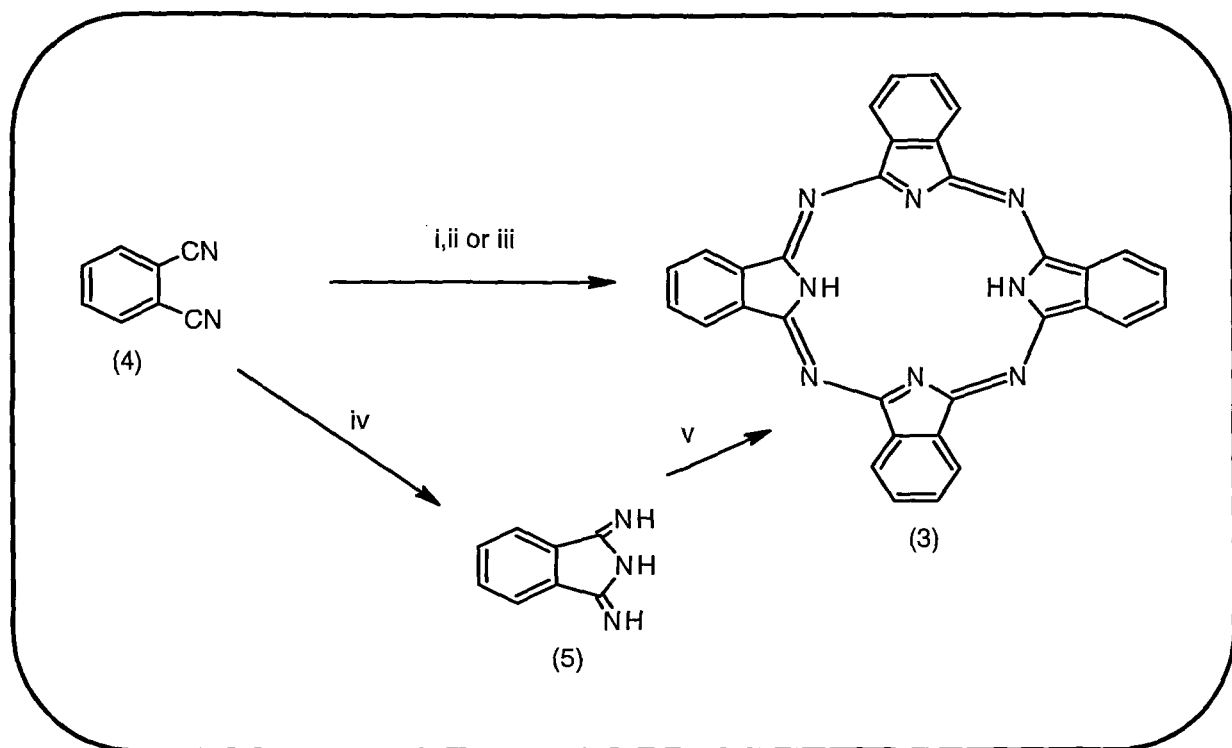
In 1927 de Diesbach and von der Weid accidentally prepared CuPc in an attempt to synthesize phthalonitrile from *o*-dibromobenzene and cuprous cyanide in pyridine. In place of a colourless product, a blue coloured product was obtained which was exceptionally stable to alkalies, sulphuric acids and heat.

In 1929 the Pc was made by Scottish Dyes. During the preparation of Phthalimide from phthalic anhydride and ammonia in an enamel vessel, a greenish blue impurity appeared. Dunsworth and Drescher carried out a preliminary examination of the compound, which was analyzed as an iron complex. It was formed in a chipped region of the enamel with iron from the vessel. Further experiments yielded FePc, CuPc and NiPc. It was soon realized that these product could be used as pigments or textile colorants. Linstead and Co-workers at the University of London discovered the structure of Pc and developed improved synthetic method for several metal Pc from 1929 to 1934. Later on the crystal structure of these large organic molecules was confirmed by X-ray diffraction experiments performed by Robertson<sup>21-24</sup>

## **2.2 Synthesis of phthalocyanine**

### **2.2.1 Synthesis of non-substituted metal free Phthalocyanine**

Synthesis of metal free phthalocyanine is given in scheme 2.2



**Scheme 2.2**

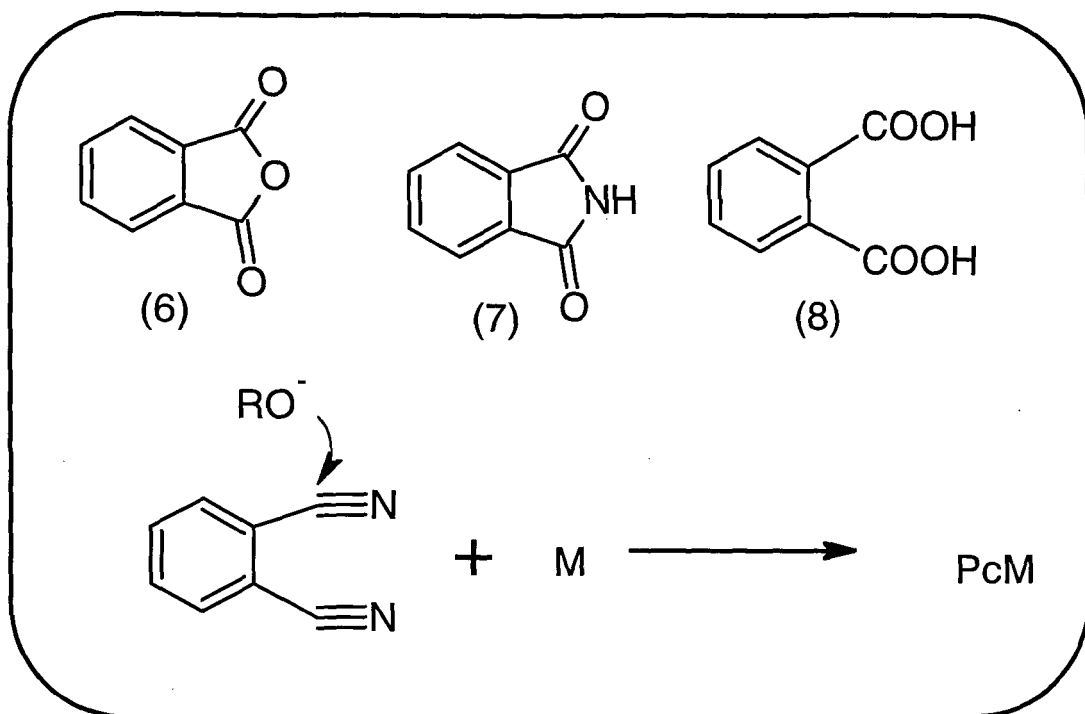
Where (i) Lithium, refluxing pentanol, followed by aqueous hydrolysis. (ii) Fuse with hydroquinone (iii) Heated with 1,8-diazobicyclo[4,3,0]non-5-ene(DBN) in a melt or in pentol solution. (iv) Ammonia (NH<sub>3</sub>), refluxing methanol and sodium methoxide. (v) Refluxing in a high boiling point alcohol<sup>25</sup>.

### 2.2.2 Synthesis of non-substituted metal phthalocyanine

MPC can be obtained from diverse precursors such as phthalonitrile (1), o-cyanobenzamide(2), 1,3-diiminoisoindoline(4), Phthalic anhydride (6), phthalimide (7),



phthalic acid (8) etc, generally in high boiling non-aqueous solvents at elevated temperature or electrochemically from phthalonitrile. In case of phthalonitrile, sodium methoxide and other strong bases are used in order to perform a nucleophilic attack at the cyano group of phthalonitrile as shown in scheme 2.3.



**Scheme 2.3**

Metal-free phthalocyanine forms metal complexes with strong (for example Fe, Cu, Ni) or weak (Mg, Sb) metals which can be synthesized (a) chemically from metals or their salts or (b) electrochemically from the bulk metals or their salts. (a) This reaction employs elemental metals or their salts, the above precursors and non-aqueous solvents having high boiling points such as nitrobenzene, o-dichloro- and trichloro-benzene, ethylene glycol,  $\alpha$ -methyl-naphthalene, quinoline etc are used. Some alcohols are also used in which

phthalonitrile are used as precursor<sup>26</sup>. (b) Electrochemical route and use of laser, ultrasonic and microwave treatment is less common for the synthesis of phthalocyanine<sup>27,28</sup>.

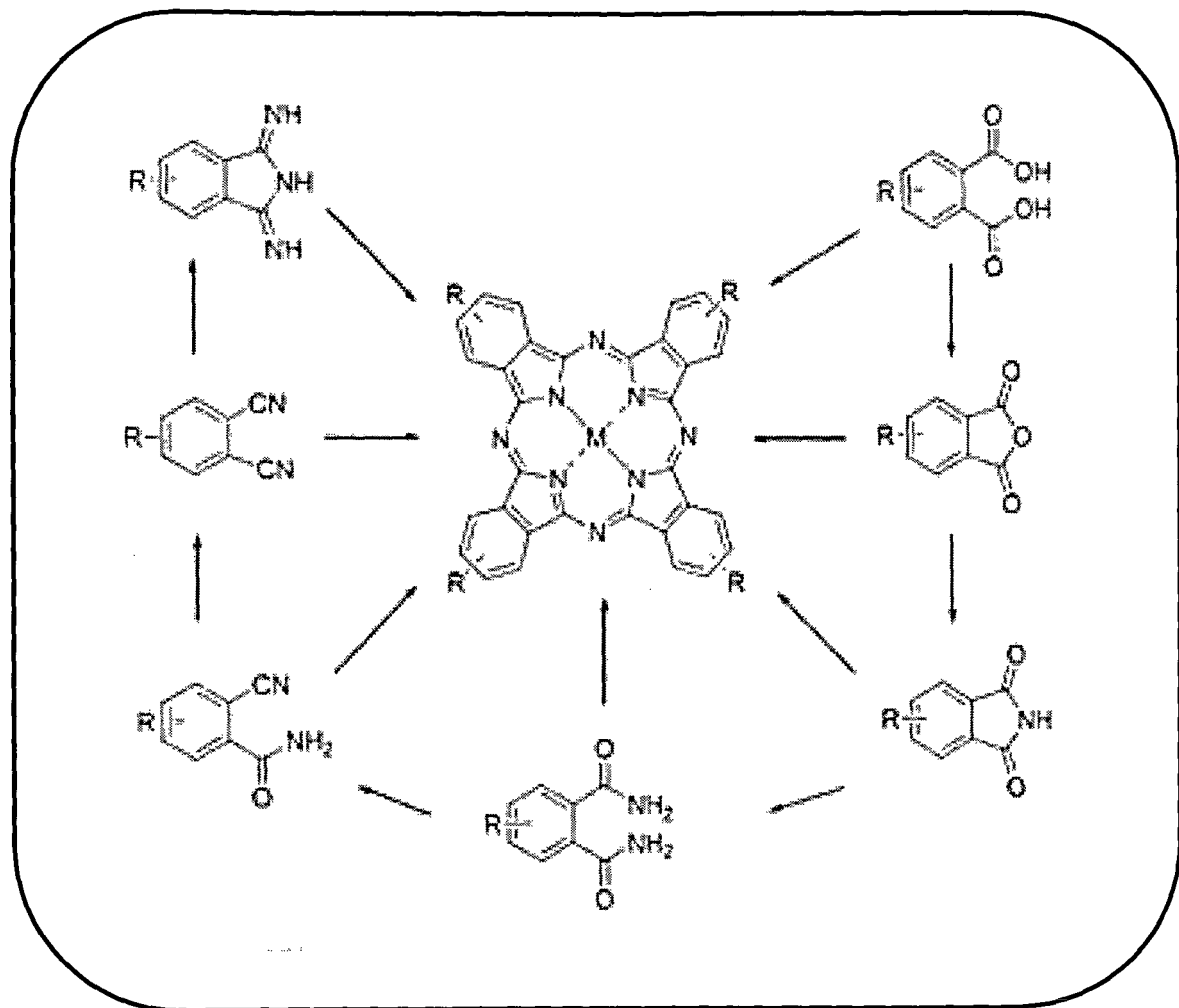
## 2.3 Synthesis of Substitute Phthalocyanine

Non substituted Pc has practically low solubility in most of the organic solvents. It shown solubility in 8M H<sub>2</sub>SO<sub>4</sub>, but the only disadvantage is that it leads to the protonation of the ring. To increase the solubility of these macrocycles, different substituent's which include aliphatic chains having capability of self-organizing into the liquid crystal state<sup>29</sup>, aromatics, amines, thiols, halides and acids can be added to the Pc framework<sup>30-32</sup>.

### 2.3.1 Tetra-substituted Phthalocyanines

Tetra substituted phthalocyanine can be obtained either by substitution on a preformed Pc ring or by condensation of an appropriately substituted precursor as shown in scheme 2.4<sup>33</sup>. The former has been used for sulphonation or chlorosulphonation of non-substituted Pc with 20-30% oleum and chlorosulphonic acid<sup>34-36</sup>. With this method, purification and isolation of the desired product is almost impossible, since complex isomeric mixtures with varying degrees of substitution are formed. The use of substituted precursor is however generally preferred since controlled substitution at 3-or-4-position is obtained. Though it is far better than the first method, the mono substituted product formed, lead to the formation of constitutional isomers. The 3-position isomer of (C<sub>4h</sub>)1,8,15,22-, (D<sub>2h</sub>) 1,11,15,25-, (C<sub>2v</sub>) 1,11,18,22- and (C<sub>s</sub>) 1,8,18,22-tetrasubstituted complexes, are shown in Fig 2.1. while the 4-position, single isomers of (C<sub>4h</sub>)2,9,16,23-, (D<sub>2h</sub>) 2,10,16,24-, ((C<sub>2v</sub>) 2,9,17,24- and ((C<sub>s</sub>) 2,9,16,24-tetrasubstituted complexes are shown in Fig 2.2. Though the separation of

regioisomer is tedious, it is made possible using HPLC. Symmetrically Tetra-substituted Pc are synthesized from tetraanhydride of 2,3,9,10,16,17,23,24-Octacarboxyphthalocyanine (OCPc) as a convenient precursor<sup>37</sup>.



Scheme 2.4

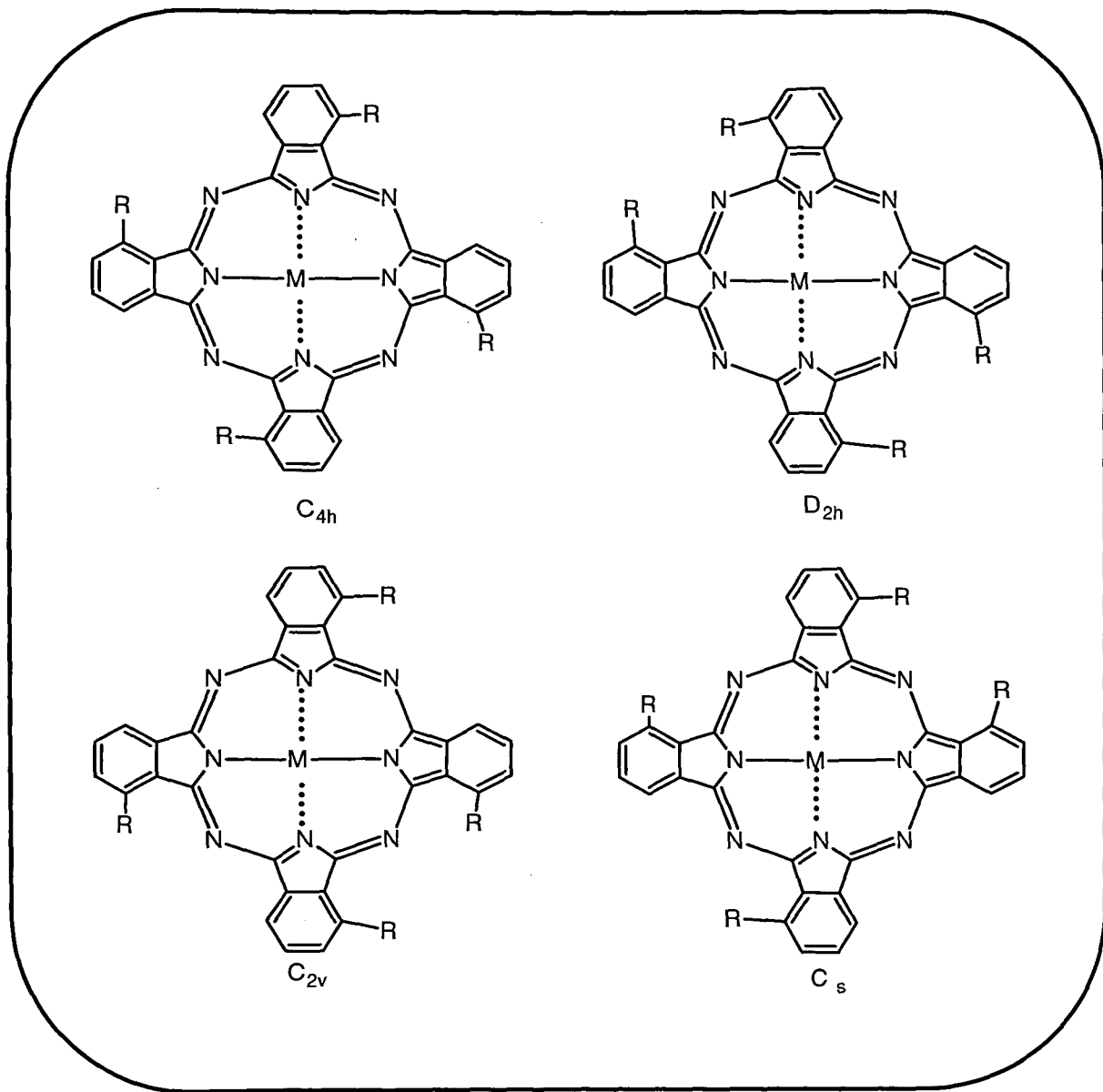


**Fig 2.1 Tetrasubstituted Pcs with substitution at 3 position**

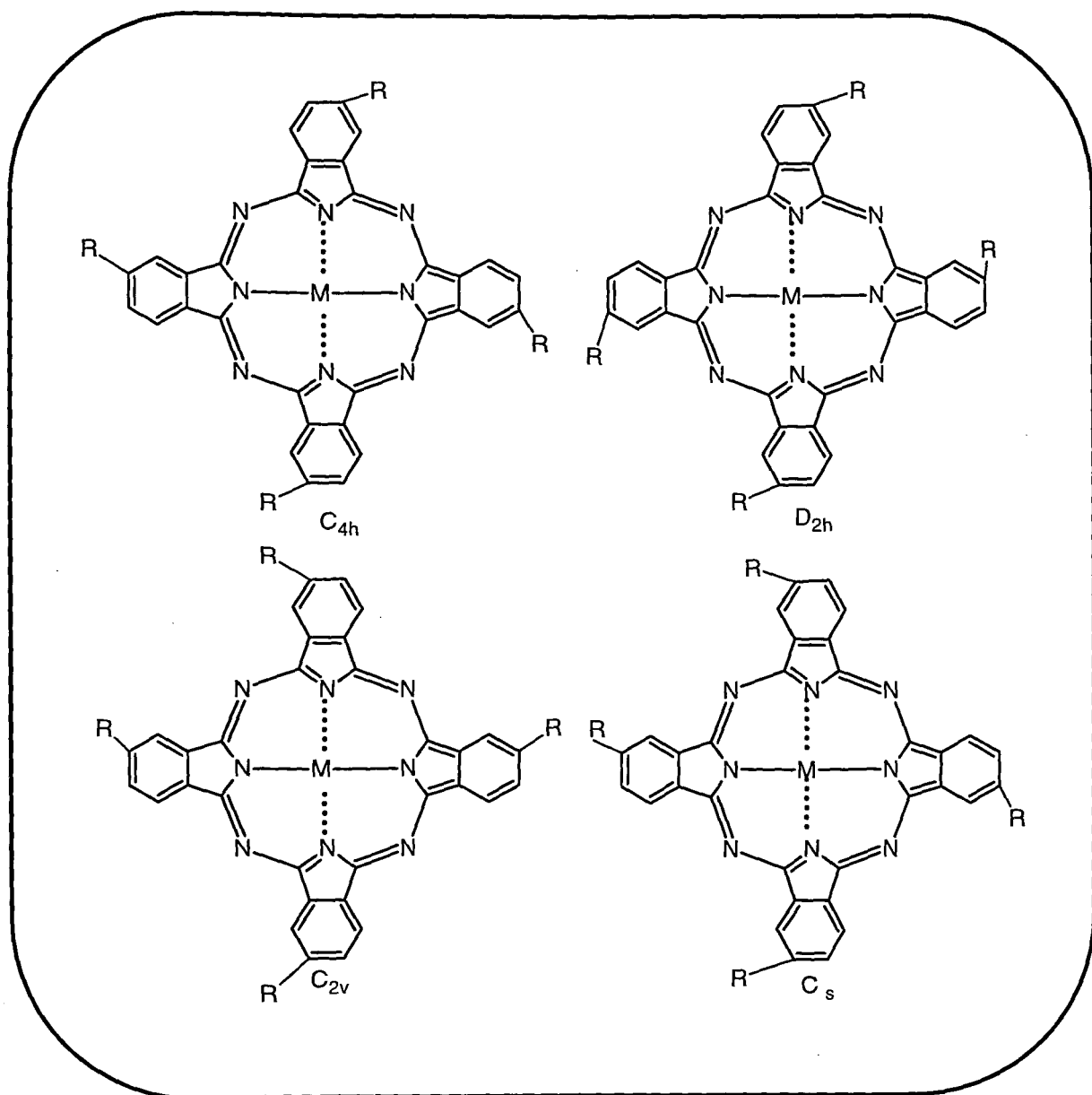


**Fig 2.2** Tetrasubstituted Pcs with substitution at 4 position

To increase conjugation, for the selective synthesis of mono substituted, tri substituted or having selective substitution at desire position, palladium catalyzed cross coupling reaction is used<sup>38-40</sup>. This technique is also used for the preparation of peptide Pc conjugates<sup>41</sup>.

### 2.3.2 Octa-substituted Phthalocyanines

The difficulty faced in the separation of isomer is overcome by synthesizing octasubstituted Pc starting from precursor having substitution at either 2,5-substitution<sup>42</sup> or 3,4 substitution<sup>43</sup>. Octa- Carboxylated Pc Cu(II) complex was prepared by the reaction of 1,2,4,5-benzenetetracarboxylic acid dianhydride, urea with CuCl<sub>2</sub> in nitrobenzene at 180°C<sup>44</sup>.

### 2.3.3 Axial substituted phthalocyanine

The cyclotetramerisation of phthalonitrile or diiminoisoindoline in the presence of silicon tetrachloride produce a-Cl<sub>2</sub>SiPc, which on hydrolysis by aqueous sodium hydroxide gave a-(OH)<sub>2</sub>SiPc, which is the intermediate precursor to the Pc-polysiloxane. Axial substitution reaction on precursor with alcohol, alkyl halide and chlorosilanes results in a range of materials having enhanced solubility in common organic solvents<sup>25</sup>. Ruthenium Phthalocyanine(RuPc) having axial polymeric bridge was synthesized and its organic conductor properties were studied by Wolfram and Michael<sup>45</sup>. DiamineRuPc is not substituted on ring but still it is water soluble and isomerically pure<sup>46</sup>. Two Pc linked to a single Lutetium (III) as a central metal atom and forming a sandwich compound is reported in literature<sup>47</sup>. Priscilla and group has increased the solubility of silicon phthalocyanine by substituting poly( $\epsilon$ -caprolactone) at axial position<sup>48</sup>.

### 2.3.4 Synthesis of phthalocyanine having macrocycle

Pc containing Macrocycles such as 15-membered oxadithiadiazole<sup>49,50</sup> crown ether,<sup>51-53</sup> Azobenzene<sup>54</sup>, Tetraaza Macrocyces<sup>55</sup> were synthesized to study their optical and electrical properties.

### 2.4 Synthesis of Sub phthalocyanine (SubPc)

Compared to Pc, Subphthalocyanine (SubPcB(X)) Fig2.3, the lower homologues of Pc, are less studied. This is mainly because of problems dealing with their purification and non-reproducible results. Apart from all this difficulties, the first SubPc with an axial halogen was synthesized in 1972 by Meller and Ossko by reaction of  $\text{BF}_3$ ,  $\text{BCl}_3$  or  $\text{PhBCl}_2$  respectively with phthalonitrile in boiling 1-chloronaphthalene for 10 minutes<sup>56</sup>. Michael Hanack and Monika Geyer could successfully synthesize and separate the structural isomers of Tri-Tert-butylsubphthalocyaninatophenylboron (III), the main aim of phenyl group as axial substituent would be to facilitate separation of the isomers and for this purpose triphenylboron as the boron reagent and Naphthalene instead of 1-chloronaphthalene as solvent are used. By this approach the unwanted chlorination of the macrocycle is avoided<sup>57</sup>. Trisulfonated Phthalocyanine and their derivatives have been successfully prepared using Boron (III) SubPc as an intermediate<sup>58</sup>. SubPhthalocyanine are extensively used for the preparation of unsymmetrical Phthalocyanine which has wide application in non-linear optics<sup>59,60</sup>. The first dimer of aromatic macrocyclic complex formed by the lateral bridging of SubPc, containing Boron in the center was prepared by Nagao Kobayashi<sup>61</sup>. SubPcdimer with  $\text{C}_{60}$  complex was found to show good photophysical properties due to extended conjugation<sup>62</sup>.

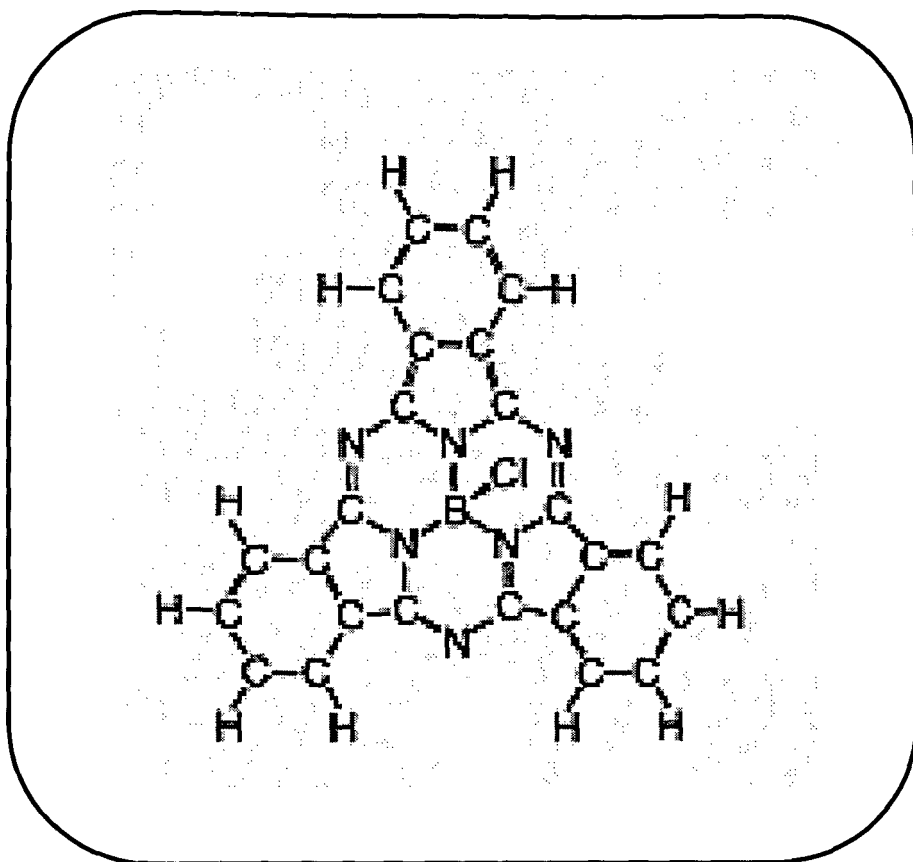


**Fig 2.3 Sub phthalocyanine**

## **2.5 Synthesis of Super phthalocyanine**

Superphthalocyanines having Uranium as a central metal atom as shown in Fig 2.4 has been synthesized and characterized by Edward and Tobin in 1981<sup>63</sup>.



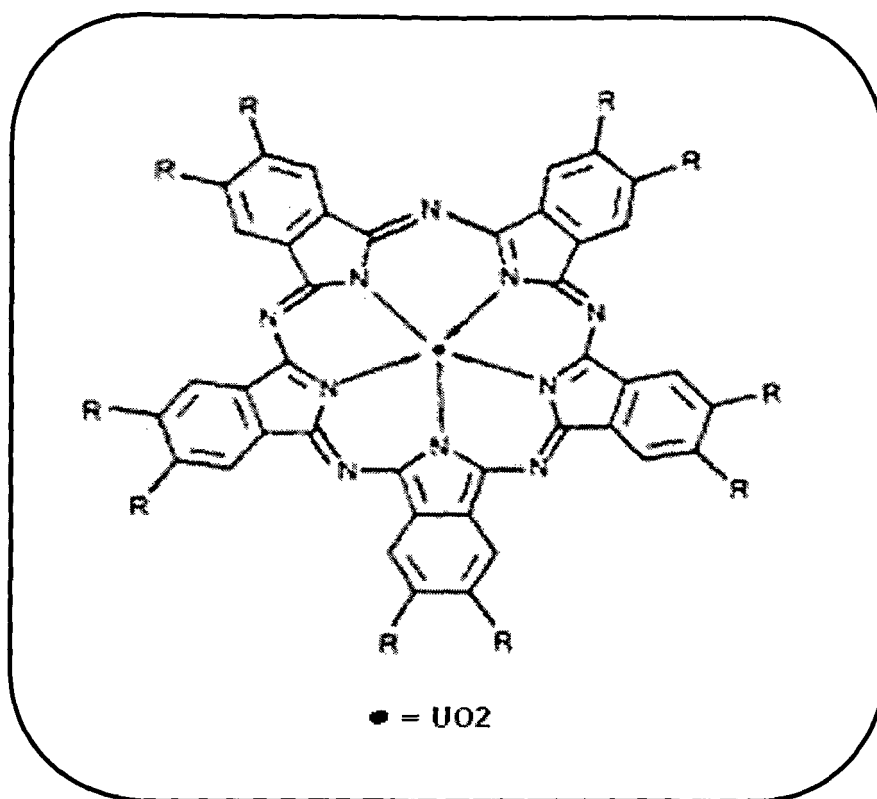


**Fig 2.4 Super phthalocyanine**

## 2.6 Related Synthetic strategies

Synthesis of metal nitro phthalocyanine starting from nitrophthalonitrile ammonium chloride, metal salt, NaOH and a catalytic amount of sodium methoxide in DMSO was carried out under reflux condition for 4 h, the product obtained was washed with alcohol and then with water, to obtain a pure product. This product was reduced to tetraamino phthalocyanine with sodium sulphide nonahydrate in water for 5 h and purified using 0.5M H<sub>2</sub>SO<sub>4</sub> and 1.0M NaOH was reported by Achar and Lokesh<sup>64</sup>. 4-Nitrophthalic acid, urea and CoCl<sub>2</sub>.6H<sub>2</sub>O and ammonium molybdate were finely grounded and placed in a 500 ml beaker covered with a glass surface vessel. The reaction mixture was heated for 5 h at 190°C followed by washing

with 1.0M HCl, 1.0M NaOH finally with water and dried in vacuum. This tetranitro Pc was reduced to tetraamino phthalocyanine with sodium sulphide in DMF at 60°C for 1 h and the product obtained was washed with water. TetraaminoCoPc thus obtained was dissolved in DMF and to that maleic anhydride was added, the reaction was kept at 50°C for 3 h, and the solution was poured in 1000 ml of water. The product obtained was dissolved in 0.1 M NaOH, followed by reprecipitation with acid, this procedure was repeated 3 times to get pure Cobalt tetra(N-Carbonylacrylic)aminePhthalocyanine<sup>65,66</sup>. Similarly Zinc tetra(N-Carbonylacrylic)amine Phthalocyanine was prepared using zinc salt and was further used for the photocatalytic degradation of 1,3-diphenylisobenzofuran<sup>67</sup>. Synthesis of tetranitro Pc in high boiling organic solvent<sup>68</sup> or using Microwave oven also for synthesis of tetrasulfo Pc is reported in literature<sup>69</sup>.

Reduction of tetranitro Pc to tetraamino Pc is well reported in literature<sup>70,71</sup>.

## 2.7 Synthesis of water soluble Phthalocyanines

Porphyrins are used in photodynamic therapy (PDT)<sup>72</sup> and as phthalocyanine is structurally similar to porphyrin, it also found application in PDT<sup>73</sup>. Research was more focused on the synthesis of water soluble phthalocyanine having sulpho, carboxy-<sup>74,75</sup> phosphono-<sup>76</sup> and acrylicgroup. The first sulphonated CuPc was reported in 1929 and further Weber and Busch synthesized sulphonated Pc from monosodium salt of sulphonic acid using metal salt heated in nitrobenzene in the presence of urea and ammonium molybdate as catalyst<sup>77</sup>. In 1960's lot of research was done to study the magnetic and electronic properties of 4,4',4'',4'''-tetrasulfophthalocyanine<sup>77,78</sup>. The Pc solubility is increased by linking deoxyribose to it, through Sonogashira coupling reaction<sup>79</sup>. Coumarin is a constituent of many

higher plants, essential oils and they are biological active as anti-coagulant, antithrombotics, antimicrobial activity. Such coumarin are coupled with Pcs, and after the cleavage of lactone ring of the peripheral 2H-1- benzopyran-2-one(coumarin)Pc, the solubility of the resulted product was found to increase<sup>80</sup>. Sonmez and Ismail have synthesized water soluble ZnPc substituted with Naphthoxy-4-Sulfonic acid sodium salt<sup>81</sup>.

## 2.8 Different tools for the characterization of phthalocyanine

### 2.8.1 Magnetic susceptibility studies

In 1965 Weber and Busch recorded magnetic moments for metal derivatives of 4,4',4'',4'''-Tetrasulfo phthalocyanine at room temperature by the Gouy method using mercury (II) tetrathiocyanatocobaltate (II) and demineralized, double distilled water as standards. The values are generally reproducible to  $\pm 0.05$  B.M for 0.025M solution and to  $\pm 0.10$  B.M for the solids<sup>82</sup>.

The magnetic susceptibility measurements of metal phthalocyanine tetrachlorides (MPTCl's) were investigated in solid state over the applied magnetic field strength of 1.33–4.45 kG. Experimental values revealed that CuPTCl and CoPTCl are paramagnetic and NiPTCl & ZnPTCl are diamagnetic. The  $\chi_m$  and  $\mu_{eff}$  for CuPTCl and CoPTCl at lower magnetic field strength are found to be higher than that expected for that of one unpaired electron and at higher field it approaches the spin only value 1.73 B.M. The observed higher magnetic moments than spin only value is due to the orbital contribution to  $\mu_{eff}$  which may arise as a result of mixing of ground state orbitals ( $b_{2g}$ )<sup>2</sup>, ( $e_g$ )<sup>4</sup> and ( $a_{1g}$ )<sup>1</sup> with higher orbitally degenerate states, ( $b_{2g}$ )<sup>2</sup>, ( $e_g$ )<sup>3</sup> and ( $a_{1g}$ )<sup>2</sup>. The orbital contribution is found to be higher at lower magnetic field than that of higher magnetic field as evidenced by higher  $\mu_{eff}$  values at

lower field strength and it may be accounted for the contribution of magnetic anisotropy of the strong phthalocyanine  $\pi$  electronic current<sup>83</sup>.

The magnetic susceptibility of the samples was determined by Guoy method at room temperature. Copper Pc and cobalt Pc were paramagnetic whereas nickel Pc is Diamagnetic and iron Pc is ferromagnetic. Higher or lower value of  $\mu_{\text{eff}}$  indicates the contribution of the direct or super exchange intermolecular interaction to spin only value. Difference in magnetic moment values and their variations may be due to the difference in intermolecular interactions, spacing and inclination of the molecules in the crystal lattice<sup>84</sup>. The nickel(II) complexes of phthalocyanine (four-coordinate, low spin) in pyridine were investigated by EPR spectroscopy and by magnetic susceptibility. The ESR spectra of Ni(II) complexes in frozen (77 K) pyridine solution exhibited well-resolved superhyperfine lines which were attributed to the formation of six-coordinated high-spin Ni(II) complex, and the interaction of the magnetic moment of the Ni(II) ions with the in-plane and out-of-plane (solvating molecules) nitrogen atoms. Due to the aggregation of the molecules, no resolved spectrum could be obtained. The ESR spectrum of the solid-state compound, which was obtained by evaporation of the solution, exhibited a single broad line. The magnetic susceptibility of this compound obeys the Curie-Weiss law<sup>85</sup>.

### 2.8.2 UV-Visible spectroscopy studies

Lot of studies are done to assign the bands observed in the UV-Visible region of the spectrum obtained by dissolving the phthalocyanine in solvents, based on that the absorption peaks observed at around 327-337 nm. This is characterized as B-band of the phthalocyanine ring which arises due to of  $a_{2u} \rightarrow e_g$  transition. The absorption peaks observed at 664-677 and 608-631 nm are attributed to the characteristic Q-band of phthalocyanine ring which are

arising because of  $a_{1u} \rightarrow e_g$  transitions. A weak band in the range 206–208 nm is observed for all the complexes and it is accounted for the C-band of the phthalocyanine molecules<sup>83,86-90</sup>. The Q-band exists in the visible region of spectra while others (B, N and C) exist in the UV region of spectra. B, N and C appear with intensities that are comparatively higher than that of Q-band. The higher energy peak of Q-band has been assigned to the first  $\pi-\pi^*$  transition on the phthalocyanine macrocycle. The lower energy peak has been explained as an excitation Peak<sup>91</sup>.

### 2.8.3 TG-DSC/DTA studies

Thermal studies have indicated the thermal stability of metal Phthalocyanines and decomposition behaviour at different temperatures. Phthalocyanines do not have sharp melting point. They decompose at elevated temperature. It is observed that CoPc is stable up to 410°C and starts decomposing at around 425°C and shows weight loss till 700°C. It was assumed that the decomposition products might be hydrocarbon, ammonia and metal oxides. FePc, NiPc and CuPc show similar thermal pattern with slightly lower decomposition temperature for FePc and NiPc<sup>84</sup>.

### 2.8.4 Fluorimetry

A spectrofluorimetric determination of sulfite is based on the co-quenching effect of sulfite and formaldehyde on the fluorescence of a red-region dye, tetra-substituted amino aluminum phthalocyanine (TAAIPc). The relationship between the fluorescence quenching of TAAIPc and the concentration of sulfite is linear over the concentration range of 8–240  $\text{ngml}^{-1}$  under optimum conditions. Therefore this method has been successfully applied to the

determination of sulfite in VK3 injections and sugar<sup>92</sup>. The phthalocyanines are considerably more fluorescent than the porphyrins, and this is attributed mainly to their shorter radiative lifetimes. The effect of peripheral substituent's is small, both on absorption and fluorescence<sup>93</sup>.

### **2.8.5 X-ray studies**

Benny and Menon have deposited CoPc in the form of thin film, they compared the different phase of CoPc in free form and after deposition. The  $\alpha$ - phase is metastable and obtained as a thin film deposited on a cold substrate in vacuum. The  $\beta$  phase can be obtained in single crystal form or as a thin film formed by deposition of phthalocyanine on heated substrates. The  $\beta$ -form is the thermodynamically stable one. The  $\alpha$ -form with tetragonal and orthorhombic structure is metastable and can be converted to  $\beta$ -form by temperature treatments. The differences in the 'd' values are attributed to higher X-ray absorption, sample purity, particle size, preferred orientation and crystal texture. Intensities of the diffracted beams are determined by the positions of the atoms within the unit cell. The XRD pattern of the deposited film shows amorphous nature, as reported by many investigators, as a single peak<sup>94</sup>.

## **2.9 Catalysis**

### **2.9.1 Catalytic Degradation**

Waste water from various industries, factories, laboratories etc is now a serious problem to environment. The discharge waste containing dyes are toxic to microorganism, aquatic life and human beings. Extensive research is underway to develop advanced

physicochemical methods for the elimination of hazardous chemical compositions from air, soil and water. Semiconductor photocatalysis has received a special attention in the decomposition of organic compounds because of their complete mineralization ability and possible application to water pollution control using solar energy, which is a renewable energy form, cost effective and completely free to degrade the organic compounds by photolysis<sup>95</sup>. Photocatalytic degradation of 4-chlorophenol in presence of TiO<sub>2</sub> is reported<sup>96,97</sup>. TiO<sub>2</sub> are used successfully for the degradation of dyes<sup>98</sup>. Ion exchanged Na Y Zeolite activated by silver metal is found effective for the photocatalytic degradation of organic contaminants and dyes in aqueous solution<sup>99</sup>. Complete oxidation of phenol to quinone and then to aliphatic acid in the presence of Fenton's reagent (H<sub>2</sub>O<sub>2</sub>/Fe<sup>2+</sup>) is reported<sup>100</sup>. Metalloporphyrins in presence of hydrogen peroxide catalyze oxidative degradation of Herbicide<sup>101</sup>. Palladium phthalocyanine sulfonate, modified organobentonite showed enhanced photodegradation of 2,4,6-Trichlorophenol<sup>102</sup>.

With the development of modern industry, a lot of waste water was produced which greatly degraded the environment. Most of it is characterized by high salinity, high toxicity and low biodegradability. The toxic organic pollutant in the solution cannot be removed efficiently by conventional technologies such as bio-treatment. Recently, the application of glow discharge electrolysis to water treatment has attracted much attention of environmental researchers, mainly because of its high efficiency, high amenability to automation and environmental compatibility, in which high energy of plasma, especially the hydroxyl radicals, as directly produced by the water discharge were mostly utilized for the destruction of Auramine dissolved in a potassium sulfate solution by means of glow discharge electrolysis under water is described, with the focus on the reaction Kinetics<sup>103</sup>. TiO<sub>2</sub> is used for the

Photocatalytic degradation of Auramine<sup>104</sup>, Naphthol Blue Black<sup>105</sup>, Methylene Blue<sup>106-111</sup>  
TiO<sub>2</sub>/Zinc Phthalocyanine nanocomposites are used as photocatalyst for waste water treatment using solar irradiation<sup>112</sup>.

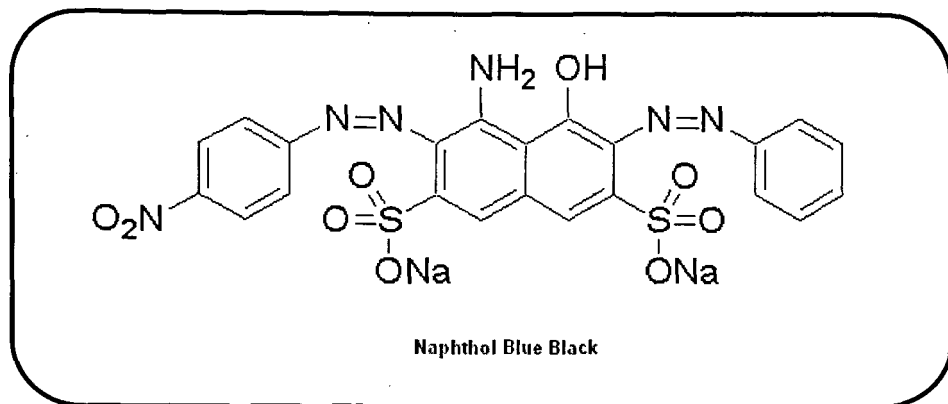


Fig. 2.5 Naphthol Blue Black

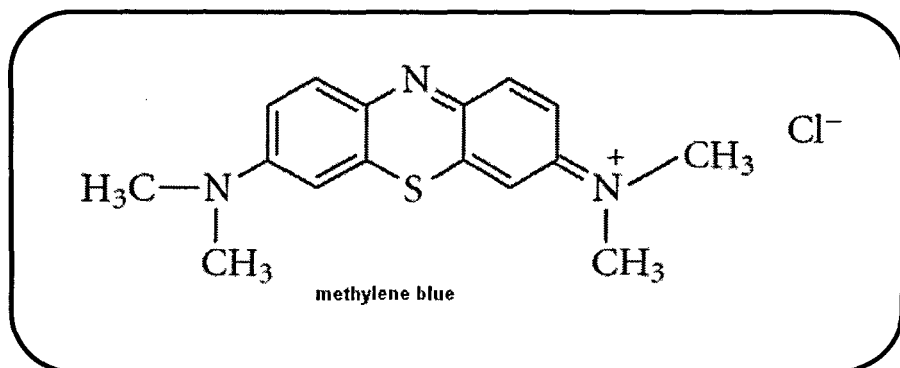


Fig. 2.6 Methylene Blue

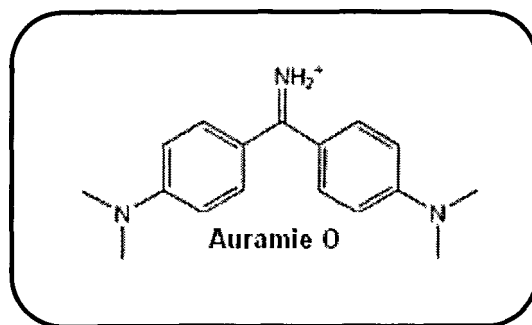


Fig. 2.7 Auramine O



## 2.9.2 Mechanism of photocatalysis

Unlike metals, which have a continuum of electronic states, semiconductors exhibit a void energy region in which no energy levels are available to promote the recombination of electron and hole produced by the photoactivation of the solid. The void region that extends from the top of the filled valence band to the bottom of the vacant conduction band is called the band gap. Absorption of a photon by semiconducting solids excites an electron ( $e^-$ ) from the valance band to the conduction band, if the photon energy  $h\nu$  equals or exceeds the band gap of the semiconductor/ Photocatalyst. Simultaneously an electron vacancy or a positive charge called a hole ( $h^+$ ) is also generated in the band (Fig 2.8). Ultraviolet (UV) or near-ultraviolet photons are typically required for this kind of reaction.



The electron hole pair thus created migrates to the photocatalyst surface where it either recombines producing thermal energy, or participates in redox reactions with the compound adsorbed on the photocatalyst. The life time of an electron hole pair is a few nanoseconds, but this is still long enough for promoting redox reactions in the solution or gas phase in contact with the semiconductor. Generally, hole oxidizes water to hydroxyl radicals (which subsequently initiate the chain of reactions leading to the oxidation of organics) or it can be combined with the electron from a donor species, depending on the mechanism of the photoreaction. Similarly, the electron can be donated to an electron acceptor such as an oxygen molecule (leading to formation of superoxide radical) or a metal ion can be reduced to its lower valence states and deposited on the surface of the catalyst. The electron transfer process is more efficient if the species are pre-adsorbed on the surface<sup>113,114</sup>.

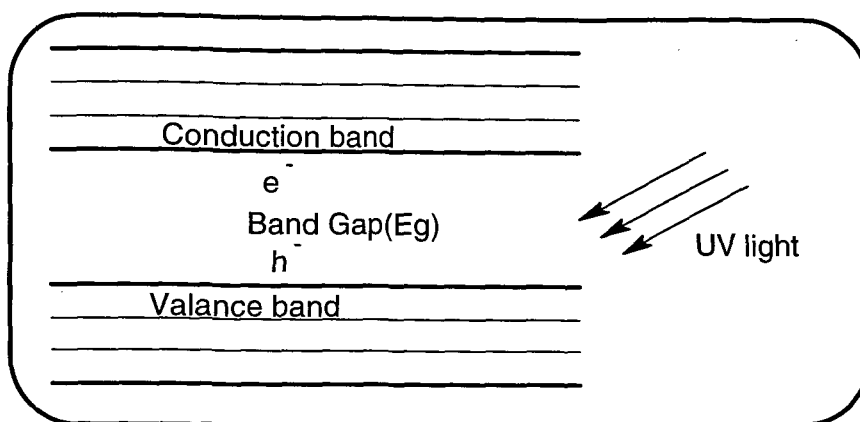


**Fig 2.8 Photo excitation of semiconductor**

### 2.9.3 Catalytic Oxidation

Nthapo and Tebello reported the oxidation of cyclohexane using tert-butyl hydrogen peroxide and chloroperoxybenzoic acid in presence of Fe and Co Pc<sup>115</sup>. Oxidation of Cis-Pinane have been reported with tert-butyl hydrogen peroxide at RT and atmospheric pressure in presence of FePc supported on activated carbons<sup>116</sup>. FePc's grafted over silica is used effectively for selective oxidation of alkynes and propargylic alcohol to  $\alpha,\beta$ -acetylenicketones, highly valuable precursors in the preparation of fine chemicals<sup>117</sup>. Substituted Pc is used as catalyst for the epoxidation of styrene using tert-Butyl hydrogen peroxide as an oxidizing agent<sup>31</sup>. Phenolic compounds are commonly used as solvent or reagents in Industrial processes and therefore they are the common contaminants in industrial waste water. In the past several years, many studies have been reported ascertaining the photocatalytic transformation of phenolic compounds using suspension of semiconductors such as  $\text{TiO}_2$  and  $\text{ZnO}_2$ <sup>118,119</sup>. Oxidation of phenol by singlet oxygen photosensitized by the Tris(2,2'-bipyridine)ruthenium(II) ion<sup>120</sup> has been reported.

#### 2.9.4 Catalytic reduction

The reaction of sodium nitrite with sodium dithionite was studied in the presence of cobalt(II)tetrasulfophthalocyanine,  $\text{CoII(TSPc)}^{4-}$ , in aqueous alkaline solution. The overall mechanism comprises the reduction of  $\text{CoII(TSPc)}^{4-}$  by dithionite, followed by the formation of an intermediate complex between  $\text{CoI(TSPc)}^{5-}$  and nitrite, which undergoes two parallel subsequent reactions with and without nitrite as a reagent. The final product of the reaction was found to be ammonia. Contrary to those found for the catalytic reduction of nitrite, the products of the catalytic reduction of nitrate were found to be dinitrogen and nitrous oxide. The striking differences in the reduction products of nitrite and nitrate are explained in terms of different structures of the intermediate complex between  $\text{CoI(TSPc)}^{5-}$  and substrate, in which nitrite and nitrate are suggested to coordinate via nitrogen and oxygen, respectively<sup>121</sup>.

#### 2.9.5 Catalytic Oxidation of benzyl to benzoine

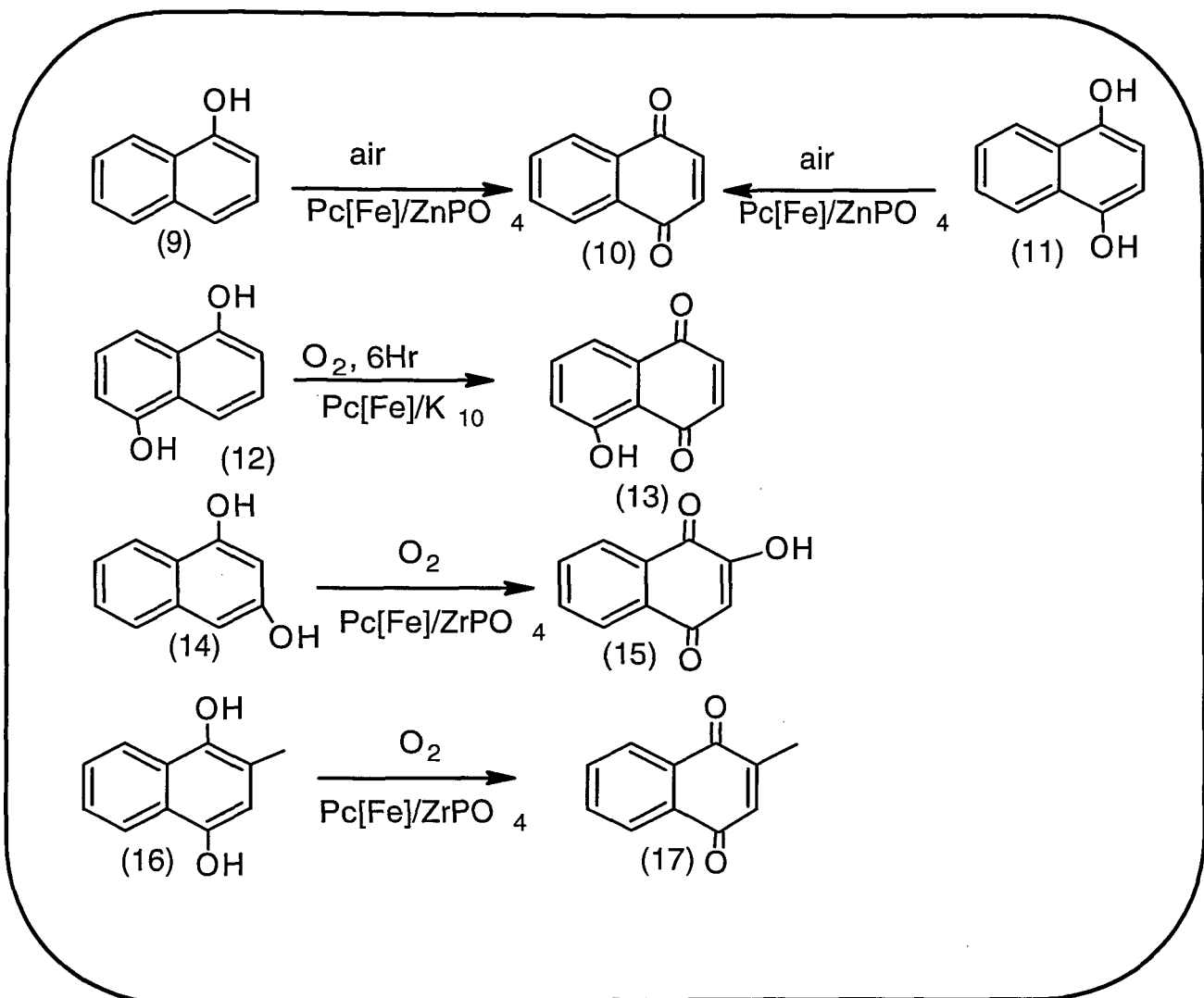
Oxidation of secondary alcohol to carbonyl compounds is an important synthetic transformation and many stoichiometric oxidants notably Chromium(VI)<sup>122</sup> and manganese reagents<sup>123,124</sup>, Bismuth nitrate<sup>125</sup>, Zirconium(IV) oxide<sup>126</sup>,  $\text{Pd(OAc)}_2$ <sup>127</sup>, producing copious amount of heavy metal wastes, have been used to accomplish the reaction. Molecular oxygen is an attractive oxidant and the development of synthetic methodology using molecular oxygen as a sole oxidant is a rewarding goal both from economic and environmental points of view. Porphyrines are used extensively for the oxidation of alcohol to its carbonyl compound<sup>128,129</sup>. Similar results are shown by Pcs. Secondary alcohols are converted to ketones under aerobic condition in xylene and powder KOH under reflux in presence of

Co(II)Pc as catalyst<sup>130</sup>.  $\alpha$ -Diketones are synthetically important building blocks and are extensively used as substrates for benzylic acid rearrangement and starting material for the synthesis of heterocyclic compounds.  $\alpha$ -hydroxyketone is oxidized to  $\alpha$ -Diketone in refluxing methanol, alkaline pH, O<sub>2</sub> at 1 atm in presence of CuPc(SO<sub>2</sub>NH<sub>2</sub>)<sub>4</sub> as catalyst<sup>131</sup>. Air oxidation of benzoin to benzyl using alumina in different organic solvent<sup>132</sup> has been reported. Plain CuCl is used as catalyst for the oxidation of secondary alcohol to ketone<sup>133</sup>.

Oxidation of benzoin to benzil in presence of cupric acetate along with ammonium nitrate<sup>134</sup> and Thallium(III)nitrate<sup>135</sup> is reported in literature. Benzil is an important compound used for the synthesis of 1,2,4-triazine<sup>136</sup> and Thiophen ring<sup>137</sup>.

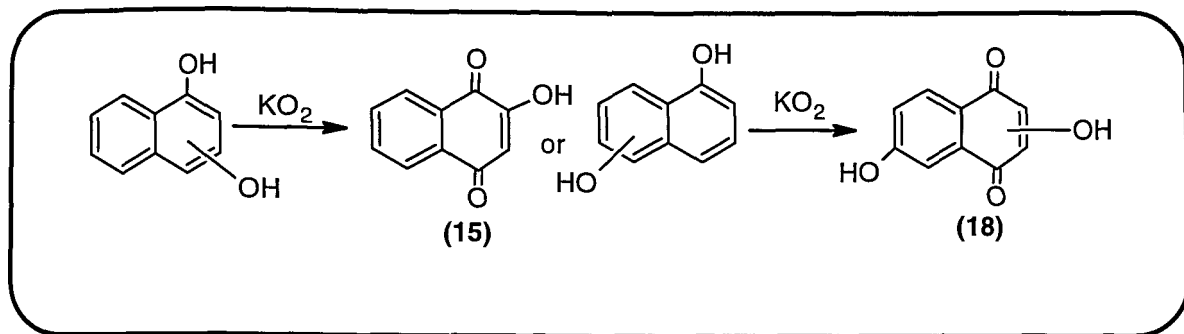
### 2.9.6 Catalytic Oxidation of 2-hydroxy Naphthol to 2-hydroxy-1,4-Naphthoquinone

The oxidation of phenols to quinones is a reaction of synthetic interest. The phenyl oxidation products are used for the synthesis of natural products such as vitamins and their intermediates. Concerning the oxidation of phenols or hydroquinones into quinones, numerous oxidants were described in literature such as chromic oxide<sup>138</sup>, silver oxide<sup>139</sup> and ceric ammonium nitrate<sup>140</sup>. However, only in few reactions, air or oxygen is used as oxidant. On economic and ecological grounds there is an increased need for the development of soft processes, without toxic salts and which do not necessitate high temperature or high pressure. Pc on supported K10 was reported to show good catalytic activity in the synthesis of plain and substituted hydroquinone to quinones<sup>141</sup>. As shown in scheme 2.5. (a) 1-naphthol(9) or 1,4-dihydroxynaphthalene(10) to naphthoquinone (11), (b) 1,5-dihydroxynaphthalene(12) to Juglone (13), 1,3-dihydroxynaphthalene (14) to 2-hydroxy-1,4- naphthoquinone (lawsone) (15) and 2-methyl-1,4-dihydroxynaphthalene (16) to Menadione (17) .



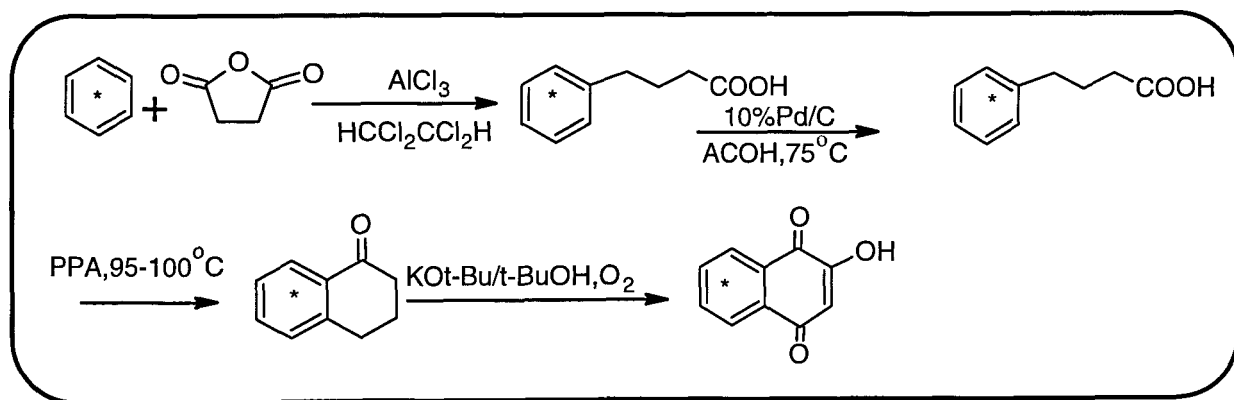
Scheme 2.5

Oxidation of Dihydronaphthalenes by potassium superoxide ( $\text{KO}_2$ ) in heterogeneous aprotic media yields mono (15) or dihydroxynaphthoquinones (18) depending on the relative position of the hydroxyl groups on the naphthalene moiety as shown in scheme 2.6<sup>142</sup>.



**Scheme 2.6**

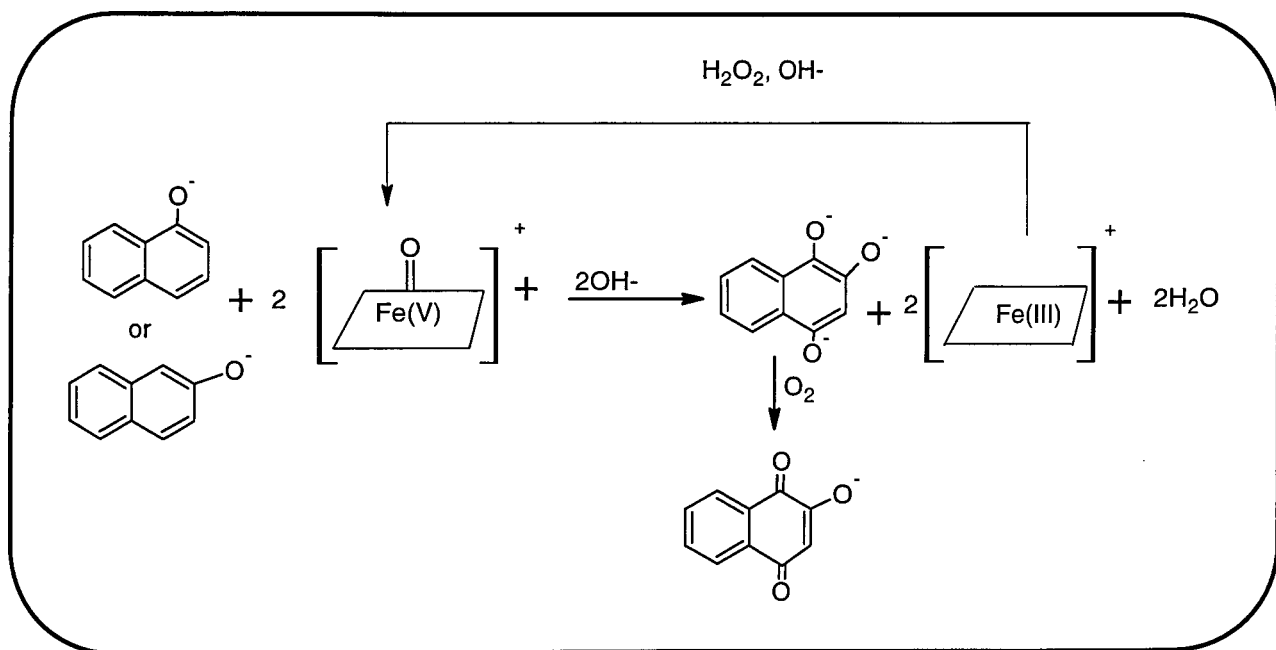
The leaves of *Lawsonia inermis* L. have been used in the Indian Subcontinent for decorating and dyeing skin and Hair. Lawsone or 2-hydroxy-1,4-Naphthoquinone was first isolated from the leaves of *Lawsonia inermis* L. in 1959. 2-hydroxy-1,4-Naphthoquinone and related compounds have been reported to possess interesting biological activities such as antitumor, antibacterial and antifungal properties<sup>143-145</sup>. It is also used as hair dye and as an ultraviolet (UV) filter in sunscreen formulation. 2-hydroxy-1,4-Naphthoquinone is mainly obtained from plants. Christopher and Giliyar synthesized<sup>14</sup>C-Labelled Lawsone starting from <sup>14</sup>C-Labelled benzene<sup>146</sup> as shown in scheme 2.7.



**Scheme 2.7**

The Catalytic conversion of 1-naphthol or 2-Naphthol to 2-Hydroxyl-1,4-Naphthquinone in the presence of  $\text{H}_2\text{O}_2$  over Iron porphyrin catalysts<sup>147</sup> as shown in scheme

2.8 and using molecular oxygen<sup>148</sup> is reported in literature. Elodie and group reported dye sensitized photooxygenations of 5-amido-1-naphthols in presence of light to 5-amido-1,4-Naphthoquinones<sup>149</sup>. Krystyna and Howard reported oxidation of 1or 2 tetralone to 2-Hydroxyl-1,4-Naphthquinone in the presence of phase transfer catalyst<sup>150</sup>. 1,3-dihydroxynaphthalene to lawsone in presence of [bis(trifluoroacetoxy)indo]benzene in acetonitrile-water<sup>151</sup>. Oxidative coupling of 1-Naphthols to 1,1-bi-2-naphthols catalyzed by solid Lewis acid using atmospheric oxygen as oxidant under reflux in Xylene<sup>152</sup> and by clay supported iron catalyst<sup>153</sup> has been reported. 2-methyl-1,4-Naphthoquinone(vitamin K3) is obtained by catalytic oxidation of 2-methyl-1-naphthalene in the presence of Iron supported catalyst<sup>154,155</sup>.



**Scheme 2.8**

2-Hydroxyl-1,4-Naphthquinone is used for the synthesis of naphthofurandiones<sup>156</sup>. Rane and group reported the coordination compound of Copper(II) with 2-Hydroxyl-1,4-Naphthquinone<sup>157</sup>.

## **2.10 Applications of Phthalocyanine**

### **2.10.1 High temperature Lubrication**

Refer to a temperature range of 427 °C to 704°C. Metal free Pc, a solid organic compound has been used successfully in this range to lubricate rolling and sliding contact bearing. However the best results are obtained by forming a film of metal Pc on the bearing before use<sup>158</sup>. Oligomeric and polymeric copper phthalocyanines are also studied as lubricants<sup>159</sup>. Phthalocyanine is doped with an electrically conductive dopant to bleed internal charge build up from the internals of turbines and large drive motors<sup>160,161</sup>.

### **2.10.2 Electro oxidation**

Electrooxidation of hydrazine catalyzed by single-walled carbon nanotube (SWCNT) functionalized with cobalt phthalocyanine (CoPc) shows that the presence of the single-walled carbon nanotubes enhances the catalytic activity of the CoPc itself, without any change in the reaction mechanism. A synergistic effect, in terms of reactivity when the new nanocomposite material was adsorbed on the GC electrode, was observed<sup>162</sup>.

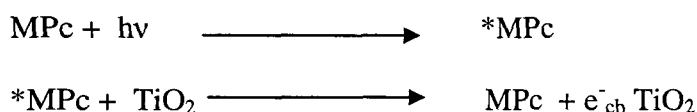
### **2.10.3 Oxidation of sulphur containing compound**

Alkyl mercaptans and other sulfur containing impurities present in petroleum are major environmental pollutants. They are also corrosive and poisoners of different catalysts during the processing and purification of petroleum. Catalytic oxidation of alkyl mercaptans to disulfide in presence of oxygen at room temperature is reported in literature<sup>163</sup>.



#### 2.10.4 Thin Film

TiO<sub>2</sub> thin films are of high practical value since the immobilization of titanium dioxide significantly reduces some of the drawbacks of practical application of heterogeneous photocatalysis in suspension, including the need to separate the powder or the tendency of titania particle to agglomerate in water. Thin films found application in fields as diverse as chemical (bio) sensing, optics, photolithography, catalysis and OLEDs in electronic devices. Similarly thin functional coatings are attractive to industry since a small amount of hybrid material imparts improved properties at low cost. MPc are potent TiO<sub>2</sub>- sensitizers enhancing the activity of titania in photocatalytic reactions under visible light by injecting electron in the conduction band of titania as shown in scheme 2.9<sup>164</sup>.



**Scheme 2.9**

Polyacrylamide polymer (PAA) coupled to CoPc electrode can be used for the determination of solubility product constant of sodium fluoride in acetonitrile<sup>165</sup>. CuPc is effective in oxidation of adrenaline, this property makes CuPc application in detection of adrenaline<sup>166</sup>. One of the challenges in electrochemical biosensor design is gaining a fundamental knowledge of the process underlying immobilization of the molecules on the electrode surface. This is of particular importance in biocomposite sensors where concern has arisen as to the nature of the interaction between the biological moiety such as glucose oxidase and synthetic molecules such as immobilized MPc<sup>167</sup>. CoPc modified electrodes are used efficiently for the electrocatalytic oxidation of hydrazine in industrial Boiler feed water<sup>168</sup>. MPc thin films have been well documented as sensitive materials for detection of

nitrogen dioxide (NO<sub>2</sub>) gas. The mechanism for detection is such that an MPc thin film acting as the electron donor possesses a strong chemical adsorption affinity towards NO<sub>2</sub> molecules acting as electron acceptors. The resulting charge-carrier complex formed significantly increases MPc thin-film conductivity. Sensors based on iron (II) phthalocyanine (FePc) thin films were fabricated by physical vapor deposition of FePc onto gold interdigitated electrodes patterned on an oxidized silicon substrate. These sensors could reliably differentiate NO<sub>2</sub> concentrations in the range of 0.5 to 2 ppm NO<sub>2</sub> under a nitrogen atmosphere, via passive monitoring of relative resistance change<sup>169-171</sup>. MnPc thick film is used as  $\gamma$ -radiation sensor<sup>172</sup> and in photoelectric cells<sup>173</sup>.

#### 2.10.5 PDT

Photodynamic therapy (PDT) is a promising new modality for the control and treatment of tumours. This technique is based on the use of a photosensitizing dye which, upon localization at the tumor site and light activation in the presence of oxygen produces cytotoxic species, including singlet oxygen, resulting in tumor necrosis. This capability to photoinactivate cancer cells in vitro as well as in vivo is well documented and particularly mono/ disulfonated, amphiphilic Pcs, chelated with diamagnetic metal ions have been shown to be capable of killing tumour cells directly. Monosulfonated Pcs are prepared using Meerwein reaction<sup>174</sup>.

Due to Pc's vast application in PDT, more focus was given in studying the Photophysical and photochemical properties of metal phthalocyanine<sup>175-177</sup>. Reactive oxygen species are produced by irradiation of some phthalocyanine derivatives<sup>178</sup>. The ability of selected Pc and metal Pc to block HIV infection has been evaluated in an epithelial Hela-CD4

cell line with an integrated LTR- $\beta$ -galactosidase gene. Sulfonated Pc itself as well as its Cu, Ni and Vanadyl chelates were the most effective in blocking viral infection<sup>179</sup>. Among some of the promising second-generation photosensitisers are phthalocyanines (Pc), which have a strong absorption band in the far-red region of the visible spectrum ( $\lambda_{\text{max}} = \text{ca.}680 \text{ nm}$ ) and can efficiently absorb light (Pc molar extinction coefficient ( $\epsilon$ ) = ca.  $10^5 \text{ M}^{-1} \text{ cm}^{-1}$ ). The efficacy of phthalocyanine derivatives as a photosensitiser can be significantly enhanced by attachment to the surface of gold nanoparticles. The surface-bound Zn(II) phthalocyanine derivative (C11Pc) exhibits a remarkable enhancement of the singlet oxygen quantum yield in the presence of an associated phase transfer reagent such as tetraoctylammonium bromide. This enhancement in singlet oxygen generation is possibly due to the phase transfer agent stabilizing an active monomeric form of the photosensitiser. Cellular experiments using the Hela cervical cancer cell line demonstrated that irradiation of the conjugates within the cells causes high cell mortality through the photodynamic effect. An extensive photodynamic effect using the C11Pc nanoparticle conjugates has been demonstrated recently in vivo where a significant decrease in the rate of growth of a subcutaneously implanted amelanotic melanoma tumour was observed. Similarly, experiments on 5RP7 rat fibroblasts cancer cells showed promising results in vivo by suppressing the tumour growth after treatment with zinc phthalocyanine-loaded single wall carbon nanohorns. Incorporation of cell-targeting peptides or antibodies onto the nanoparticle surface is highly desirable for therapeutic applications, as it would enable selective cell and/or nuclear targeting. Direct physisorption of fluorescently tagged antibodies to the surface of gold nanoparticles has been used for some time to produce 'immunogold'. However, such simple methods of nanoparticle functionalisation results in poor orientation of the recognition component (the F (ab)<sub>2</sub> region) of the antibody, non

specific binding of the nanoparticle conjugates and agglomeration of small gold nanoparticles. These drawbacks can be overcome by modification of the nanoparticle's surface with polyethylene glycol (PEG), which has been approved for human intravenous application and which stabilizes the nanoparticles by steric repulsion to inhibit colloidal aggregation in physiological conditions. The use of a heterobifunctional PEG with two different terminal moieties allows covalent attachment of an antibody to the outer end of the polyethylene glycol chain, thus maintaining availability of antibody binding sites to cell surface receptors. The complete 4-component system of photosensitizer-nanoparticle conjugates is shown in Fig 2.9<sup>180</sup>.

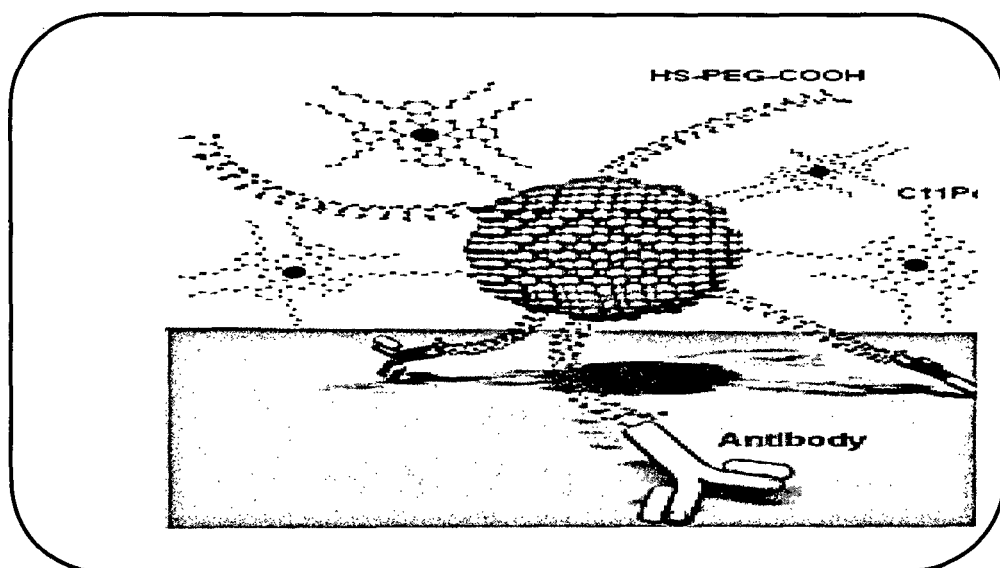


**Fig 2.9 Photosensitizer-nanoparticle conjugates.**

### **2.10.6 Photoluminescence**

CuPc belongs to a group of metal Pc, consisting of a central metallic atom bonded to ligands with extended  $\pi$  conjugated system. Among the various metal Pc, CuPc is most comprehensively studied. It has been used in a variety of optoelectronic and electronic

devices, both in the form of thin film and nano/microstructures. CuPc can be used as donor materials in organic photovoltaic cells. While in organic light emitting diodes it can serve as hole injection layer or emitting layer. Infrared photoluminescence studies are done on  $\alpha$  and  $\beta$  CuPc nanostructures<sup>181</sup>,  $\mu\text{m}$  near-Infrared electrophosphorescence from organic light emitting diode based on CuPc<sup>182</sup>. In recent years, a lot of effort has gone into the search of organic donor acceptor systems for providing an efficient light induced charge transfer in order to produce organic solar cells. Fullerenes as electron acceptors play a very important role in most of these concepts. Highly soluble pyrrolidinofullerene bearing three chelating pyridyl groups and ZnPc are used in organic solar cell<sup>183</sup>. Photoluminescence studies on Nitro substituted Europium (III) Pc<sup>184</sup>, Magnesium, Chloroaluminium, Bromoaluminium and metal free Pc solid films<sup>185</sup>, Upconversion Fluorescence from CuPc<sup>186</sup> and Upconversion Luminescence of highly soluble ZnPc epoxy derivative<sup>187</sup> and Fluorescence efficiency on solid Pc<sup>188</sup> is reported in literature. Because of this properties Pc is extensively used in optical recording devices<sup>189</sup>.

### 2.10.7 Antimicrobial activity

The phototoxicity of chemical compounds towards microorganisms was first published at the turn of the 20<sup>th</sup> century. Oskar Raab observed that the toxicity of acridine hydrochloride against *Paramecia caudatum* was dependent on the amount of light, which was incidental on the experimental mixture. In addition, HvTappeiner, reported that the toxic effects in the presence of light are not due to heat. After further experiments to exclude direct influence of light, Hv Tappeiner coined the term “photodynamic reaction” in 1904. Additional investigations demonstrated the involvement of oxygen in killing the bacteria because the anti-bacterial activity of fluorescent dyes against the facultative anaerobic species

*Proteus vulgaris* could not be demonstrated in the absence of oxygen. Photodynamic inactivation of microorganisms is based on the concept that a dye, known as a photosensitizer (PS), should be localized preferentially in the bacteria and not in the surrounding tissues or cells, and subsequently activated by low doses of visible light of an appropriate wavelength to generate free radicals or singlet oxygen that are toxic to target microorganisms. Since the middle of the last century, anti-microbial photodynamic therapy was forgotten because of the discovery of antibiotics. Certainly, in the last decades the total worldwide rise in antibiotic resistance has driven research to the development of new anti-microbial strategies<sup>190</sup>. The abnormal aggregation of protein monomers is commonly associated with the transmissible spongiform encephalopathies (TSEs) and over 20 other diseases, including type II diabetes and Alzheimer's, Parkinson's, and Huntington's diseases. The pathogenesis of TSEs involves the conversion of the normally protease-sensitive prion protein (PrP<sup>sen</sup> or PrP<sup>C</sup>) to a protease-resistant amyloidogenic oligomer/multimer, called PrP<sup>res</sup> or PrP<sup>S</sup>. The relative abilities of differently sulfonated and metal-bound phthalocyanines to inhibit PrP<sup>res</sup> accumulation were compared by using a murine neuroblastoma cell line and it was found that aluminum(III) phthalocyanine tetrasulfonate was both the poorest anti-TSE compound and the least prone to oligomerization in aqueous media<sup>191</sup>. Antimicrobial activity is shown by many substituted phthalocyanine<sup>192,193</sup>.

*Staphylococcus citreus* is pyogenic and involved in nosocomial infections<sup>194</sup>; *Serratia marcescens*<sup>195,196</sup>, *Proteus vulgaris* involved in emerging UTI infections<sup>197</sup>, and *Bacillus subtilis* often encountered as laboratory contaminant or in casual handling of food<sup>194,198</sup>. *Pseudomonas fluorescens* is known to be resistant for many frontline antibiotics<sup>199</sup>.

# CHAPTER 3

## *EXPERIMENTAL*

## 3.1 Synthesis of Phthalocyanine

### 3.1.1 Synthesis of non-substituted Phthalocyanines

Phthalocyanines were prepared using three different experimental techniques.

- Synthesis using reflux method
- By Melt method and
- By Microwave oven

#### a) Synthesis using reflux method

4 moles of phthalic anhydride, 1 moles of metal salt, ammonium molybdate and 4 moles of urea were suspended in Nitrobenzene and heated at 190 °C for 4 - 5 h. The product obtained was filtered, washed with nitrobenzene followed by methanol, further the crude product was boiled for 2 h first with 1 N HCl and then with 1 N NaOH between HCl and NaOH washing. Finally the water washing were given, to the product then with methanol and dried at 105 °C. The reaction is shown in scheme 3.1.

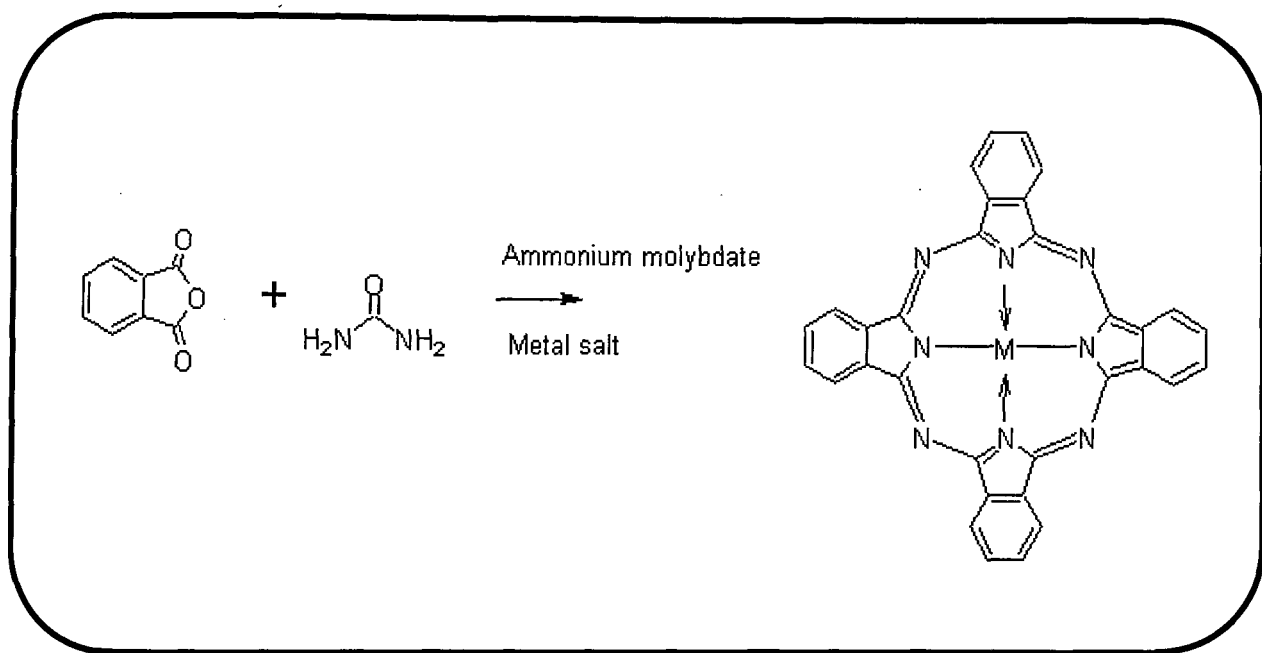
#### b) Melt Method

4 moles of phthalic anhydride, 1 moles of metal salt, ammonium molybdate and 15 moles of urea were mixed homogenously using motor and pestle, the resulting mixture was transferred in a beaker and heated at 260 °C on sand bath for 1h, further the crude product was boiled for 2 h first with 1 N HCl and then with 1 N NaOH between HCl and NaOH washing. Finally the water washing were given, to the product then with methanol and dried at 105 °C.



### c) Microwave method

Same quantities of the reactants were taken as that of melt method. Reactants were placed in microwave oven for 5 min and same procedure for purification was used as that of melt method.

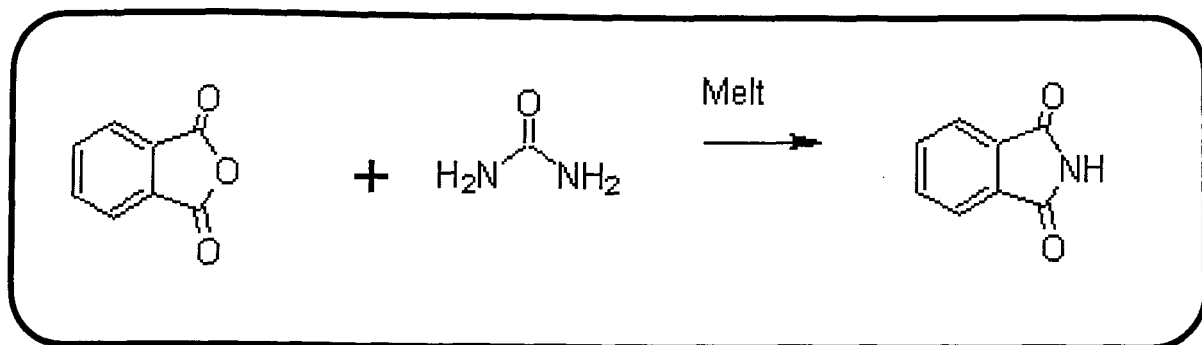


**Scheme 3.1**

### 3.1.2 Synthesis of substituted Phthalocyanines

#### a) Preparation of phthalimide

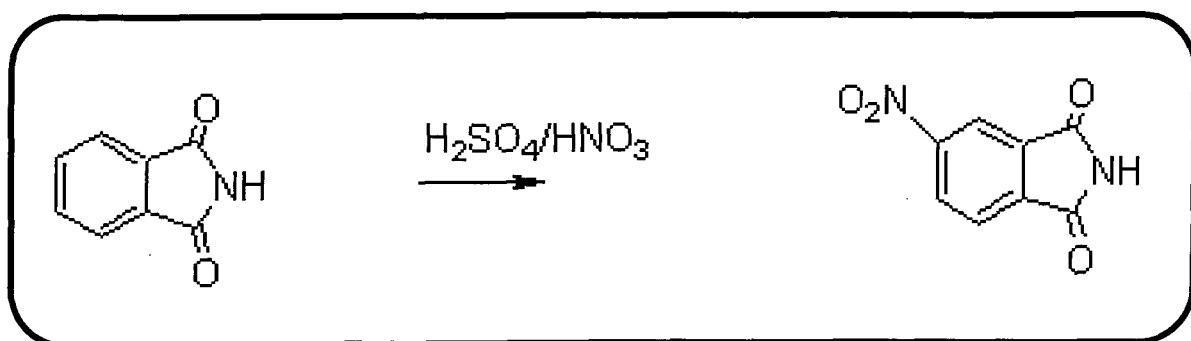
75 g of phthalic anhydride was mixed with 15 g of urea and heated on sand bath. Heating was carried out till the mixture melted and a clear liquid was formed. On further heating it slowly, a white shiny solid reformed. It was then allowed to cool and washed with water and filtered. The product obtained is phthalimide, which was dried at 100 °C<sup>200</sup>. The reaction is shown in scheme 3.2.



**Scheme 3.2**

### b) Preparation of 4-nitrophthalimide

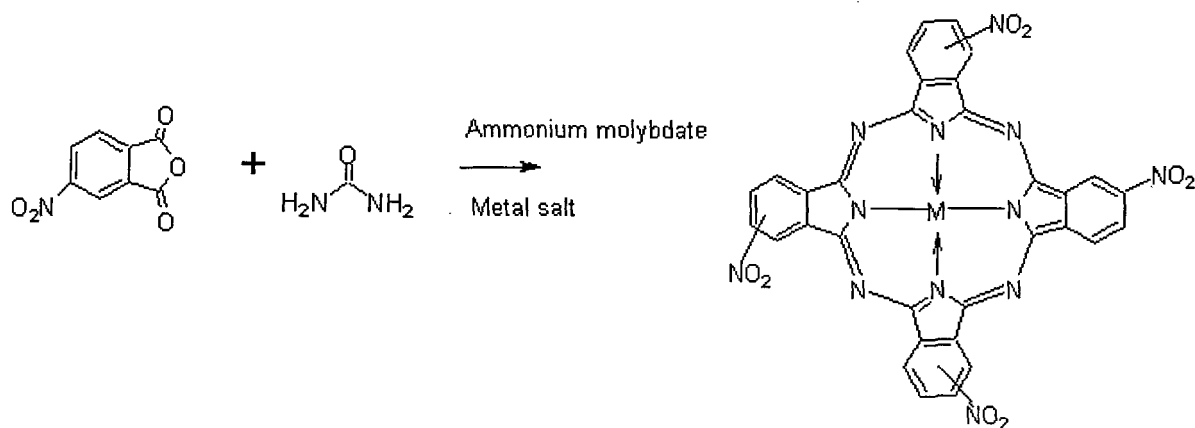
40 g of phthalimide was transferred slowly to 250 ml of nitrating mixture maintained at 0 °C containing concentrated sulphuric acid and nitric acid in a ratio of 3 : 1 at an interval of 15 min. The temperature was raised to about 35 °C so that all phthalimide dissolved and a pale yellow colored clear solution was obtained. This solution is transferred slowly with stirring to a 1000 ml beaker filled with ice cubes. Yellow colored product thus formed was then filtered using Buchner funnel. It was then washed thoroughly with distilled water till the filtrate was colourless. This could wash away the 3-nitro phthalimide formed in the reaction mixture and only 4-nitro phthalimide was retained on the filter paper and was dried at 80 °C<sup>201</sup>. The reaction is shown below in scheme 3.3.



**Scheme 3.3**

### c) Preparation of Tetranitro metal Phthalocyanine (TNMPc)

9.8 g of 4-nitro phthalimide, 15 g of urea, 0.15 g of ammonium molybdate and  $1 \text{ M}$  metal salt were mixed together. The same procedure was adopted as that of melt and microwave oven for the formation and also for the purification of product. The reaction is shown in scheme 3.4.

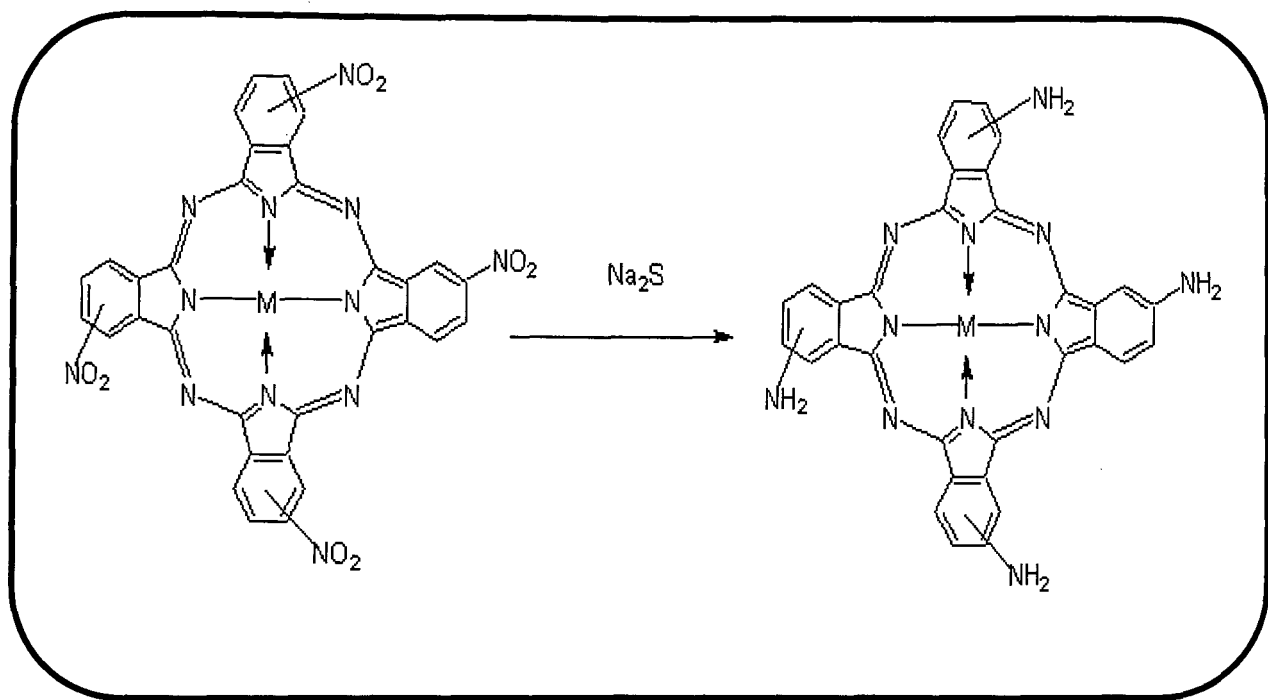


Scheme 3.4

### d) Preparation of Tetraamino Metal Phthalocyanine (TAMPc)

The 7 g of TNMPc was transferred to 500 ml beaker with about 100 ml water and kept on boiling on water bath for 20 min. Similarly 21 g of  $\text{Na}_2\text{S}$  was separately dissolved in 250 ml beaker and kept on boiling water bath for 20 min. After 20 min both the beakers were removed from the water bath and  $\text{Na}_2\text{S}$  solution was slowly transferred to 500 ml beaker containing MnTNPC solution when warm, the resulting mixture was allowed to stand at room temperature for 15 min. Further the solid residue obtained was washed with HCl (1 N) and

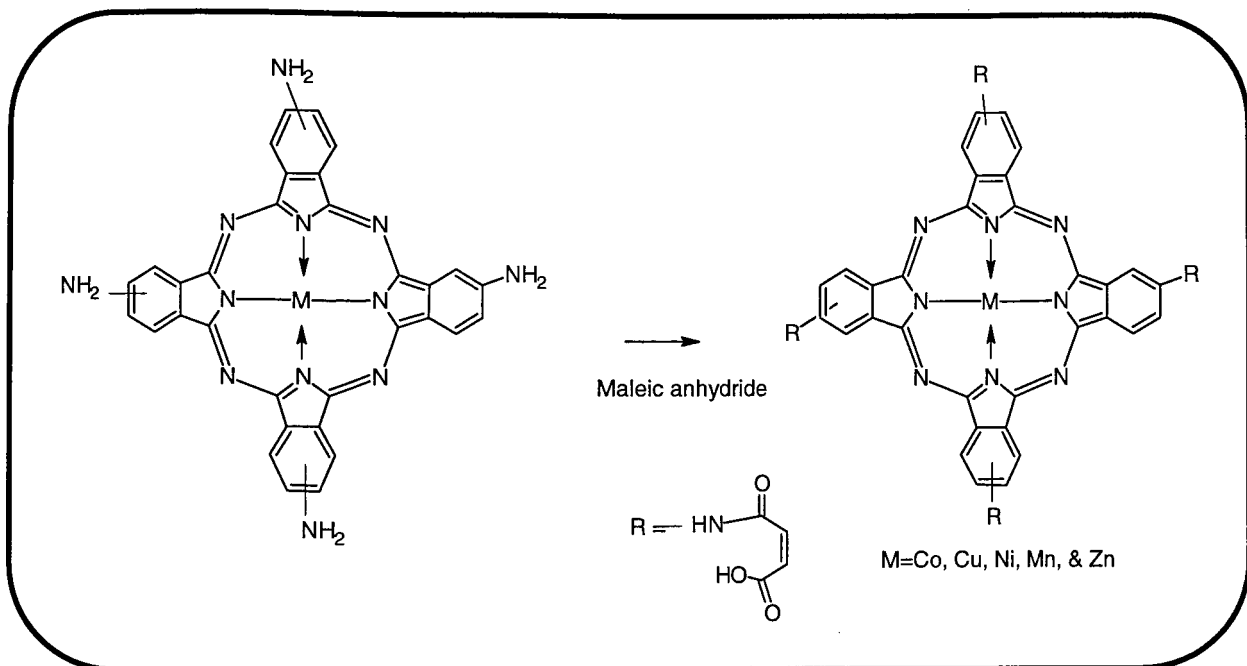
NaOH (1 N) respectively. After filtration the product was washed to neutralization with water and dried in vacuum. The reaction is shown in scheme 3.5.



**Scheme 3.5**

**e) Preparation of Tetra (n-carboxylacrylic) amine Metal Phthalocyanine(TAMPc)**

4 g (1 mol) of TAMPc was dissolved in 75 ml DMF, further to this 2.5 g (4 moles) of maleic anhydride was added and the reaction was kept at 50 °C for 3 h. Later the solution was poured into 1 L water, filtered and dissolved in 0.1 N NaOH, and precipitated with 0.1 N HCl. The precipitate obtained was washed with water till free from chloride ions, then further washed with Ethanol and diethyl ether and dried over vacuum. The scheme 3.4 shows the reaction.



**Scheme 3.6**

### 3.2 Characterization

The phthalocyanines prepared were characterized by Vibration spectroscopy, UV-Visible spectroscopy, X-ray diffraction technique, Elemental analysis and NMR. Other instrumental techniques were employed such as B.E.T. liquid nitrogen adsorption method, SEM, Magnetic susceptibility, thermal studies, ESR and Photoluminescence studies.

### **3.2.1 Infrared spectroscopy (IR spectroscopy)**

Infrared spectroscopy is a vibration spectroscopy and it depends on the excitation of vibrations in molecules, which occurs if a dipole moment changes during vibration. A non linear molecule containing N atoms has  $3N-5$  possible modes of vibration whereas linear molecule containing N atoms has  $3N-6$  possible modes of vibration. However not all vibrations modes causes absorption of IR, the basic condition is that a particular molecule will absorb in IR only if it causes the change in dipole moment of the molecule.

The energy required for the stretching vibration is more and the bands are seen in the region  $4000-1600\text{ cm}^{-1}$  whereas the energy required for bending vibration is less and bands appear in the region from  $1600-400\text{ cm}^{-1}$ . The IR was recorded on a Shimadzu FTIR instrument model IRPrestige-21, using KBr as a carrier. The spectra were recorded in diffuse reflectance mode.

### **3.2.2 UV-Visible spectroscopy**

The UV-visible spectroscopy were recorded for all the phthalocyanines, intermediate and the catalytic oxidation product obtain in oxidation in the range 200-800 nm on a UV-visible spectrophotometer (UV-2450) by dissolving in different solvents. The solution was scanned using glass cuvetes, each solution showed maximum absorption with respect to that of molecule as well as that of solution in which molecule is dissolved. A sharp Q-band is observed at around 700 nm and B bands are observed at around 350 nm.

### **3.2.3 X-ray powder diffraction technique**

The prepared samples are characterized by recording X-Ray powder diffractogram using Cu-K $\alpha$  radiation, filtered through Ni absorber at a scanning rate of 1°/min. The samples were identified by comparing the observed inter planar d-spacings and relative peak intensities, with those reported in literature (ICDD-PDF data files).

### **3.2.4 Elemental analysis**

The elemental analyses of water soluble phthalocyanine were recorded on Prostar Varian C, H, N analyzer (model Varian 500-MS).

### **3.2.5 UV-visible reflectance study**

Diffuse reflectance spectroscopy (DRS) is a technique based on the reflection of light in the ultra violet, visible and near infra red region by powdered sample. In a DRS spectrum, the ratio of the light scattered from an infinitely thick closely packed catalyst layer and the scattered light from an infinitely thick layer of an ideal non – absorbing reference sample, is collected in an integration sphere and detected. The samples showed absorption in visible region i.e. between 500–600 nm which can be attributed to the d-d transition occurring in the compounds due to which the prepared metallophthalocyanines showed characteristic colour. The UV-VIS-DRS spectra were recorded on UV-visible spectrophotometer model with BaSO<sub>4</sub> as a reference material. The samples were taken in a form of a 2 mm thick self supported pellets to measure the reflectance. Samples were scanned from 200 to 800 nm. Band gap energy was calculated at absorption edge shown by each sample in the spectra.

### 3.2.6 B.E.T. method (surface area measurement)

Surface areas of the prepared samples under study were measured using BET nitrogen adsorption method on SMARTSORB 91. Specific surface area of the catalyst was calculated with the help of well-known Brunauer, Emmet and Teller (BET) expression.

$$P/V(P_0-P) = 1/V_m C + (C-1)/V_m C \times P/P_0 \dots\dots\dots(1)$$

Where P is the equilibrium pressure P<sub>0</sub> is the saturated vapour pressure of the gas at the temperature of the adsorption. V is the volume of the adsorbed gas at S.T.P, C is the constant related to the heat of adsorption and V<sub>m</sub> is the volume of the gas at S.T.P required to form the monolayer. Various quantities from the above equation like P, P<sub>0</sub> and V could be determined experimentally. V<sub>m</sub> and C can be obtained by plotting P/V(P<sub>0</sub>-P) versus P/P<sub>0</sub>. Plot should give a straight line with slope (S) = C-1/V<sub>m</sub>C and Intercept (I) = 1/V<sub>m</sub>C which proves the validity of equation (1).

It can be shown from equation (1) that V<sub>m</sub> = 1/S+I and C = S/I+1. Since V<sub>m</sub> is the volume of gas at 0 °C and 1 atmospheric pressure necessary to cover the surface with one layer of the gas, it is easy to convert it to the no of molecules involved. Assuming 16.2 °Å as the value of the cross sectional area of single nitrogen molecule at liquid nitrogen temperature Brunauer, Emmet and Teller have shown that,

$$\text{Surface area} = 4.38 V_m (\text{C.C.,S.T.P.})\text{m}^2/\text{g}\text{-----}(2)$$

### 3.2.7 Magnetic Susceptibility Measurements

The magnetic susceptibility 'χ<sub>g</sub>' in air of the samples was determined by Gouy's method at room temperature. A field of the order of 8,000 Gauss was employed. A sensitive analytical balance of DHONA was used to measure the difference in weights. Mercury tetra



thiocyanatocobaltate  $\{\text{Hg}[\text{Co}(\text{SCN})_4]\}$  was used as standard material. The sample tube was washed, dried and filled with the standard material up to a certain mark and Hanged between the electromagnets of the Gouy balance.

The weight was recorded before and after applying the appropriate magnetic field. The procedure was repeated for the sample whose  $\chi_g$  is to be determined. The magnetic susceptibility of the sample was calculated by using the following calculations.

In the first part, tube constant or  $\beta$ - constant is calculated, as  $\chi_g$  value of the standard material is known. Using the relation,

$$\beta\text{- constant} = \chi_g \times W / \Delta W (\chi_g = 16.44 \times 10^{-6} \text{ cgs units for } \{\text{Hg}[\text{Co}(\text{SCN})_4]\})$$

$W = (W_3 - W_1)$  = wt of the standard material taken.

$\Delta W = \Delta W' + \Delta W''$  (+ve for paramagnetic and -ve for diamagnetic)

$\Delta W' = (W_4 - W_3)$  and  $\Delta W'' = (W_1 - W_2)$  where

$W_1$  = weight of empty tube

$W_2$  = weight of empty tube with field

$W_3$  = weight of tube with standard material and

$W_4$  = weight of tube and standard material with field

Hence  $\beta$ - constant was calculated. In the second part, to calculate  $\chi_g$  of the sample, substitute

$\beta$ - constant in the above relation, gives the magnetic susceptibility. Further this data is utilized

to calculate unpaired electrons present in the sample as follows.

$\chi_m = \chi_g \times \text{molecular weight of the sample}$

Where  $\chi_m$  = molar susceptibility and

$\chi_g$  = gram susceptibility

The magnetic moment  $\mu$  effective ( $\mu_{\text{eff}}$ ) of the sample was calculated by using the equation given below.

$$\mu_{\text{eff}} = 2.84\sqrt{\chi_m \times T} \text{ B.M where } T = \text{absolute temperature}$$

$\mu_{\text{eff}}$  is the magnetic moment

### 3.2.8 Thermal studies

The thermal technique of Thermogravimetric analysis (TG) and Differential scanning calorimetry (DSC) was carried out using NETZSCH Geratebau GmbH Thermal Analyzer. TG was used to study the heat effects, associated with the physical and chemical changes of the substances in the temperature range from room temperature to 800°C. Thermal effects, exothermic or endothermic preceding physical and chemical changes were studied by differential method, in which the sample temperature was continuously compared against the temperature of thermally inert reference material. TG was recorded to study the behaviour of weight loss of the precursor sample.

The samples, in a powder weighing between 5 to 10 mg were placed in alumina crucible covered with lid. Sample was continuously weighed as it is heated at a constant linear rate of 10 °C/min.

### 3.2.9 Electron spin resonance spectroscopy (ESR)

In case of paramagnetic phthalocyanine, one or more unpaired electrons may reside either on phthalocyanine ring or in the central metal system or in both. The basic features of ESR spectra are strongly dependent on the number as well as the location of the unpaired electrons in a system. The ESR spectra of  $\text{CuPcNH}_2$ ,  $\text{MnPcNH}_2$ ,  $\text{FePcNH}_2$  and  $\text{NiPcNH}_2$  were

recorded at room temperature. Further, ESR signals were used to calculate g-factor or Lande's splitting factor, number of unpaired electrons and line width. The results were recorded on Varian E-112 X-band ESR spectroscopy.

### **3.2.10 Proton magnetic resonance spectroscopy**

The starting material 4-nitrophthalimide used for the synthesis of TNMPc was first hydrolyzed in presence of NaOH to 2-amido, 4-nitro-benzoic acid was recorded in DMSO. The chemical shifts were recorded with respect to tetra methyl silane as a reference material. The NMR model used was Bruker 400 MHz spectrometer.

### **3.3 Photoluminescence studies**

Luminescence spectroscopy is a powerful tool for the characterization of semiconductors, especially those applicable for optoelectronic devices. It is a nondestructive technique that can yield information on fundamental properties of semiconductors. It is also sensitive to impurities and defects that affect materials quality and device performance. Luminescence is the word for light emission after some energy was deposited in the material. There are several ways to excite the sample to cause luminescence. The most common method is Photoluminescence, which describes light emission stimulated by exposing the material to light - by necessity with a higher energy than the energy of the luminescence light. Photoluminescence is also called fluorescence if the emission is less than about 1  $\mu$ s after the excitation and phosphorescence it takes long times- up to hours and days - for the emission. One possible way is to excite the sample by applying an external current, called as electroluminescence. Electroluminescence is particularly important in the production of

optoelectronic devices such as Light Emitting Diodes (LED), and Light Amplification By Stimulated Emission of Radiations (LASERS). Other ways are Cathodo-luminescence, describes excitation by energy-rich electrons, chemo-luminescence provides the necessary energy by chemical reactions and thermo-luminescence describes production of radiation from sample by heating.

### 3.3.1. Photoluminescence

Photoluminescence (PL) is a non-destructive optical technique used for the characterization, investigation, and detection of point defects or for measuring the band-gaps of materials. Photoluminescence involves the irradiation of the crystal to be characterized with photons of energy greater than the band-gap energy of that material. In the case of a crystal scintillator, the incident photons will create electron hole pairs. When these electrons and holes recombine, this recombination energy will transform partly into non-radiative emission and partly into radiative emission. Photoluminescence consists of impinging relatively high frequency ( $h\nu > E_g$ ) light onto a material, exciting atomic electrons. Subsequent relaxation may result in the production of photons that are characteristic of the crystal or defect site that emits the light. The luminescent signals detected could result from the band to band recombination, intrinsic crystalline defects (growth defects), dopant impurities (introduced during growth or ion implantation), or other extrinsic defect levels (as a result of radiation or thermal effects). When bombarded with photons of energy greater than the band gap of the material, an impurity energy level may emit characteristic photons via several different types of radiative recombination events, allowing the resultant PL spectra to be used to determine the specific type of semiconductor defect. This interaction provides a

highly sensitive, qualitative measurement of native and extrinsic impurity levels found within the material band gap. We can briefly say photoluminescence process includes three main phases as shown in Figure 3.1. 1) Excitation: Electrons can absorb energy from external sources, such as lasers, arc-discharge lamps, and tungsten-halogen bulbs, and be promoted to higher energy levels. In this process electron-hole pairs are created. 2) Thermalization: Excited pairs relax towards quasi-thermal equilibrium distributions. 3) Recombination: The energy can subsequently be released, in the form of a lower energy photon, when the electron falls back to the original ground state. This process can occur radiatively or non-radiatively. When a semiconductor absorbs a photon of energy greater than the bandgap, an electron is excited from the valence band into the conduction band leaving behind a hole. When the electron returns to its original state, it may do so through radiative (release of a photon) or non-radiative (no photon production) recombination.

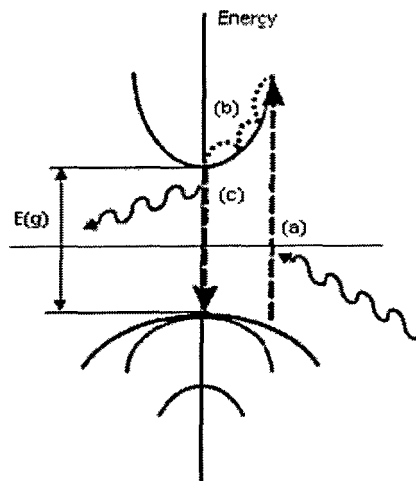


**Figure 3.1. Photoluminescence schematic. (a) An electron absorbs a photon and is promoted from the valence band to the conduction band. (b) The electrons cool down to the bottom of the conduction band. (c) The electron recombines with the hole resulting in the emission of light with energy  $h\nu$ .**

When the electron and hole recombine through radiative recombination, a photon is emitted and the energy of the emitted photon is dependent on the change in energy state of the electron-crystal system. Indirect band gap semiconductor, photon emission requires the aid of a phonon (energy in the form of lattice vibrations) to conserve momentum within the lattice structure. With the introduction of impurities in semiconductor material discrete energy levels are formed within the semiconductor's forbidden energy gap. Shallow donor levels are defined as levels just below the conduction band, whereas, shallow acceptor levels are defined as levels just above the valence band. These donor or acceptor level traps can act as recombination centers for transitions within the band gap. By studying the nature of these trap levels, information about the impurity or defect can be resolved. Figure 3.2 represents the energy band diagram of a semiconductor, illustrating the most common radiative and non-radiative transitions. (The conduction band ( $E_C$ ), occupied by free electrons, and the valence band ( $E_V$ ), occupied by free holes, are represented in addition to donor ( $E_D$ ) and acceptor ( $E_A$ ) trapping centers within the forbidden gap) These transitions are band-to-band transition, free-to-bound transition, donor –acceptor pair transition, excitonic transition, auger transition.

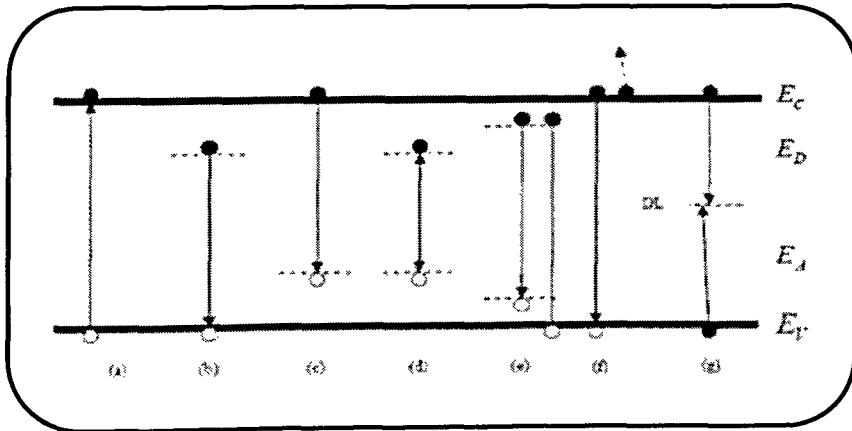


**Figure 3.2. Most common radiative transition observable with photoluminescence and non-radiative transitions.**

### 3.3.2 Upconversion luminescence

An Upconversion process is the one where emission is found to exceed excitation energies by approx 10-100 times. This Upconversion phenomenon is violating Stokes law in its basic statement. This exists in Lanthanide doped compounds, where the coupling between lanthanide f ions and transition-metal d ions, this embedded system later deviate the normal luminescence principle, producing upconversion emissions of the anti-Stokes types under moderate to strong excitation density. Though some aspects of its theoretical behavior are rather analogous with upconversion by energy transfers, its efficiency is usually much weaker. This is because it involves quasi-virtual pair levels between which transitions have to be described in a higher order of perturbation due to their double-operator nature.

### 3.3.3. Set up of Photoluminescence

The basic equipment setup needed to perform conventional photoluminescence consists of three main parts: (1) a light source to provide above or below band gap excitation; (2) a dewar to maintain the samples at low temperatures while allowing optical access to the sample surface; and (3) a detection system to collect and analyze the photons which are emitted from the sample. A diagram describing the experimental PL set-up is presented in Figure 3.3.

In the present study the photoluminescence studies were carried out on Shimadzu RF-5301PC spectrofluorophotometer, with a Xenon flash lamp. The sample loaded on a powder holder provided by Shimadzu (the powder samples were densely packed on this holder) was mounted at about 45° to the excitation source for PL measurement. All samples were analyzed with the same slit to measure the excitation and emission spectra with wavelength

resolution of 1 nm. The upconversion luminescence was obtained by irradiating samples at 625 nm and recording the emission from 400 to 575 nm.

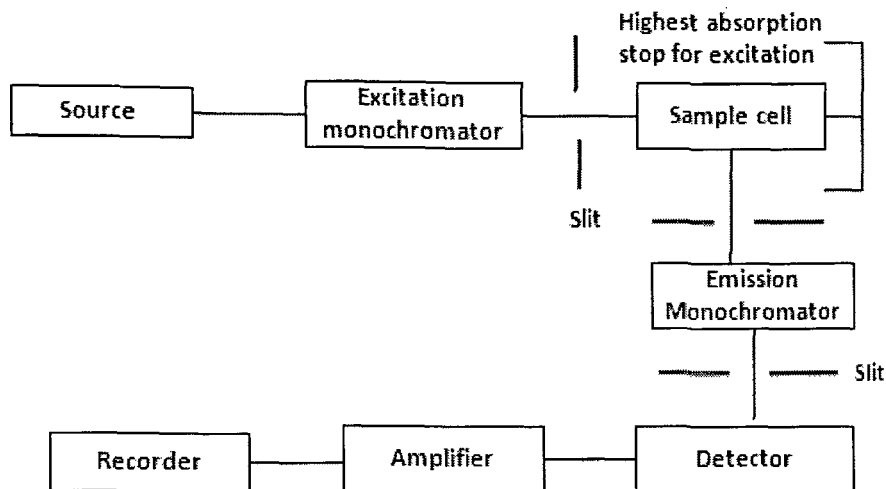


**Figure 3.3. Block diagram of a spectrofluorimeter.**

### 3.4 Scanning Electron Microscopy

Scanning electron microscopy is a straightforward technique to study overall topography of a material. SEM scans over a sample surface with probe of electrons (5-50 kV) and detect the yield of either secondary or back-scattered electrons as a function of the position of the primary beam. Parts of the surface facing the detector appear brighter than parts of the surface with their surface normal pointing away from the detector. Magnification of 20000 – 30000 times is possible with a resolution of about 150 nm. A gold coating was deposited on the sample to avoid charging of the surface. Particle shape, size and distributions are easily obtained for particles larger than 150 nm. The crystallite size and morphology of



the compounds of the present study were examined using a JEOL model 5800LV scanning electron microscope

### 3.5 Photocatalytic Studies

Photocatalytic degradation of Amido Black 10B was studied which has a  $\lambda_{\max}$  617-619 nm using MnPc, CoPc, NiPc, CuPc and ZnPc. This study was carried out at different pH i.e. neutral (pH=7), alkaline (pH=8) and acidic (pH=6).

Photocatalytic degradation of Auramine was studied which has a  $\lambda_{\max}$  430-432 nm using MnPc, CoPc, NiPc, CuPc and ZnPc. This study was carried out at neutral (pH=7).

Photocatalytic degradation of methylene blue was studied which has a  $\lambda_{\max}$  664-666 nm was studied using MnTAPc, CoTAPc, NiTAPc, CuTAPc, ZnTAPc, MnTNPc, CoTNPc, NiTNPc, CuTNPc and ZnTNPc. This study was carried out at neutral (pH=7).

The photocatalytic degradation reaction was carried out in a 150 ml glass reaction with a stopper to prevent loss of solution by evaporation. The reaction is kept in sunlight for the degradation process. Periodic rate of degradation was monitored using UV-visible spectrophotometer.

### 3.6 Catalytic Oxidation

Water soluble phthalocyanines were used for the oxidation of benzoin to benzyl.

Catalytic oxidation of beta naphthol to 2-hydroxy 1,4 naphthaquinone (Lawson) a naturally occurring compound using different substituted and non-substituted phthalocyanine was studied. Out of which only Cu unsubstituted and Cu tetranitrophthalocyanine could show the catalytic conversion.

In both the cases reaction mixture was taken in a 150 ml conical flask with a magnetic needle to carry out uniform mixing. To control the temperature water bath was used. The reaction vessel was covered with Aluminium foil.

### 3.7 Antimicrobial Activity

TCNiPc, TCCuPc and TCZnPc were individually dissolved in alkaline buffer to obtain a corresponding solution, having a final concentration of 100 µg/ml and 2mg/ml, respectively. Antibacterial activity of these phthalocyanines was tested against five emerging opportunistic bacterial pathogens. Twenty four hour old seed cultures of *Staphylococcus citreus*, *Serratia marcescens*, *Bacillus subtilis*, *Proteus vulgaris* and *Pseudomonas fluorescense* pregrown in nutrient broth, were plated on to separate nutrient agar, for matt growth. Subsequently, wells were bored into the agar, with a sterile 10 mm diameter cork borer, aseptically for agar well diffusion assay<sup>202</sup>. Different concentration of individual phthalocyanines in the range of 0.2 µg to a maximum of 1 mg was added into separate wells. All plates were incubated at appropriate temperature and monitored for growth, zones of inhibition of growth and exhibition around the well, if any, periodically.

Further the antimicrobial activity of MPcs (M= Al, Co, Cu, Fe, Mn, Ni and Zn) was studied by dissolving them individually in Dimethyl sulphoxide (DMSO) to obtain a corresponding solution, having a final concentration of 4 µg/ml, respectively. Antibacterial activity of these Pcs was tested against four emerging opportunistic bacterial pathogens. Twenty four hour old seed cultures of *Staphylococcus aureus* (ATCC 6538P), *Escherichia coli* (ATCC 8739), *Salmonella typhi* (ATCC 14028) and *Pseudomonas aeruginosa* (ATTC 9027) pregrown in nutrient broth, were plated on to separate mueller-hinton agar, for matt growth. Subsequently, wells were bored into the agar, with a sterile 10 mm diameter cork

borer, aseptically for agar well diffusion assay<sup>202</sup>. 100  $\mu$ l of individual phthalocyanines with a concentration of 4  $\mu$ g was added into separate wells. All plates were incubated at appropriate temperature and monitored for growth, zones of inhibition of growth and exhibition around the well, if any, periodically.

# CHAPTER 4

## *CHARACTERIZATION AND SPECTROSCOPIC STUDIES*

## Introduction

Various techniques such as FT-IR, UV-Visible, XRD, Elemental analysis, TG-DSC were used for the characterization of substituted, non substituted phthalocyanine and the intermediates used for the synthesis of MPcs.

### 4.1 FTIR Spectroscopy

FTIR technique is most commonly used for the characterization of Organic as well as metal organic compounds. The FTIR spectra for non substituted Pcs are shown in Figs.4.1-4.5. The following peaks such as 1121-1123  $\text{cm}^{-1}$ , 1090-1095  $\text{cm}^{-1}$ , 1067-1070  $\text{cm}^{-1}$ , 947-949  $\text{cm}^{-1}$ , 872-885  $\text{cm}^{-1}$ , and 754  $\text{cm}^{-1}$  are assigned to the phthalocyanine skeletal vibration. The peak observed at 1286-1290  $\text{cm}^{-1}$  is due to C-N stretching, 900-905  $\text{cm}^{-1}$  is due to C-N bending and 1332-1335  $\text{cm}^{-1}$ , 1419-1425  $\text{cm}^{-1}$  is due to aromatic phenyl rings. In addition to this, the peak observed at 1610-1616  $\text{cm}^{-1}$  is due to C=C, C=N and ring stretching, also peak at 770-730  $\text{cm}^{-1}$  and 1165  $\text{cm}^{-1}$  are due to C-H out of plane bending and C-H in plane bending vibration were observed.

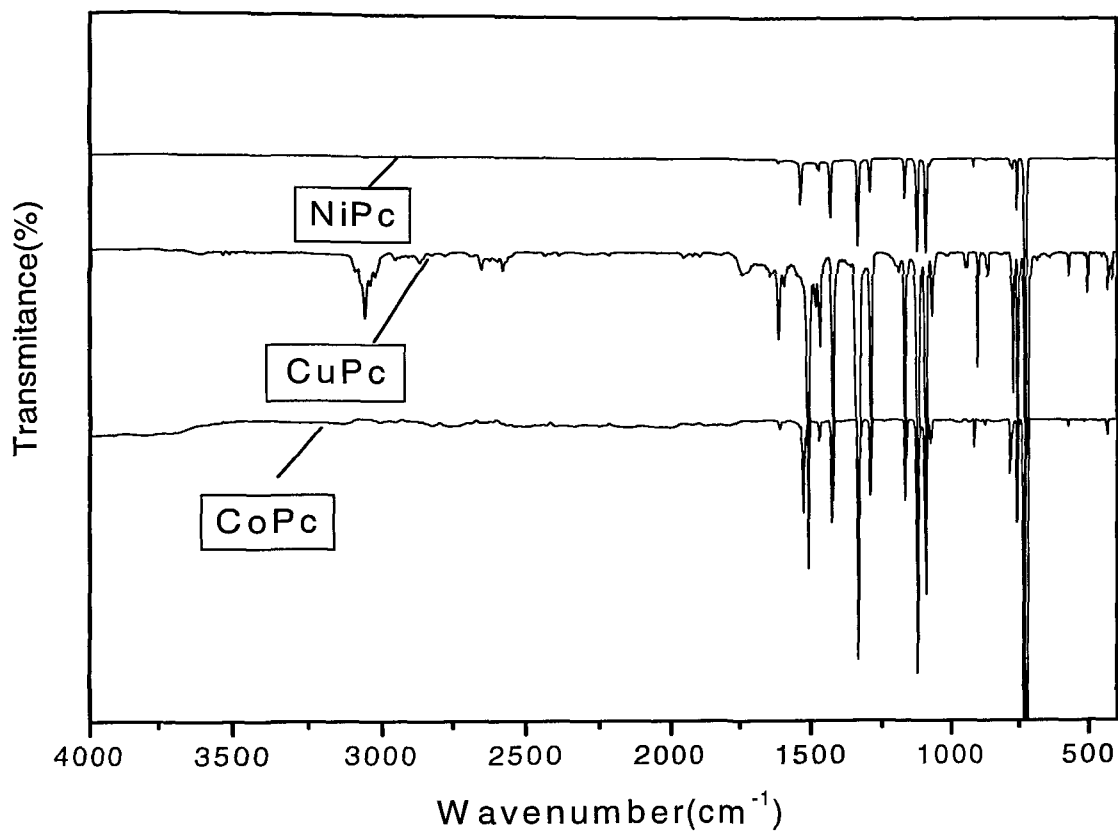


**Fig 4.1 IR spectra of NiPc, CoPc and CuPc**

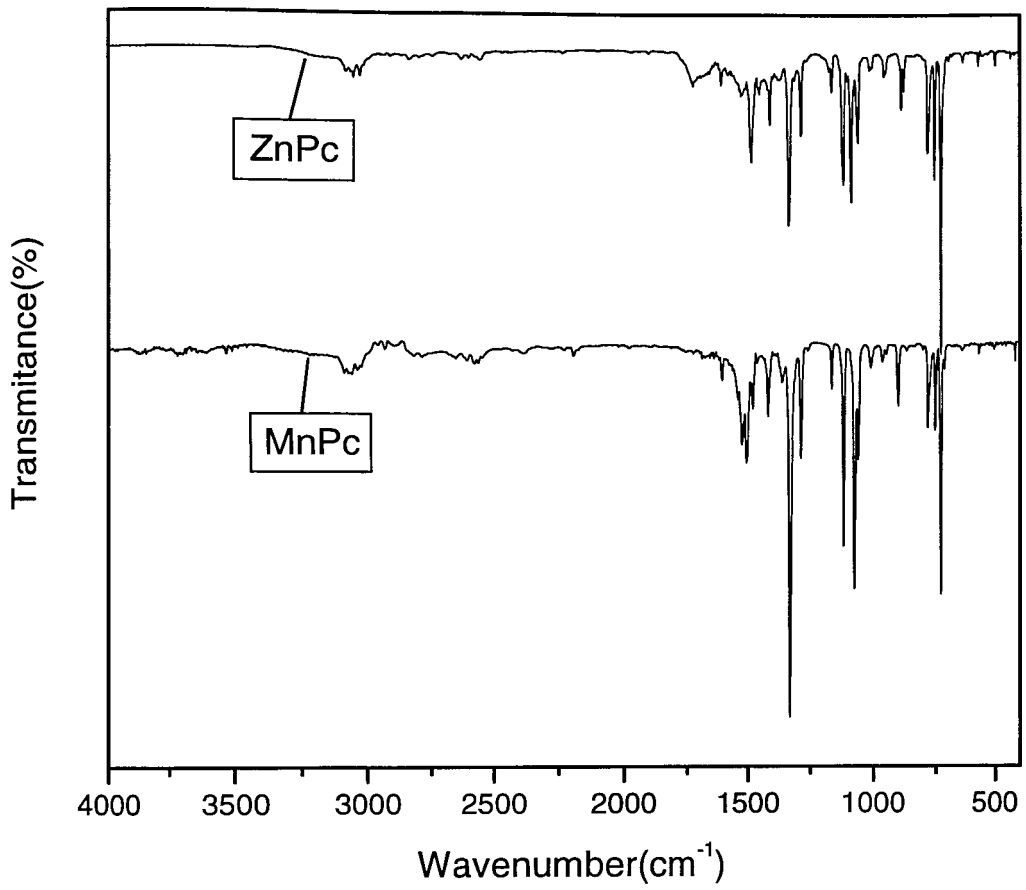


**Fig 4.2 IR spectra of ZnPc, and MnPc**

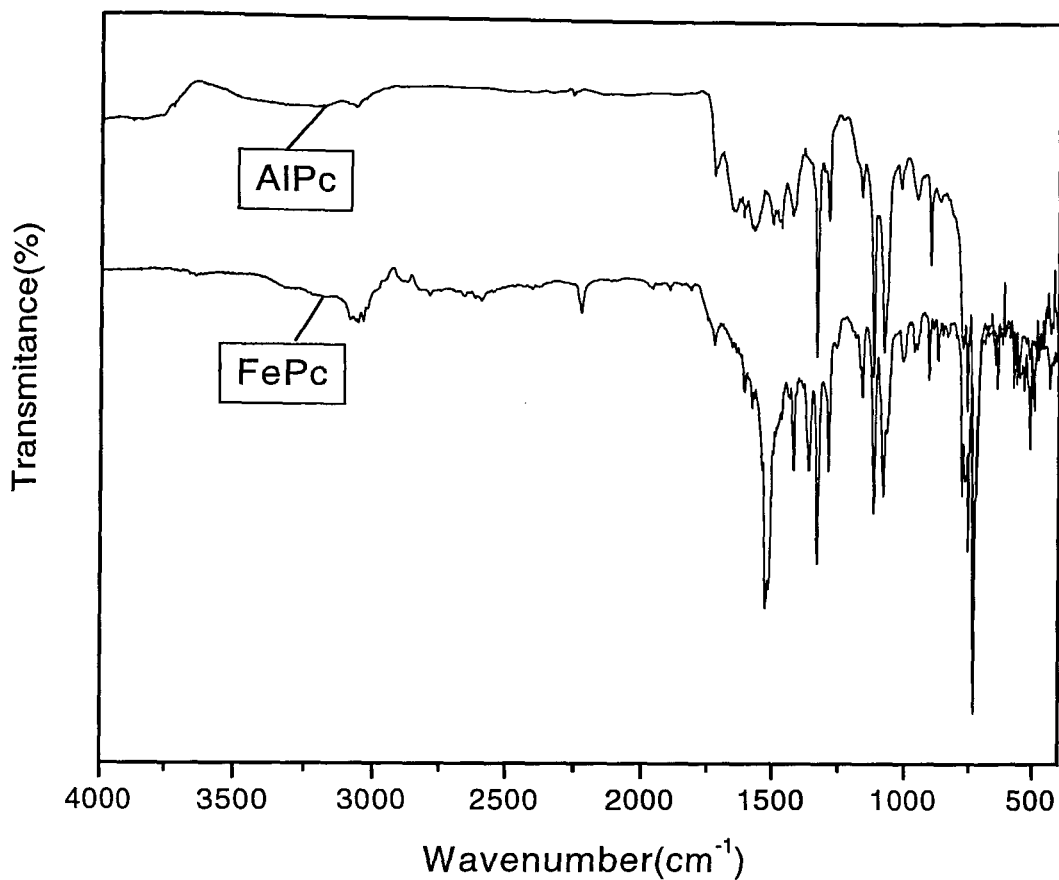


**Fig 4.3 IR spectra of AlPc and FePc**

IR spectroscopy is used effectively for the characterization of precursors employed for the synthesis of substituted phthalocyanine as shown in Fig. 4.4. Phthalimide prepared from phthalic anhydride and urea showed characteristic peak at  $3200\text{ cm}^{-1}$  which is due to N-H stretching, which moves to higher wave number on substitution of nitro group and can be seen at  $3333\text{ cm}^{-1}$  in case of 4-nitrophthalimide. The most prominent peak at  $1547\text{ cm}^{-1}$  due to N=O stretching is also seen which strengthens the observation.



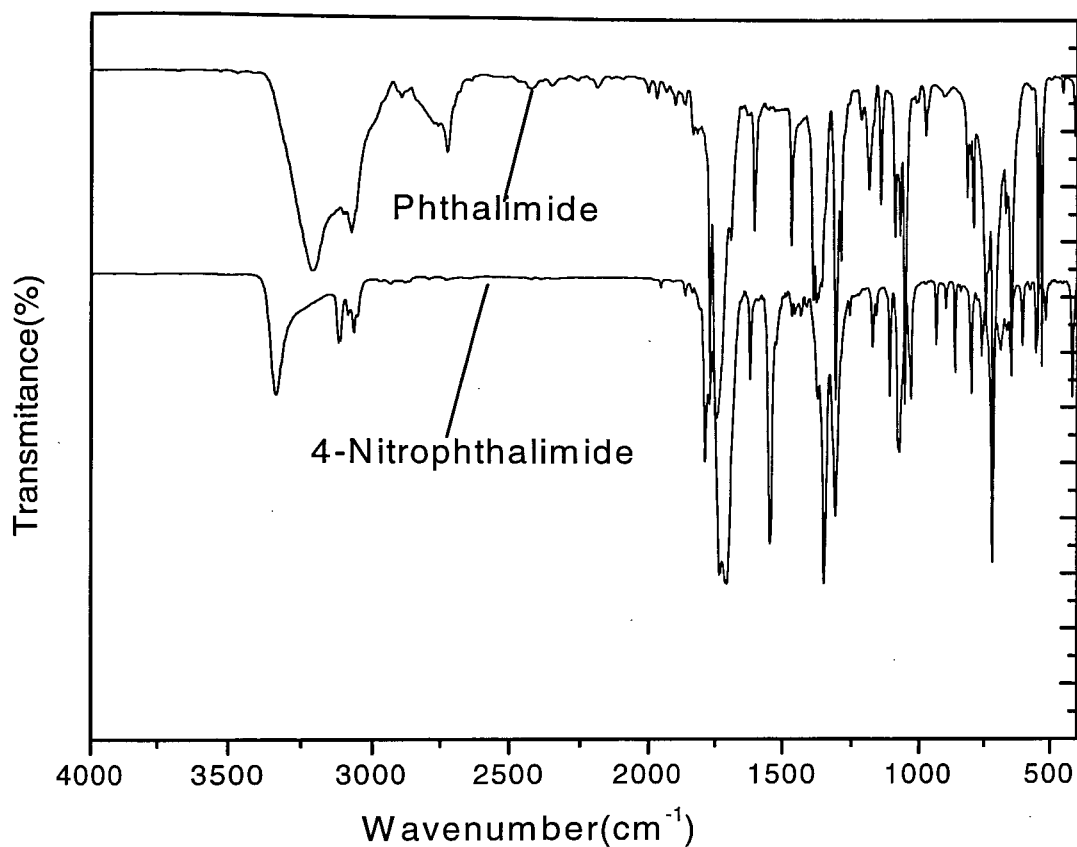


**Fig 4.4 IR spectra of Phthalimide and Nitrophthalimide**

Substituted Pcs were effectively characterized using FT-IR spectroscopy. The characteristic IR spectra for Nitro substituted, amino substituted and acrylic acid substituted Pc with respect to their individual metal are shown in each figure from 4.5 to 4.10. In case of nitro substituted Pc, apart from all the peaks which appear in the case of non substituted Pc, a characteristic peak due to nitro group is observed at around  $1519\text{ cm}^{-1}$ . On reduction of nitro group for the synthesis of amino substituted Pcs, Characteristic peaks of primary amine is

observed at around  $3353\text{ cm}^{-1}$  and  $3212\text{ cm}^{-1}$  with disappearance of peak due to nitro group. Further on acrylic acid substitution, characteristic peak of primary amine disappears with appearance of a new peaks due to  $\text{C}=\text{O}$  stretching at  $1720\text{ cm}^{-1}$ .

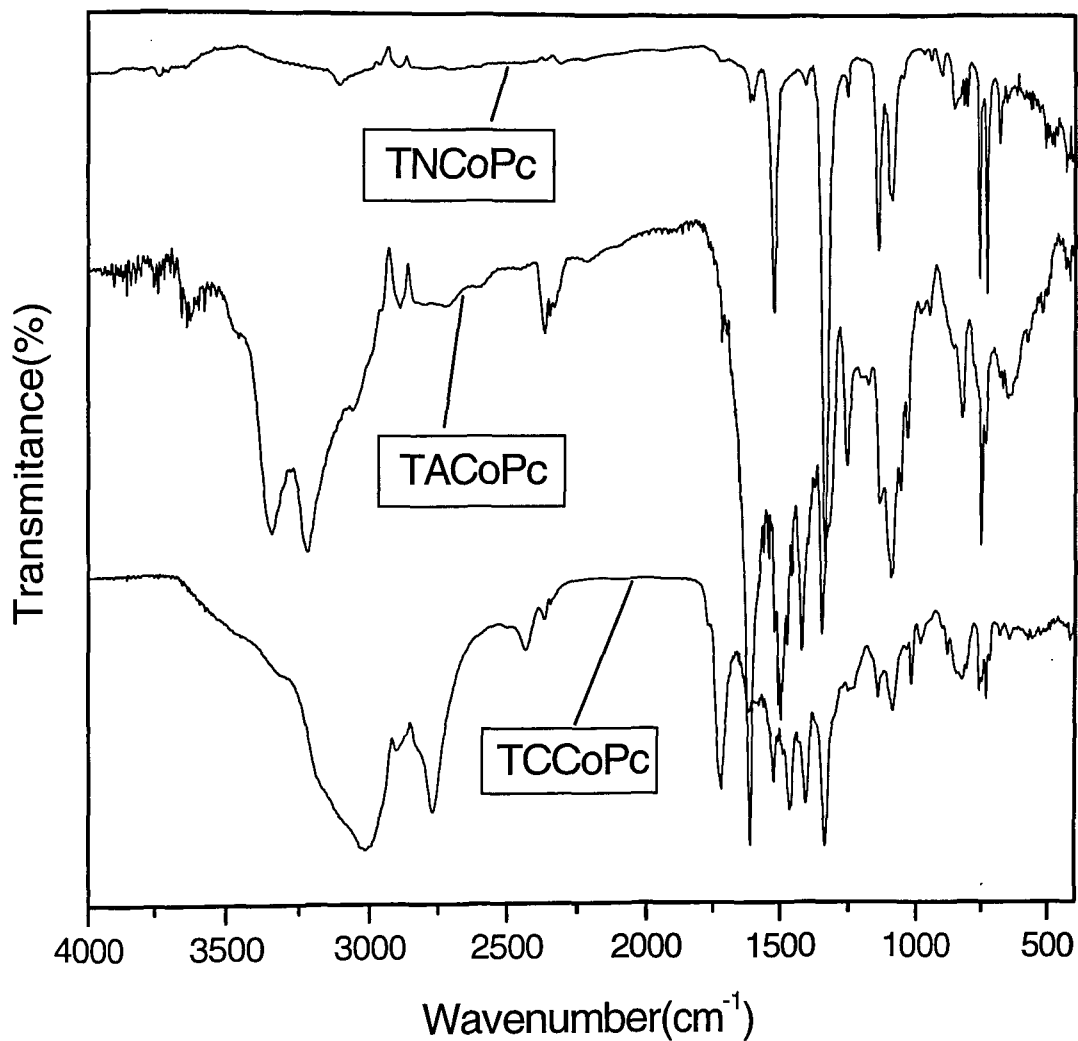


**Fig 4.5 IR spectra of TNCOPc, TACOPc and TCCOPc**

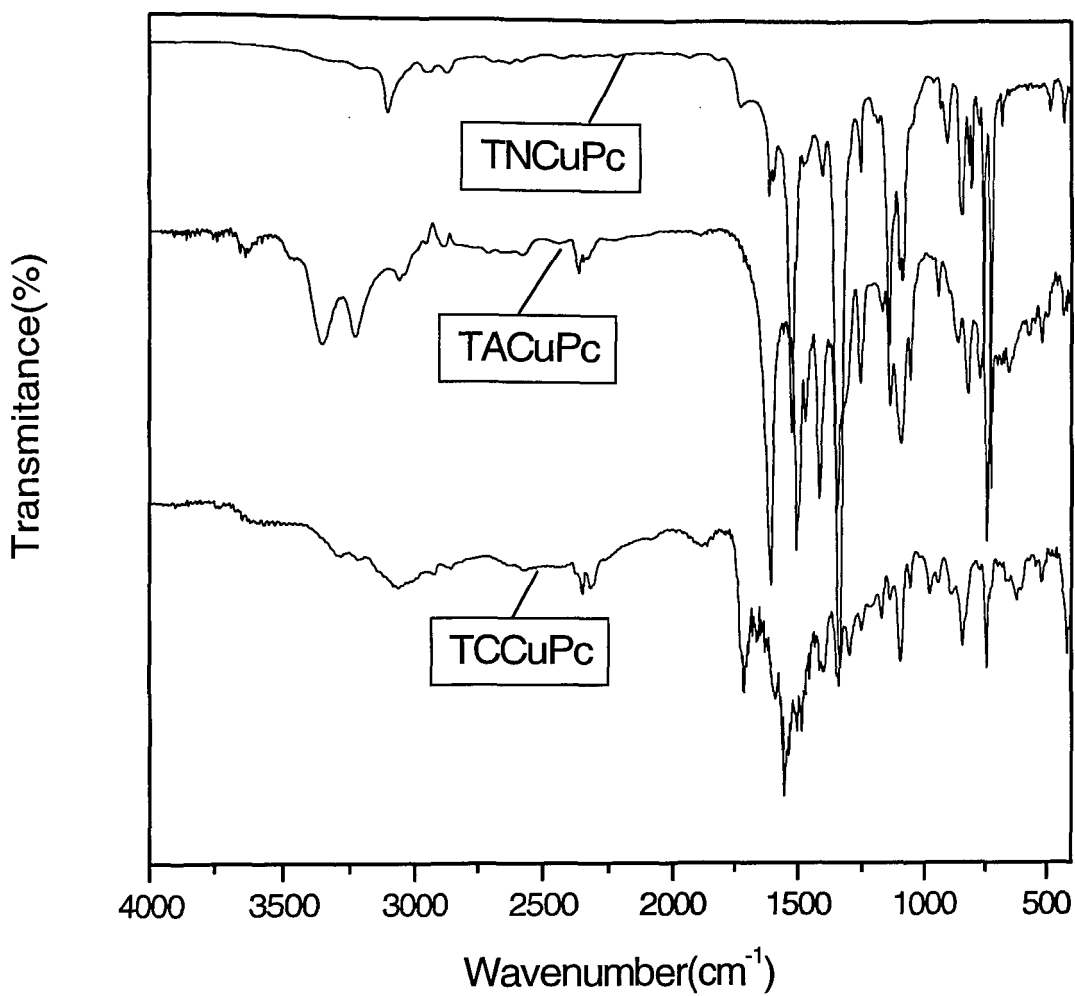


**Fig 4.6 IR spectra of TNCuPc, TACuPc and TCCuPc**

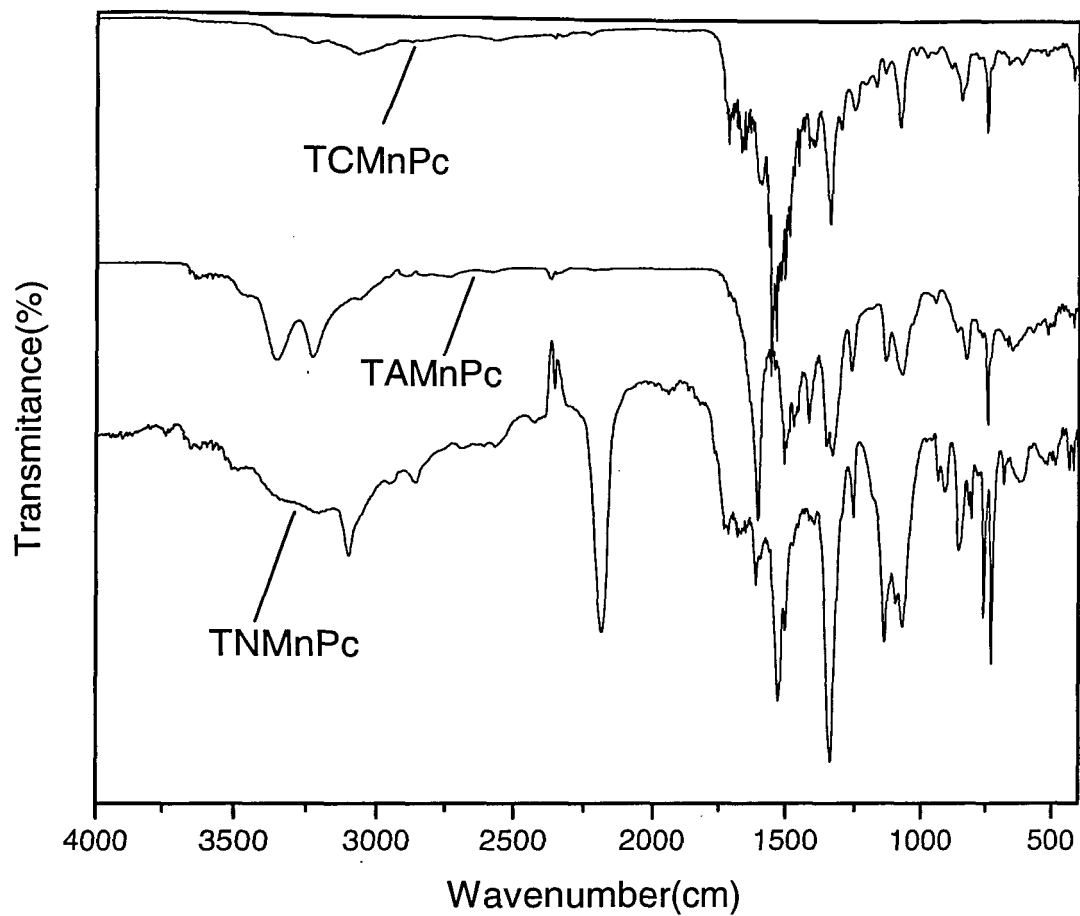


**Fig 4.7 IR spectra of TNMnPc, TAMnPc and TCMnPc**

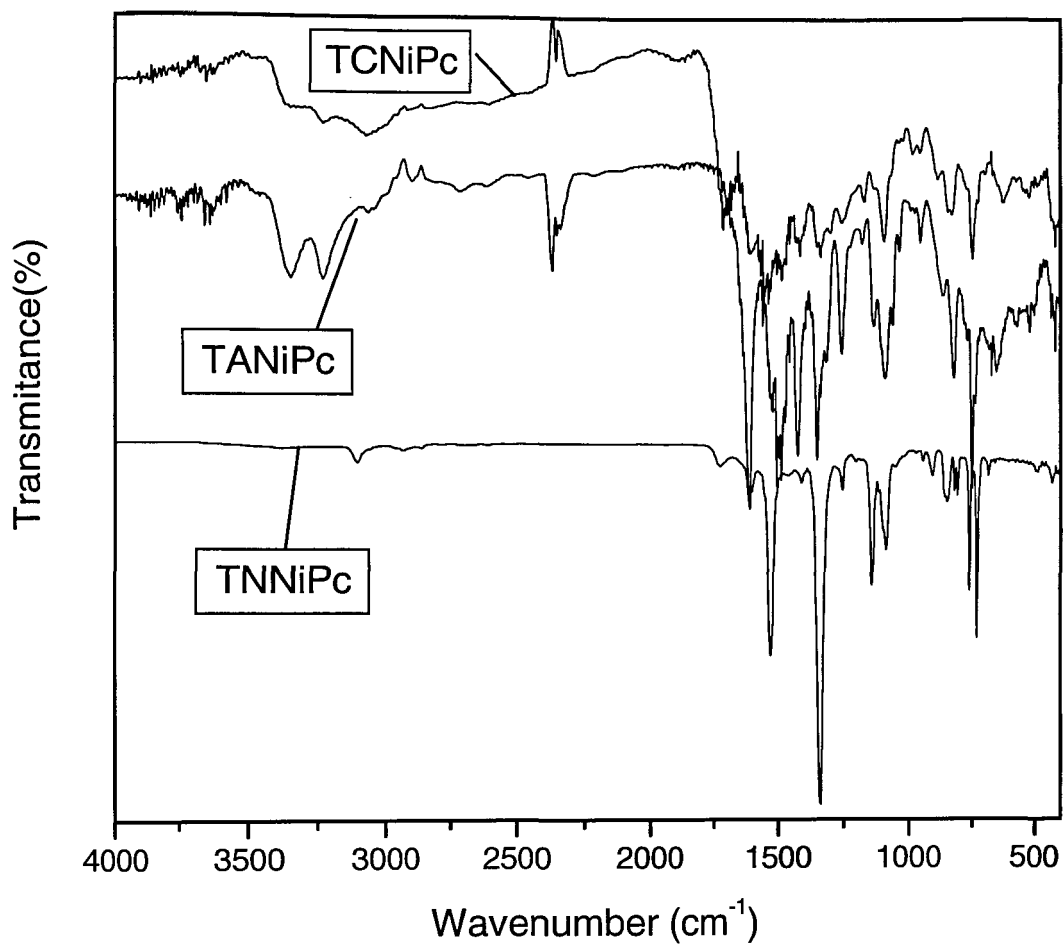


**Fig 4.8 IR spectra of TNNiPc, TANIpc and TCNiPc**

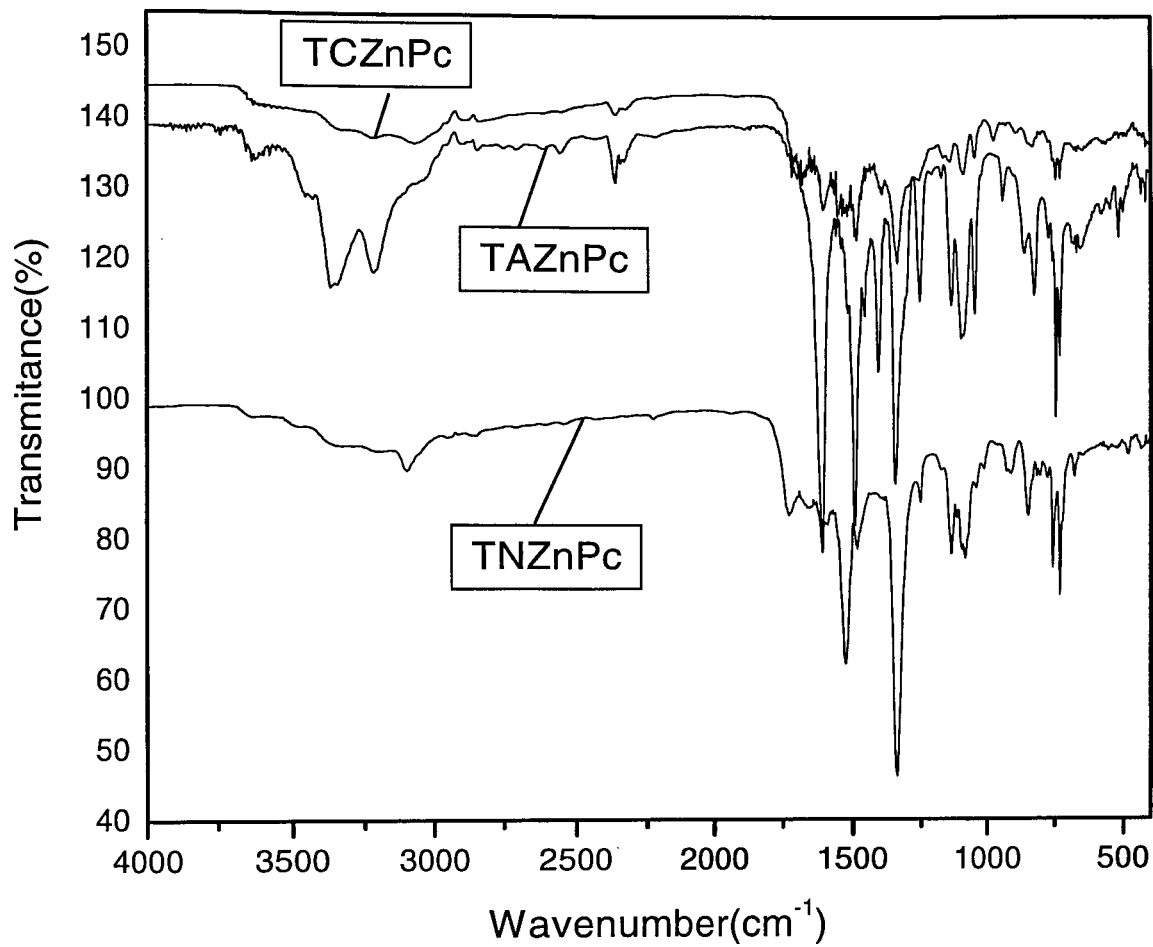


**Fig 4.9 IR spectra of TNZnPc, TAZnPc and TCZnPc**

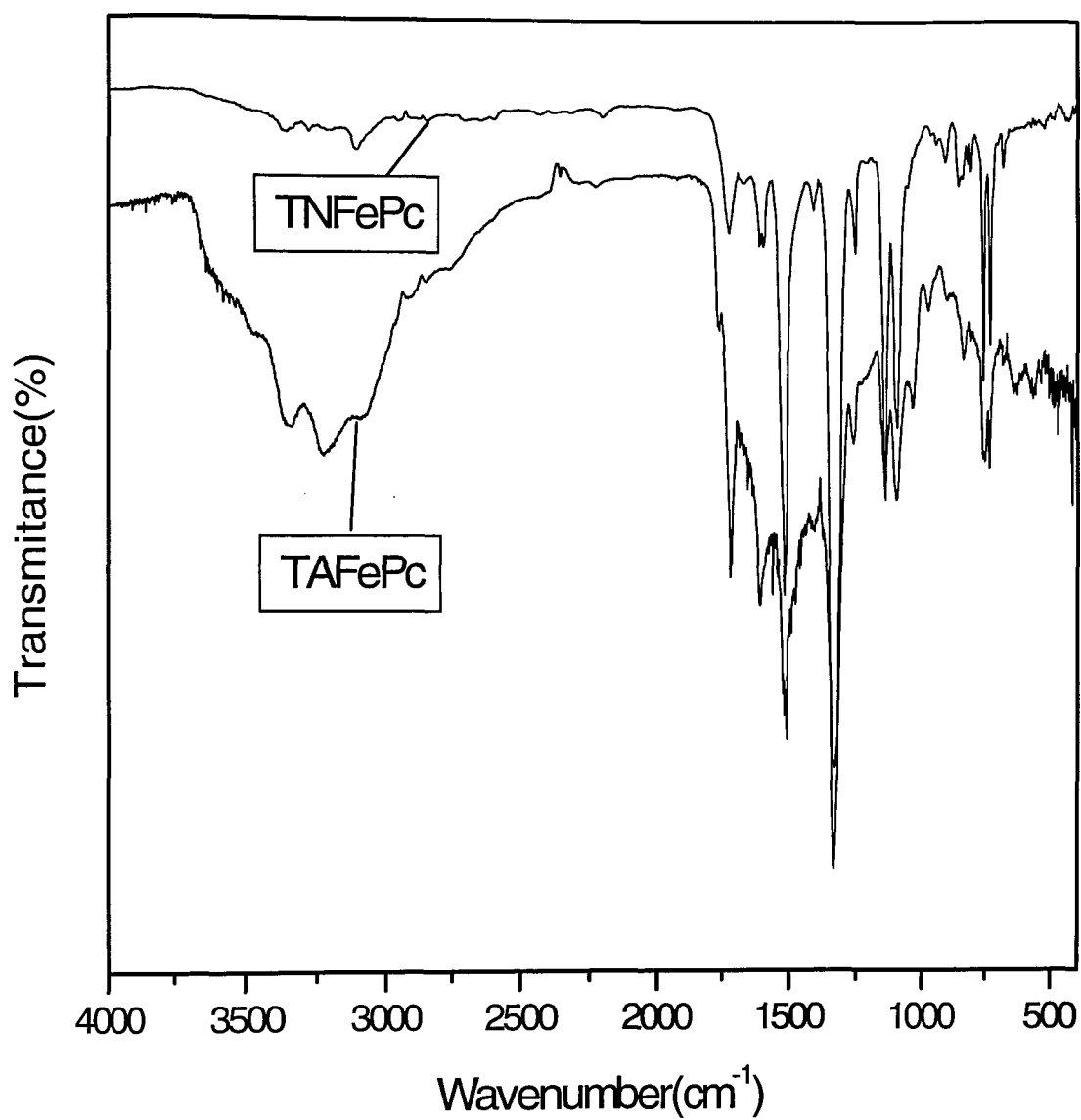


**Fig 4.10 IR spectra of TNFePc and TAFEPC**

## 4.2 UV-Visible spectroscopy

The Characteristic Q and B bands are observed in case of different metal substituted Pcs when dissolved in dimethyl sulphoxide as shown in Fig 4.11 and in Table 4.1. The maxima obtained and the intensity of Q band with respect to B band depends on the central metal atom in the Pc ring. Compared to all other MPcs, the MnPc showed Q and B band at higher wavelength.

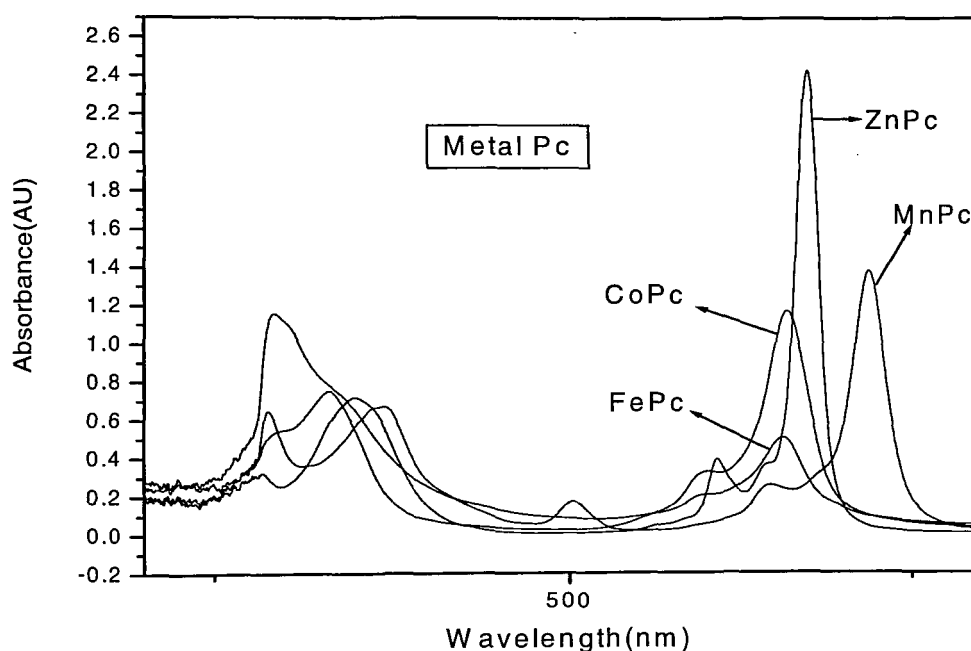


Fig. 4.11 UV-Visible spectrum for CoPc, ZnPc, MnPc and FePc



**Table 4.1 UV-Visible data of metal Pcs**

<b>Compound</b>	<b>B Band (nm)</b>	<b>Q band (nm)</b>
ZnPc	347	672
MnPc	367	717
CoPc	328	658
FePc	291	657
CuPc	287	670
NiPc	289	675
AlPc	359	680

Substituted Pcs were effectively characterized using UV-Visible spectroscopy. The characteristic UV-Visible spectra for nitro substituted (1), amino substituted (2) and acrylic acid substituted (3) Pcs with respect to their individual metal are shown as Figs. 4.12 - 4.17 and combined data for all Pcs are shown in Table 4.2. The common thing which is observed in all the cases is that when the nitro substituted Pcs gets reduced to amino substituted Pcs there is an increase in the value of Q band and, it shifts to the red region, where as, on the other hand when amino group gets substituted with acrylic acid group blue shift is observed.

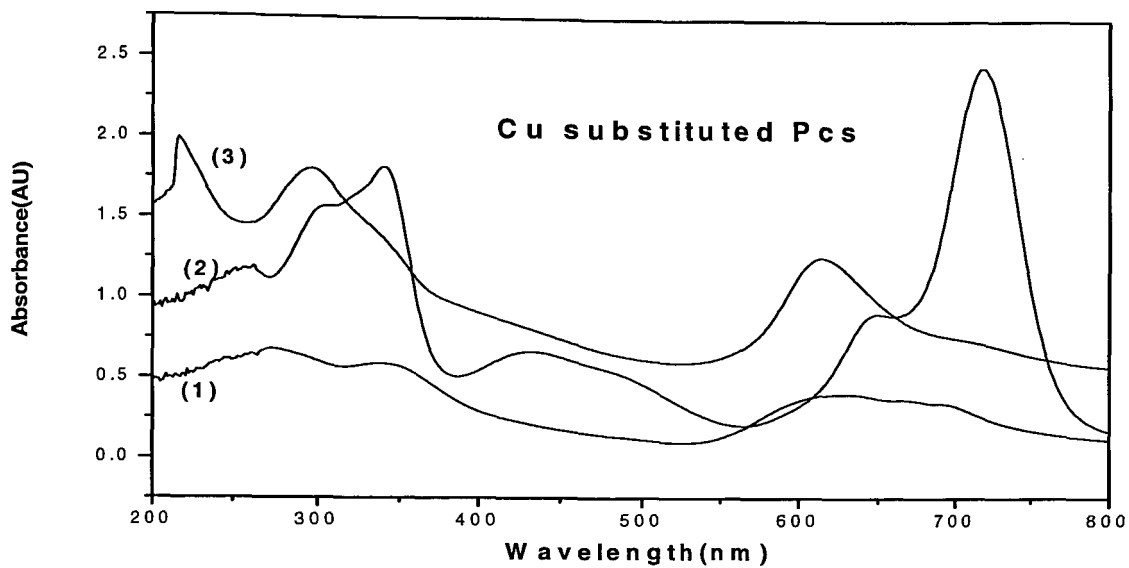


**Fig 4.12 UV-Visible spectra for 1)TNCuPc, 2)TACuPc and 3)TCCuPc**

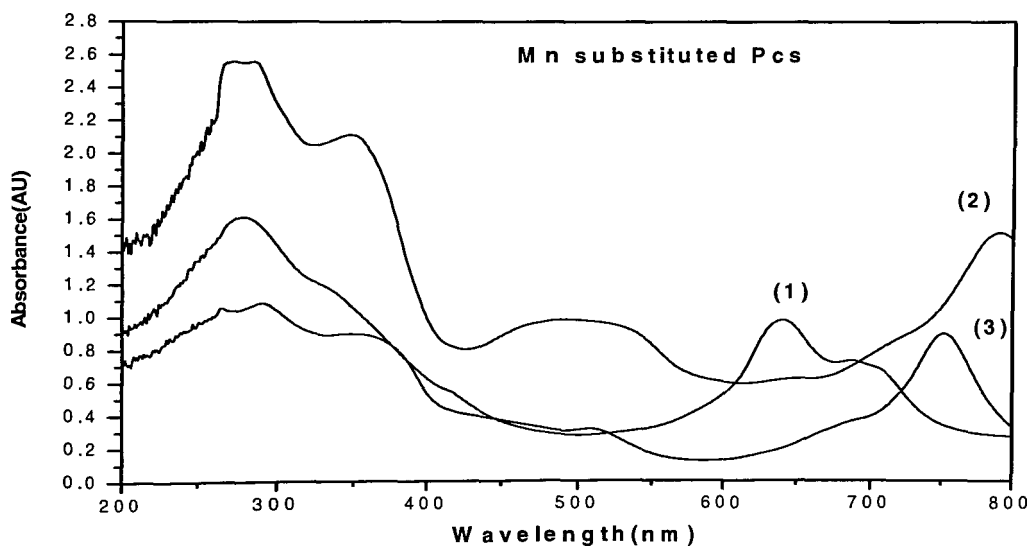


**Fig 4.13 UV-Visible spectra for 1)TNMnPc, 2)TAMnPc and 3)TCMnPc**

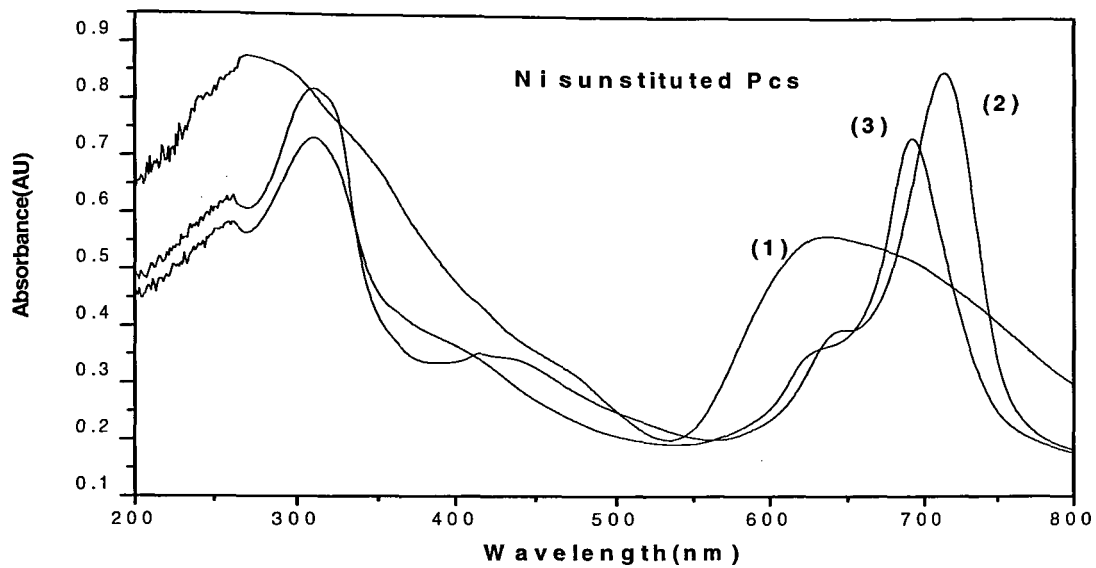


**Fig 4.14 UV-Visible spectra for 1) TNNiPc, 2) TANiPc and 3)TCNiPc**

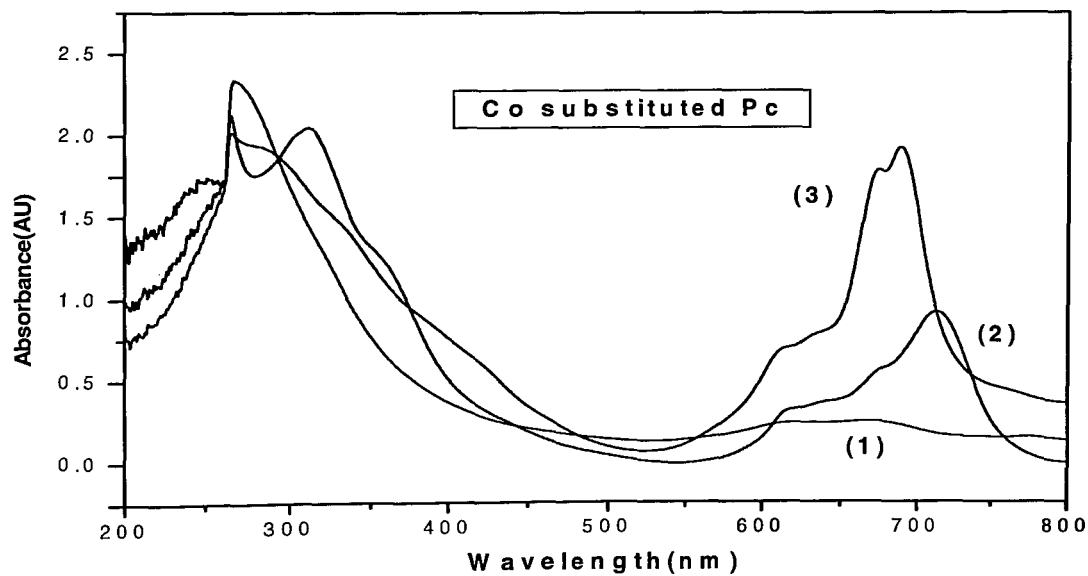


**Fig 4.15 UV-Visible spectra for 1)TNCOPc, 2) TACOPc and 3) TCCOPc (3)**

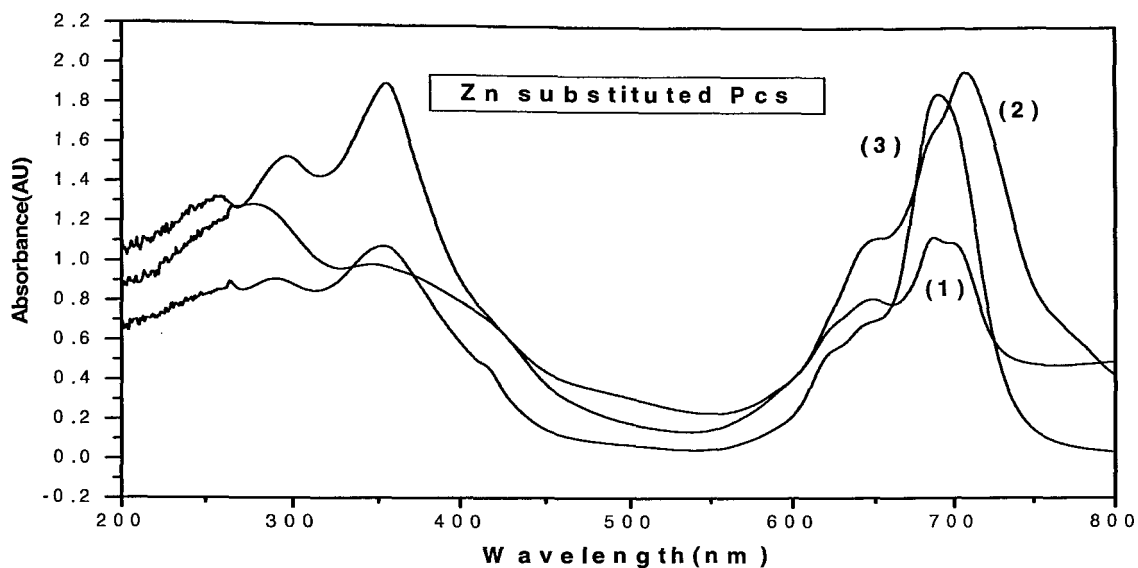


Fig 4.16 UV-Visible spectra for 1) TNZnPc, 2) TAZnPc and 3) TCZnPc

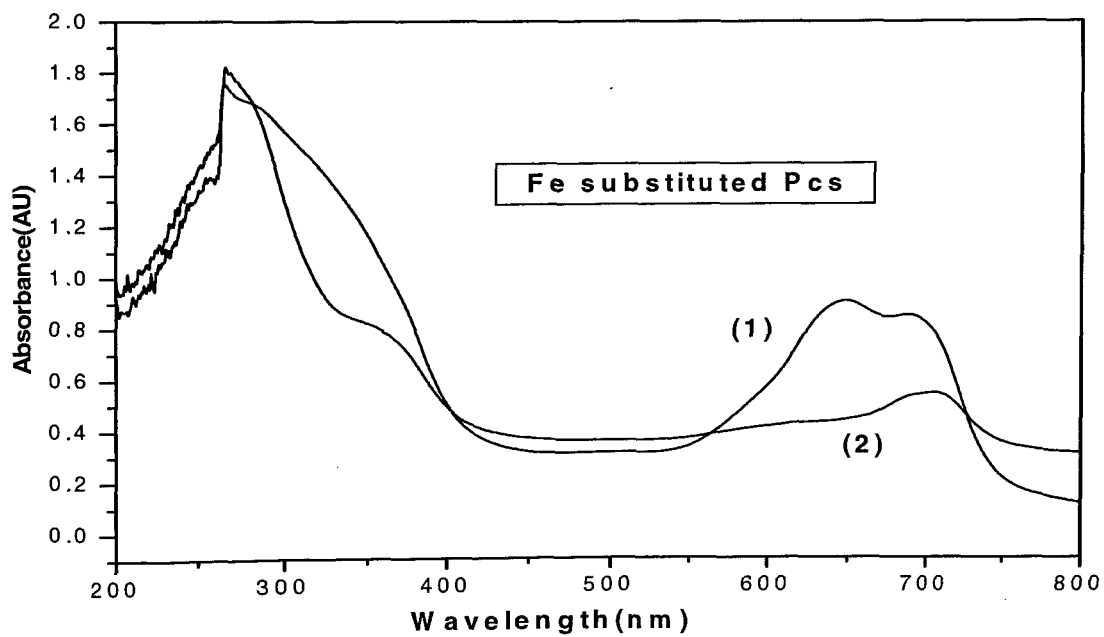


Fig 4.17 UV-Visible spectra for 1) TNFePc and 2) TAFEPC

**Table 4.2 UV-Visible data for substituted metal Pcs**

<b>Name</b>	<b>B band(nm)</b>	<b>Q band(nm)</b>
<b>TNMnPc</b>	<b>279</b>	<b>693</b>
<b>TAMnPc</b>	<b>350</b>	<b>791</b>
<b>TCMnPc</b>	<b>357</b>	<b>750</b>
<b>TNCuPc</b>	<b>340</b>	<b>625</b>
<b>TACuPc</b>	<b>339</b>	<b>717</b>
<b>TCCuPc</b>	<b>297</b>	<b>613</b>
<b>TNNiPc</b>	<b>269</b>	<b>634</b>
<b>TANiPc</b>	<b>311</b>	<b>713</b>
<b>TCNiPc</b>	<b>311</b>	<b>692</b>
<b>TNCoPc</b>	<b>267</b>	<b>670</b>
<b>TACoPc</b>	<b>314</b>	<b>713</b>
<b>TCCoPc</b>	<b>266</b>	<b>687</b>
<b>TNZnPc</b>	<b>346</b>	<b>687</b>
<b>TAZnPc</b>	<b>354</b>	<b>706</b>
<b>TCZnPc</b>	<b>353</b>	<b>691</b>
<b>TNFePc</b>	<b>266</b>	<b>688</b>
<b>TAFcPc</b>	<b>265</b>	<b>708</b>

### 4.3 X-ray diffraction

The MPcs were characterized by X-ray diffraction Technique. The  $2\theta$ ,  $I/I_0$  and  $d$  spacing values obtained are represented in Table 4.3. The powder X-ray diffraction patterns of the non substituted MPcs showed the diffraction peaks and the  $2\theta$  values were matched with the corresponding JCPDS files which indicates that these MPcs have a  $\beta$  planar monoclinic structure. Figs. 4.18 - 4.29 show the diffraction patterns of some representative Pcs.

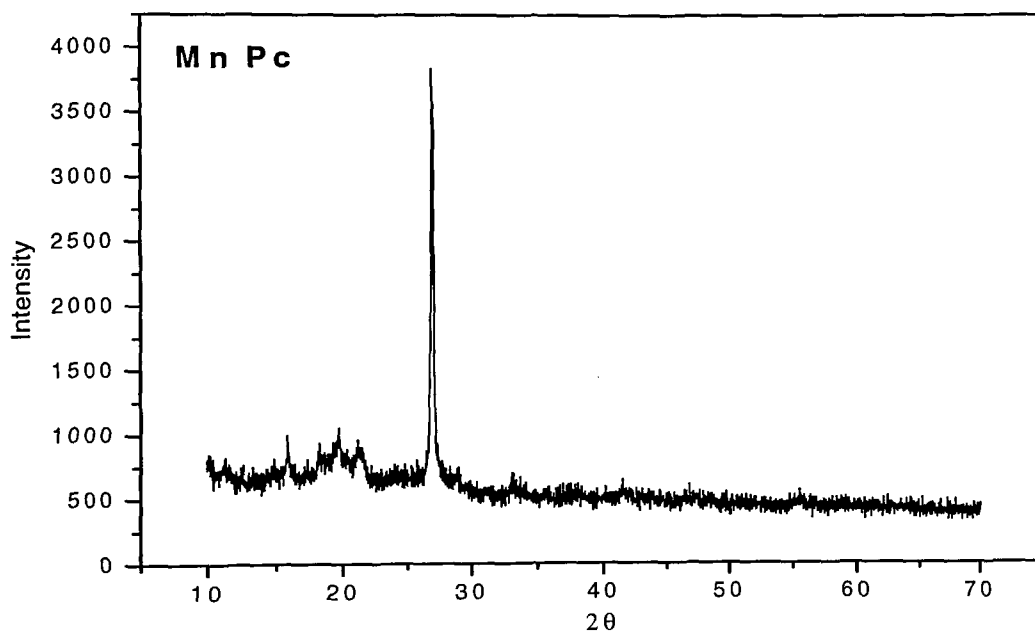
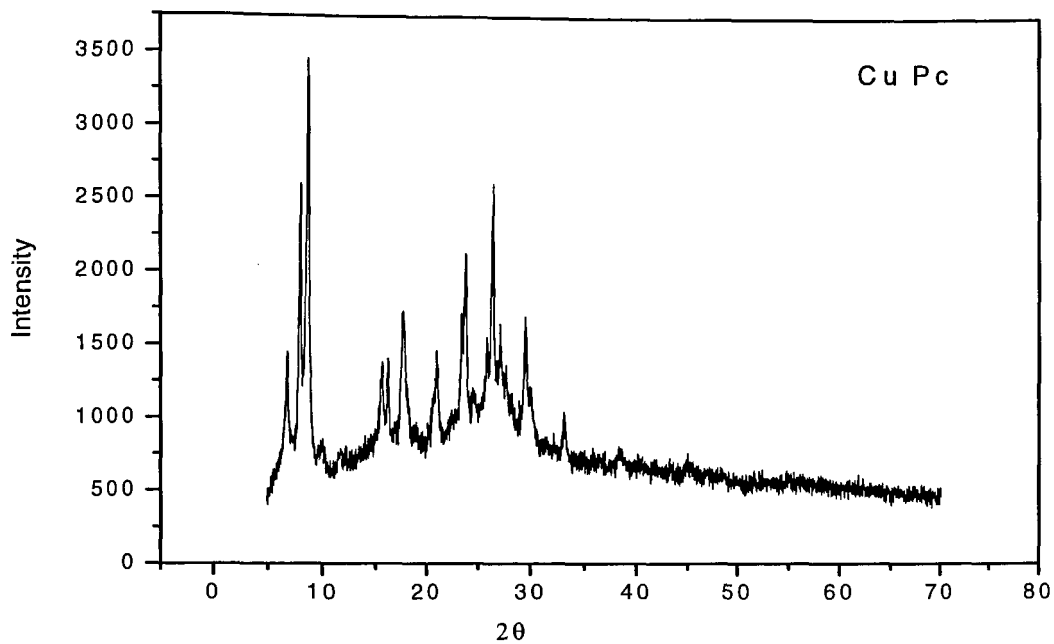
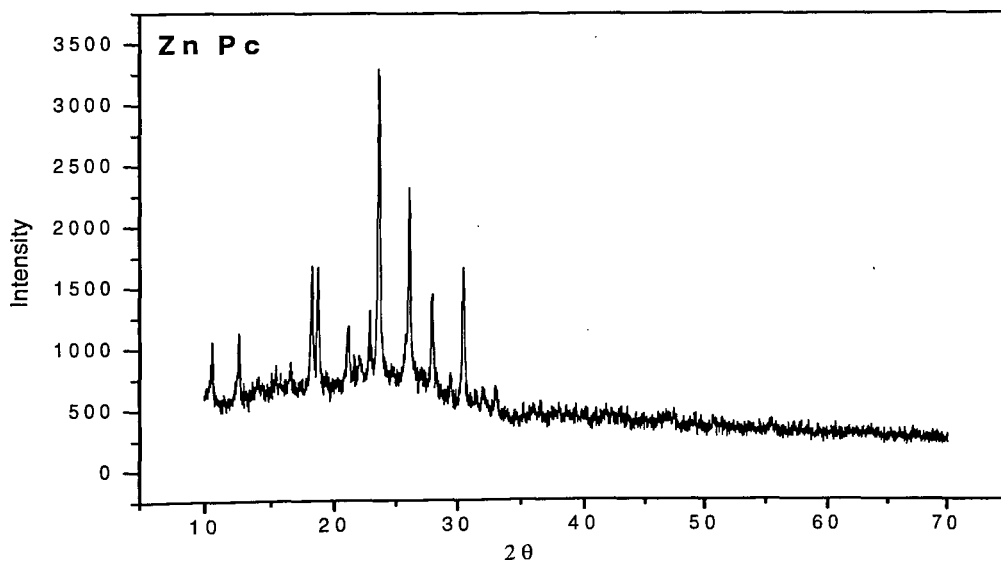


Fig 4.18 XRD pattern of MnPc



**Fig 4.19 XRD pattern of CuPc**

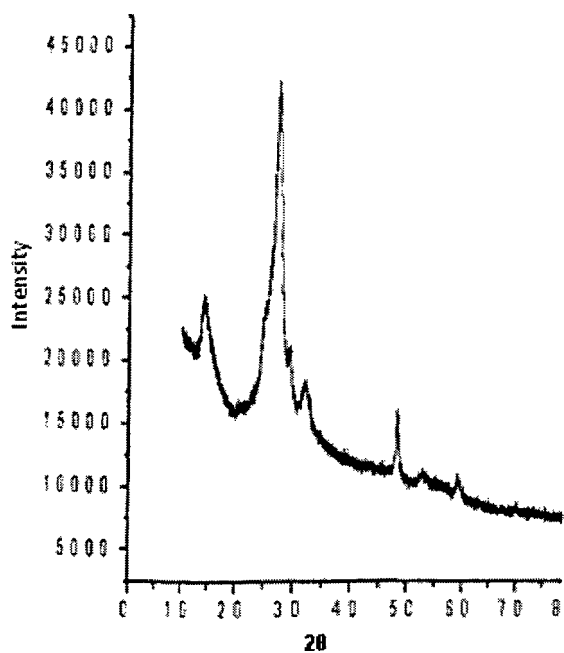


**Fig 4.20 XRD pattern of ZnPc**

**Table 4.3 XRD value of MnPc, CuPc and ZnPc**

Sr. no.	Samples	2 $\theta$	d spacing calculated	d spacing from literature	I/I <sub>t</sub>
1	Mn Pc	15.871	5.57	5.71	14.34
		19.703	4.50	4.47	16.52
		27.017	3.29	3.38	100
2	CuPc	6.8227	12.94	12.60	31.80
		8.8248	10.008	9.61	100
3	Zn Pc	10.563	8.365	8.29	22.38
		12.635	6.998	6.99	24.28
		18.218	4.863	4.87	43.80
		18.681	4.744	4.73	43.33
		22.76	3.902	3.87	30.95
		23.56	3.771	3.75	100
		26.086	3.296	3.40	66.19
		30.441	2.93	2.92	42.85

**Table 4.4 XRD value of TACuPc**

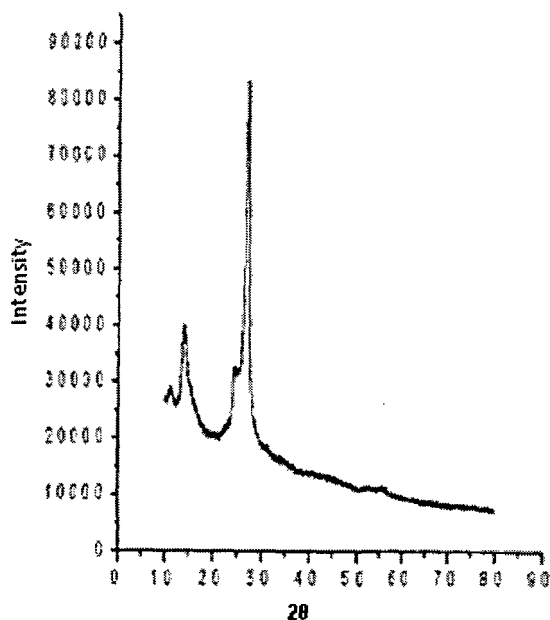


2 $\theta$	I/I <sub>t</sub>	d
14.2370	37.62	6.2208
27.2807	100	3.2689
29.3315	28.71	3.0448
32.0235	21.78	2.7947
48.0753	20.79	1.6958
52.5592	4.9	1.7411
59.1060	5.94	1.5629

**Fig 4.21 XRD pattern of TACuPc**



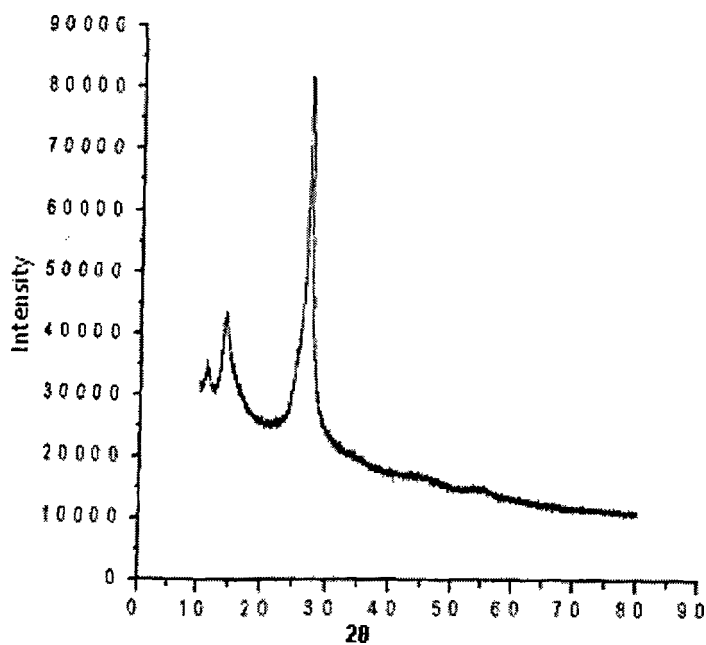
**Table 4.5 XRD value of TNCuPc**



2θ	I/I <sub>t</sub>	d
11.2917	19.64	7.8360
14.1514	35.71	6.2582
27.1389	100	3.2856

**Fig 4.22 XRD pattern of TNCuPc**

**Table 4.6 XRD value of TNNiPc**



2θ	I/I <sub>t</sub>	d
11.1676	43.75	7.9927
14.0452	53.97	6.3053
26.9410	100	3.3093

**Fig 4.23 XRD pattern of TNNiPc**

**Table 4.7 XRD value of TANiPc**

$2\theta$	$I/I_t$	d
14.3638	58.64	6.1662
20.3207	45.86	4.3701
23.0201	53.38	3.8634
26.7661	100	3.3306

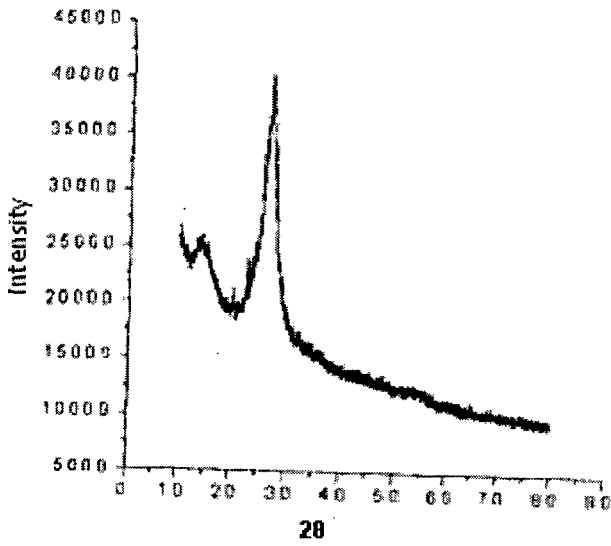


**Fig 4.24 XRD pattern of TANiPc**

**Table 4.8 XRD value of TNCOPc**

$2\theta$	$I/I_t$	d
11.00	40.2	8.0444
14.25	50.0	6.2147
24.61	30.5	3.6173
27.47	100.0	3.2473

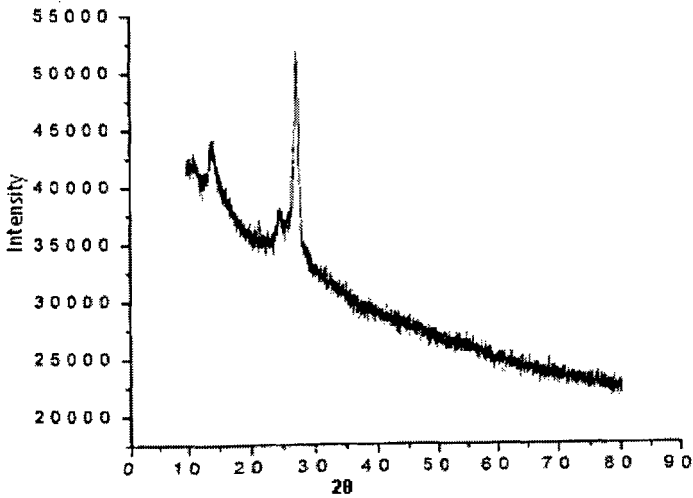


**Fig 4.25 XRD pattern of TNCOPc**

**Table 4.9 XRD value of TNZnPc**

$2\theta$	$I/I_t$	d
18.90054	45.03	4.6951
27.27620	39.69	3.2694
27.50970	100	3.2422

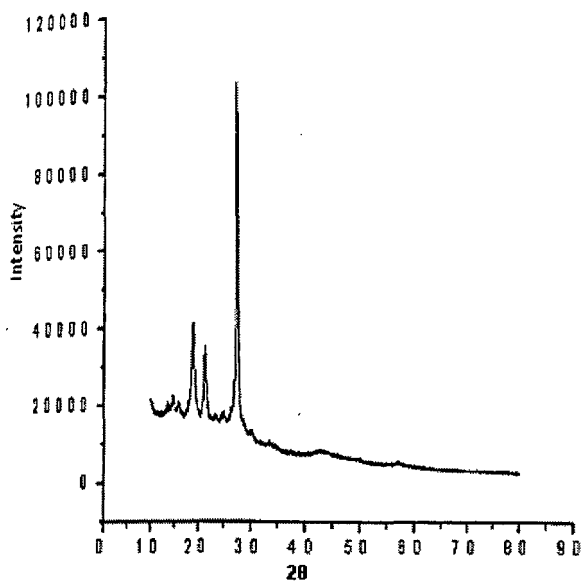


**Fig 4.26 XRD pattern of TNZnPc**

**Table 4.10 XRD value of TAMnPc**

$2\theta$	$I/I_t$	d
10.29	52.7	8.5994
13.40	51.6	6.6096
15.35	52.7	5.7709
26.74	100.0	3.3344

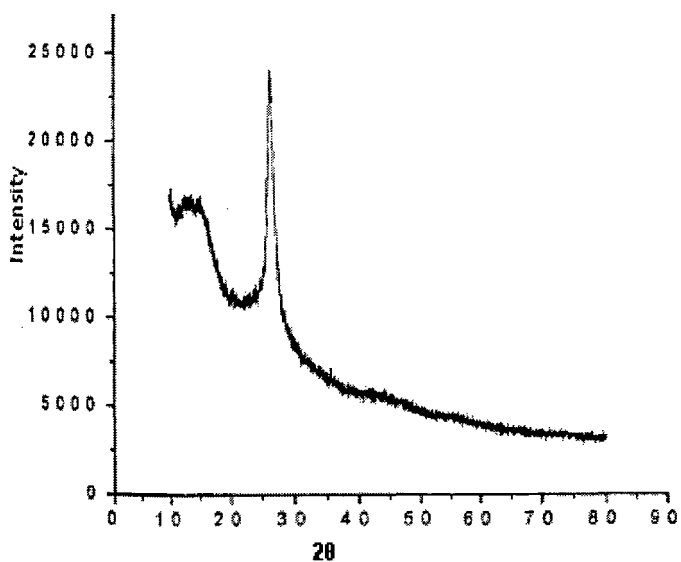
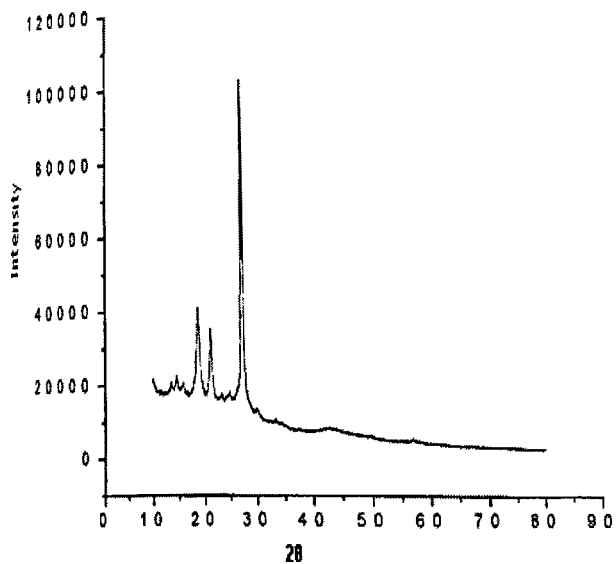


**Fig 4.27 XRD pattern of TAMnPc**

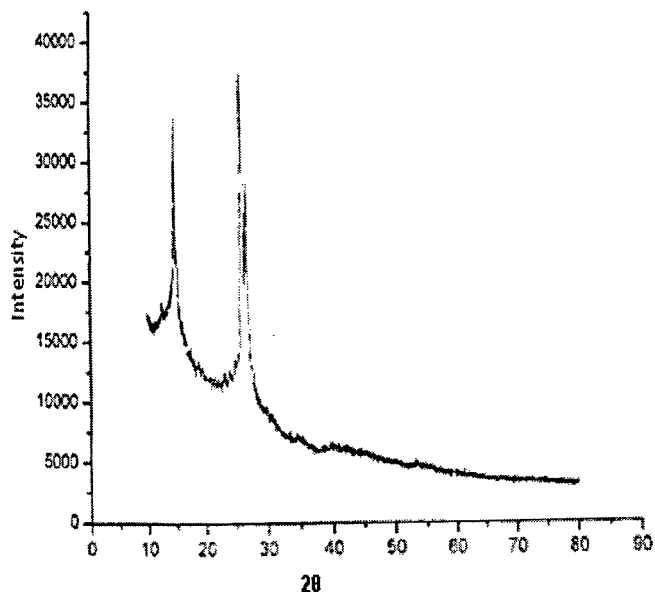
**Table 4.11 XRD value of TAZnPc**



$2\theta$	$I/I_t$	d
27.58	100.0	3.2341
21.42	26.8	4.1482
18.94	29.6	4.6854
14.62	21.3	6.0587
10.00	23.2	8.8451

**Fig 4.28 XRD pattern of TAZnPc**

**Table 4.12 XRD value of TNMnPc**



$2\theta$	$I/I_t$	d
12.50	33.9	7.0808
14.85	84.4	5.9660
26.11	100.0	3.4132
26.96	66.1	3.3071

**Fig 4.29 XRD pattern of TNMnPc**

#### 4.4 Elemental Analysis

Elemental analysis was carried out on TCMPcs and the observed values were compared with the calculated values as shown in Table 4.13. There is a slight difference in the calculated and observed values, but they are within experimental errors.

**Table 4.13 CHN Data for TCMPc**

Calculated (%)				Observed(%)		
Name of Pc	C	H	N	C	H	N
TCMnPc	56.53	2.75	16.49	56.86	2.99	16.91
TCNiPc.2H <sub>2</sub> O	54.41	3.04	15.86	53.63	2.64	16.48
TCCuPc.H <sub>2</sub> O	55.10	2.89	16.06	55.95	3.11	15.64
TCZnPc.3H <sub>2</sub> O	53.17	3.16	15.50	52.95	3.01	16.40
TCCoPc.3H <sub>2</sub> O	56.3	2.73	16.4	57.07	2.94	14.94

## 4.5 TG-DSC

Pcs are well known for their high thermal stability. The TG-DSC studies were done to understand the thermal behavior and to know the thermal stability of these compounds. From the TG-DSC curves it was concluded that Pcs do not melt and there is no phase change but they undergo decomposition at higher temperature above 350 °C. It was also observed that the thermal stability changes with the change in central metal atom and also with a change in the substituent at peripheral positions. TG-DSC for non substituted MPcs is shown in Figs. 4.30-4.33 for CoPc, CuPc, FePc and NiPc.

The thermal stability of MnPc, NiPc and ZnPc was found to be 438 °C, 456 °C and 430°C respectively.

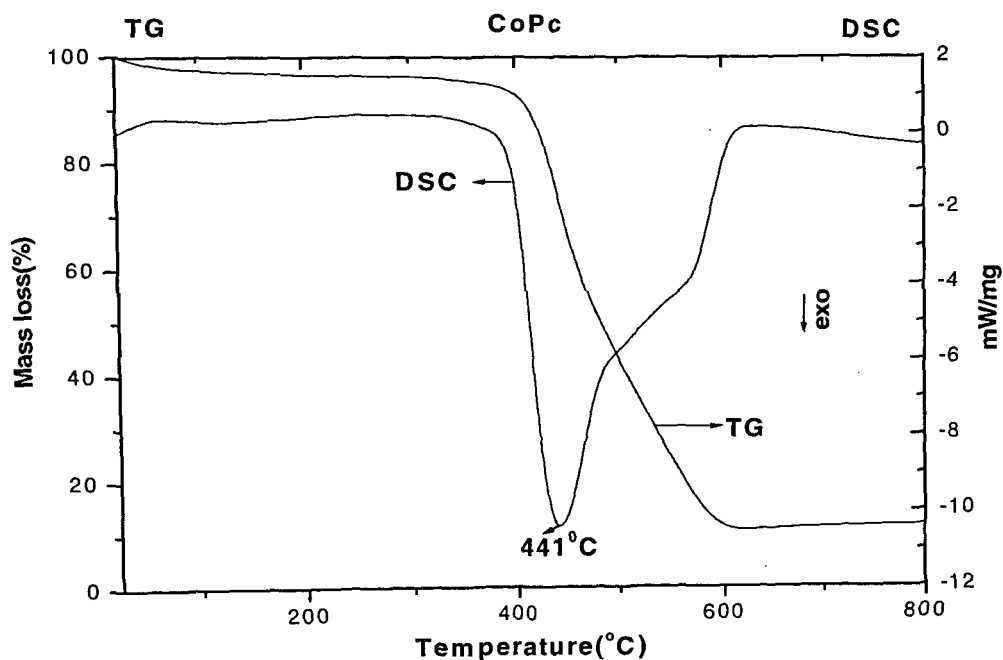
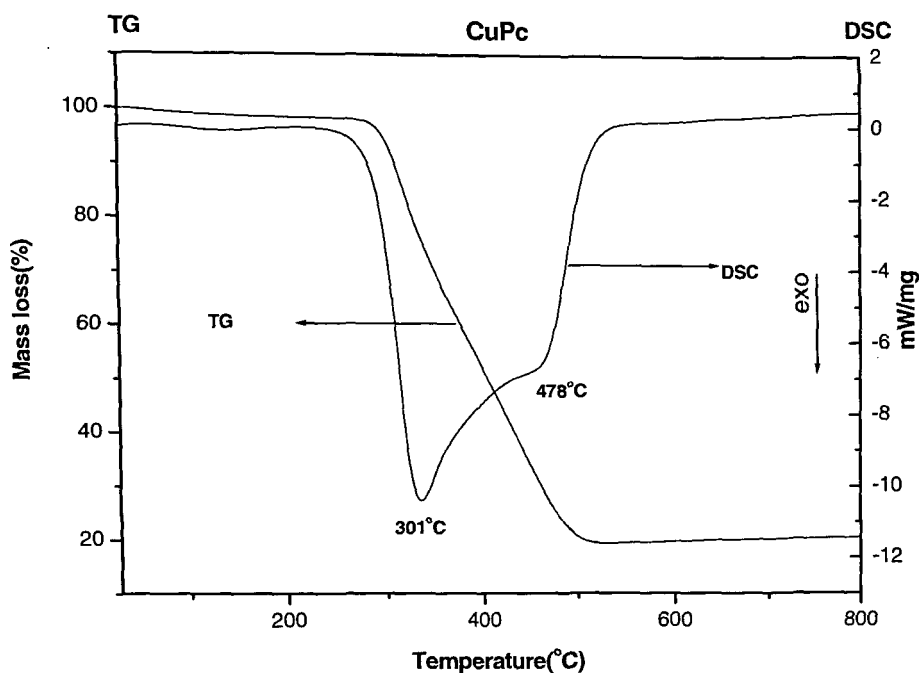


Fig 4.30 TG-DSC for CoPc

In case of CoPc, an exotherm of DSC is observed at 441 °C with gradual weight loss up to 600 °C as shown by TG graph. In addition to this an adjacent exotherm is also observed at around 570 °C. The remaining residue after TG/DSC was attributed for the formation of cobalt oxide.



**Fig 4.31 TG-DSC for CuPc**

The DSC exotherm pattern observed for CuPc is similar to that of CoPc, but in case of CuPc the decompositions begins at 301 °C, which is almost 100 °C less than that of CoPc. CuPc is found to have least decomposition temperature as compared to that of other Pcs. The residual mass is attributed for the formation of copper oxide.

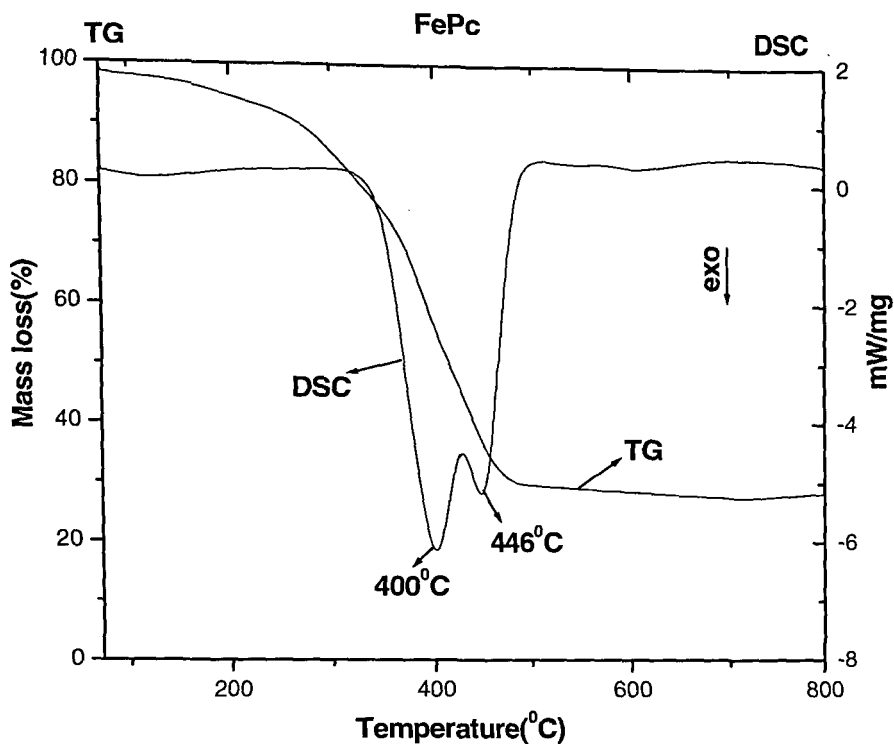


**Fig 4.32 TG-DSC for FePc**

In case of FePc, two separate exotherms are observed for DSC, one at 400 °C and other at 446 °C with subsequent loss of weight from 400 – 450 °C. The formation of two separate exotherms in case of Fe may be due to the different decomposition pattern. The residual mass shown by TG is due to the formation of metal oxide.



The TG-DSC pattern for the Tetra nitro substituted Pcs, such as TNCuPc, TNMnPc and TNZnPc are shown in Figs. 4.33-4.35. The decomposition temperature observed for TNCuPc – 405°C, TNFePc – 354 °C and TNNiPc – 430 °C respectively.

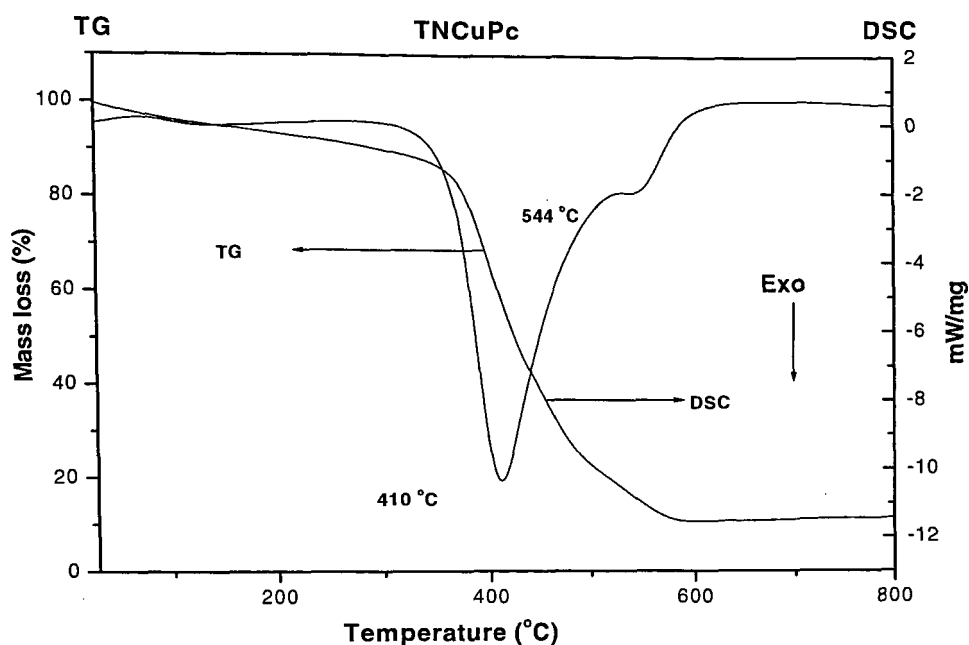


**Fig 4.33 TG-DSC for TNCuPc**

In case of TNCuPc the exotherms in DSC are observed at 410 °C and 544 °C, with a TG graph showing weight loss gradually from 400-600 °C. A residual mass of less than 10% is observed at 600 °C. Substitution of Nitro group at the peripheral position increases the thermal stability of CuPc.

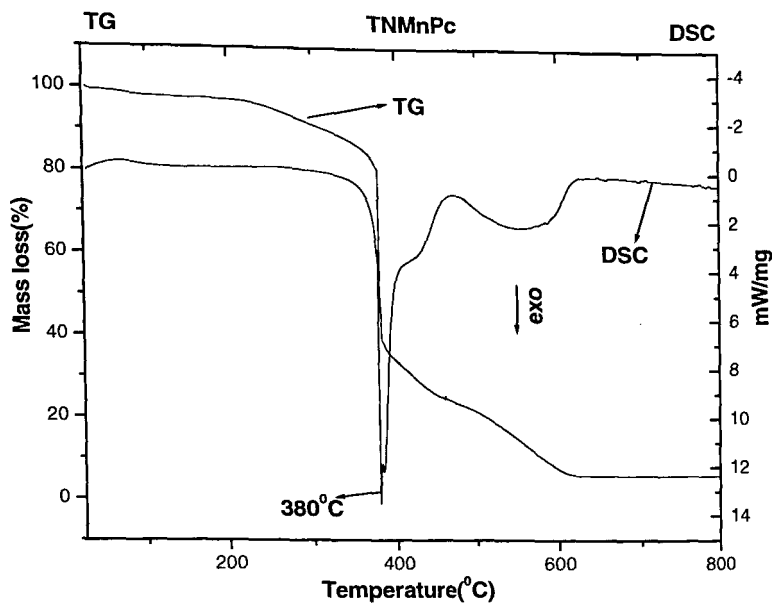


**Fig 4.34 TG-DSC for TNMnPc**

In case of TNMnPc a sharp exotherm is observed at 380 °C with fast weight loss as shown by TG in Fig. 4.34. Subsequently at 500 °C, a broad exotherm is observed with a gradual weight loss as shown by TG up to 600 °C. The actual pattern of decomposition is not known, but the Phthalocyanine ring attach to the central metal atom decomposes depending upon the stability of the complex formed.

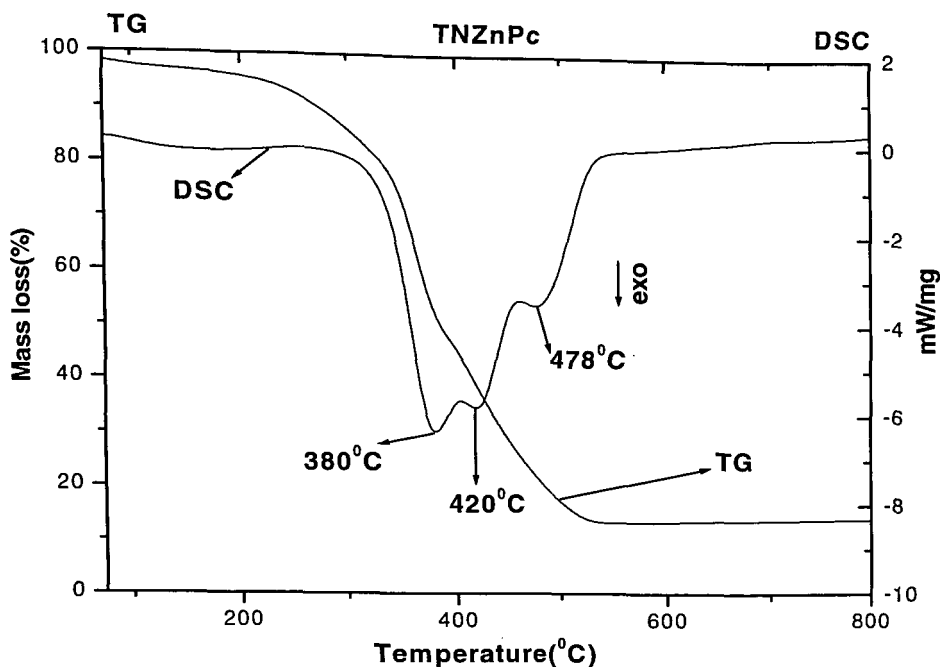


**Fig 4.35 TG-DSC for TNZnPc**

In case of TNZnPc three exotherms are observed at 380 °C, 420 °C and 478 °C with mass loss as shown in TG from 380 °C to 500 °C. No activity in the TG-DSC pattern is observed with a further increase in temperature as indicating the formation of ZnO with a stable mass up to 800 °C.

The TG-DSC patterns for Tetra amino substituted Pcs TACuPc, TANiPc and TAZnPc are shown in Figs. 4.36-4.38 .The decomposition temperature values obtained for TACoPc , TAFEPC, and TAMnPc are 430°C, 375 °C and 380 °C respectively.

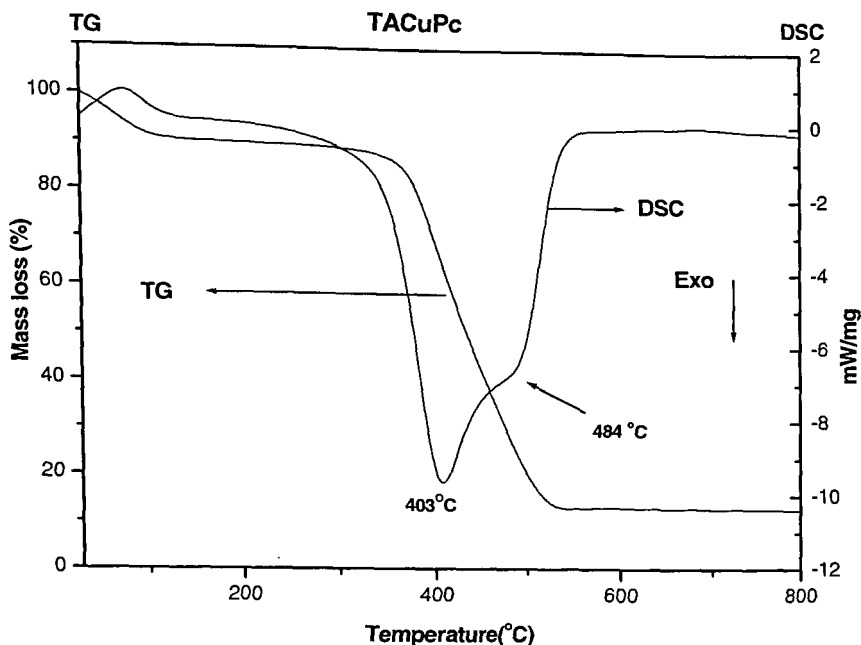


**Fig 4.36 TG-DSC for TACuPc**

TACuPc as shown in Fig. 4.36 have similar TG- DSC pattern in comparison to that of CuPc and TNCuPc. The only difference is that an endotherm is observed at 105 °C which is attributed to loss of water molecule. The decomposition temperature observed is 403 °C. The 10% mass remaining after 600 °C is due to the formation of CuO.

The TANiPc as shown in Fig 4.37 also shows an endotherm at 105 °C as that observed in the case of TACuPc . This endotherm is due to the loss of water molecule. From the TG curve it can be concluded that around 10% weight loss is due to the water molecules. Further complete decomposition is observed at 410 °C with gradual weight loss up to 500 °C. No further loss in weight is seen due to the formation of metal oxide.

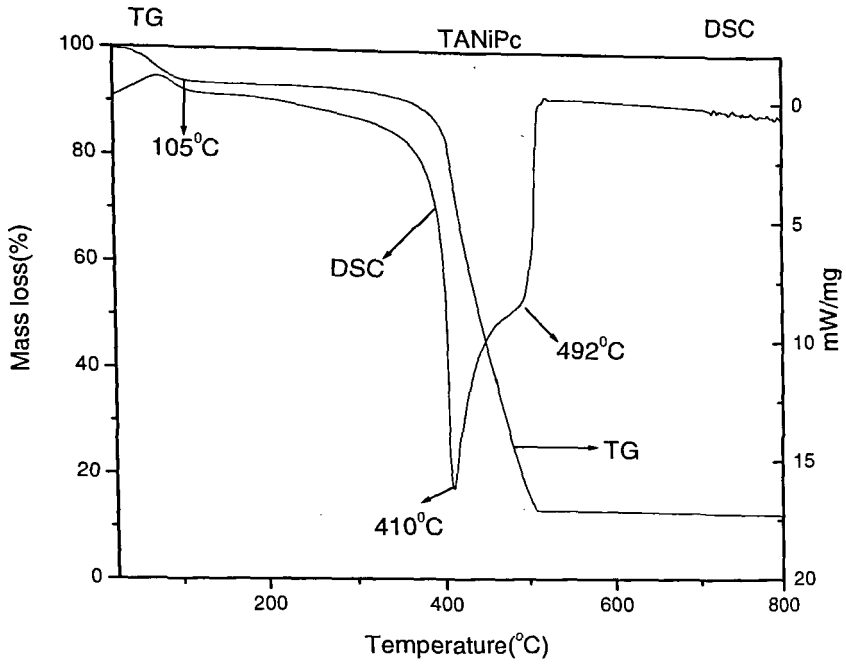


**Fig 4.37 TG-DSC for TANiPc**

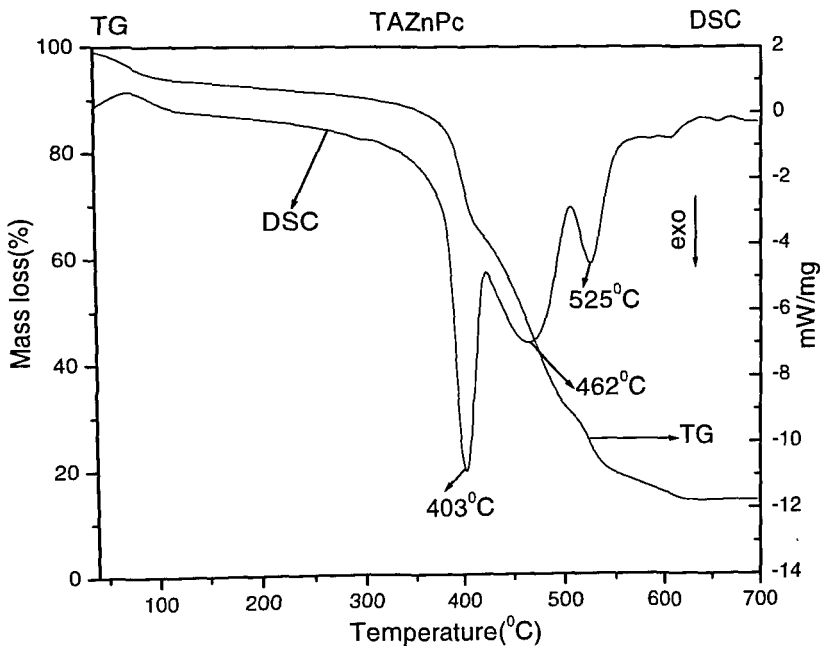


**Fig 4.38 TG-DSC for TAZnPc**

TAZnPc as shown in Fig. 4.38 have similar TG- DSC pattern in comparison to that of TNZnPc. The decomposition temperature observed is at 403 °C with subsequent two other exotherms observed at 462 °C and 525 °C with continuous mass loss as shown by TG. The remaining mass after 600 °C is due to the formation of ZnO.

The TG-DTA pattern of Tetra acrylic acid substituted Pcs TCCoPc and TCZnPc are shown in Figs. 4.39-4.40. Differential thermal analysis (DTA) pattern observed in both the case is similar irrespective of central metal atom, which is very much different to that observed in the case of non-substituted, tetra nitro and tetra amino Pcs. An endotherm is observed at 105 °C ue to loss of water molecule. A small exotherm is observed at 445 °C in case of TCCoPc and 513 °C in case of TCZnPc with a marginal weight loss as shown in TG. A prominent exotherm is observed at 535 °C for TCCoPc and at 613 °C for TCZnPc with huge weight loss. The final mass is due to the formation of metal oxide. The decomposition temperature values obtained for TCCuPc , TCMnPc and TCNiPc are 397°C, 391 °C and 416 °C respectively.

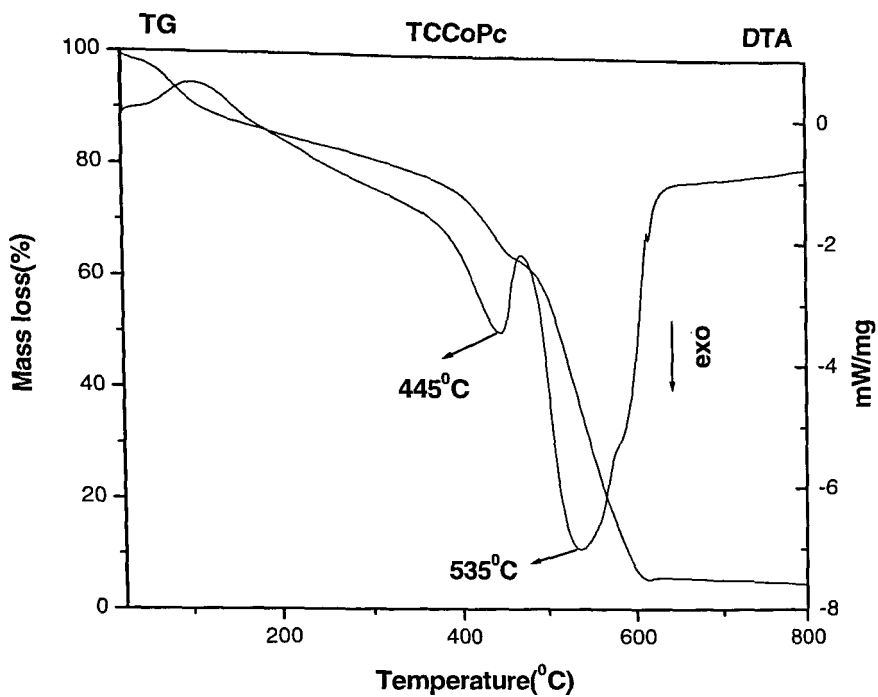


Fig 4.39 TG-DTA for TCCoPc

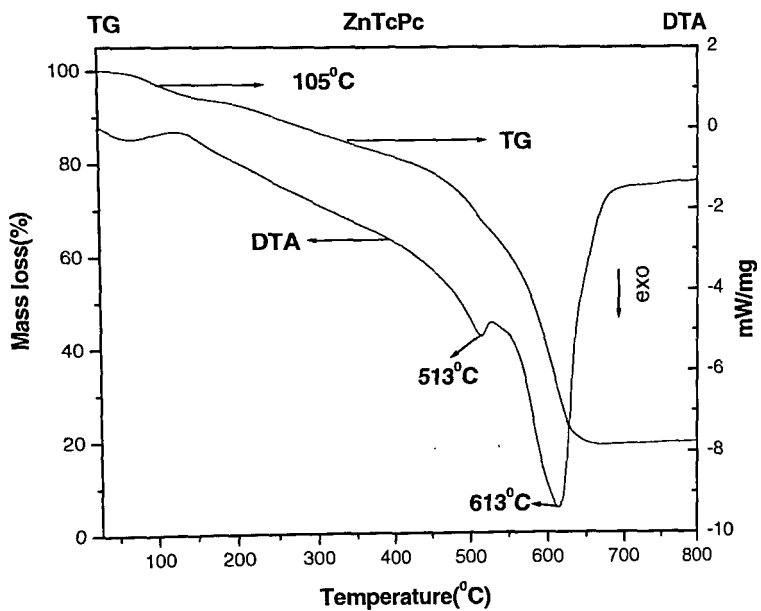


Fig 4.40 TG-DTA for TAZnPc

## 4.6 Magnetic Susceptibility

The magnetic susceptibility values for the different MPcs were determined by Guoy balance at room temperature, using field strength of 8500 gauss. The magnetic moments in Bohr magneton were calculated using an expression  $\mu_{\text{eff}} \text{ (B.M)} = 2.84 \sqrt{\chi_m} \text{ T}$ . Where  $\sqrt{\chi_m}$  is the molar magnetic susceptibility at room temperature (as discussed in chapter 3). The observed gram susceptibility values at room temperature are presented in Table 4.14. Higher magnetic moment is observed in case of Pc having Mn as a central metal atom followed by Co and least by Cu, where as Ni and Zn were found to be diamagnetic. Higher or lower value of  $\mu_{\text{eff}}$  indicates the contribution of direct or super exchange intermolecular interaction to spin only value. Difference in magnetic moment values and their variation may be due to the difference in intermolecular interactions, spacing and inclination of the molecule in the crystal lattices.

**Table 4.14 Magnetic Susceptibility of metal Pcs**

Sr.No	Name of Pcs	$\chi_g$ (CGS unit)	$\mu_{\text{eff}}$ (B.M)
01	MnPc	$13.2 \times 10^{-6}$	4.2
02	CoPc	$5.65 \times 10^{-6}$	2.8
03	CuPc	$2.60 \times 10^{-6}$	1.9
04	NiPc	Diamagnetic	-
05	ZnPc	Diamagnetic	-



The magnetic susceptibility of Tetra amino MPcs are shown in Table 4.15. The relation observed in case of non substituted MPc (M = Mn, Co and Cu) giving different  $\chi_g$  and  $\mu_{\text{eff}}$  values but there is overall decrease in the value of magnetic moment due to the decrease in the metal content in a molecule because of the substitution indicating the presence of different unpaired electrons in the compounds.

**Table 4.15 Magnetic Susceptibility of Tetra amino metal Pcs**

<b>Sr.No</b>	<b>Name of Pcs</b>	<b><math>\chi_g</math>(CGS unit)</b>	<b><math>\mu_{\text{eff}}</math> (B.M)</b>
<b>01</b>	<b>TAFcPc</b>	<b><math>15.776 \times 10^{-6}</math></b>	<b>1.548</b>
<b>02</b>	<b>TAMnPc</b>	<b><math>11.568 \times 10^{-6}</math></b>	<b>1.3247</b>
<b>03</b>	<b>TACoPc</b>	<b><math>15.946 \times 10^{-7}</math></b>	<b>0.4934</b>
<b>04</b>	<b>TACuPc</b>	<b><math>8.4320 \times 10^{-7}</math></b>	<b>0.3601</b>
<b>05</b>	<b>TANiPc</b>	<b>Diamagnetic</b>	<b>-</b>
<b>06</b>	<b>TAZnPc</b>	<b>Diamagnetic</b>	<b>-</b>

#### 4.7 Diffuse Reflectance UV- visible Spectroscopy (DRS)

The spectra were recorded in solid state by loading the sample in a sample holder. The sample was scan from 200-800 nm. The technique is non-destructive and used to determine the band gap energy ( $E_g$ ) in semiconductors. The band-gap ( $E_g$ ) for the given Pcs were calculated by using formula, band gap (eV)  $E_g = 1239/\lambda_{\max}$ , where  $\lambda_{\max}$  is the maxima observed in UV/ visible region. The compounds are coloured in nature and therefore show absorption in the visible region.  $E_g$  is the measure of energy required to transfer an electron from valence band to conduction band. The absorbance spectra for MPcs in shown in Fig. 4.41 and the calculated band gaps are shown in Table 4.16

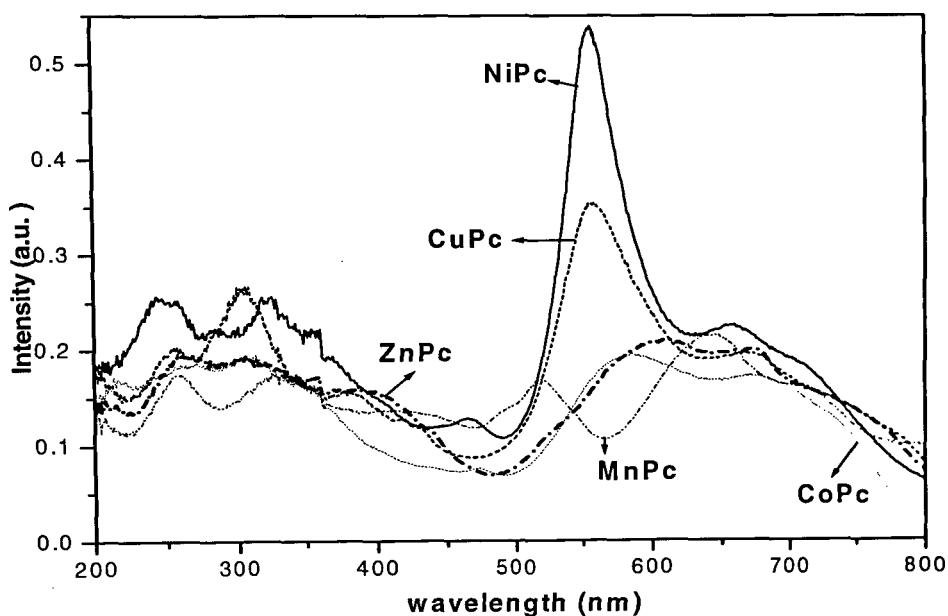
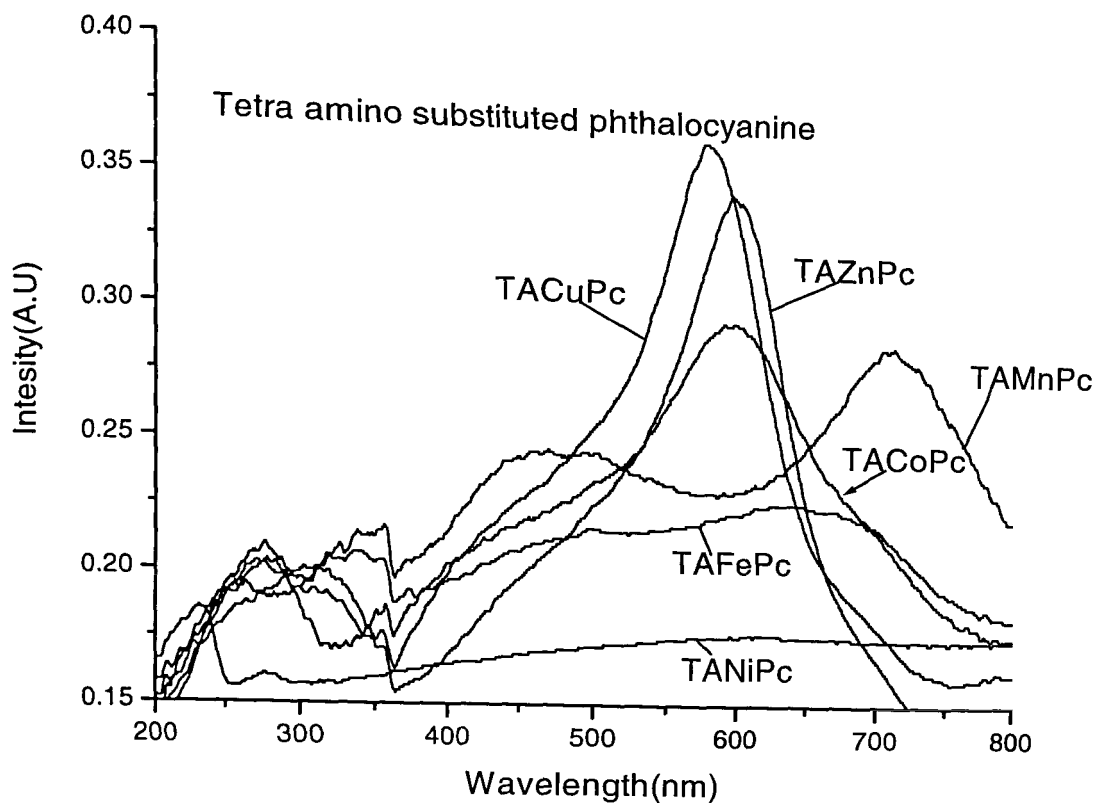


Fig 4.41 Absorbance spectra for metal Pcs

**Table 4.16 Band gap values of Metallophthalocyanines**

<b>Samples</b>	<b><math>\lambda_{\max}</math> (nm)</b>	<b>Band gap (eV)</b>
Mn Pc	324.96	3.812
Co Pc	308.3	4.021
Ni Pc	323.36	3.835
Cu Pc	303	4.091
Zn Pc	305.91	4.052

Under similar conditions the studies were extended to Tetra amino Pcs and the absorbance spectra for Tetra amino metal Pcs is shown in Fig. 4.42. The calculated band gaps are shown in Table 4.17. In both the cases of tetra substituted and non substituted Pcs, Mn as a central metal atom was found to have lower band gap energy, whereas similar relation is not valid in case of other metal substituted Pcs. This could be due to the interaction of different central metal atom with the electron donating amino group on the periphery of Phthalocyanines.



**Fig 4.42 Absorbance spectra for tetra amino metal Pcs**

**Table 4.17 Band gap values for Metallophthalocyanines**

Name	$\lambda_{(max)}(nm)$	Band Gap (eV)
TAMnPc	357	3.47
TAFcPc	354	3.50
TACoPc	357	3.47
TACuPc	305	4.06
TAZnPc	316	3.90
TANIcPc	276	4.49

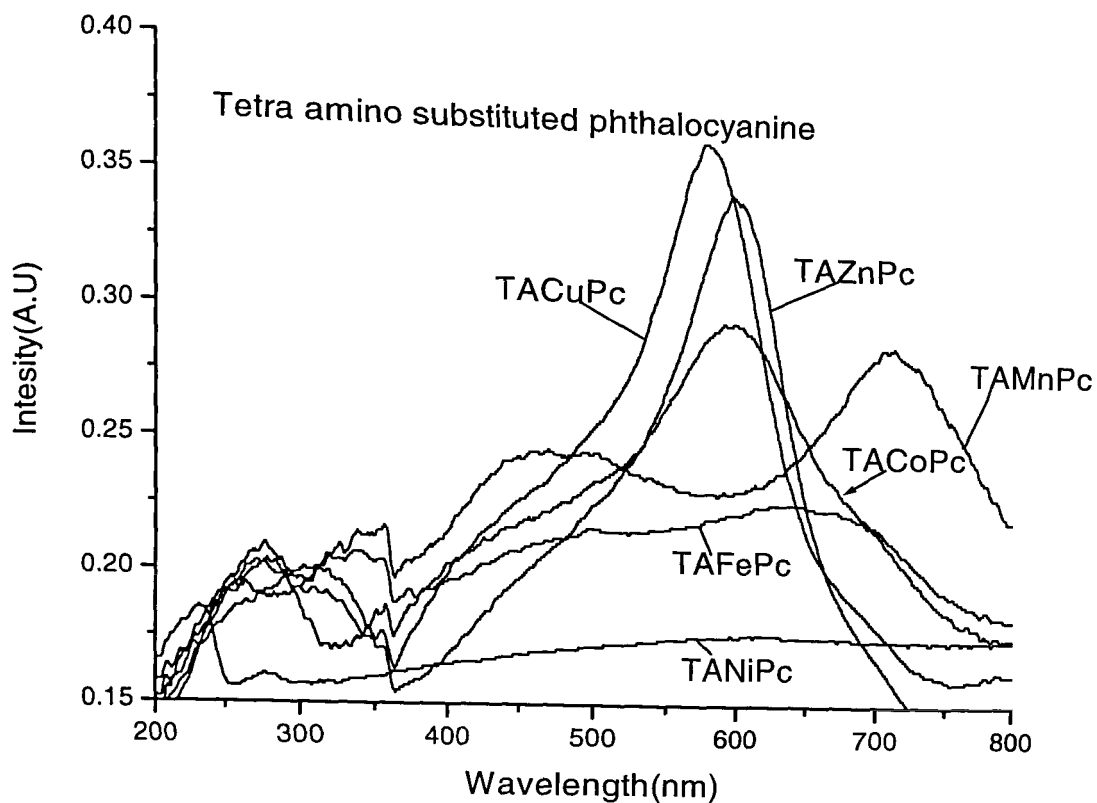


**Fig 4.42 Absorbance spectra for tetra amino metal Pcs**

**Table 4.17 Band gap values for Metallophthalocyanines**

Name	$\lambda_{(\max)}$ (nm)	Band Gap (eV)
TAMnPc	357	3.47
TAFcPc	354	3.50
TACoPc	357	3.47
TACuPc	305	4.06
TAZnPc	316	3.90
TANIcPc	276	4.49

## 4.8 Electron spin resonance

The basic feature of ESR spectra is strongly dependent on the number as well as the location of the unpaired electrons in a system. The information available from magnetic studies is used for the selection of the samples for ESR spectroscopy. ESR spectra of TACoPc, TACuPc, TAMnPc and TNFePc were recorded at room temperature as shown in Figs. 4.43- 4.46 and Table 4.18 which gives the calculated gyromagnetic (g) values and line-width. The g value indicated that the central metal is in +2 oxidation state. The spin- lattice relaxation for TACoPc at room temperature is sufficiently high to give sharp ESR peak with shorter line width. With change in central metal atom, the spin-orbital coupling is strongly coupled to the lattice vibration. This reduces the spin relaxation time, broadening the spectra with the increased line-width which depicts the increasing paramagnetic nature of the compound.

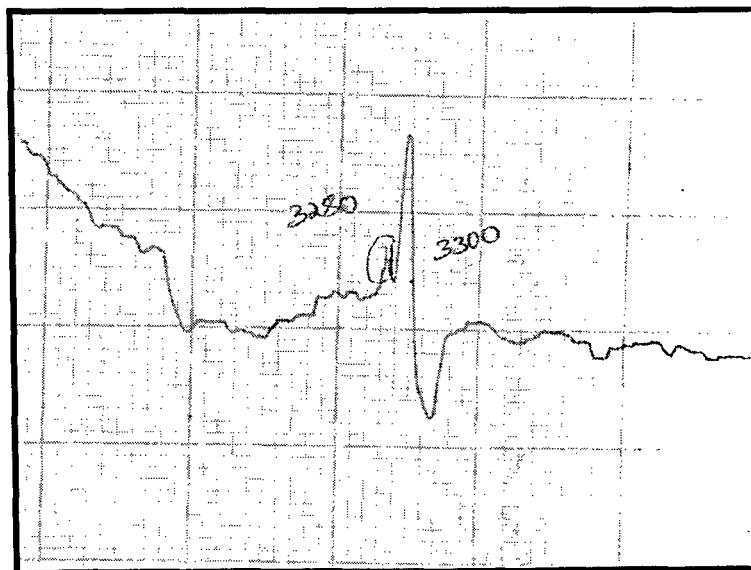


**Fig 4.43 ESR spectra of TACoPc**

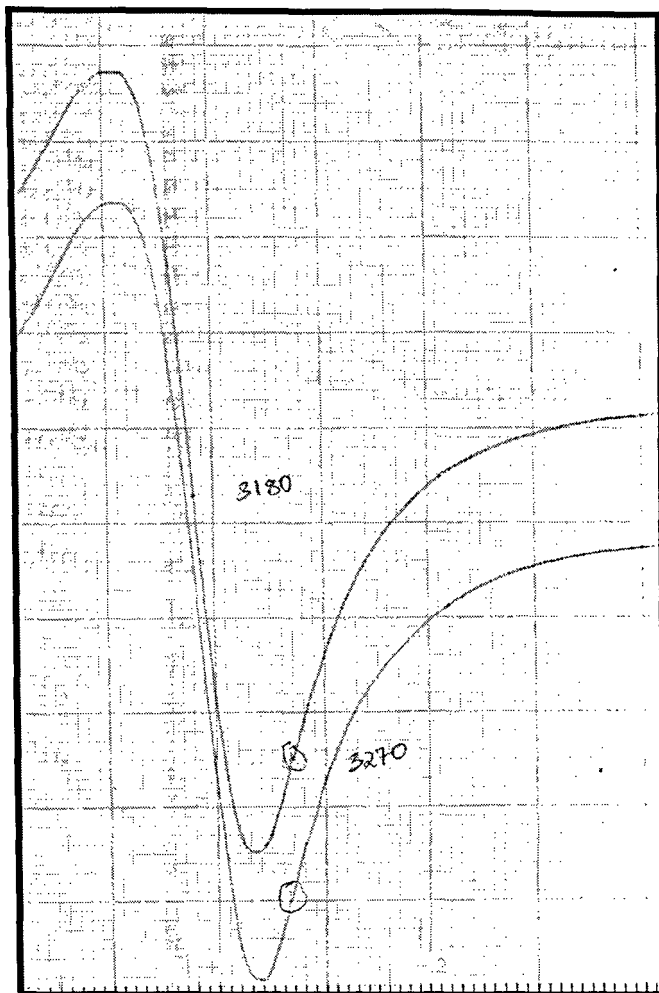


Fig 4.44 ESR spectra of TACuPc

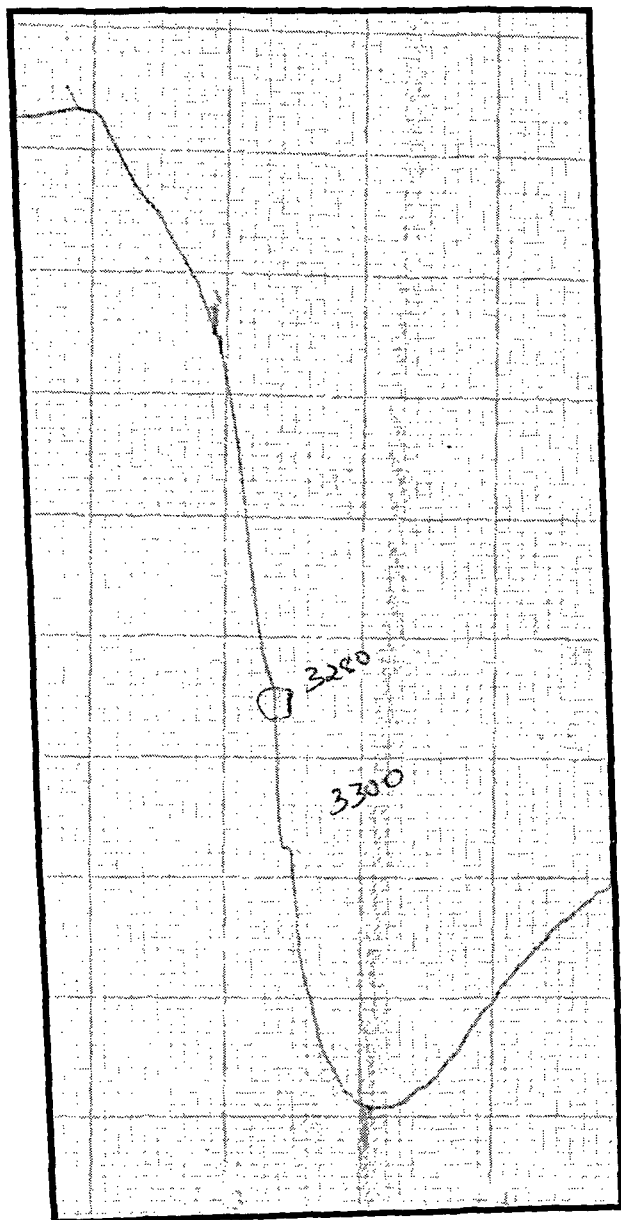


Fig 4.45 ESR spectra of TAFEPC



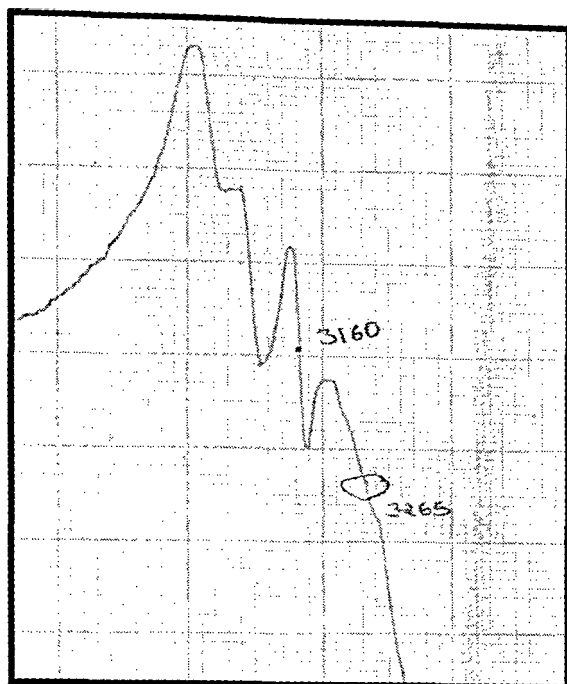


Fig 4.46 ESR spectra of TAMnPc

Table 4.18 ESR measurement for TAMnPc, TACoPc, TAFcPc and TACuPc

Name	g calculated	Line-width (G)
TAMnPc	2.07	30
TACoPc	1.99	30
TAFcPc	1.99	220
TACuPc	2.059	110

## 4.9 NMR spectroscopy

To study the structure of 4-nitrothalimide, the compound was hydrolyzed to its corresponding acid and the NMR was recorded in DMSO solution as shown in Fig 4.47. The Value obtained were assigned as follow 7.64 (d,  $J=8.4$  Hz,  $H_3$ ), 8.20 (dd,  $J=2.4$  Hz,  $H_5$ ), 8.36 (d,  $J=2.4$  Hz,  $H_6$ ), 8.94 (br.s,  $J=2.4$ Hz, -N-H).

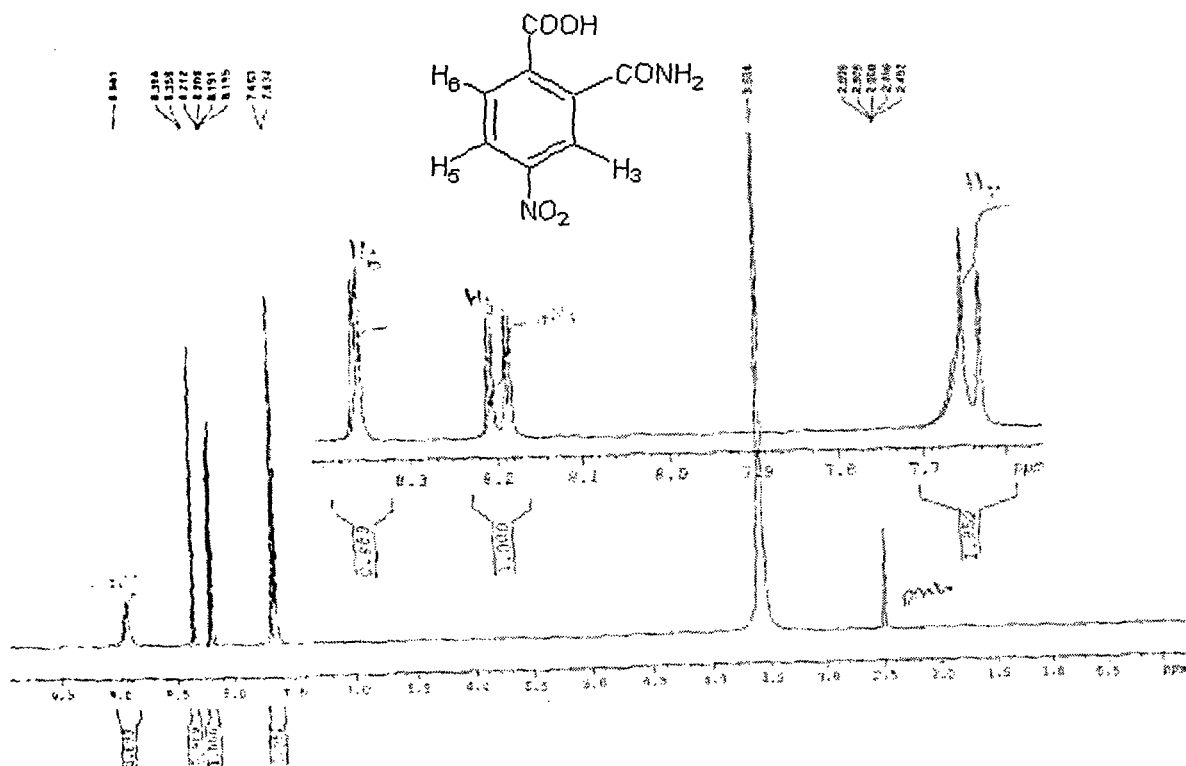


Fig 4.47 NMR spectrum of 2-carbamoyl-4-nitrobenzoic acid

#### 4.10 Photoluminescent studies

The luminescence properties of the materials were studied by analyzing the photoluminescence spectra of the material in the visible region from 400-800 nm. The photoluminescence spectra and the corresponding excitation spectra were recorded at the room temperature using Shimadzu RF-5301 PC Spectrofluorometer with Xe flash lamp.

Figs.4.48-4.50 show the photoluminescence spectra for the non substituted MPcs

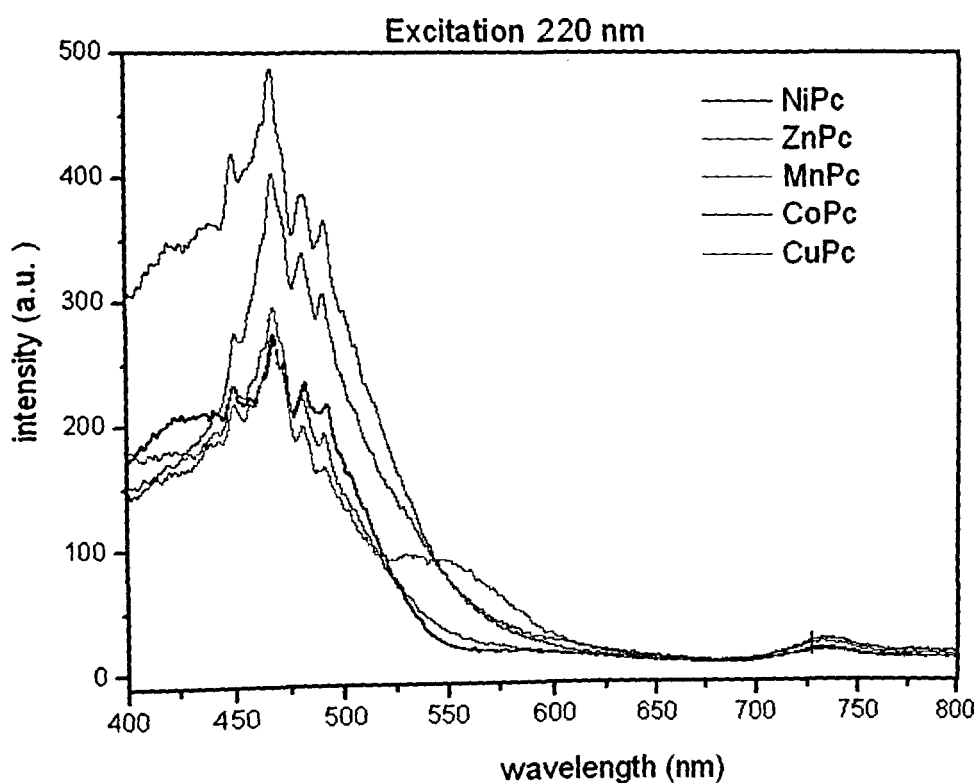
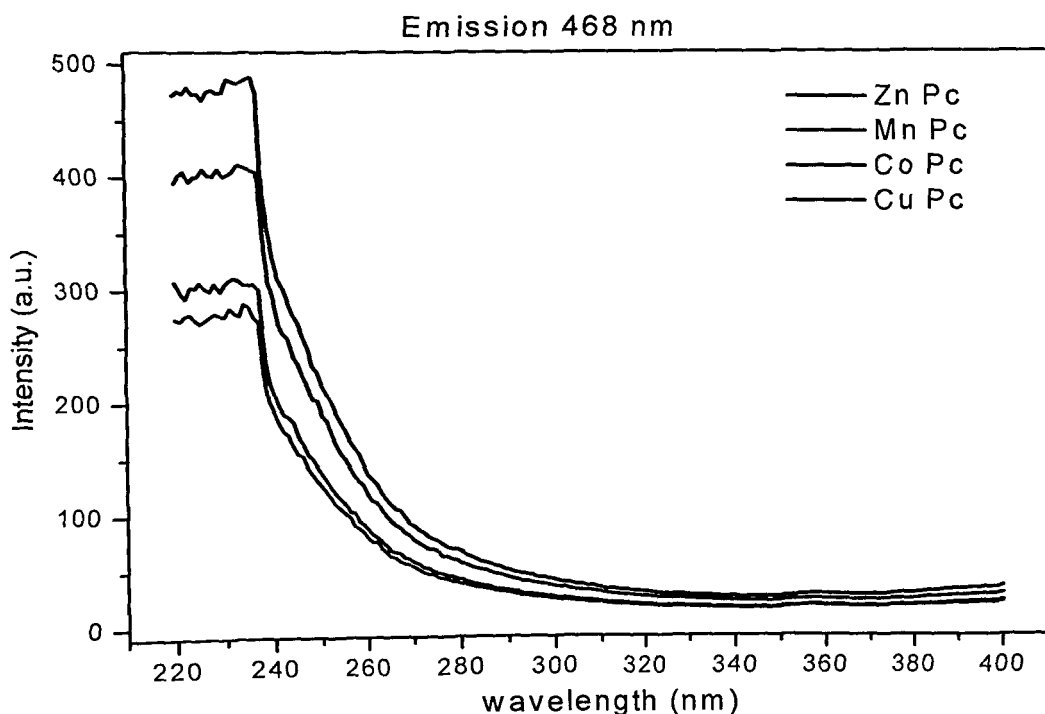


Fig. 4.48 PL spectra with excitation at 220 nm

Samples on excitation at wavelength of 220 nm show emission in the blue-green region i.e. from 430-550 nm. All the samples show same spectra with several emission lines in blue green region showing maximum emission at 468 nm. Presence of several intrinsic levels in the conduction bands gives this complex spectrum. Influence of transition metals resulted in different intensities. The emission intensity of cobalt phthalocyanine is maximum followed by zinc phthalocyanine, copper phthalocyanine, nickel phthalocyanine and manganese phthalocyanine. Zinc phthalocyanine, copper phthalocyanine and nickel phthalocyanine show low intensity because of non radiative processes that occurs more than the radiative processes.



**Fig. 4.49** Excitation spectra of 468 nm PL emission for MPc

The excitation pattern observed is in the range of 220-240 nm and the intensity is similar to that observed in the emission spectra.

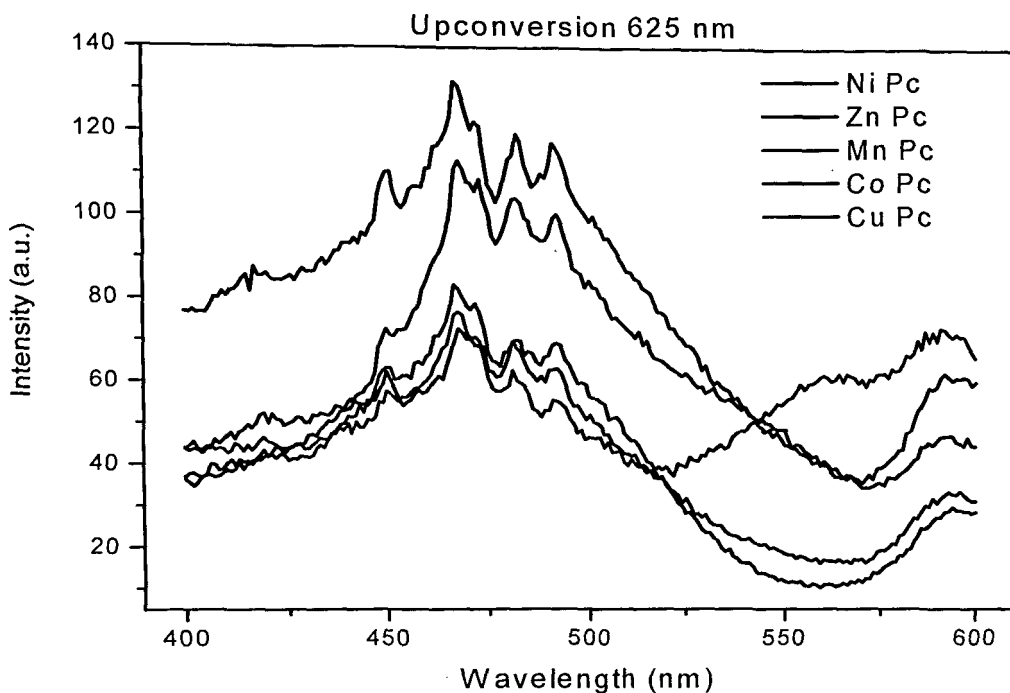


**Fig. 4.50 PL spectra with Up-conversion at 625 nm**

Up-conversion is observed in all the samples by keeping the slit width same. Sample was excited with *different wavelength in the range 580-650 nm*, of which 625 nm showed the up-conversion at 440-550 nm with maximum intensity. The up-conversion pattern was similar to for the excitation at 220 nm and 625 nm emission patterns were similar, indicating that in both the cases, the emission centers are same. The up-conversion process may be explained by anti stokes two photon theory i.e. when the samples are irradiated at 625 nm, the first photon pumps the electron from the conduction band to the intermediate level and the second photon ionizes it to the conduction. When the electrons are recaptured or transfer energy in the valence band, intrinsic emission occurs and while the

recombination or transfer of energy in the intermediate level gives the emission at lower wavelength. Similar observation were also recorded on TCMPC as shown in Figs. 4.51 – 4.53 , but the order of intensity was not comparable with that of non substituted MPcs. This could be attributed for the different level of interaction between the central metal atom and that of the substituted group on the periphery of the phthalocyanine ring.

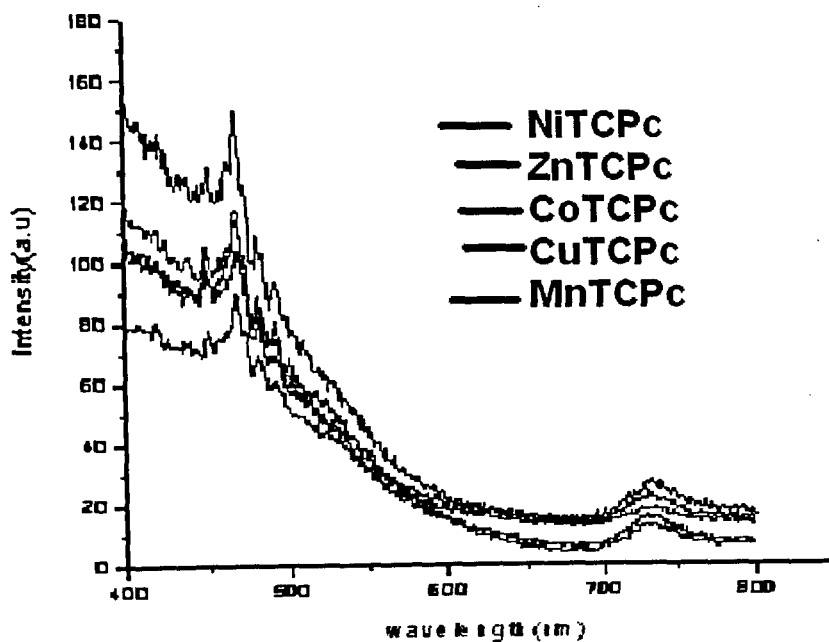


Fig. 4.51 PL spectra with excitation at 220 nm for TCMPC

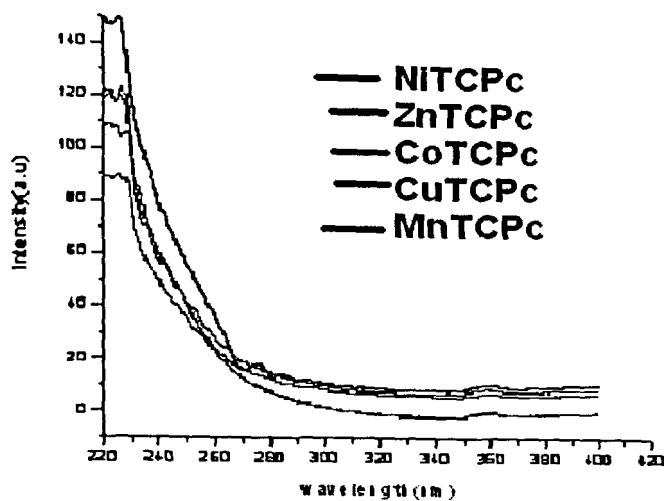


Fig.4.52 Excitation spectra of 468 nm PL emission for TCMPC

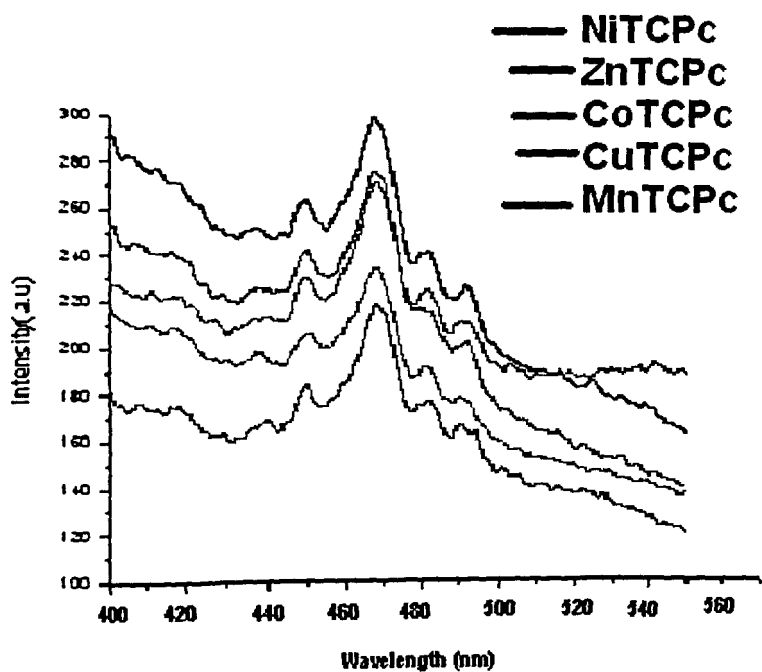
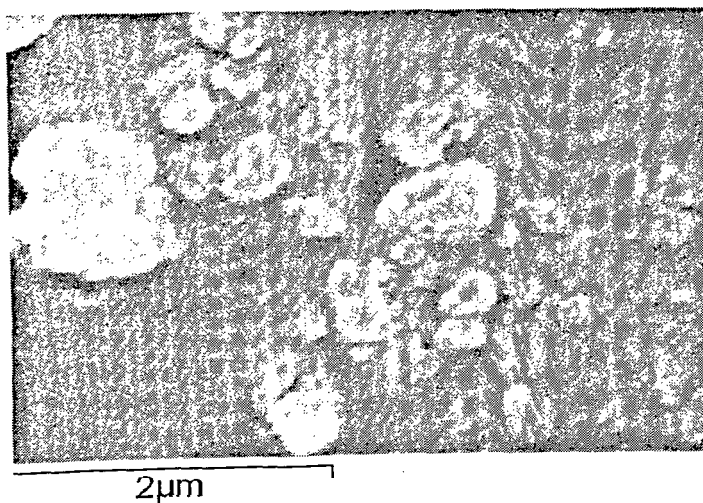


Fig.4.53 PL spectra with Up-conversion at 625 nm for TCMPC

#### 4.11 Scanning Electron Microscopy

SEM was recorded with a resolution of 2  $\mu\text{m}$ . A gold coating was deposited on the sample to avoid charging of the surface. The SEM images for TACoPc, TANiPc, TAFcPc, TCNiPc and TCCoPc are shown in Figs. 4.54-4.58. From the image it was observed that the sample exist in an agglomerate form with a particle size < 100 nm but the particle size was not uniform and due to agglomeration exact measurement was difficult. In case of TAFcPc less agglomeration was observed as compared to others. The TCCoPc also showed good surface morphology with less agglomeration. If a comparison is made between TANiPc and TCNiPc and also with TACoPc and TCCoPc the surface morphology obtained after substitution of acrylic group is better than the amino group. The main reason behind this is the precipitation technique used for the purification of compound which leads to decrease in the size of the particle.



**Fig.4.54 SEM of TACoPc**



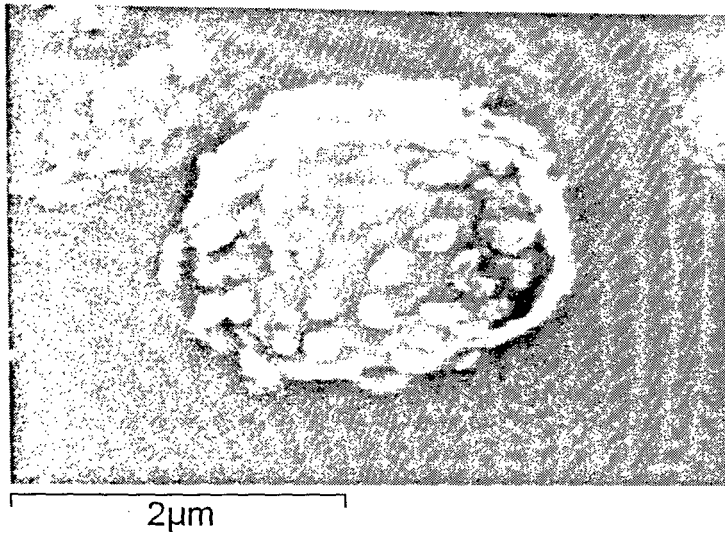


**Fig.4.55 SEM of TANiPc**

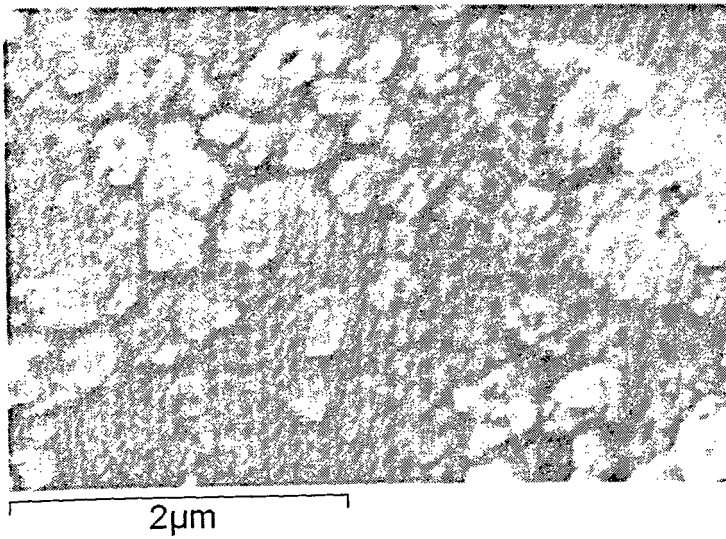


**Fig.4.56 SEM of TAFEPC**

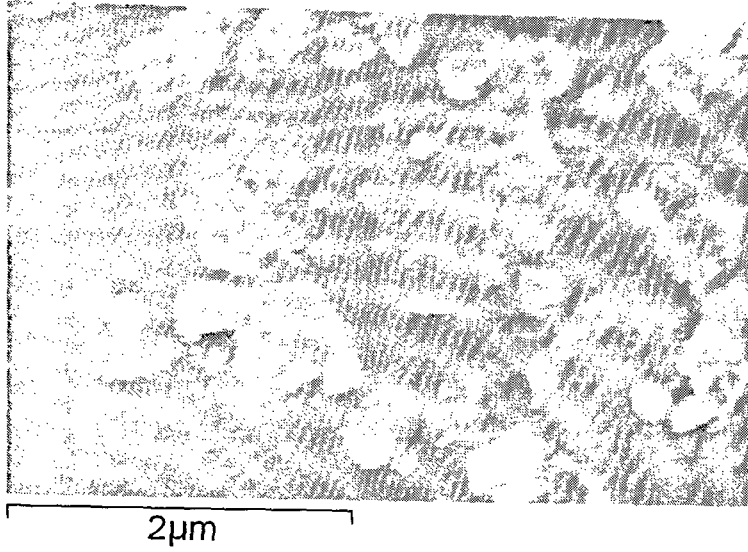


**Fig.4.57 SEM of TCNiPc**

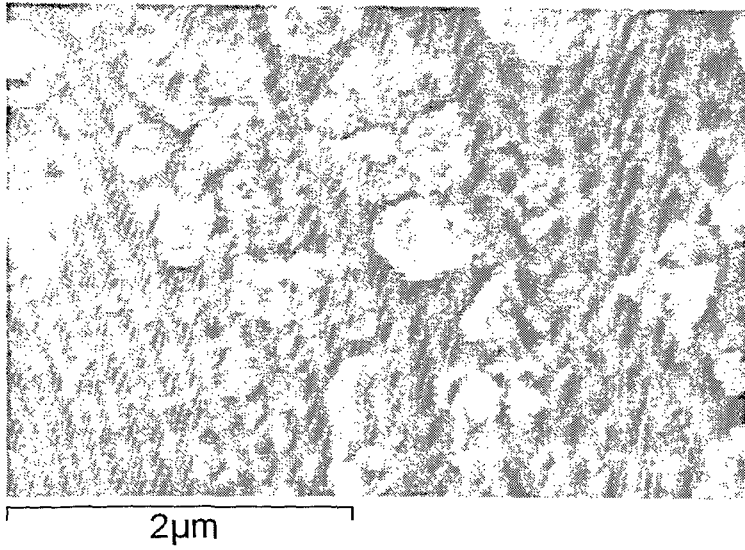


**Fig.4.58 SEM of TCCoPc**

# CHAPTER 5

*CATALYTIC*

*AND*

*ANTIMICROBIAL*

*STUDIES*

## Introduction

Semiconductor photocatalysts are excellent materials for the degradation of various pollutants. Pcs are well known semiconductors their photocatalytic activities were studied on different dyes. Water soluble Pcs synthesized were used for catalytic oxidation of Benzoin to Benzil. Naturally occurring Lawson was synthesized by heterogeneous catalytic oxidation of 2-hydroxy naphthalene in aqueous medium. Antimicrobial activities of Pcs were tested on different microbial pathogens.

### 5.1 BET Surface area measurement

The surface area of the sample was measured using BET instrument SMATSORB 90/91 at the boiling of nitrogen temperature. The results obtained for different non substituted Pc in comparison to that of tetra nitro metal Pc was higher, highest surface area was recorded in case of MnPc and lowest in case of TNCuPc. The recorded value of surface area are shown in Table 5.1

**Table 5.1 Surface area measurement**

Sr. No.	Sample	Surface area
1	CoPc	21.13
2	TNCoPc	19.12
3	CuPc	10.45
4	TNCuPc	3.43
5	MnPc	26.2
6	TNMnPc	10.15

## 5.2 Photocatalytic degradation of Amido Black 10B

Photocatalytic degradation was studied on Amido Black 10B which has a  $\lambda_{\max}$  617-619 nm using MPcs such as MnPc, CoPc, NiPc, CuPc and ZnPc. This study was carried out at different pH i.e. neutral (pH=7), alkaline (pH=8) and acidic (pH=6).  $10^{-5}$  M solution of the dye was prepared. The solution was oxygenated by bubbling with air for 5 minutes. 20 mg of the catalyst was weighed and added to 100 ml of the oxygenated dye solution. The solutions were then irradiated under sunlight. The absorbance of each solution was recorded at different time interval i.e. 1 h, 2 h, 3 h, and 4 h using UV-visible spectrometer.

Similar procedure was repeated in alkaline medium wherein the dye solution was made alkaline by adding drop wise 0.5 N NaOH till pH 8. Similarly the dye solution was made acidic by adding 0.5 N HNO<sub>3</sub> till pH 6. Table 5.2, 5.3 and 5.4 represents the absorbance data in neutral, alkaline and acidic medium respectively. Fig. 5.1, 5.2 and 5.3 shows absorbance against time plots

**Table 5.2 Absorbance data at pH=7**

Samples	Absorbance in nm				
	0 h	1 h	2 h	3 h	4 h
Blank	0.2572	0.2568	0.2562	0.2555	0.2551
MnPc	0.2572	0.206	0.2141	0.2137	0.1879
CoPc	0.2572	0.2515	0.2396	0.2383	0.1737
NiPc	0.2572	0.2545	0.2515	0.2458	0.2301
CuPc	0.2572	0.2154	0.1334	0.040	0.034
ZnPc	0.2572	0.2556	0.2559	0.2562	0.2565

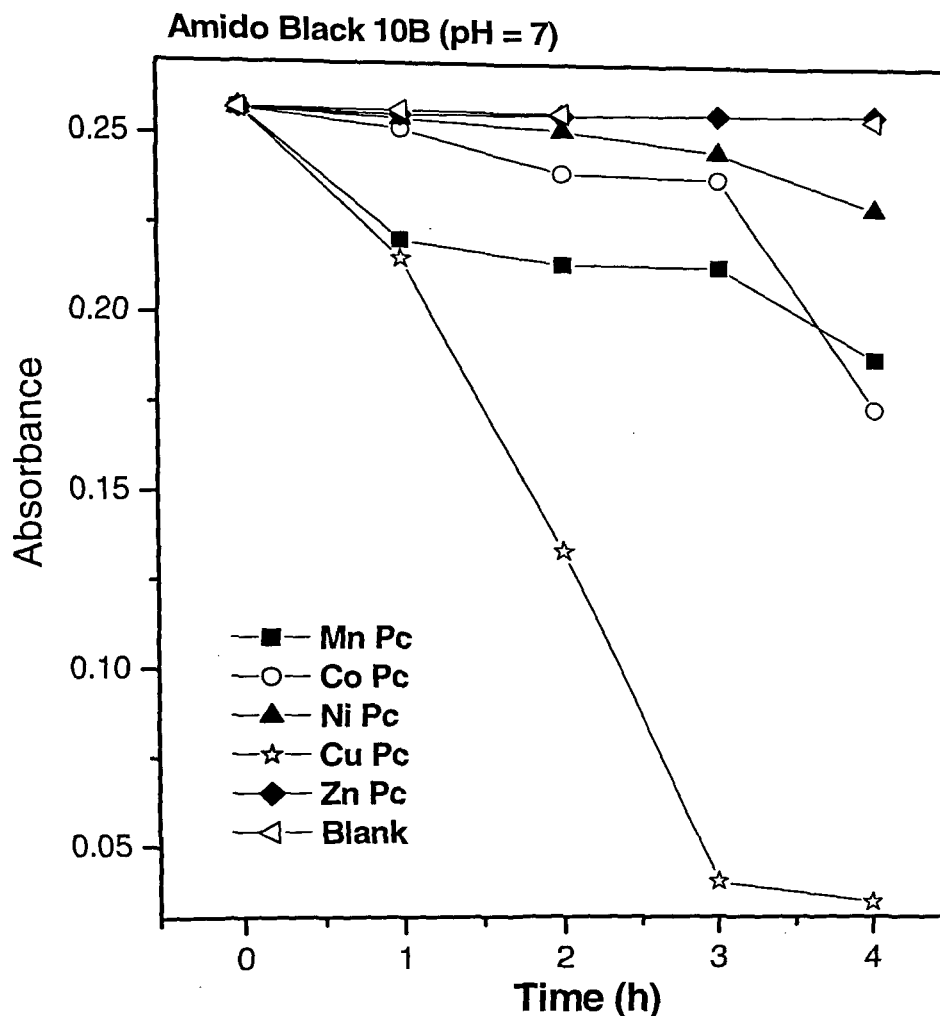


**Fig. 5.1 Absorbance against time plot at pH=7**

In neutral pH copper phthalocyanine showed high catalytic activity as compared to other phthalocyanines. Manganese phthalocyanine and cobalt phthalocyanine showed less catalytic activity whereas zinc phthalocyanine and nickel phthalocyanine did not showed any appreciable degradation of the dye.

**Table 5.3 Absorbance data at pH=8**

Samples	Absorbance in nm				
	0 h	1 h	2 h	3 h	4 h
Blank	0.2783	0.2776	0.2768	0.2761	0.2755
MnPc	0.2783	0.2711	0.2007	0.1929	0.1661
CoPc	0.2783	0.2258	0.2040	0.1540	0.1190
NiPc	0.2783	0.2781	0.2779	0.2775	0.2773
CuPc	0.2783	0.1943	0.1750	0.1150	0.0910
ZnPc	0.2783	0.2784	0.2786	0.2790	0.2792

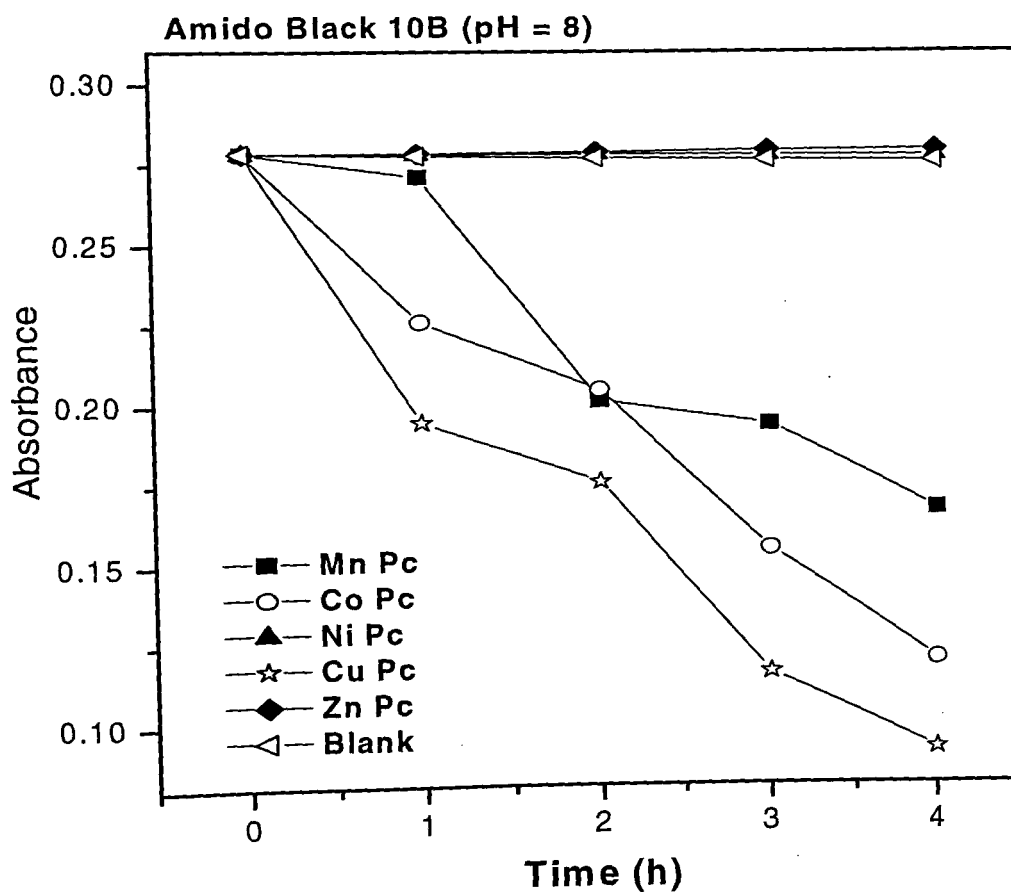


**Fig. 5.2 Absorbance against time plot at pH=8**

In alkaline pH copper phthalocyanine retained its activity as that in neutral pH. The catalytic activity of manganese phthalocyanine and cobalt phthalocyanine increased in alkaline medium but no degradation of dye was observed in presence of nickel phthalocyanine and zinc phthalocyanine.

**Table 5.4 Absorbance data at pH=6**

Samples	Absorbance in nm				
	0 h	1 h	2 h	3 h	4 h
Blank	0.2193	0.2189	0.2187	0.2184	0.2182
Mn Pc	0.2193	0.1325	0.1206	0.1150	0.0750
Co Pc	0.2193	0.2100	0.1910	0.1850	0.1590
Ni Pc	0.2193	-	-	-	0.1981
Cu Pc	0.2193	0.1170	0.0916	0.0480	0.0400
Zn Pc	0.2193	-	-	-	0.2182



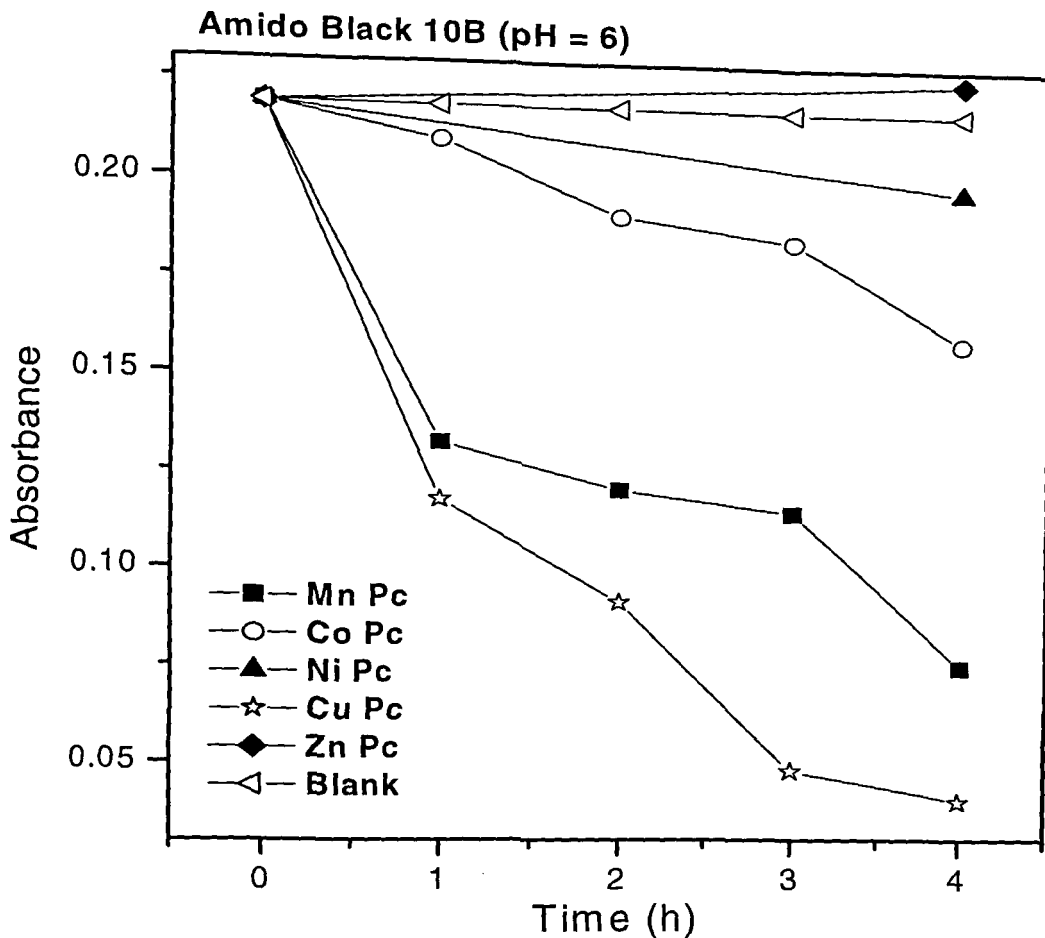


**Fig. 5.3 Absorbance against time plot at pH=6**

In acidic pH copper phthalocyanine showed the highest rate of dye degradation. Manganese phthalocyanine showed increase in activity than in neutral pH but cobalt phthalocyanine showed less activity. There was no effect of pH on nickel phthalocyanine and zinc phthalocyanine as it did not show any activity. Fig 5.4 and 5.5 show representative UV-visible spectra of degradation pattern on CuPc at pH 7 and pH 6. The main reason for CuPc showing maximum activity as compared to others may be because of the ability of Cu to go in +1 oxidation state which is not observed in case of Zn and other metal.

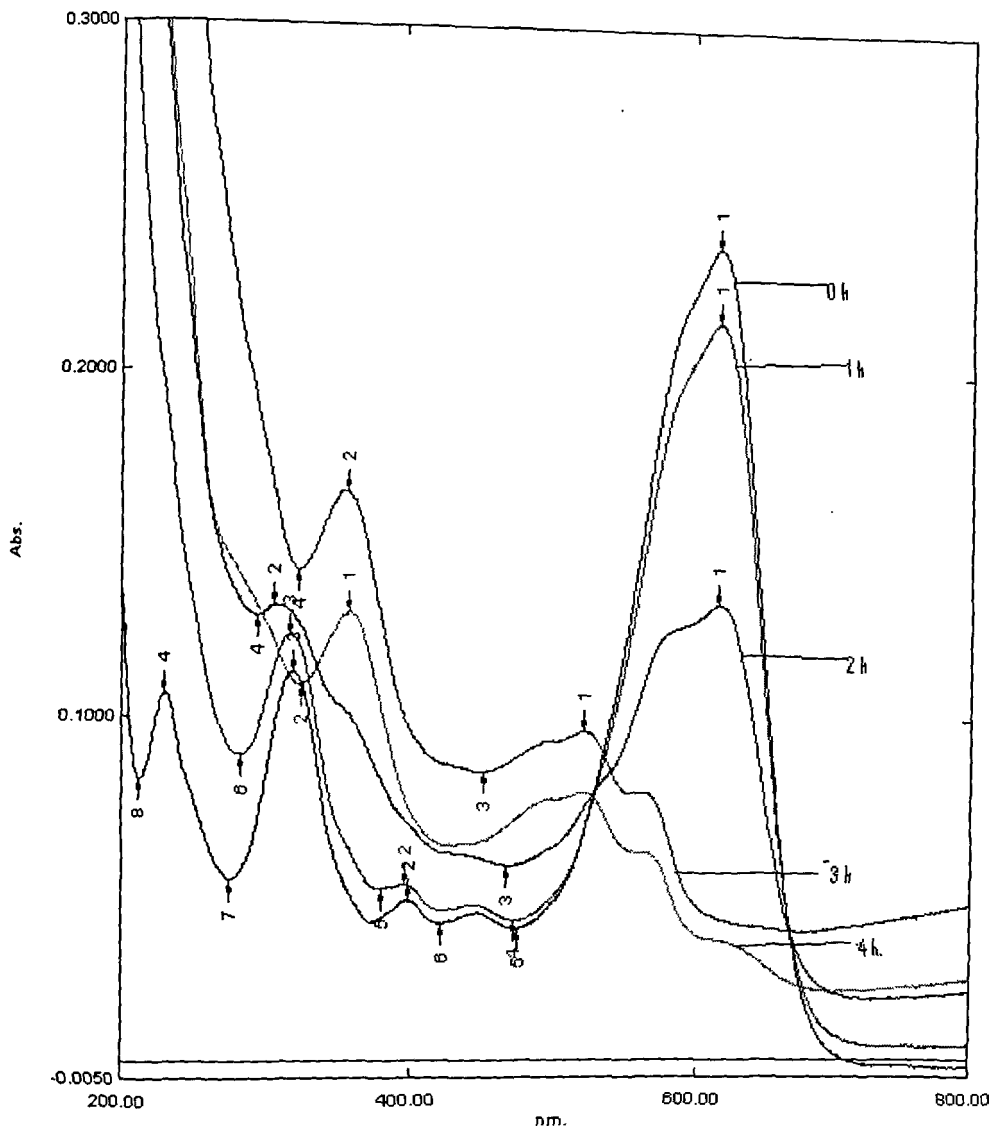


**Fig. 5.4 UV-visible spectra of Amido Black 10B over CuPc catalyzed reaction at pH=7 at different interval period.**

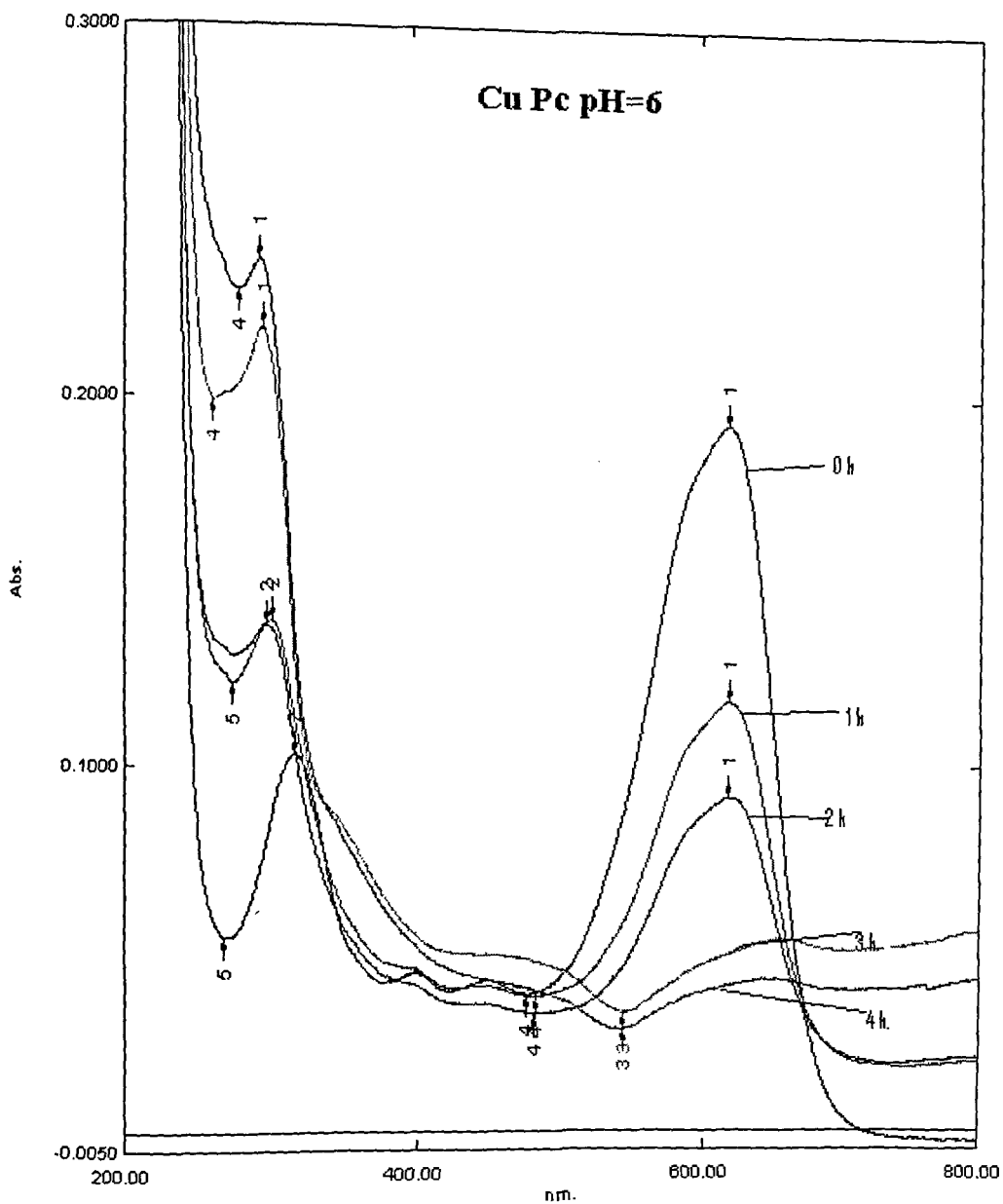


**Fig. 5.5 UV-visible spectra of Amido Black 10B over CuPc catalyzed reaction at pH=6 at different interval period.**

### 5.3 Photocatalytic degradation of Auramine O

Photocatalytic degradation was studied on Auramine O which has a  $\lambda_{\max}$  430-432 nm using MPcs such as MnPc, CoPc, NiPc, CuPc and ZnPc. This study was carried out at neutral (pH=7).  $10^{-5}$  M solution of the dye was prepared. The solution was oxygenated by bubbling with air for 5 minutes. 100 mg of the catalyst was weighed and added to 100 ml of the oxygenated dye solution. The solutions were then irradiated under sunlight. The absorbance of each solution was recorded at different time interval i.e. 1 h, 2 h, 3 h, and 4 h using UV-visible spectrometer. Table 5.5 represents the absorbance data in neutral medium respectively. Fig. 5.6 shows absorbance against time plots of dye degradation.

**Table 5.5 Absorbance data at neutral pH**

Samples	Absorbance in nm				
	0 h	1 h	2 h	3 h	4 h
MnPc	0.3293	0.2255	0.1882	0.1412	0.0469
CoPc	0.2866	0.1740	0.1520	0.1510	0.114
NiPc	0.2866	0.1792	0.1782	0.1608	0.1571
CuPc	0.2995	0.1034	0.0826	0.0551	0.0344
ZnPc	0.2995	0.0958	0.0717	0.0620	0.0570

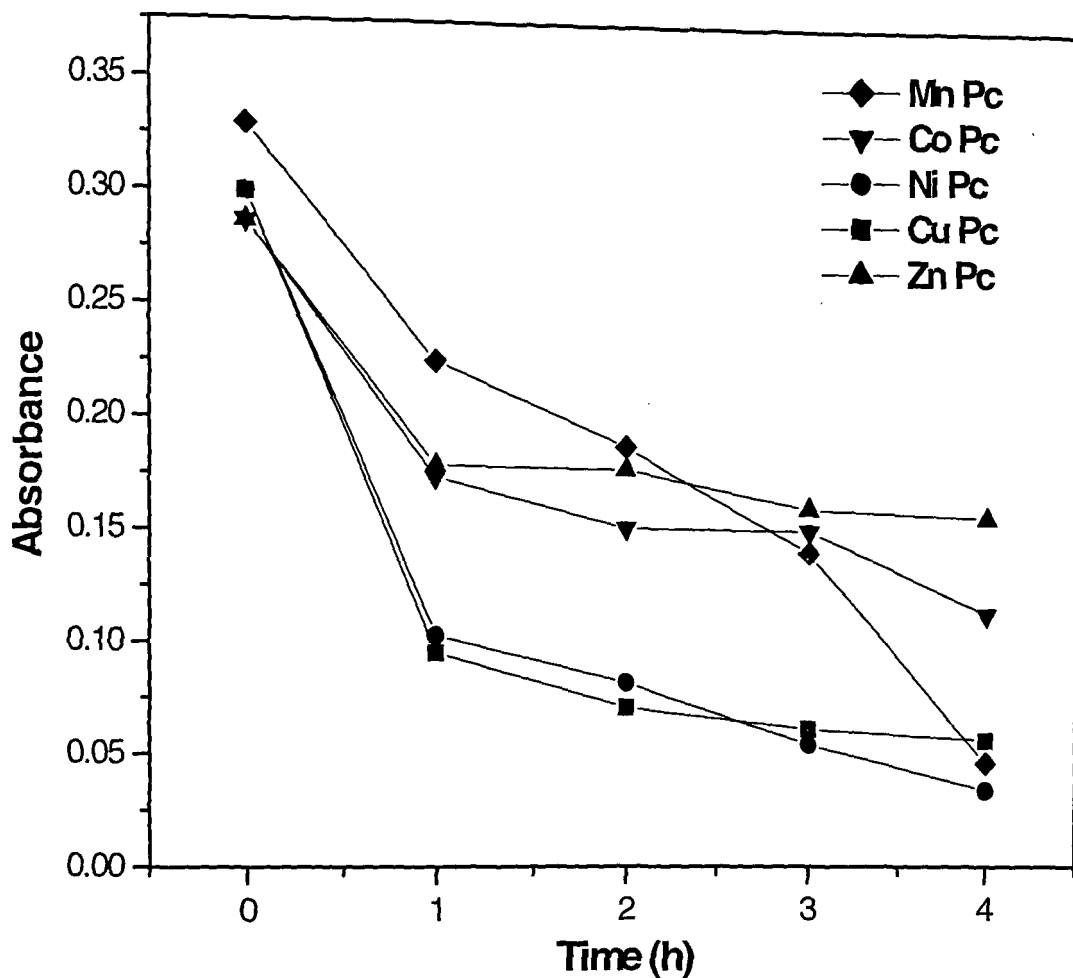


**Fig. 5.6 Absorbance against time for the degradation of Auramine**

Copper and Nickel phthalocyanine showed high catalytic activity as compared to other phthalocyanines. Manganese phthalocyanine and cobalt phthalocyanine showed less catalytic activity but Manganese phthalocyanine showed good activity at the end of 4 h. Whereas zinc phthalocyanine did not show appreciable degradation of the dye. Fig. 5.7-5.8 show representative UV-Visible spectra of Auramine O degradation using CoPc, MnPc and ZnPc.

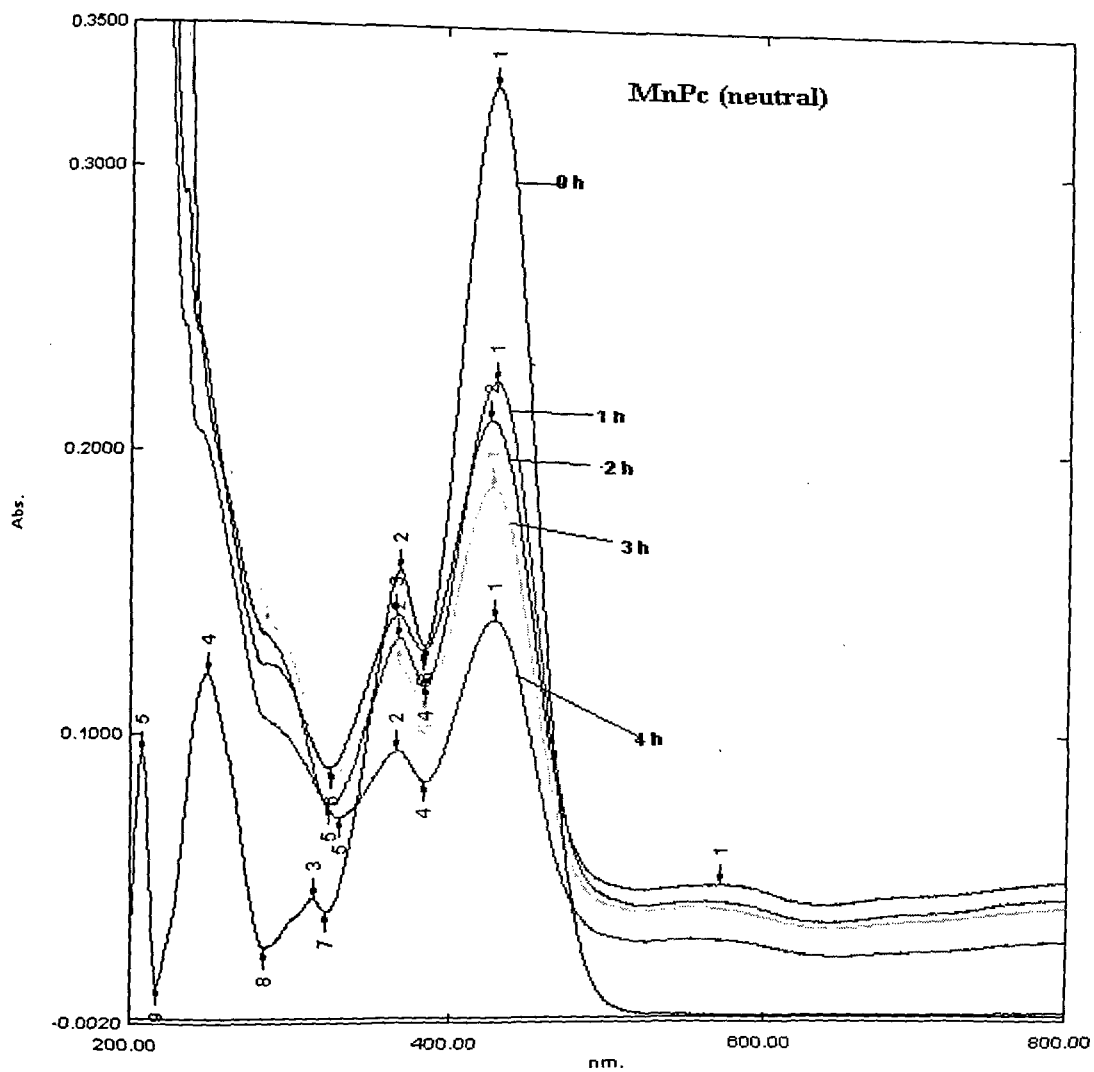


Fig. 5.7 UV-visible spectra of MnPc catalyzed degradation of Auramine O

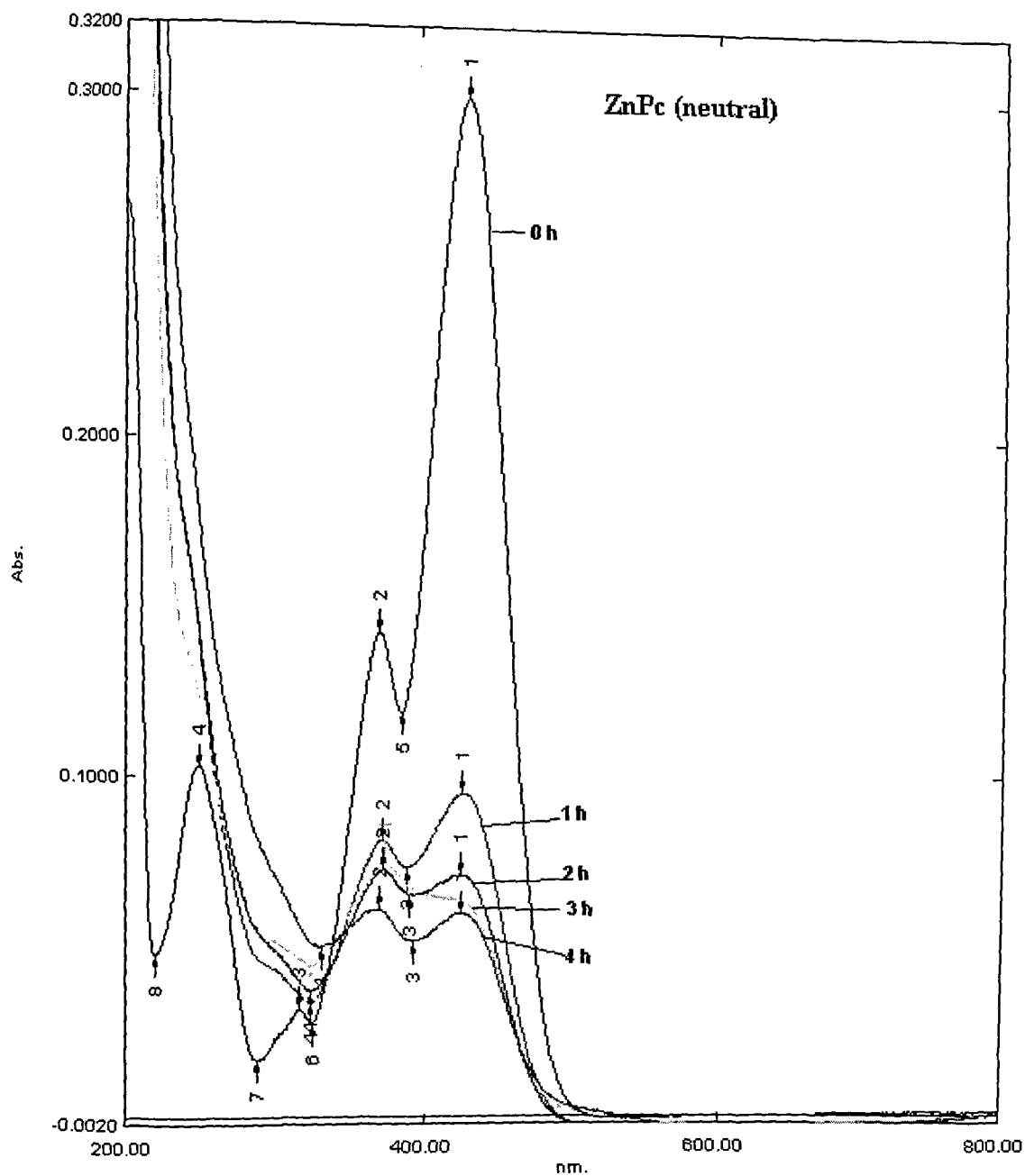


Fig. 5.8 UV-visible spectra of ZnPc catalyzed degradation of Auramine O

#### 5.4 Photocatalytic degradation of Methylene blue

Photocatalytic degradation was studied for Methylene blue which has a  $\lambda_{\max}$  663-665 nm using TNMnPc, TNCOPc, TNNiPc, TNCuPc , TNZnPc , TAMnPc, TACOPc, TANiPc, TACuPc and TAZnPc. This study was carried out at neutral (pH=7). $10^{-5}$  M solution of the dye was prepared. The solution was oxygenated by bubbling with air for 5 minutes. 100 mg of the catalyst was weighed and added to 100 ml of the oxygenated dye solution. The solutions were then irradiated under sunlight. The absorbance of each solution was recorded at different time interval i.e. 1 h, 2 h, 3 h, and 4 h using UV-visible spectrometer.

Based on the time required for degradation, the data is divided into two groups in group I there are Pcs where degrade methylene blue after 3 and 4 hours where as in group II there are Pcs where methylene blue degrade after 1 and 2 hours Fig. 5.9 shows absorbance with time plots for group I and Fig. 5.10 shows absorbance with time plots for group II.

Figs 5.11-5.12 are UV-Visible spectra of methylene blue degradation using CuTAPc and CuTNPc.



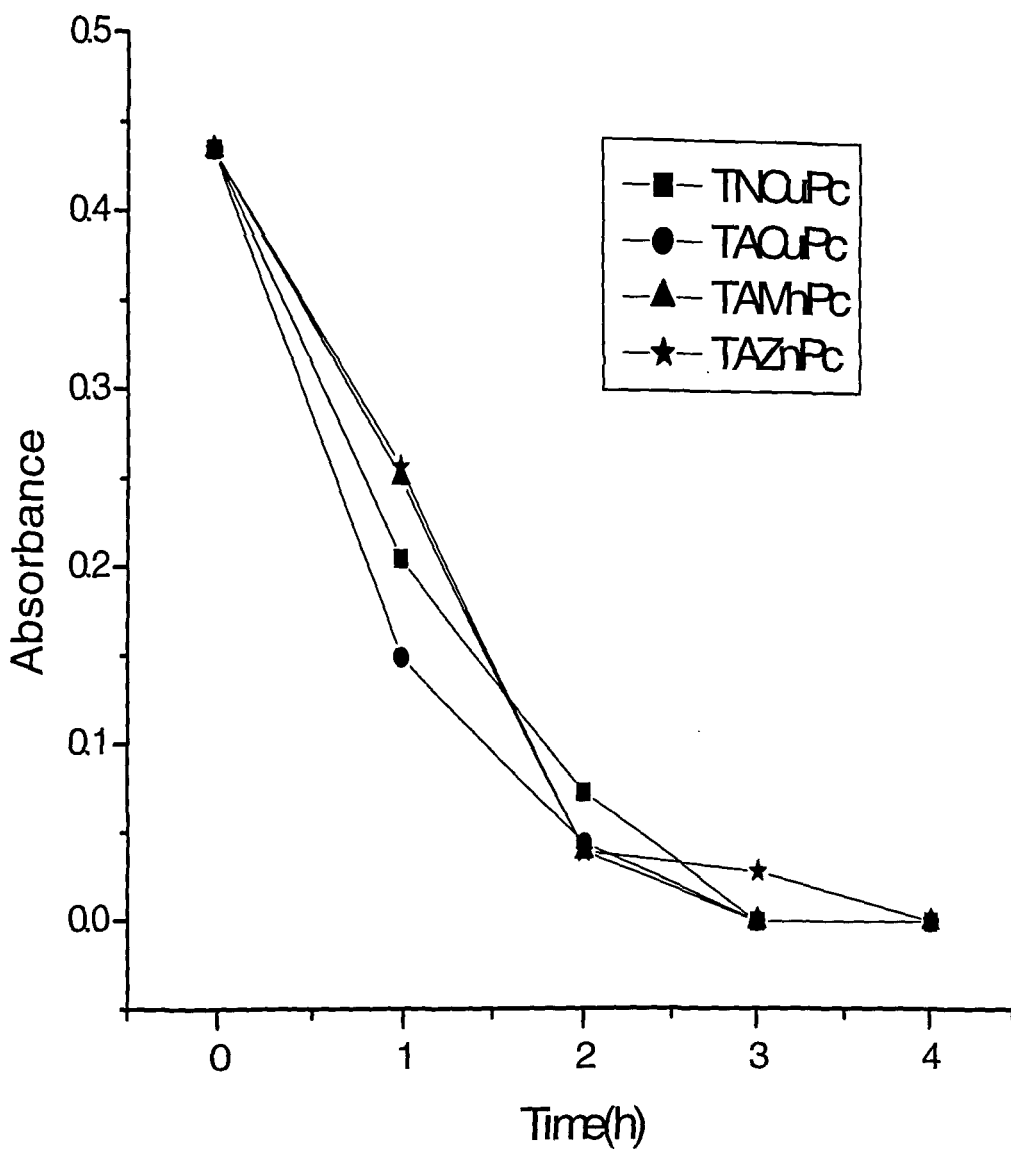


Fig. 5.9 Absorbance against time for the degradation of Methylene Blue by group I Pcs

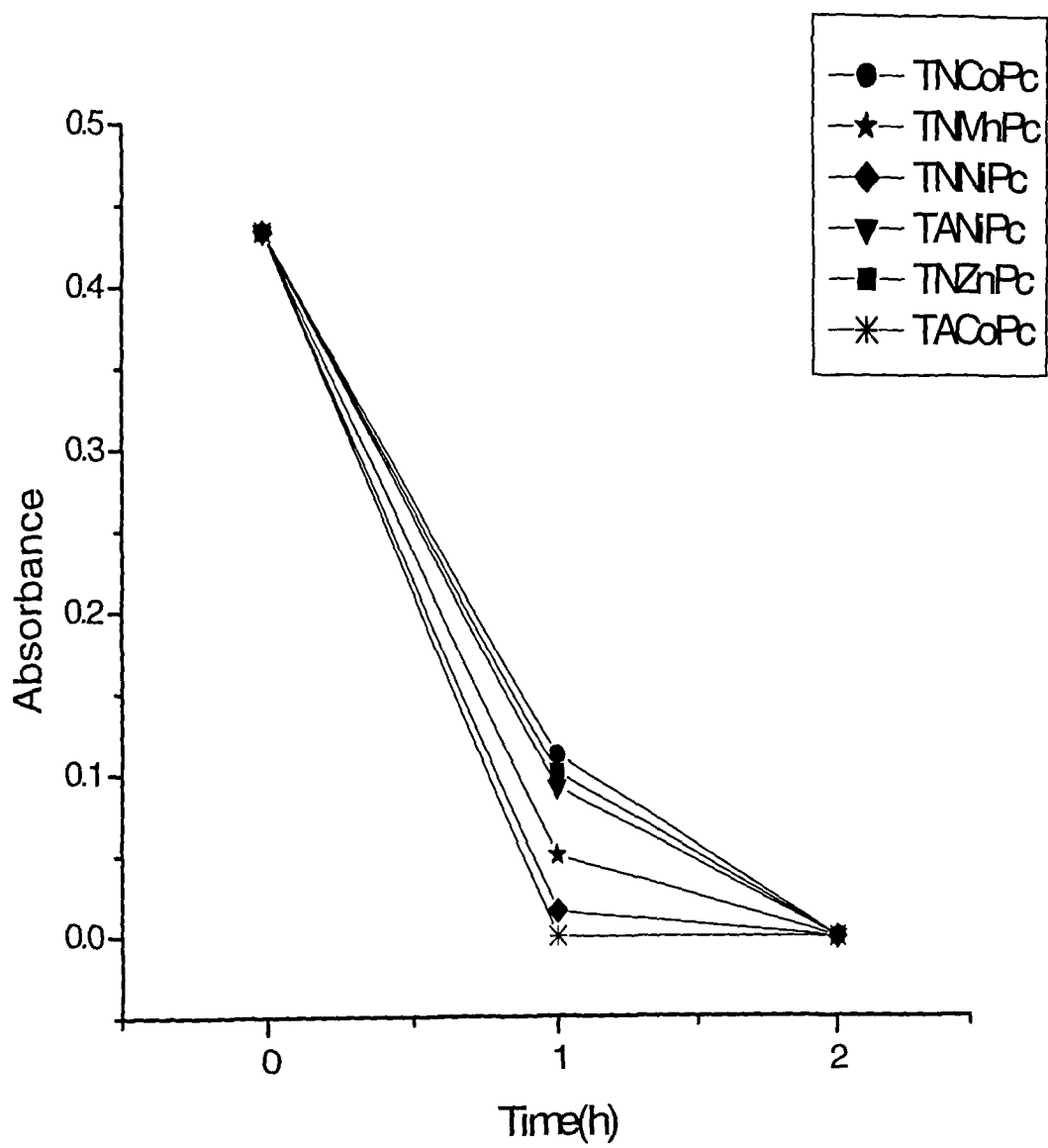
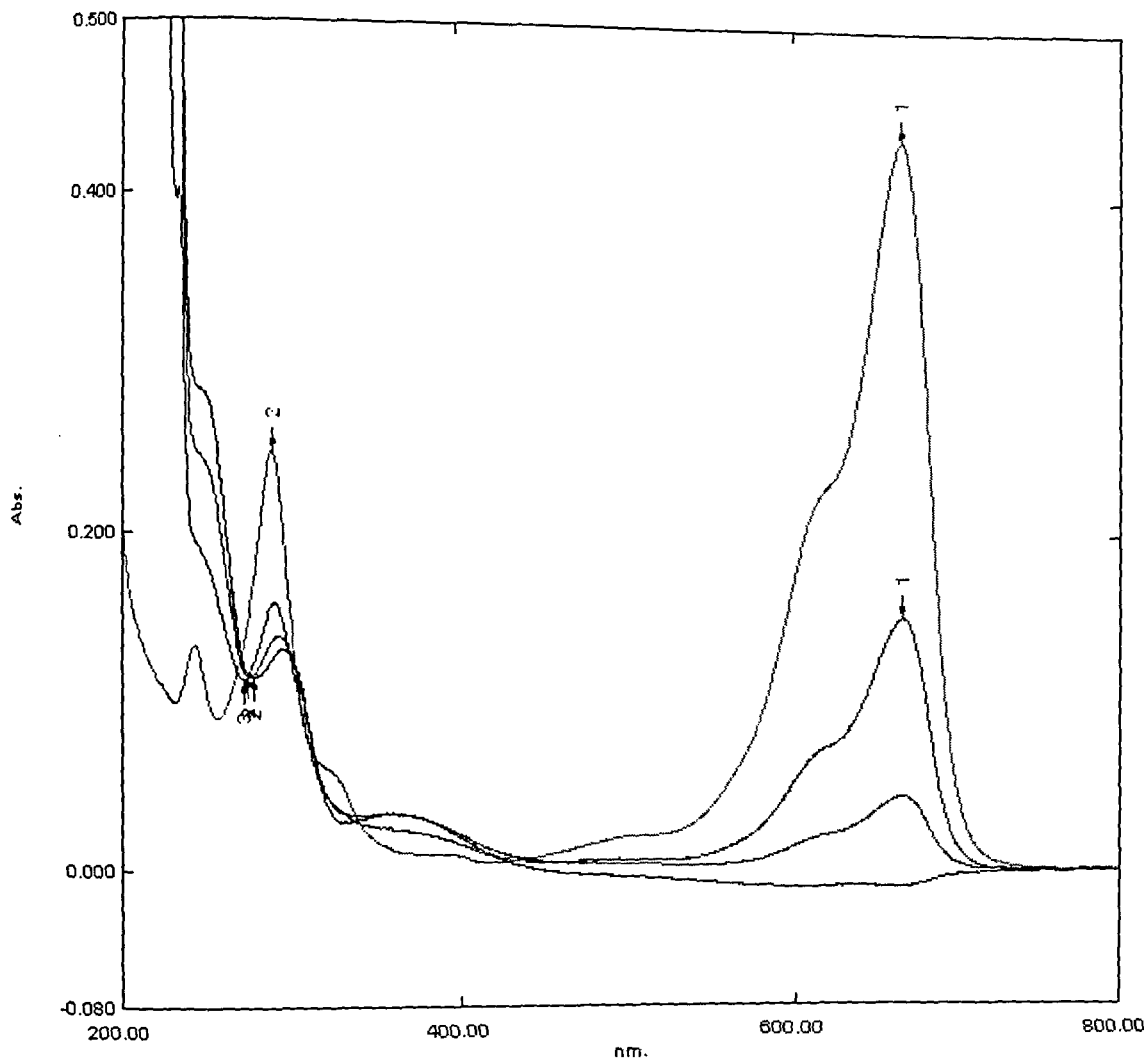
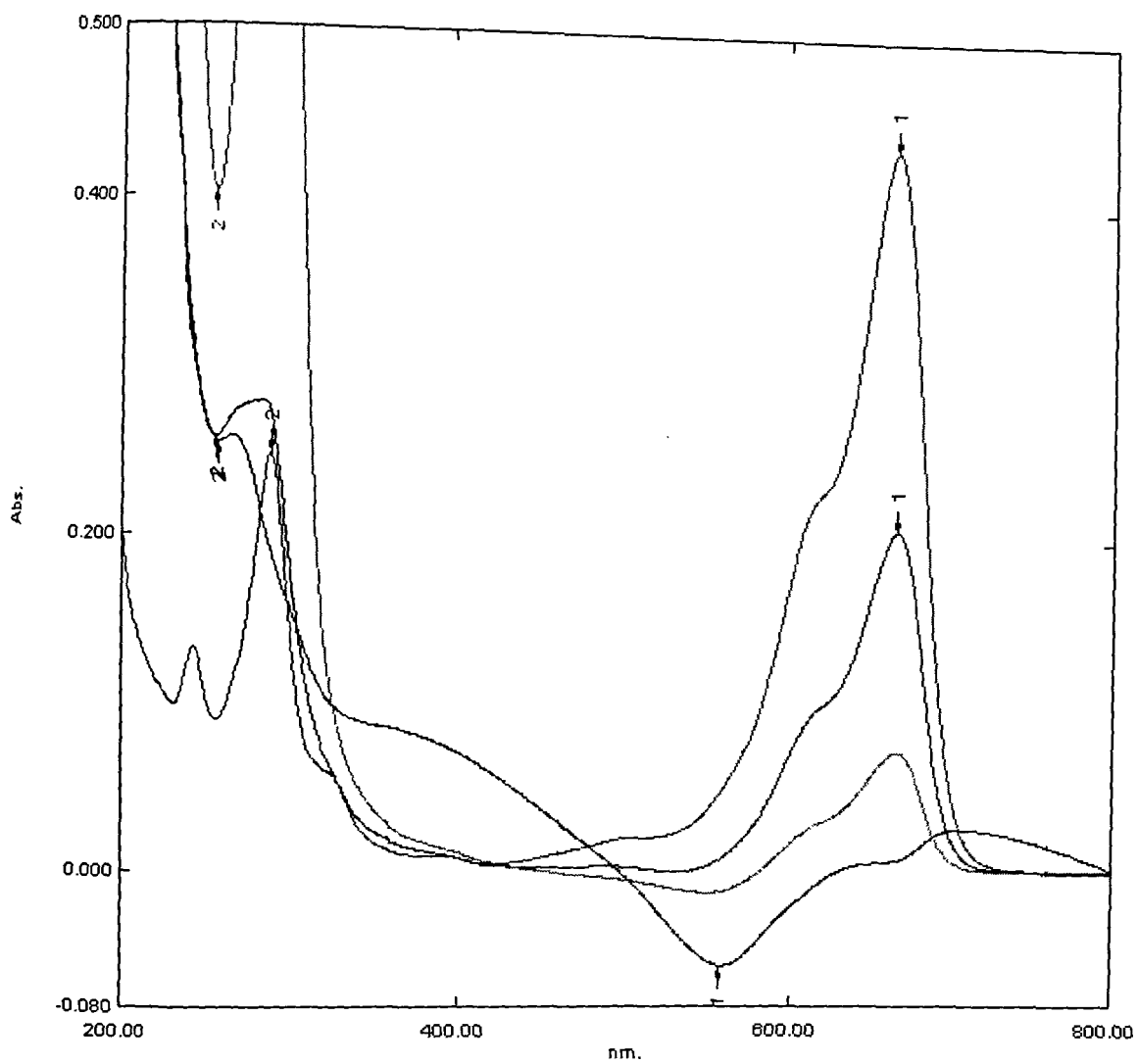


Fig. 5.10 Absorbance against time for the degradation of Methylene Blue by group II Pcs



**Fig. 5.11 UV-visible spectra of CuTAPc catalyzed degradation of Methylene Blue**



**Fig. 5.12 UV-visible spectra of CuTNPC catalyzed degradation of Methylene Blue**

## 5.5 Mechanism for photocatalytic reaction

Many investigators have suggested various mechanisms for the degradation of dye pollutants. When photocatalyst absorbs radiation from sunlight or illuminated by light source (fluorescent lamps), it will produce pairs of electrons and holes. The electron of the valence band of semiconductor becomes excited when illuminated by light. The excess energy of this excited electron promoted the electron to the conduction band of semiconductor therefore creating the negative-electron ( $e^-$ ) and positive-hole ( $h^+$ ) pair. This stage is referred as the semiconductor's 'photo-excitation' state. The energy difference between the valence band and the conduction band is known as the 'Band Gap'. Wavelength of the light necessary for photo-excitation is:  $1240 \text{ (Planck's constant, } h) / (\text{band gap energy})$  as shown in Fig 5.1. This electron is then trapped by molecular  $O_2$  forming  $O_2^-$  ions. The valence band generates hydroxyl radicals ( $OH^\cdot$ ) From hydroxyl ions, this can easily attack the adsorbed dye, thus leading finally to their complete mineralization as shown in scheme 5.1.

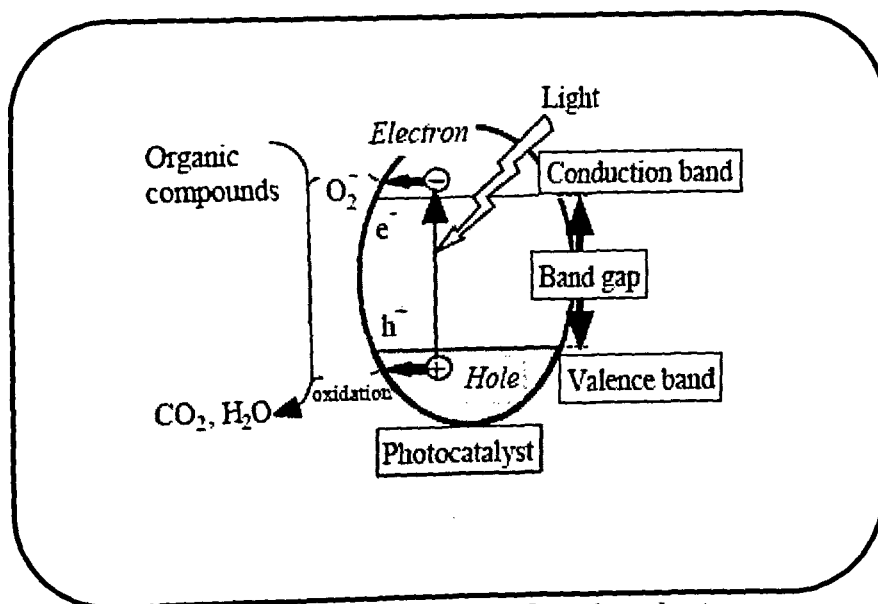
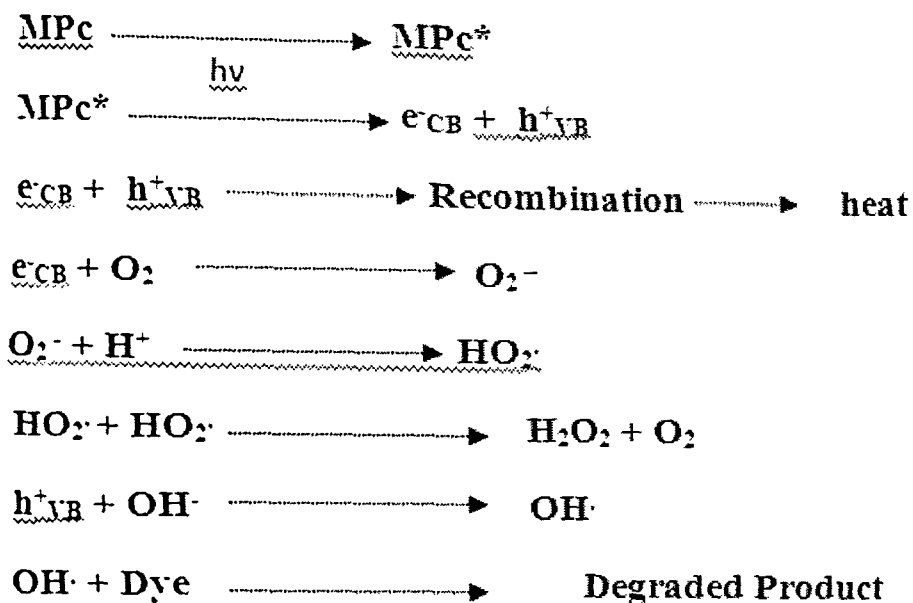


Fig 5.13 Photo excitation of semiconductor



Scheme 5.1

### 5.6 Catalytic oxidation of 2-hydroxynaphthalene

Lawsonia is a naturally occurring compound first isolated from leaves of *Lawsonia inermis* L. in 1959 and was used traditionally for dyeing and also in treatment of diseases like cancer. Lot of research is underway for the synthesis of this molecule having large commercial value. Oxidation of 2-hydroxynaphthalene to 2-hydroxy-1,4-Naphthoquinone (Lawsonia) was carried out in aqueous medium in presence of CuPc.

### 5.6.1 Procedure for the oxidation of 2-hydroxynaphthalene to 2-hydroxy-1,4-Naphthoquinone:

2 g of NaOH was dissolved in 50 ml of water to that 20 mg of 2-hydroxynaphthalene was added, followed by addition of 100 mg of CuPc. The reaction mixture was stirred for 30 min on a magnetic stirrer; stirring was stopped and to this 0.9 ml of H<sub>2</sub>O<sub>2</sub> was added. The reaction mixture was allowed to stand at room temperature for 30 min. The resulting mixture was neutralized with dilute HCl and further extracted with diethyl ether. The ether layer obtained was first washed with water twice and was dried over sodium sulphate. The ether layer was evaporated to dryness and residue obtained was crystallized in ethanol. The product obtained was compared with that of authentic sample procured from sigma Aldrich. The overlying IR spectra are shown in Fig. 5.14 and the overlying UV-Visible spectra was shown in Fig. 5.15. The authentic sample and product both were dissolved in ethanol and run on TLC with a mobile phase of 10% methanol in Chloroform. Both authentic sample and product have same R<sub>f</sub> of 0.26.

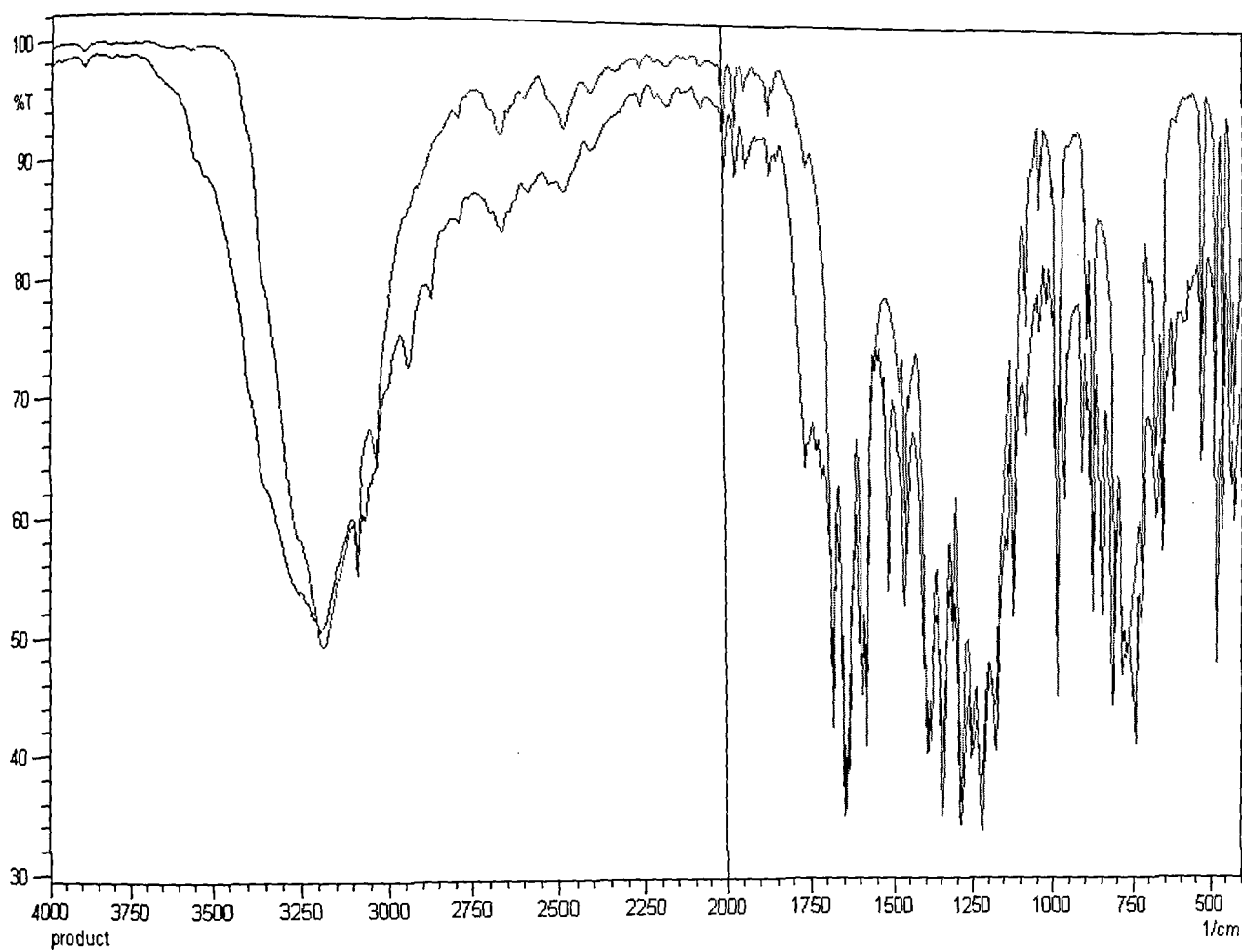


**Fig 5.14 The overlying IR spectra of product with that of authentic sample of Lawsone**



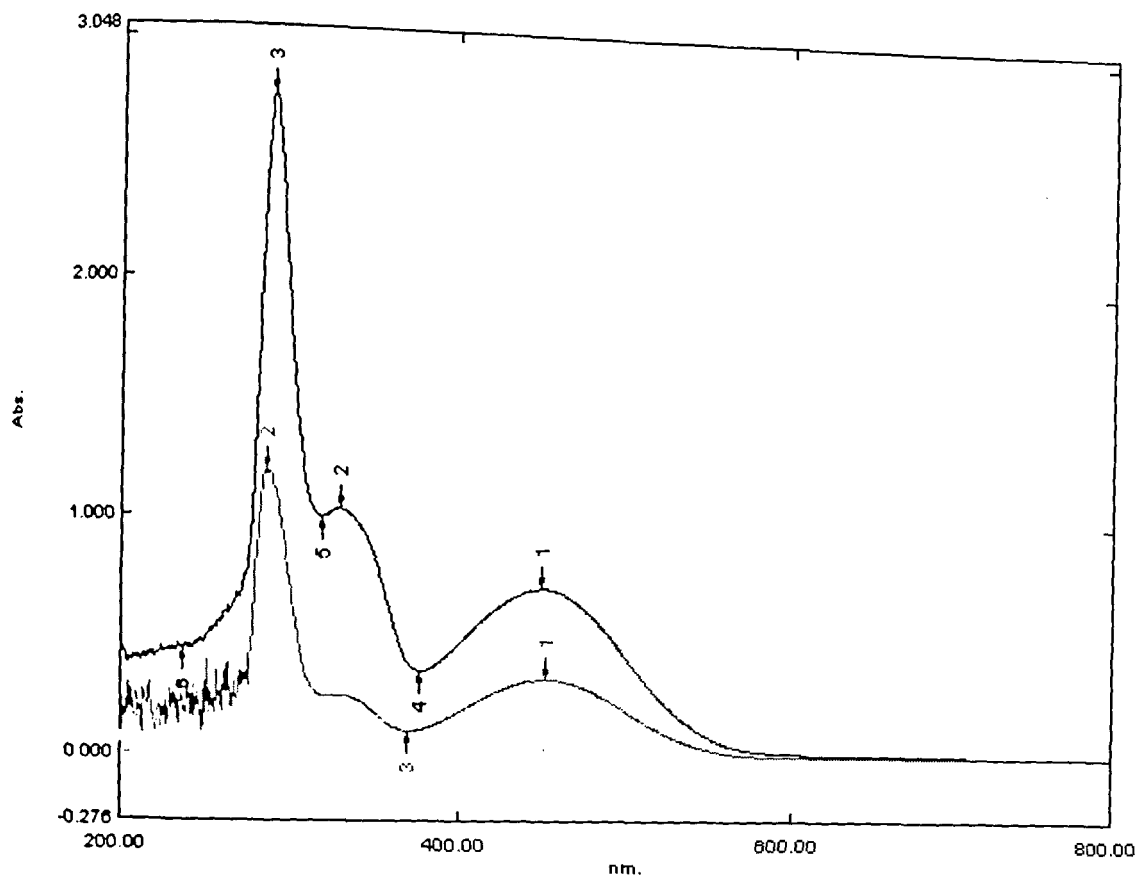


**Fig 5.15** The overlying UV-Visible spectrum of product with that of authentic sample of Lawsone.

Different parameters were studied to optimize reaction conditions, and the product obtained in each case was quantified using UV-Visible spectroscopy. The UV-Visible spectroscopic method was developed and partially validated to quantify the amount of product formed. 2-hydroxy-1,4-Naphthoquinone is soluble in 0.1 N NaOH and has maxima in visible region at 453 nm. Whereas the starting material (2-Hydroxynaphthalene) after dissolving in 0.1 N NaOH is not having any absorbance at around 400-500 nm region as shown in figure 5.16.

The linearity studies were done for five different levels from 4 ppm to 20 ppm. The concentration level and their absorbance is reported in Table 5.6 and the Linearity graph in Fig. 5.17 with correlation coefficient of 0.999.

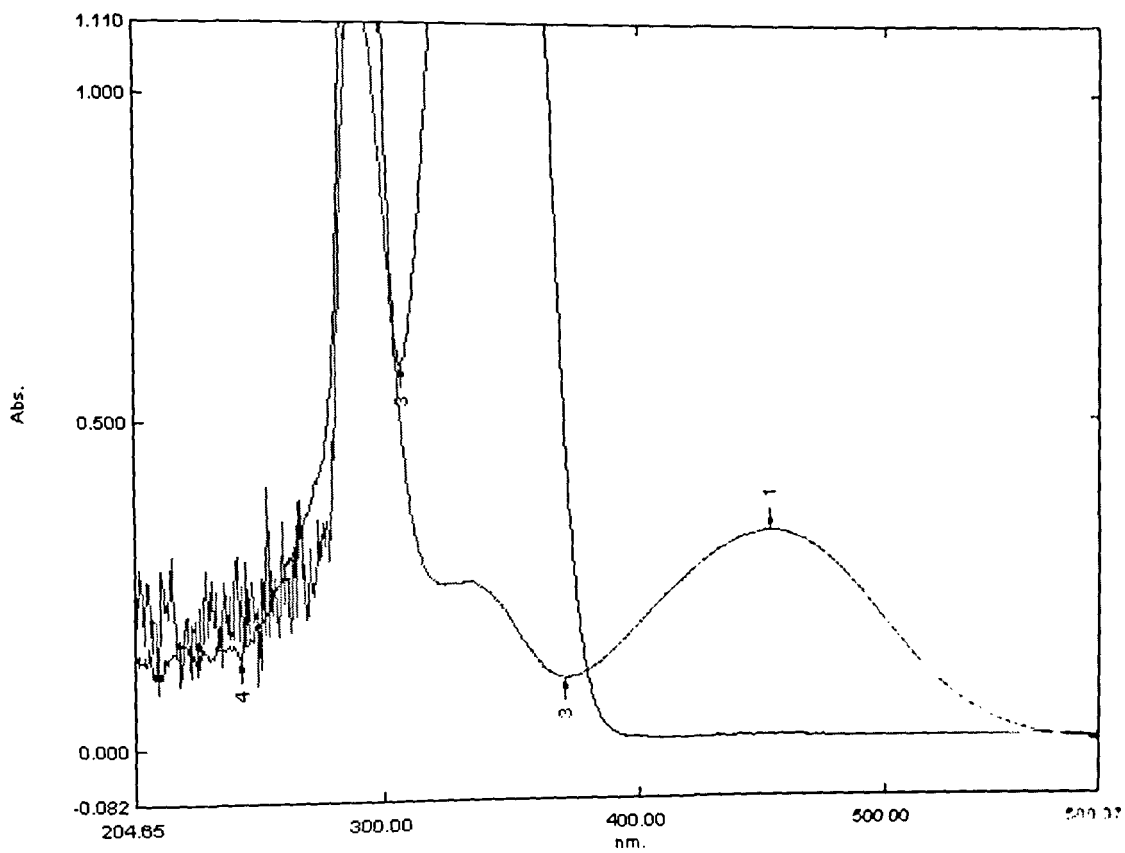


**Fig 5.16 The UV-Visible spectrum of product and that of starting material**

**Table 5.6 Concentration level and their absorbance**

Sr.No	Conc. in ppm	Absorbance at 453 nm
1	4	0.068
2	8	0.133
3	12	0.200
4	16	0.264
5	20	0.334

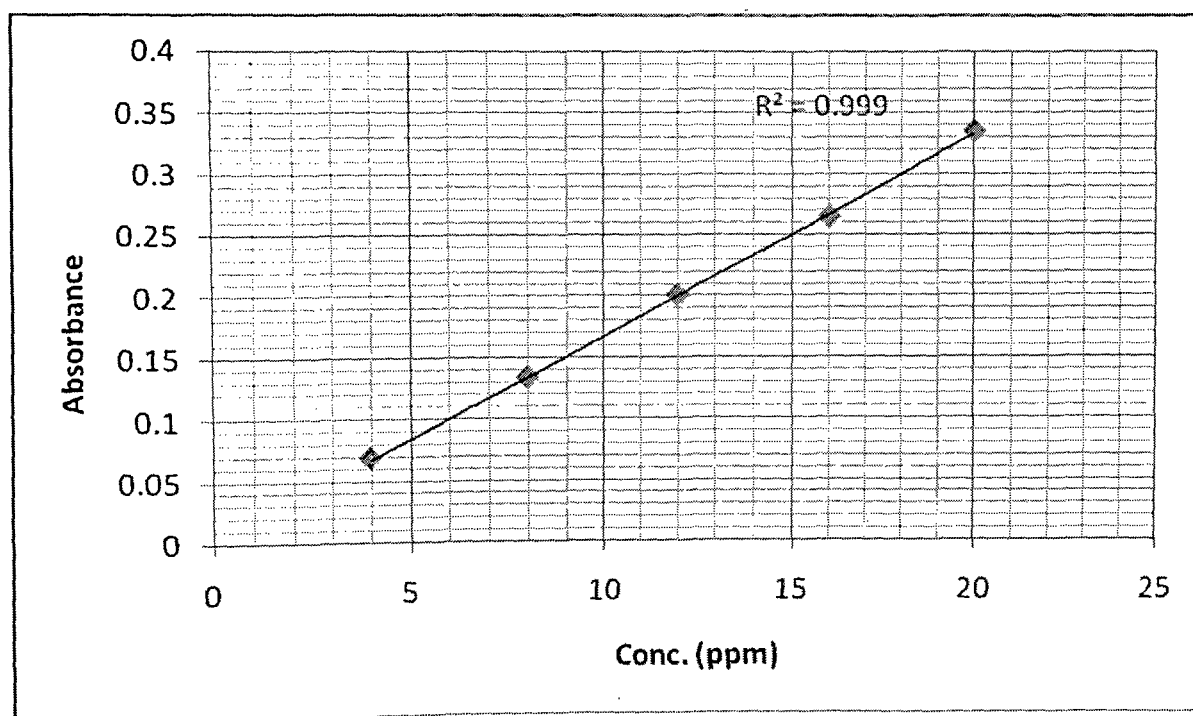


**Fig 5.17 Linearity graph for different conc. of Lawsone against Absorbance**

### 5.6.2 Effect of amount of 2-Hydroxy naphthalene on the rate of reaction

This reaction was carried out with different concentration of 2-Hydroxy naphthalene rest of the reaction condition were kept constant. 50 ml of water , 100mg of CuPc , 2g of NaOH and 0.9 ml of H<sub>2</sub>O<sub>2</sub>. After 30 min on addition of H<sub>2</sub>O<sub>2</sub>, 8 ml of the reaction mixture (on filtration) was neutralized with dilute HCl and extracted with diethyl ether. The ether layer obtained was first washed with water twice and was dried over sodium sulphate. The ether layer was evaporated to dryness and residue obtained was dissolved in 0.1 N NaOH and diluted to 50 ml with 0.1 N NaOH. The percentage of product obtained is shown in Table 5.7 and also graphically in figure 5.18.

**Table 5.7 Represent the percentage product formation for different concentration of 2-Hydroxy naphthalene (mg)**

Sr.No.	Wt of 2-Hydroxy naphthalene (mg)	Product Formation (%)
1	20	59
2	40	44
3	60	42
4	80	32
5	100	27

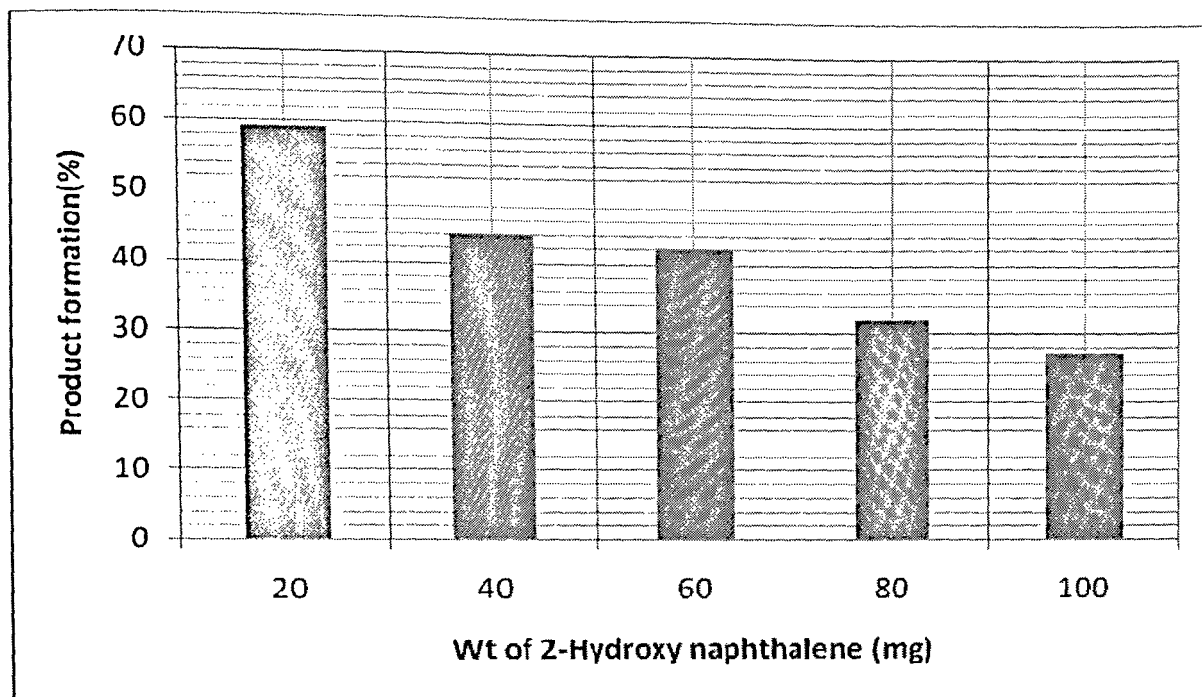


**Fig 5.18 Graphical representation of percentage product formation for different concentration of 2-Hydroxy naphthalene (mg)**

### **5.6.3 Effect of amount of Catalyst on the rate of reaction**

This reaction was carried out with different concentration of catalyst (CuPc) rest of the reaction condition were kept constant 50 ml of water, 20 mg of 2-Hydroxy naphthalene, 2g of NaOH and 0.9 ml of H<sub>2</sub>O<sub>2</sub>. After 30 min on addition of H<sub>2</sub>O<sub>2</sub>, 8 ml of the reaction mixture (on filtration) was neutralized with dilute HCl and extracted with diethyl ether. The ether layer obtained was first washed with water twice and was dried over sodium sulphate. The ether layer was evaporated to dryness and residue obtained was dissolved in 0.1 N NaOH and diluted to 50 ml with 0.1 N NaOH. The percentage of product obtained is shown in Table 5.8 and also graphically in Fig. 5.19. The product spectrums are shown in Fig 5.20.

**Table 5.8** Represent the % product formation for different concentration of CuPc (mg)

<b>Sr.No.</b>	<b>Wt of CuPc (mg)</b>	<b>Product Formation (%)</b>
<b>1</b>	<b>5</b>	<b>12.5</b>
<b>2</b>	<b>20</b>	<b>24.3</b>
<b>3</b>	<b>50</b>	<b>53.3</b>
<b>4</b>	<b>100</b>	<b>59.4</b>
<b>5</b>	<b>150</b>	<b>47.8</b>

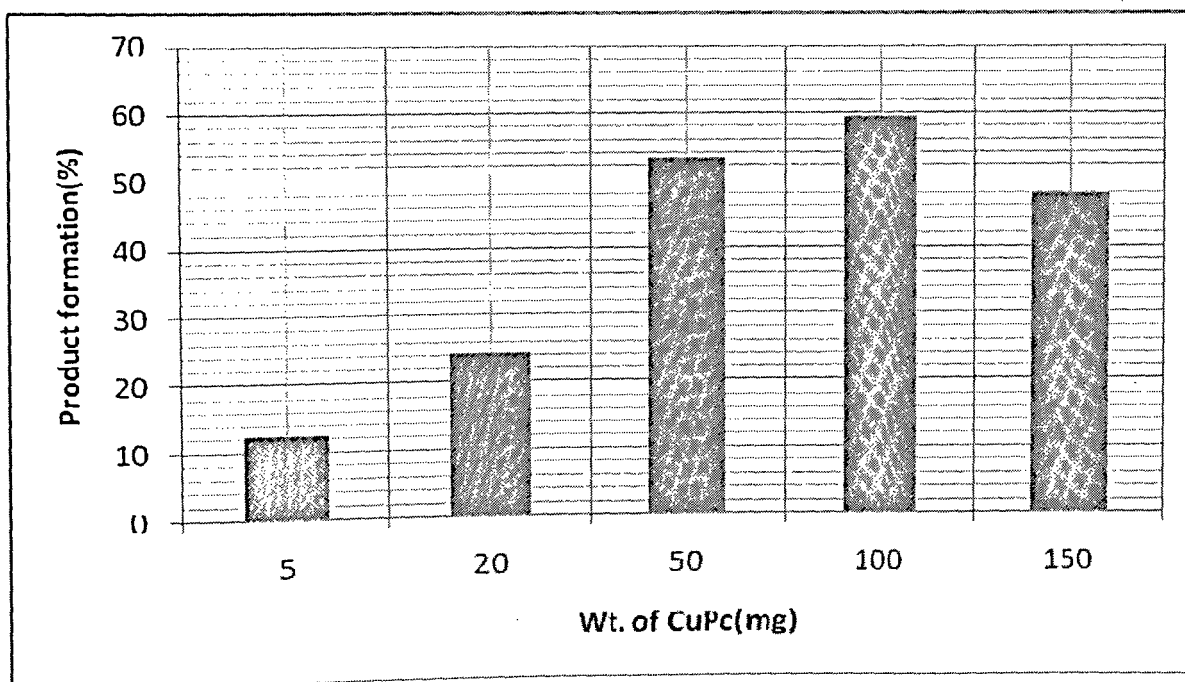


**Fig 5.19** Graphical representation percentage of product formation for different concentration of CuPc (mg)

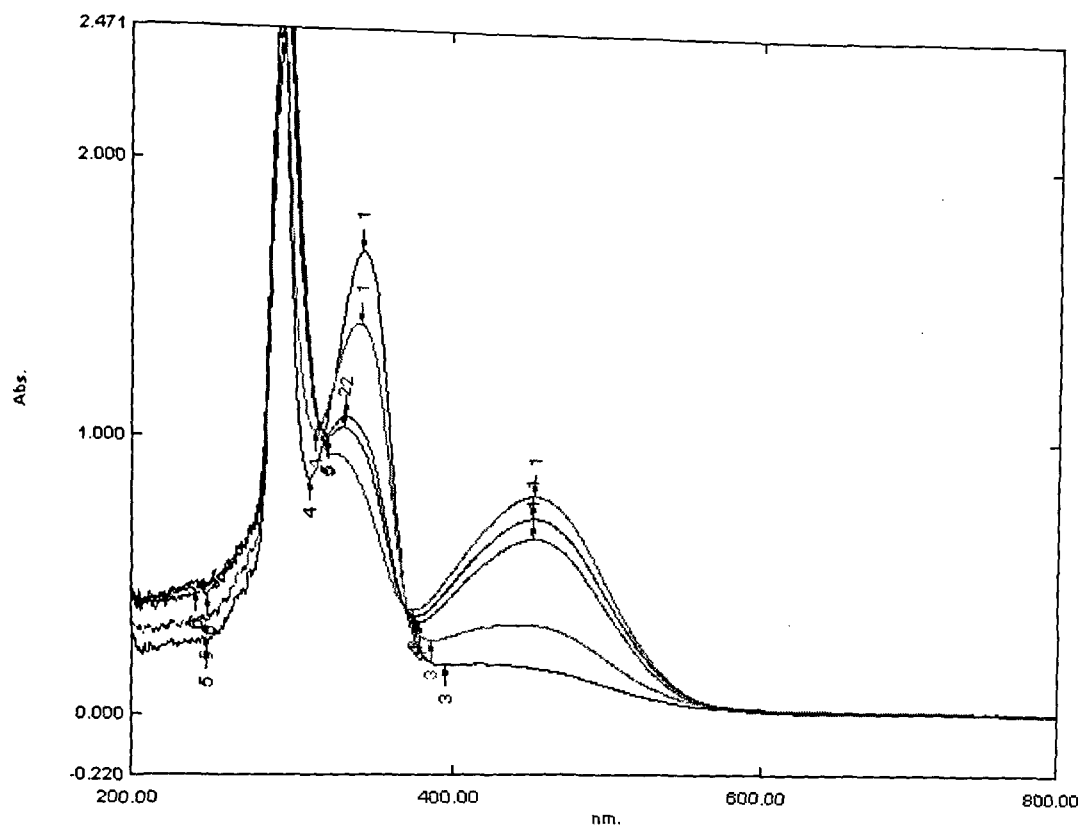


**Fig 5.20 UV-Visible spectrum of Lawsone formed at different concentration of CuPc (mg)**

#### **5.6.4 Effect of amount of NaOH the rate of reaction**

This reaction was carried out with different concentration of NaOH rest of the reaction condition was kept constant. 50 ml of water, 20 mg of 2-Hydroxy naphthalene, 20 mg of CuPc and 0.9 ml of H<sub>2</sub>O<sub>2</sub>. After 30 min on addition of H<sub>2</sub>O<sub>2</sub>, 8 ml of the reaction mixture (on filtration) was neutralized with dilute HCl and extracted with diethyl ether. The ether layer obtained was first washed with water twice and was dried over sodium sulphate. The ether layer was evaporated to dryness and residue obtained was dissolved in 0.1 N NaOH and

diluted to 50 ml with 0.1N NaOH .The % of product obtained is shown in Table 5.9 and also graphically in Fig. 5.21. The product spectrums are shown in Fig. 5.22.

**Table 5.9 Represent the percentage product formation for different concentration of NaOH (g)**

Sr.No.	Wt of NaOH (g)	Product Formation (%)
1	0.2	5.2
2	0.5	13.9
3	1.0	21.2
4	2.0	24.7
5	3.0	21.1

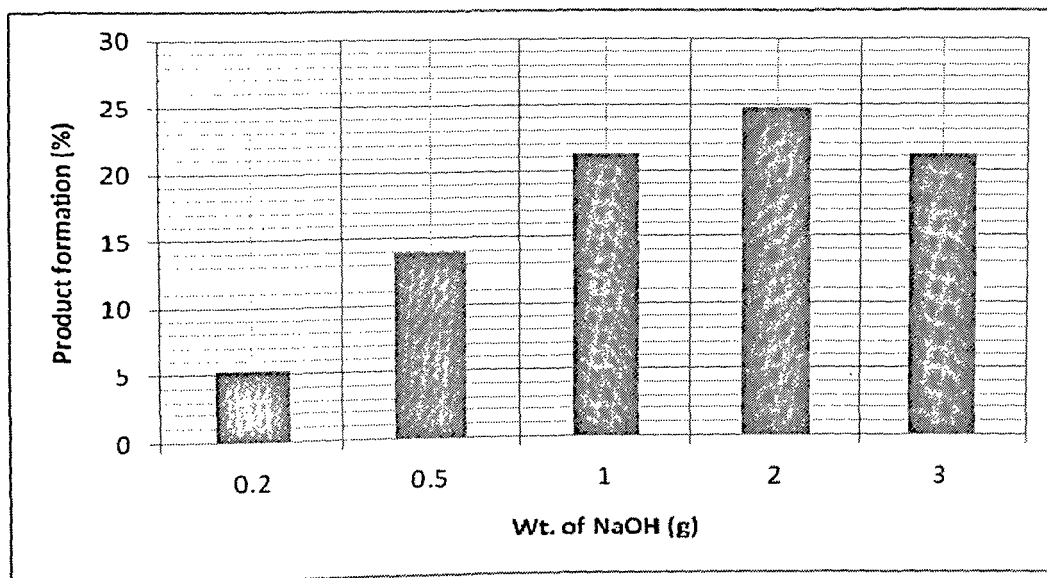


**Fig 5.21 Graphical representation of % product formation for different concentration of NaOH(g)**



As the reaction was carried out at different concentration of NaOH the ideal concentration of NaOH was found to be 2 g for 50 ml of water and further increase in the concentration of NaOH results in decrease in the rate of product formation.

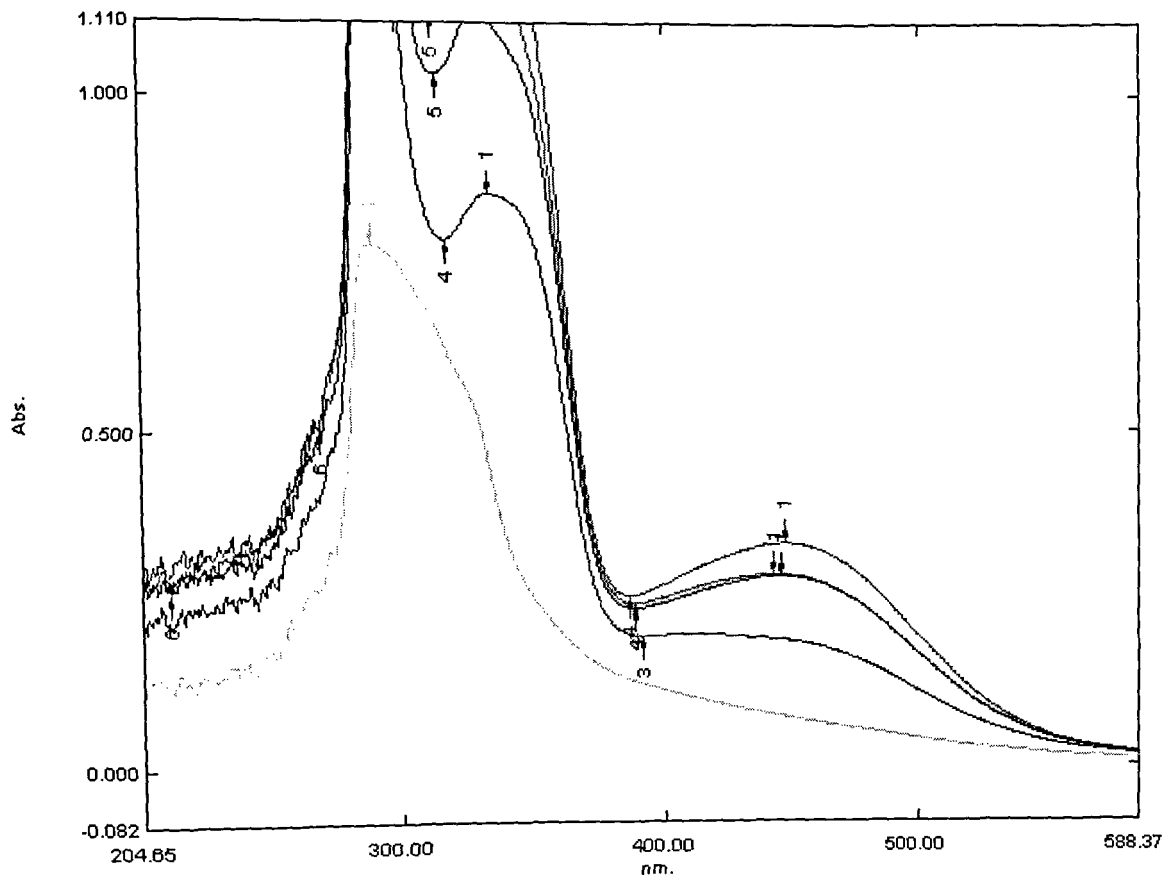


**Fig 5.22 UV-Visible spectrums of Lawsone formed at different concentration of NaOH (g)**

### 5.6.5 Effect of amount of H<sub>2</sub>O<sub>2</sub> on the rate of reaction

This reaction was carried out with different concentration of NaOH rest of the reaction condition was kept constant. 50 ml of water, 20 mg of 2-Hydroxy naphthalene, 20 mg of CuPc and 0.9 ml of H<sub>2</sub>O<sub>2</sub>. After 30 min on addition of H<sub>2</sub>O<sub>2</sub>, 8 ml of the reaction mixture (on filtration) was neutralized with dilute HCl and extracted with diethylether. The ether layer obtained was first washed with water twice and was dried over sodium sulphate. The ether layer was evaporated to dryness and residue obtained was dissolved in 0.1 N NaOH and diluted to 50ml with 0.1 N NaOH. The percentage of product obtained is shown in Table 5.10 and also graphically in Fig. 5.23. The product spectrums are shown in Fig. 5.24.

**Table 5.10 Represent the percentage of product formation for different Volume of H<sub>2</sub>O<sub>2</sub>**

Sr.No.	Amount of H <sub>2</sub> O <sub>2</sub> (ml)	Product Formation (%)
1	0.2	7.0
2	0.5	17.1
3	0.9	24.3
4	1.3	10.1
5	1.5	10.0
6	2.0	9.1

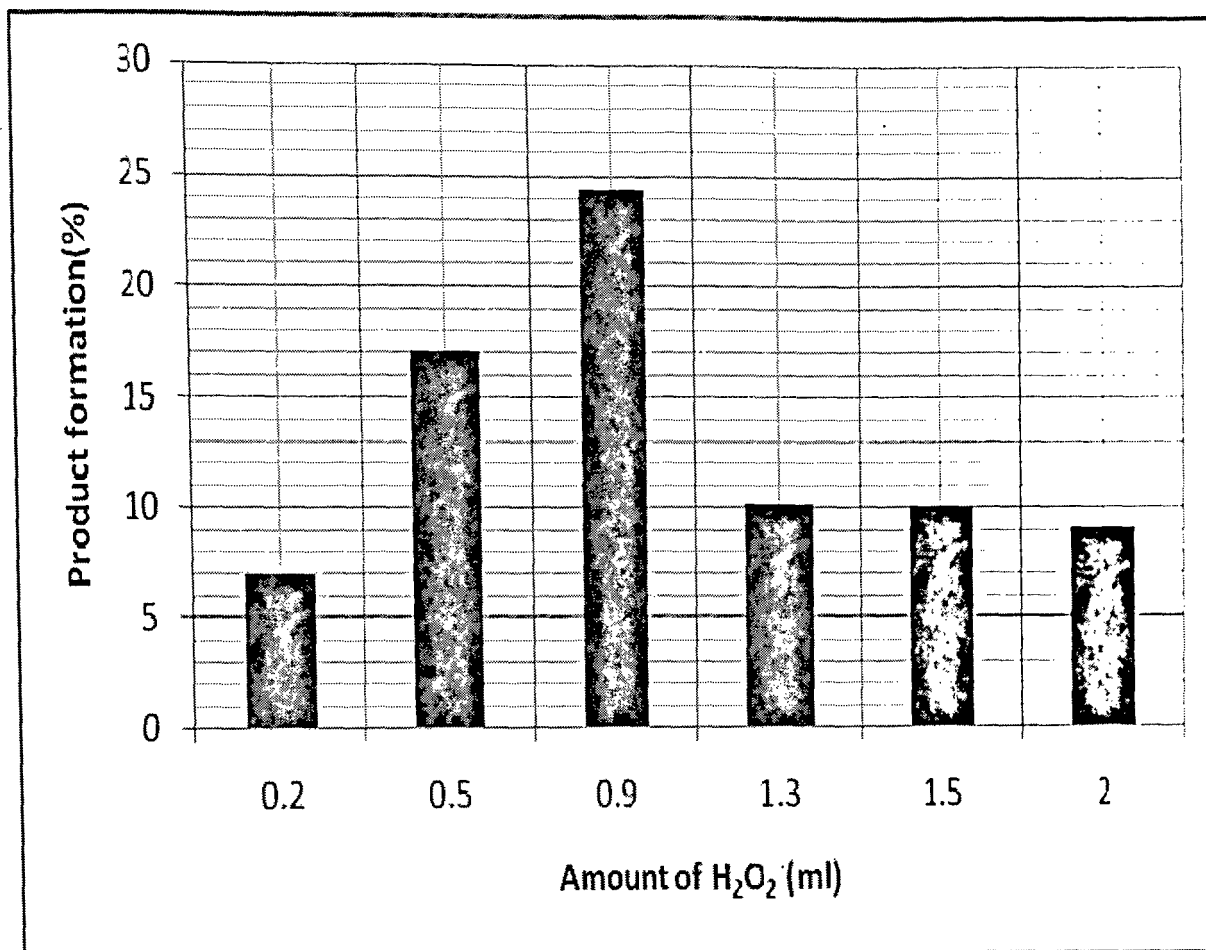


**Fig 5.23 Graphical representation percentage of product formation for different Volume of H<sub>2</sub>O<sub>2</sub>**

As the reaction was carried out at different volume of H<sub>2</sub>O<sub>2</sub> the ideal concentration of H<sub>2</sub>O<sub>2</sub> was found to be 0.8 ml for 50 ml of water and further increase in the concentration of H<sub>2</sub>O<sub>2</sub> results in decrease in the rate of product formation.

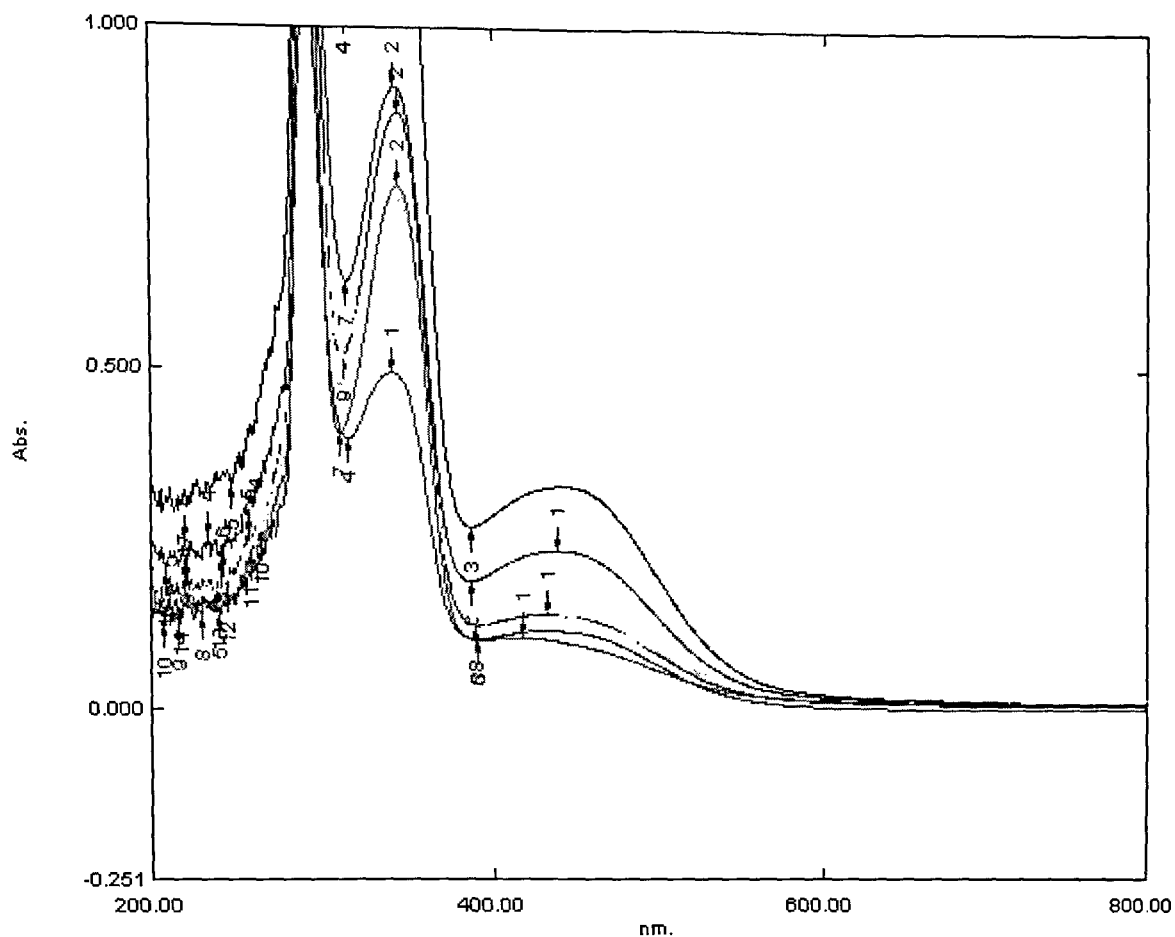


**Fig 5.24 UV-Visible spectrums of Lawsones formed at different Volume of H<sub>2</sub>O<sub>2</sub> (ml).**

The reaction is economical though amount of catalyst required is little large but after the reaction the catalyst can be washed with water followed by methanol and after drying at 105 °C it can be reused. No effect on the rate of reaction is observed even after using for 3 times. This observation is also supported by overlaying IR data obtained as shown in Fig. 5.28 for CuPc before catalytic activity and after catalytic activity as shown in Fig. 5.25.

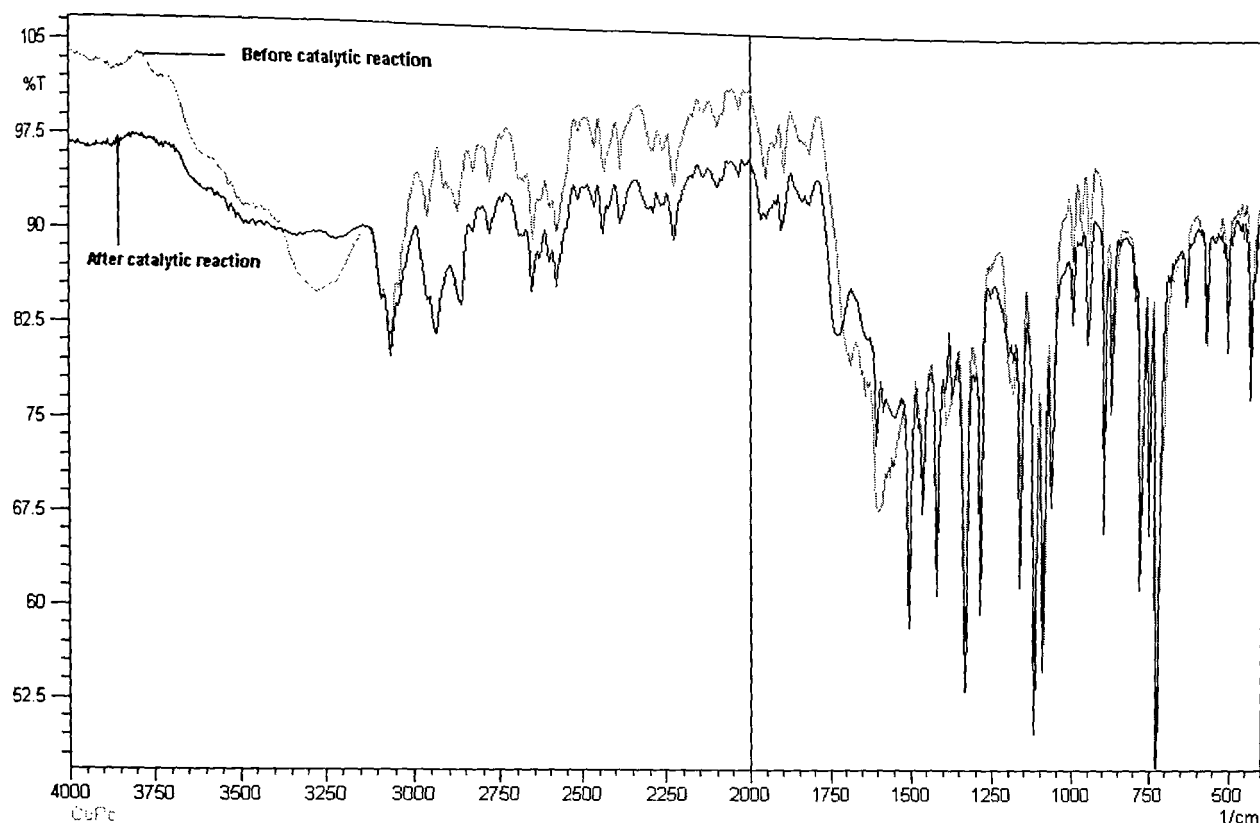


**Fig 5.25 IR spectrum of CuPc before catalytic activity and after catalytic activity**

The oxidation studies were done in other organic solvent such as methanol, IPA and also by varying conditions such as amount of NaOH, temperature, Exposure to sunlight etc.

The following cases and their results are listed below.

### Case I

47.5 ml of MeOH + 2.5 ml of 2 N NaOH cooled and added 200 mg of 2-hydroxynaphthalene + 10 mg of CuPc. Further 1 ml of H<sub>2</sub>O<sub>2</sub> was added drop wise maintaining the reaction temperature of 0-5 °C. The reaction was monitor after 30 min and subsequently after every 2 h for 8 h and finally after 24 h.

**Results** – No formation of product.

#### **Case II**

47.5 ml of MeOH + 2.5 ml of 2 N NaOH cooled and added 200 mg of 2-hydroxynaphthalene + 10 mg of CuPc. Further 1 ml of H<sub>2</sub>O<sub>2</sub> was added drop wise after attaining room temperature in the reaction mixture. The reaction was monitor after 30 min and subsequently after every 2 h for 8 h and finally after 24 h.

**Results** – No formation of product.

#### **Case III**

Same as Case II only 2.5 ml of 2 N NaOH was not added. And 50 ml of MeOH in place of 47.5 ml was taken.

**Results** – No formation of product.

#### **Case IV**

Same as Case II only catalyst is not added

**Results** – No formation of product.

#### **Case V**

Same as Case II only MeOH replaced by IPA

**Results** – Formation of product was observed with yield of 3.8% after 24 h.

#### **Case VI**

Same as Case II only the reaction vessel was kept in sunlight.

**Results** – No formation of product.

#### **Case VII**

Same as Case II only the reaction mixture was heated at 60 °C for 5 h

**Results** – No formation of product.

#### Case VII

50 ml of MeOH + 2 g of NaOH cooled and added 200 mg of 2-hydroxynaphthalene + 10 mg of CuPc. Further 1 ml of H<sub>2</sub>O<sub>2</sub> was added drop wise after attaining room temperature in the reaction mixture. The reaction was monitor after 30 min and subsequently after every 2 h for 8h and finally after 24 h.

**Results** – Formation of product was observed with yield of 2.3% after 24 h.

#### Case VIII

50 ml of MeOH + 2 g of NaOH cooled and added 200 mg of 2-hydroxynaphthalene + 10 mg of CuPc. Further 1 ml of H<sub>2</sub>O<sub>2</sub> was added drop wise maintaining the reaction temperature of 0-5 °C. The reaction was monitor after 30 min and subsequently after every 2 h for 8 h and finally after 24 h.

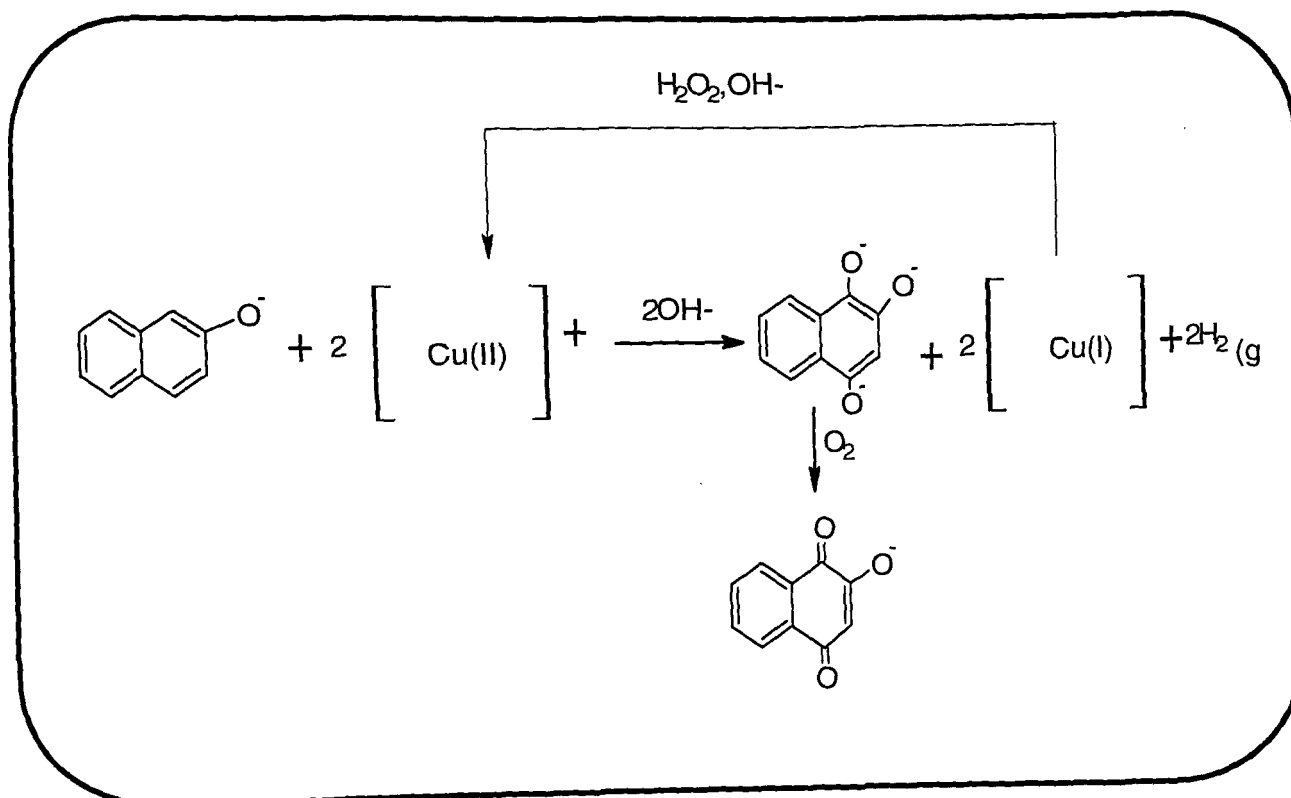
**Results** – Formation of product was observed with yield of 1.4% after 24 h.

The oxidation were studied using CuPc, TNCuPc ,TACuPc, TCCuPc ,CoPc, TNCuPc ,TACuPc, TCCuPc , FePc , TNFePc ,TAFePc , MnPc, TNMnPc ,TAMnPc, TCMnPc ,NiPc, TNNiPc ,TANiPc, TCNiPc , ZnPc, TNZnPc ,TAZnPc and TAZnPc. Only CuPc, TNCuPc and TACuPc were able to catalyzed the reaction out of which CuPc showed total product formation of 59% where as TACuPc 11.8% and TNCuPc only 1.72%.

From the above observation a very meaningfully conclusion can be drawn and also with respect to the reference<sup>156-157</sup> where Iron porphyrin from V to III oxidation state. Similarly only Copper can go from II to I oxidation state and reverse without affecting the structure of the Pc. Also Such reactions are not possible when the catalyst is in homogeneous phase as in case of TCCuPc. TNCuPc showed lower result as compared to that of TACuPc which inturn showed lower as compared to CuPc. This is mainly because of Copper content in

Different Pc is as follow  $\text{TNCuPc} < \text{TACuPc} < \text{CuPc}$ . The result obtained also complies with this observation.

Based on above observation following mechanism was proposed for the oxidation of 2-hydroxynaphthalene to Lawsone as shown in scheme 5.2

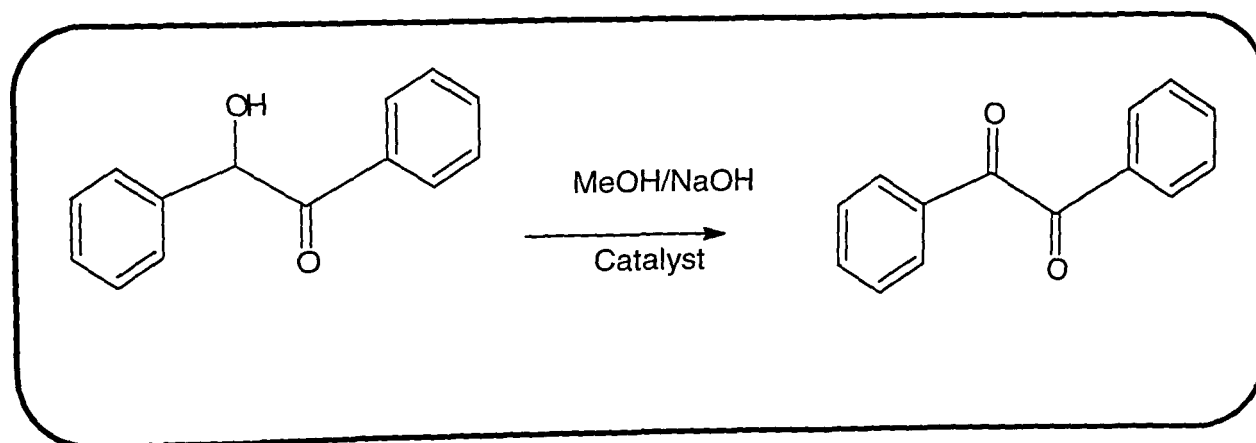


Scheme 5.2



## 5.7 Catalytic oxidation of benzoin to benzil

500 mg of benzoin was taken in 100 ml conical flask, to that 25 ml of MeOH, 500 mg of NaOH and 20 mg of TCMPc (where M = Cu, Ni and Zn) as a was added. The resulting mixture was kept open with intermediate stirring until the benzoin was no longer detectable by TLC analysis. The reaction mechanism is suggested as per scheme 5.3. The mixture was filtered to separate the catalyst and to the filtrate 25 ml of water was added, it was further neutralized with dilute HCl and extracted with ethyl acetate. The ethyl acetate layer was washed 3 times with water further dried over anhydrous sodium sulphate, filtered and solvent was removed under reduced pressure. The product formed was further purified by crystallization in ethanol and characterized using UV and IR technique as shown in Fig. 5.34 and compared with that of authentic commercial sample. Yield obtained was about 80-85%. The catalyst can be dissolved in water and precipitated with 0.1 M HCl. The precipitate obtained was washed with water till free from chloride ions then washed with Ethanol and diethyl ether, finally dried over vacuum and reused.



Scheme 5.3 oxidation of benzoin to Benzil

The oxidation of benzoin to benzyl was carried out using all three metal tetra (n-carboxylacrylic) aminophthalocyanines in methanol at room temperature the reaction was completed in 20 min irrespective of central metal atom. Further the oxidation was carried out at room temperature using Zn tetra (n-carboxylacrylic) aminophthalocyanine in different solvents and the effect of solvent on the rate of reaction and selectivity is shown in Table 5.11. The oxidation was carried out in methanol as solvent in presence of Zn tetra (n-carboxylacrylic) aminophthalocyanine as catalyst at different temperature and effect of temperature on the rate of reaction is shown in Table 5.12 and Fig 5.26. In both above case the volume of solvent and amount of NaOH is kept constant. The reaction did not start in neutral and acidic medium.

**Table 5.11 Effect of solvent on conversion of benzoin to benzyl under same reaction condition.**

Sr. No	Solvent	Time required(min)	Selectivity
1.	Methanol	20	100%
2.	50% Methanol water	30	100%
3.	Ethanol	30	100%
4.	Acetone	–	Benzyl formed gets Converted into benzoic acid
5.	Isopropyl alcohol	–	Benzyl formed gets Converted into benzoic acid
6.	Water	–	No product formation after 24Hr

**Table 5.12 Effect of temperature on the rate of reaction.**

Sr. No	Temperature ( $^{\circ}\text{C}$ )	Time for 100% reaction (min)
1.	0	60
2.	11	50
3.	25	20
4.	35	15
5.	45	5
6.	55	15

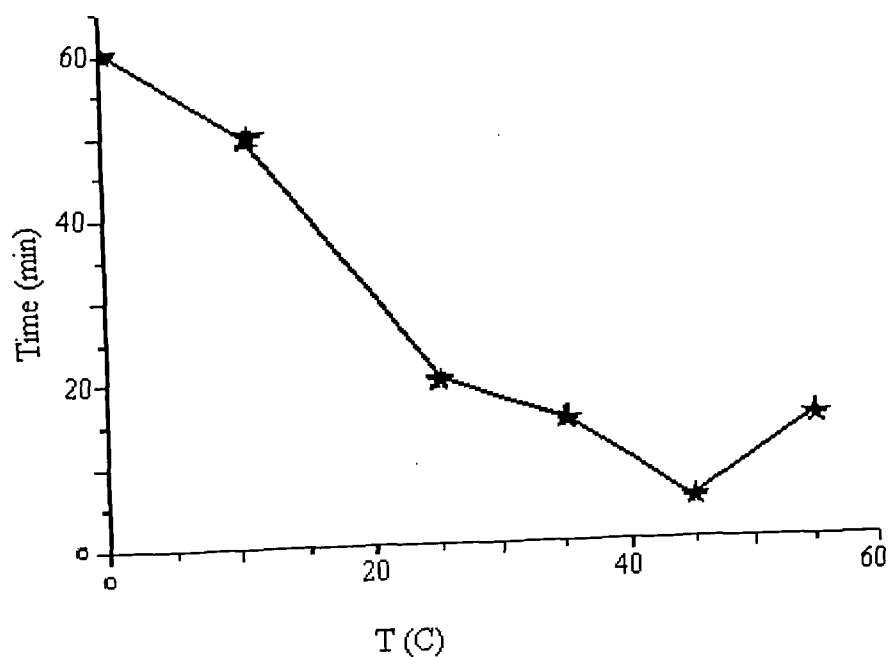


**Fig. 5.26 Effect of temperature on the rate of reaction.**

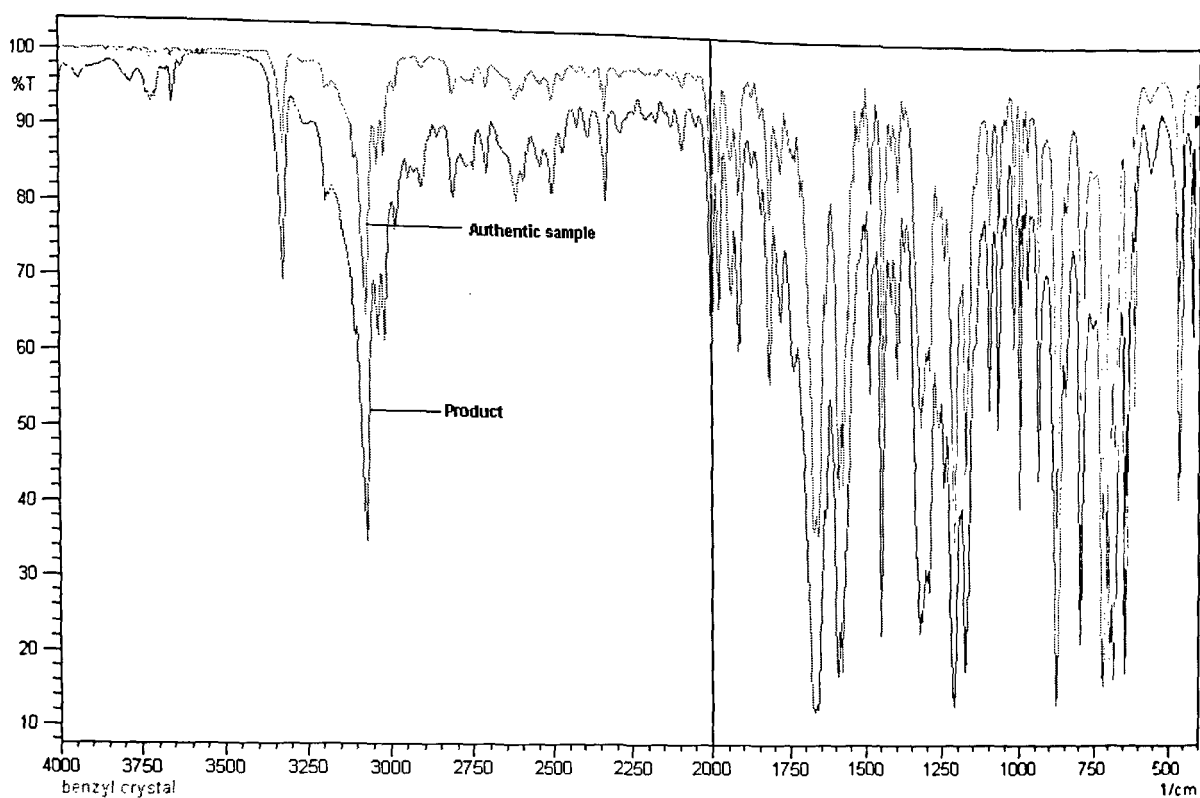


**Fig 5.27 The overlying IR spectra of product with that of authentic sample of Benzil**

The oxidation of benzoin to benzil is studied under extremely mild condition with high yield. The recovery of the catalyst, use of environmental friendly solvent, room temperature and use of atmospheric oxygen makes this process economical and Green. The other Pcs were not that active under similar reaction conditions.

## 5.8 Effect of Phthalocyanines on Microbial cultures

### 5.8.1 Antimicrobial activity on water soluble Pcs

Antibacterial activity tests were performed on different MPcs. Fig 5.28 shows a representative figure of TCMnPc, TCNiPc, TCCuPc and TCZnPc indicating positive test to antibacterial activity. Different concentration of TCCuPc, TCNiPc and TCZnPc was prepared in alkaline buffer solution and its antimicrobial activities were studied for *Staphylococcus citreus*, *Serratia marcescens*, *Bacillus subtilis*, *Proteus vulgaris* and *Pseudomonas fluorescens* plated on to separate nutrient agar, for matt growth. A representative photo of plate with different concentration of TCZnPc for its antimicrobial activity on *Proteus vulgaris* is shown in Fig 5.29.

Based on different zones of inhibition with respect to different micro organism for different concentration of TCMPC is shown in Figs. 5.30 - 5.32. As observed in Fig. 5.30-5.32 inhibition of growth with TCCuPc and TCNiPc occurred at minimum of 10 µg and 20 µg in case of *Staphylococcus citreus*, *Serratia marcescans*, *Proteus vulgaris*, *Pseudomonas fluorescens*; *Staphylococcus citreus*, *Serratia marcescans*, *Bacillus subtilis*, and *Proteus vulgaris* respectively. The adverse effect of TCCuPc and TCNiPc, in terms of size of growth inhibition zone was in the order of: *Pseudomonas fluorescens* = *Staphylococcus citreus* > *Serratia marcescans* = *Proteus vulgaris* and *Serratia marcescans* > *Bacillus subtilis* > *Staphylococcus citreus*, respectively. Further as evident in TCZnPc at 200 µg, 400 µg and 600 µg affected growth of *Staphylococcus citreus* > *Serratia marcescans*, *Proteus vulgaris* and *Bacillus subtilis* respectively. It is noteworthy that the growth of *Pseudomonas fluorescens* was inhibited only by TCCuPc. TCCuPc and TCNiPc are potent at a ten fold lower concentration than those of TCZnPc. The observation therefore an evidence of

antimicrobiocity/ antibiocity of metal pthalocyanines against *Staphylococcus citreus*, *Serratia marcecans*, *Proteus vulgaris*, *Bacillus subtilis* and *Pseudomonas fluorescense* which is dose dependent and bacteria as well as metal specific.

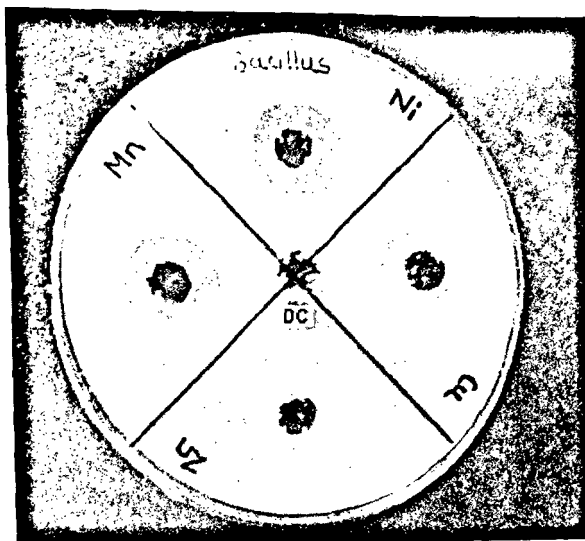
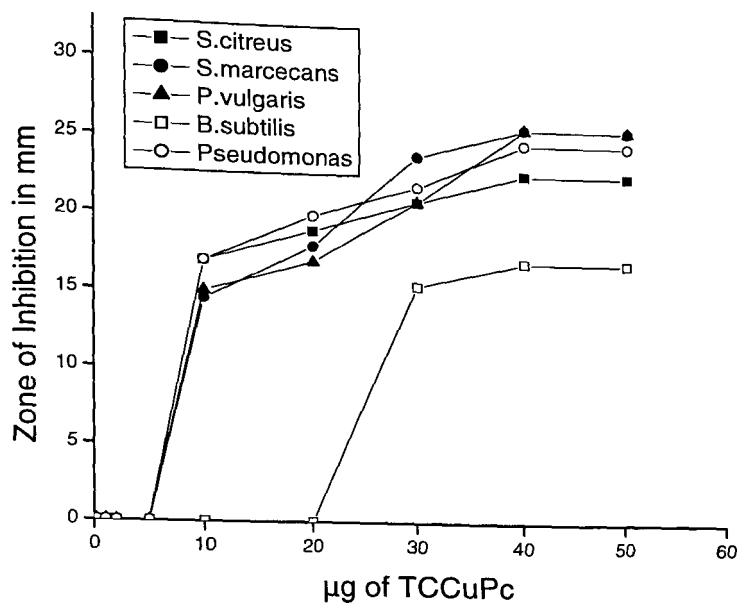


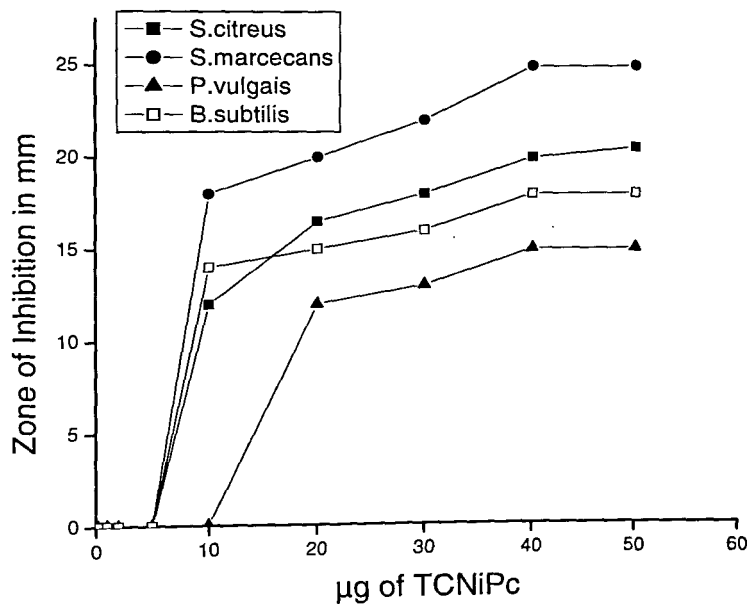
Fig. 5.28 Antimicrobial activity of TCMnPc, TCNiPc, TCCuPc and TCZnPc against *Bacillus subtilis*



Fig. 5.29 Antimicrobial activity against *Proteus vulgaris* at different concentration of TCZnPc



**Fig. 5.30** Antimicrobial activity of TCCuPc



**Fig. 5.31** Antimicrobial activity of TCNiPc

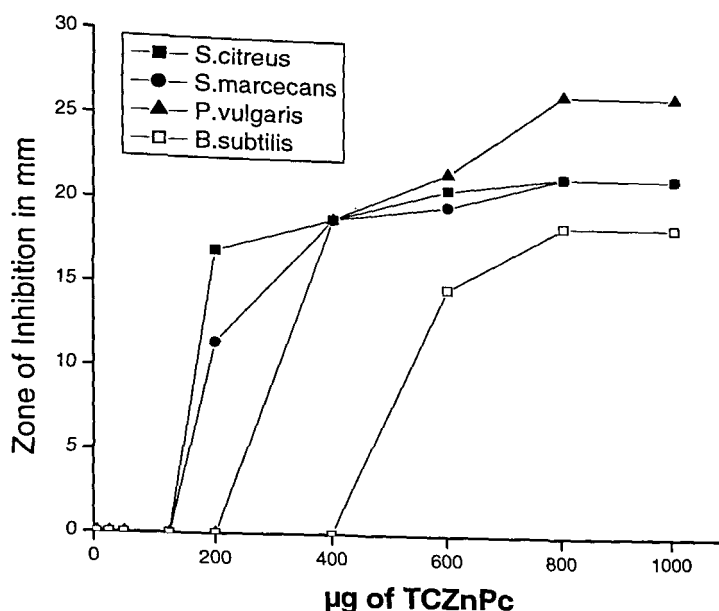


**Fig. 5.32 Antimicrobial activity of TCZnPc**

### 5.8.2 Effect of solvent on the antimicrobial activity of TCCoPc and TCMnPc

To study the effect of solvent in which the Pcs are dissolved the studies were extended by changing the solvent from aqueous to organic. TCCoPc and TCMnPc are water soluble at alkaline pH. Initial when the activity was not observed at lower concentration, a concentrated solution of concentration of 100 µg /100 µl was prepared in alkaline solution and the activity was studied on *Staphylococcus aureus* (ATCC 6538P), *Escherichia coli* (ATCC 8739), *Salmonella typhi* (ATCC 14028) and *Pseudomonas aeruginosa* (ATTC 9027) plated on to separate mueller-hinton agar, for matt growth. No zone of inhibition were observed in all the cases, but a diffusion of the TCCoPc and TCMnPc on the plate mounted with *Pseudomonas aeruginosa* was observed as shown in Fig 5.33, This experiment was repeated by dissolving TCCoPc and TCMnPc in DMSO in an concentration of 4 µg /100 µl.



The zone of inhibition was observed in all the stains as shown in Fig 5.34 (plate mounted with *Pseudomonas aeruginosa* ), except in the case of *Staphylococcus aureus* where TCMnPc did not show any activity but TCCoPc had shown good activity. The comparison of antimicrobial activity among TCCoPc and TCMnPc in DMSO with respect to different strains of micro organism is shown in Fig. 5.35.

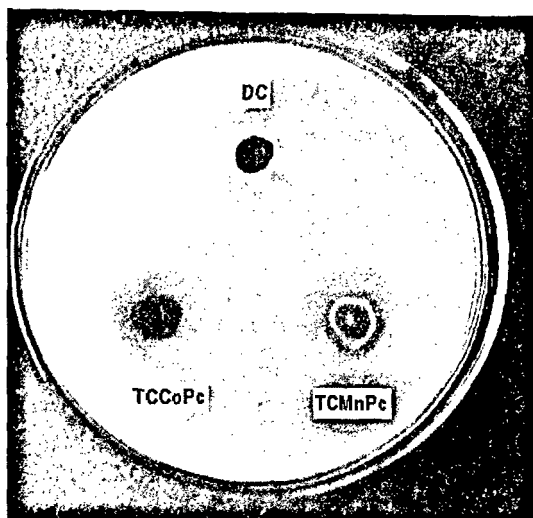
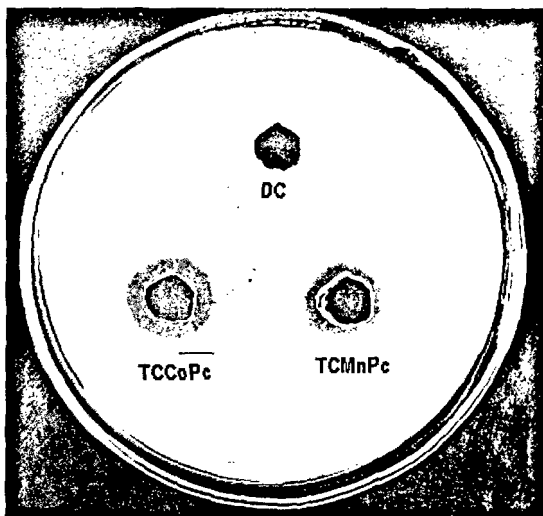
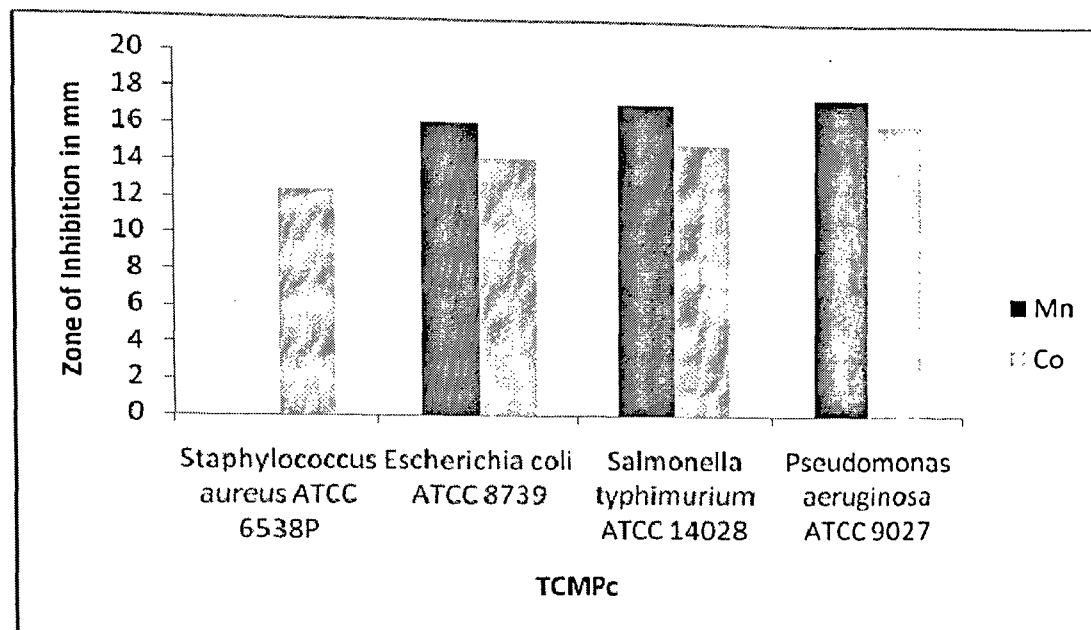


Fig 5.33 Diffusion of TCMnPc on mueller-hinton agar loded with *Pseudomonas aeruginosa*



**Fig 5.34 Antimicrobial activity of TCMnPc against *Pseudomonas aeruginosa***



**Fig.5.35 Antimicrobial activity of TCCoPc and TCMnPc on different strains of microorganism.**

From the above observation it can be concluded that the mode of attack of Pcs in all is cases is not identical, as it is revealed from above case of *Staphylococcus aureus*, where TCMnPc has not shown any activity. But in case of *Escherichia coli*, *Salmonella typhi* and *Pseudomonas aeruginosa*, TCMnPc has shown better activity than that of TCCoPc. If antimicrobial activity is explained in terms of production of singlet oxygen, than TCMnPc when dissolved in organic solvent, have absorption maxima in the red region as compared to that of TCCoPc. Therefore the ability of TCMnPc to produce singlet oxygen will be more than that of TCCoPc. Additional conclusion, which can be inferred from above observation, is that MnPc is active against *Staphylococcus aureus*, but on substitution at peripheral position its activity has completely subsided.

### 5.8.3 Antimicrobial activity on non substituted MPcs

The studies were extended by using MPcs (M= Al, Co, Cu, Fe, Mn, Ni and Zn) in Dimethyl sulphoxide (DMSO) to obtain a corresponding solution, having a final concentration of 4 µg /ml respectively. The activity was studied on *Staphylococcus aureus* (ATCC 6538P), *Escherichia coli* (ATCC 8739), *Salmonella typhi* (ATCC 14028) and *Pseudomonas aeruginosa* (ATTC 9027) plated on to separate muller-hinton agar, for matt growth. Based on different zones of inhibition with respect to different micro organism for different MPcs are shown in Figs. 5.36 - 5.39. These studies were carried out at very low concentration level of 4 µg and in triplicate. In case of *Staphylococcus aureus* ZnPc showed maximum activity whereas FePc showed minimum activity. In case of *Escherichia coli* FePc showed maximum activity whereas CoPc showed minimum activity. In case of *Salmonella typhi* FePc showed maximum activity whereas CoPc and ZnPc showed minimum activity. In case of *Pseudomonas aeruginosa*, AlPc showed maximum activity whereas NiPc showed minimum activity. Such inhibition of growth, seen with antibiotics is termed as antimicrobial effect and is taken as the criteria for measure of evaluating potency of antibiotics<sup>203</sup>. Thus our preliminary results clearly indicate that the Pcs are potent '*bacteriocides*' and that their potency can be affixed in terms of *Minimum inhibitory Concentration (MIC)* against the bacterial cultures used in the study.

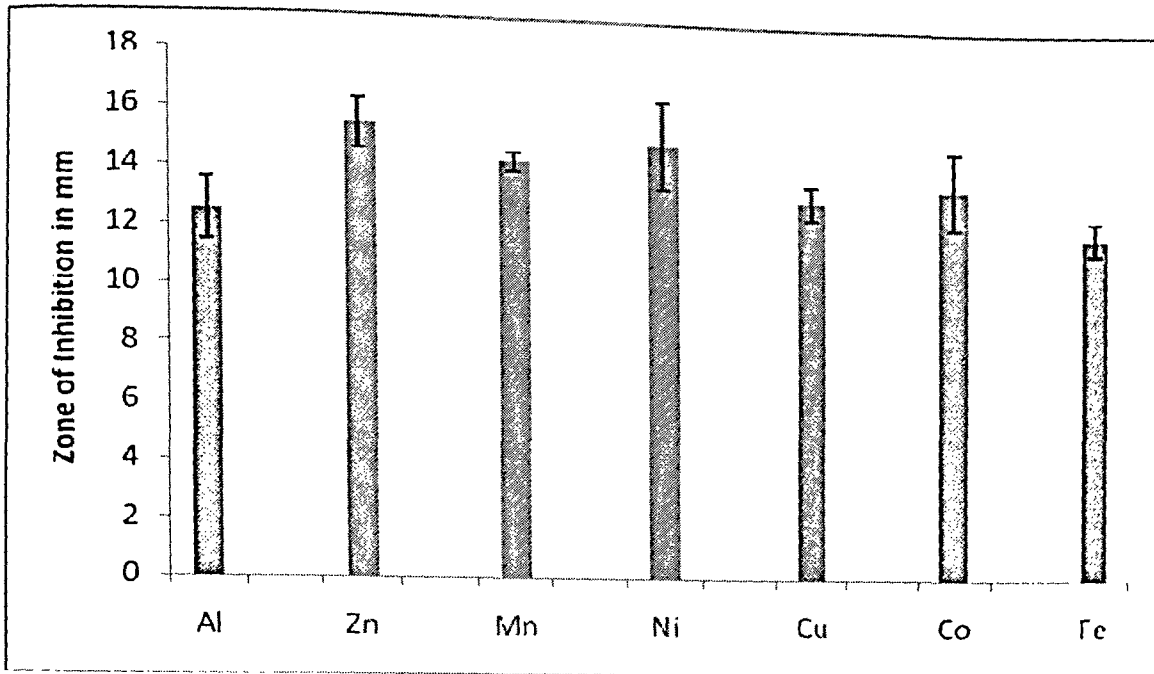


Fig. 5.36 Antimicrobial activity of MPs on *Staphylococcus aureus*

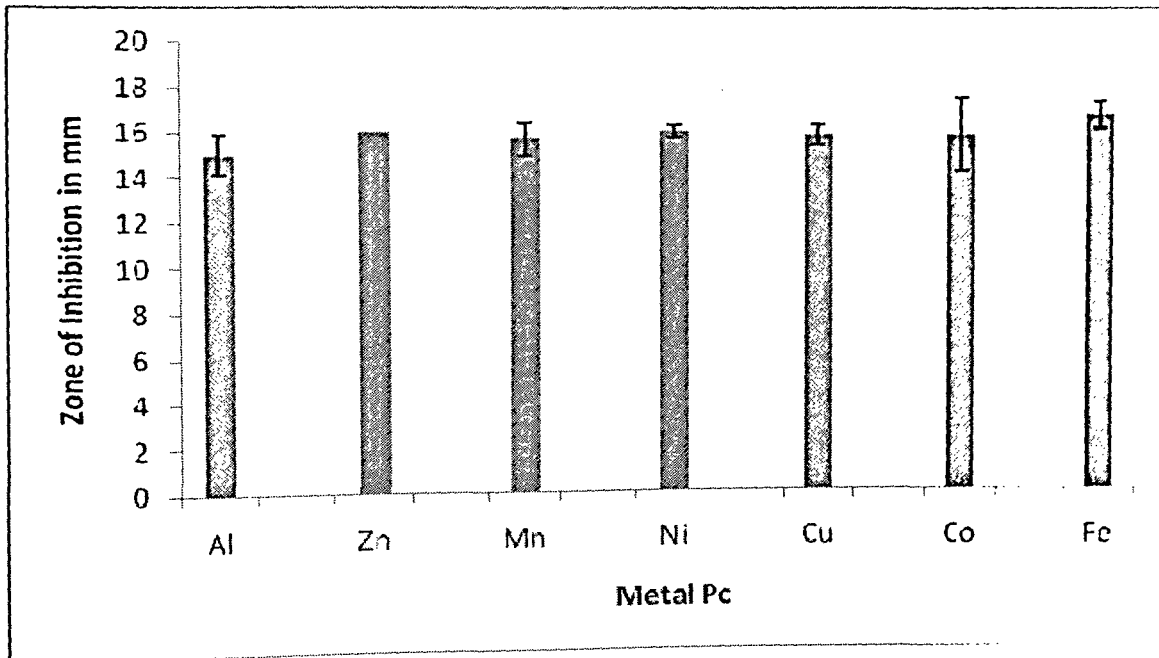
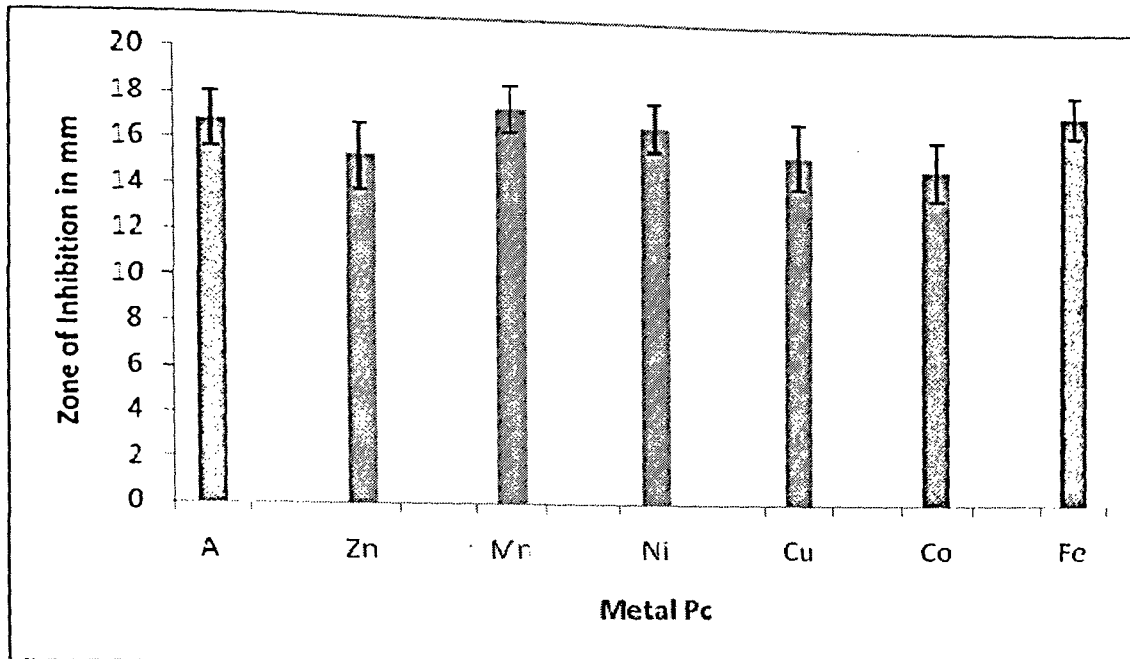
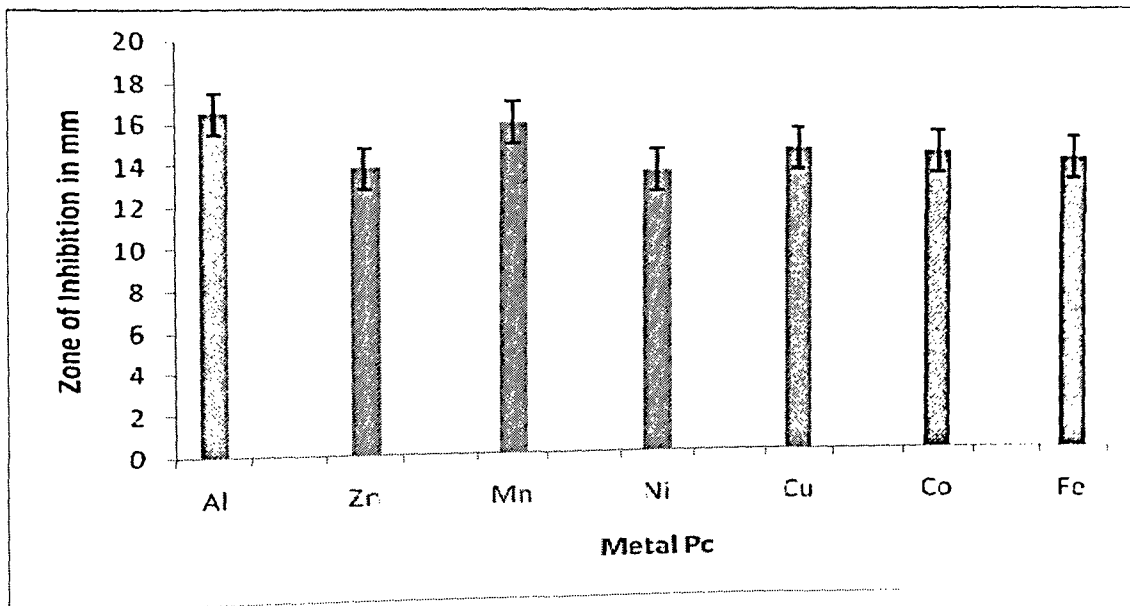


Fig. 5.37 Antimicrobial activity of MPs on *Escherichia coli*



**Fig. 5.38 Antimicrobial activity of MPcs on *Salmonella typhi***



**Fig. 5.39 Antimicrobial activity of MPcs on *Pseudomonas aeruginosa***

These compounds have excellent property to provide or make available oxygen species for the oxidation and there is every chance that such reactions may be more effective in presence of light. Since these compounds are light harvesting and have photoluminescence property including up-conversion, may be playing a vital role as antibacterial activity. The phthalocyanine compounds in solution have potency of generating singlet oxygen if dissolved oxygen is present in presence of light. However, the activity may be increased by taking oxygen enriched solution. The photodynamic therapy may also work based on similar phenomenon. Singlet oxygen has high potentiality to kill all types of bacteria present around. It depends on the efficiency of singlet oxygen generation capability by individual compounds under given condition.

# CHAPTER 6

*SUMMARY*

*AND*

*CONCLUSIONS*

## 6.0 Summary and Conclusion:

Green chemistry has focussed the concentration of many chemists both from environmental and also from economic point of view. Any reaction which make use of less organic solvents, low temperature, low cost, harmless by-products, use of solar radiation, microwave oven, use of catalyst and nano materials have continuously attracted attention of all the Scientists and Technologists.

Our first aim was to synthesize water soluble Phthalocyanines (PCs) using easily available starting material. Method was standardized for the synthesis of simple MPcs using solvent, melt and microwave oven. By carrying out these synthesis we were in a better position to understand the molecules in terms of their stability, solubility and quantity of precursor required for the synthesis of Pcs. The 4-Nitrophthalimide was the precursor required for the synthesis of TNMPcs and it was prepared by nitration of phthalimide using nitrating mixture. By this method both 3-nitro and 4-nitro phthalimide were formed, out of which 3-nitrophthalimide was water soluble and therefore can be separated from 4-nitrophthalimide.

The 4-nitro phthalimide was used for the synthesis of TNMPcs, which was further reduced to TAMPC using sodium sulfide in water. TAMPCs were further used for the synthesis of water soluble TCMPCs on reaction with malic anhydride in DMF. The products formed were well characterized using UV-Visible, FT-IR spectroscopy and Elemental analysis to confirm the formation of the product.

Thermal analysis using TG-DSC were carried out on all substituted as well as non substituted Pcs to study their thermal stability and thermal behaviours. In some cases an endothermic peak was observed at around 105 °C, this was due to the loss of water molecule. In all the cases the molecules were found to be stable up to 350 °C, further on



heating gradually MPcs were found to undergo decomposition and finally resulting to metal oxide in case of MPcs at 800 °C. This high thermal stability makes their application possible as high temperature catalyst and as lubricants at higher temperature.

Magnetic susceptibility studies were done on MPcs, it was observed that MnPc, CoPc and CuPc are paramagnetic whereas NiPc and ZnPc are diamagnetic. Similar observations were also recorded in case of TAMPcs. But the value of magnetic moment was less as compared to that of non substituted Phthalocyanine. Based on this observation ESR studies were done on TAMPcs and it was observed that Fe, Mn, Co, and Cu are in 2+ oxidation state in TAMPcs.

XRD studies were done on some MPcs and the  $2\theta$  values obtained were in agreement with that reported in the literature. On comparison with the  $2\theta$  value reported in literature it was also found that the MPcs have  $\beta$  monoclinic structure.

From UV-Visible spectroscopy it was observed that phthalocyanines have Q bands in visible region greater than 600 nm and highest value of Q band was observed in the case of TAMnPc which decreases on substitution. Pcs have distinct B band in the UV region.

A perfect relation was build between the different signals obtained in IR spectrum on change in substituent's at peripheral position. In case of tetranitro substituted metal Pcs a band is observed at around  $1550\text{ cm}^{-1}$ , which gradually disappears on reduction of nitro to amino group in case of tetra amino phthalocyanine with the appearance of new band at around  $3300\text{ cm}^{-1}$  due to primary amino group. This band due to primary amino group disappears on substitution with carboic acrylic group, with appearance of new band at around  $1700\text{ cm}^{-1}$  due to carbonyl group. Similar type of observations were also recorded

in the case of nitration of phthalimide to 4-nitrophthalimide, where band was observed at  $1550\text{ cm}^{-1}$  due to nitro group.

Elemental analyses of TCMPcs were done and the result obtained were in accordance with that on the theoretical value, further this observation also strengthens the formation of TNMPcs and TAMPcs.

Pholuminescence studies showed absorption maxima at 468 nm after excitation at 220 nm and also at lower energy wavelength of 625 nm, such phenomena of excitation with lower wavelength and emission at higher wavelength is called as up-conversion, which makes application of these molecules in laser technology. The ability of this molecules to undergo solid state excitation in visible region lead to their applications in solar cell. Now a days due to large requirement for power generation, though the nuclear plant provide the satisfactory source but the risk involve in terms of leakage and the damage to the nuclear power plant can be caused by natural calamities, for example in Japan where the nuclear plant was damaged by tsunami, therefore the naturally available solar energy is in need to be looked as a future energy source. A systematic research is required to use phthalocyanine molecules having high stability, wide absorption maxima, semiconductor properties, provision of extending the linkage, and also advantage of synthesizing with different central metal atom.

MPcs were used for the degradation of Amido black 10B in presence of sun light and oxygen at different pH, to study the effect of pH on the rate of degradation reaction, the pH played an important role with respect to the different central metal atom present in the phthalocyanine ring, though the external ring was same in all the cases. In terms of activity at neutral pH (pH=7), CuPc showed maximum activity followed by MnPc and CoPc. The NiPc showed less activity whereas ZnPc showed almost no activity. At alkaline pH

(pH=8) CuPc has shown maximum activity same as that shown at neutral pH, MnPc and CoPc have showed improved the activity with increase in pH whereas NiPc showed decrease in activity and therefore did not show any degradation same as that of ZnPc. In case of acidic pH (pH=6) CuPc has shown better activity as compared to basic pH, while comparing MnPc and CoPc, MnPc showed higher activity in acidic pH and CoPc showed better activity at alkaline pH. And the activity of NiPc has improved in acidic pH. ZnPc has not shown any activity in all pH range. As Amido black 10B is an azo dye it was decided to study the activity of these phthalocyanines on another azo dye such as Auramine O at neutral pH. In this case NiPc has shown highest activity followed by MnPc, CuPc and CoPc . In this case even ZnPc has shown some activity. The above studies have indicated that the catalytic activities are very much dependent on the nature of substrate and on central metal atoms. Overall CuPc is a very good photo-catalyst.

To study the effect of substitution on the peripheral ring by electron withdrawing group such as nitro and that of electron donating group such as amino, degradation studies were done on a most commonly used dye such as Methylene blue. The observation and the inferences drawn were that, all the substituted metal Pcs showed very good activity. It was found that nitro substituted Pc showed better activity with an exception in case of Co whereas Cu amino substituted showed better activity, this could be attributed to their capacity to accept the electron and go to lower oxidation state. Direct use of Pcs for dye degradation in case of effluent treatment may not be that economical as it would be difficult to recover the catalyst. But if a systematic research is done to impregnate this Pcs on supports which can be dipped in the tanks for the degradation of dyes in presence of molecular oxygen and sunlight. So that after the completion of activity the Pcs along with the support can be removed, reactivated and reused.

Oxidation of alcohol to ketone is always an important chemical reaction. The oxidation of  $\alpha$ -hydroxy aromatic ketone to a diketone is an important reaction as diketones are used as a starting material for the synthesis of different products<sup>136,137</sup>. In earlier work water soluble Pcs are used for the oxidation of benzoin to benzil under reflux condition in methanol for 1 h<sup>131</sup>. In the present work, tried to use water soluble TCMPc in methanol at different temperature and it was observed that at 45 °C the reaction was completed in just 5 minutes with yield greater than 80%. The effects of different solvents were also studied and it was observed that in methanol the time required for the completion of reaction was 20 min whereas in ethanol and 50% methanol in water, 30 min were required. In water alone the reaction was not started. In acetone and isopropyl alcohol formation of benzoic acid was observed. This indicates that the rate of oxidation in acetone and isopropyl alcohol was so fast that it lead to the formation of benzoic acid.

Lawson is a naturally occurring compound in henna leaves, having large commercial value as a dye, antioxidant agent and also as a precursor for the synthesis of other pharmaceutical active ingredient. To synthesize this molecule by normal conventional route, many steps are involved. This molecule is also synthesized from  $\beta$ -naphthol using iron porphyrin to give 57% yield. As Pc is a structural homologue of porphyrine and in terms of cost and stability it is cheaper as well as more stable, an attempt was made for the oxidation of  $\beta$ -naphthol to lawson. Successful results for the oxidation of  $\beta$ -naphthol to lawson using CuPc as catalyst and hydrogen peroxide as an oxidizing reagent in water were obtained. The reaction was totally Green as water was used as solvent and H<sub>2</sub>O<sub>2</sub> which was used as an oxidizing agent and not generating any harmful waste by-products. Further more the reaction was carried out at room temperature and over all reaction time was only 1 h and the yield obtained was more than 60%. The product obtained was

compared with that of authentic sample and though large amount of catalyst was required the catalyst was reusable. One important thing which was observed was that only CuPc was able to catalyze the reaction and all other substituted and non substituted Pc were not able to show the good activity. The reason is that only Cu can go in +1 oxidation state under these reaction conditions. Further the activity was reduced with decrease in Cu content in catalyst i.e. CuPc showed higher activity followed by TACuPc and then by TNCuPc. The reaction was not reported in presence of homogeneous TCCuPc.

Large amount of exposure to UV radiation, wrong eating habits, Industrialization, the number of cancer cases have increased and lot of research is done in this field to find the new ways to cure the diseases. PDT has given an promising solution to the problem, sodium salt of tetrasulphonated Pcs are used in this phenomena. In this work preparation of water soluble TCMPcs using chemicals with low cost was undertaken. Cost plays an important role, when a new thing is required to be launched in market. This phthalocyanine is required to be studied for their photodynamic activity and commercial viability.

In the present studies antimicrobial activities of water soluble and plain phthalocyanines on different strains of micro organism were tested. In comparison with TCNiPc and TCZnPc, TCCuPc showed better activity and also in case of Pseudomonas only TCCuPc could show the activity.

## References

1. Frank E. Dayan, Emilie A Dayan, *Am. Scient.* 66(3) (2011) 236.
2. Lionel R. Milgrom, *J. Chem. Edu.* 75(4) (1998) 420.
3. Gerd Lobbert, *Ency. Ind. Chem.*(2003) Wiley-VCH, Weinheim,10.102/14356007.920-213
4. L. E. Webb, E. B Fleischer, *J. Chem. Phys.* 43 (1965) 3100.
5. M.S. Fischer, D.H. Templeton, A. Zalkin, M. Calvin, *J. Am. Chem. Soc.* 97 (1975) 2676.
6. G.P.Moss, *Pure Appl. Chem.* 59 (1987) 779.
7. C. Grazia Bezzu, Madeleine Helliwell, John E. Warren, David R. Allan, Neil B. McKeown [www.sciencemag.org/cgi/content/full/327/5973/1627/DC1](http://www.sciencemag.org/cgi/content/full/327/5973/1627/DC1)
8. Marly E. Osugi, Patrícia A. Carneiro and Maria Valnice B. Zanoni, *J. Braz. Chem. Soc.* 14(4) (2003) 660.
9. US Patent US7,527,657B2
10. US Patent US4,521,217
11. Xun Wang, Jung Zhuang, Qing Pong, Yadong Li, *Nature.* 437 (2005) 121.
12. H.H. Krause, S.L. Cosgrove, and C.M. Allen, *J. Chem. and Eng. Data.* 6(1) (1961) 112.
13. US Patent US4,950,413
14. US Patent US4,975,210
15. US Patent US4,769,163
16. S. Venugopal Rao, D. Narayana Rao, *J. Porphyrins. Phthalocyanines.* 6 (2002) 233.
17. Michael Hanack, Thorsten Schneider, Markus Barthel, James S. Shirk, Steven R. Flom, Richard G.S. Pong, *Coordination Chem. Rev.* 219 (2001) 235.
18. Jong Dae Lee, Hong Bae Kim, *Korean J. Chem. Eng.* 26(3) (2009) 673.

19. A.B. El-Bosaty, T.A. El-Brolossy, S. Abdalla, S. Negm, R.A. Abdella, H. Talaat, Egypt. J. Solids, 29 (1) (2006) 121.
20. S.Radhakrishnan and S.D.Deshpande, Sensors. 2 (2002) 185.
21. Phthalocyanine Colorant III<sup>rd</sup> Edition Vol 4
22. Industrial Dyes: Chemistry, Property ,Application by Klaus Hunger Wiley-VCH (2003).
23. J. Monteath Robertson, J Chem. Soc. (1935) 615.
24. Phthalocyanine material synthesis, structure and Function , By Neil B. Mckeown.
25. Phthalocyanine materials synthesis, structure and function- by Neil B, MCKeown. Cambridge Universiy Press 1998.
26. R.L.M. Allen, Colour chemistry. Imperial Chemical Industry Limited Nelson. Pg 231.  
B.I. Kharisov, U. Ortiz Mendez, J. L. Almaraz Garza, J. R. Almaguer Rodriguez, New J. Chem. 29 (2005) 686.
27. Ki Suck Jung, Jong Ho Kwon, J. Mat. Sci. 39 (2004) 723.
28. Jose A. Duro, Gema de La Torre, Tomas Torres, Tetrahedron Lett. 36 (44) (1995) 8079.
29. O. G. Lutsenko, V. P. Kulinich, G. P. Shaposhnikov, Russ. J. Gen. Chem. 73(9) (2003) 1463.
30. Sindhu Seelan, M.S. Agashe, D. Srinivas, S. Sivasanker, J. Mol. Cat. A: Chem. 168 (2001) 61.
31. Metin Ozer, Ahmet Altındal, Ali Rıza Ozkaya, Mustafa Bulut, Ozer Bekaroglu, Polyhedron 25 (2006) 3593.
32. Wöhrle, D, Eskes, M. Shigehara, K. Yamada, A. Synthesis (1993) 194.
33. US Patent US 2,187,816
34. US Patent US 7,034,149

35. Keiichi Sakamoto, Eiko Ohno, *Dyes and Pigments*. 35(4) (1997) 375.
36. Nagao Kobayashi, Yoshiyuki Nishiyama, Toshie Ohya, Mitsuo. Sato, *J. Chem. Soc. Chem. Commun.* (1987) 390.
37. Hasrat Ali, Johan E. van Lier, *Tetrahedron Lett.* 38 (7) (1997) 1157.
38. Hongjian Tian, Hasrat Ali, Johan E van Lier, *Tetrahedron Lett.* 41 (44) (2000) 8435.
39. Minquan Tian, Tatsuo Wada, Hiroyuki Sasabe, *J. Heter. Chem.* 37(5) (2000) 1193.
40. Hasrat Ali, Samia Ait-Mohand, Simon Gosselin, Johan E. van Lier, Brigitte Guerin, *J. Org. Chem.* 76 (6) (2011) 1887.
41. Detao Gao, Haitao Xu, Tiantang Yan, Bixian Peng. *J. Chin. Chem. Soc.* 48 (2001) 1189.
42. Metz, Otto Schneider, Michael Hanack, *Inorg. Chem.* 23 (1984) 1065.
43. B. wang and H.zh. Ma, *Synth. React. Inorg. Met. Org. Chem.* 34(6) (2004) 1009.
44. Wolfram Koble and Michael Hanack, *Inorg. Chem.* 25 (1986) 103.
45. Gerald E. Bossard, Michael J. Abrams, Marilyn C Darkes, Jean F. Vollano, Robert C. Brooks, *Inorg. Chem.* 34 (1995) 1524.
46. Sebnur Merey and Ozer Bekaroglu, *J. Chem. Soc. Dalton Trans.* (1999) 4503.
47. Priscilla P.S. Lee, To Ngai, Jian-Dong Huang, Chi wu, Wing-Ping Fong, Dennis K. P Ng, *Macromolecules.* 36 (2003) 7527.
48. Erbil Agar, Selami sasmaz, Nesuhi Akdemir, Ibrahim Keskin, *J. Chem. Soc. Dalton Trans.* (1997) 2087.
49. Gulay Gumus, Z.Ziya ozturk, Vefa Ahsen, Ahmet Gul and Ozer Bekaroglu, *J. Chem. Soc. Dalton Trans.* (1992) 2485.
50. Hongwei Lui, Yaohu Liu, Minghua Liu, Chuanfu chen, Fu Xi, *Tetrahedron Lett.* 42 (2001) 7083.



51. M Salih Agirtas, Mehment sonmez, Mehmet Kandaz, Ozer Bekaroglu, *Ind. J. Chem.* 40B (2001) 1236.
52. Nagoa Kabayashi, A.B.P. Lever, *J. Am. Chem. Soc.* 109 (1987) 7433.
53. Ki-Jong Han, Kwang-Yol Kay, *Bull Korean Chem. Soc.* 26(8) (2005) 1274.
54. Makbule Kacak, Ali Cihan, Ali I. Okur, Ozer Bekaroglu, *J. Chem. Soc. Chem. Commun.* (1991) 577.
55. Johannes Rauschnabel, Michael Hanack, Pergamon. (1995) 1629.
56. Michael Hanach, Monika. Geyer, *J. Chem. Soc. Chem. Commun.* (1994) 2253.
57. Svetlana V. Kudrevich, Sandra Gilbert, Johan E. Van Lier, *J. Org. Chem.* 61 (1996) 5706.
58. Angela Sastre, Belen del Rey, Tomas Torres, *J. Org. Chem.* 61 (1996) 8591.
59. Angela Sastre, Tomas Torres, Michael Hanach, *Tetrahedron Lett.* 36(46) (1995) 8501.
60. Nagoa Kabayashi, *J. Chem. Soc. Chem. Commun.* (1991) 1203.
61. G.M. Aminur Rahman, Dork M Guldi, *Chem. Commun* (2005) 2113.
62. Edward A Cuellar, Tobin J Marks, *Inorg. Chem.* 20 (1981) 3766.
63. B.N. Achar, K.S. Lokesh, *J. Org. Met. Chem.* 689 (2004) 3357.
64. Yong Pan, Wenxing Chen, Sufang Lu, Yifeng Zhang, *Dyes and Pigments.* 66 (2005) 115.
65. Wenxing Chen, Baoyan Zhao, Yong Pan, Yuyuan Yao, Shenshui Lu, Shiliang Chen, Lijuan Du, *J. Coll. Interf. Sci.* 300 (2006) 626.
66. Xiaoyuan Shen, Wangyang Lu, Guihua Feng, Yuyuan Yao, Wenxing Chen, *J. Mol. Cat. A: Chemical.* 298 (2009) 17.
67. T. V Rao, K.N.Rao, S. L. Jain, B. Sain, *Synth. Commun.* 32 (2002) 1151.

68. Shaabani A, Safari N, Bazgir A, Bahodoran f, Sharifi N, Jammal P R, *Syn Commun* 33(10) (2003) 1717.
69. US Patent US 5,739,319
70. Achar B. N, Fohlon G. M, Parker J.A, Keshavayya J, *Polyhedron* 6(6) (1887) 1463.
71. André R. da Silva, Alessandra C. Pelegrino, Antonio C. Tedesco, Renato A. Jorge, J. *Braz. Chem. Soc.* 19(3) (2008) 491.
72. Maha Fadel , Kawser Kassab , Doa Abdel Fadeel, *Lasers Med Sci.* 25 (2010) 283.
73. Dorina M. Opris, Frank Nuesch, Christiane Lowe, Martin Molberg, Matthias Nagel, *Chem. Mater.* 20 (2008) 6889.
74. O. V. Petrova, N.Sh Lebedeva, A.I. Vugin, V. E. Maizlish, G.P. Shaposhnikov, *Russ. J. Coord. Chem.* 32(10) (2006) 740.
75. Wesley M Sharma, Svetlana V. Kudrerich, Johan E. van Lier, *Tetrahedron Lett.* 37(33) (1996) 5831.
76. Weber .J. H, Busch D.H, *Inorg. Chem.* 4 (1965) 469.
77. Louis D Rollmann and Reynold T. Iwamoto, *J. Am. Chem. Soc.* (1968) 1455.
78. Mamida Ramesh Reddy, Norioshibata, Hideyuki Yoshiyama, Shurichi Nakamura, Takeshi Toru, *Synlett.* 4 (2007) 0628.
79. Aliye Asli Esenpinar, Mustafa Bulut, *Dyes and Pigments.* (2006) 1.
80. Sonmez Arslan , Ismail Yilmaz, *Inorg. Chem. Comm.* 10 (2007) 385.
81. James H Weber, Daryle H. Busch. *Inorg. Chem.* 4(4) (1965) 469.
82. M.P. Somashekarappa, K.R. Venugopala Reddy, M.N.K. Harish, J. Keshavayya, *J. Mol. Struct.* 753 (2005) 190.
83. Pritam borker, A.V.Salker, *Ind. J. Chem. Tech.* 13 (2006) 341.
84. A.R. Harutyunyan, A.A. Kuznetsov, *Chem. Phy. Lett.* 241 (1995) 168.

85. P.C. Minor, M.Gouterman, A.B.P. Lever, *Inorg. Chem.* 24 (1985) 1894.
86. Li Kao Lee, Nora H. Sabell, P. R. LeBreton, *J. Phys. Chem.* 86 (1982), 3926.
87. J. Spadavecchia, G. Ciccarella, P. Siciliano, S. Capone, R. Rella, *Sensors and Actuators B.* 100 (2004) 88.
88. Gregory Kalyuzhny, Alexander Vaskevich, Gonen Ashkenasy, Abraham Shanzer, Israel Rubinstein, *J. Phys. Chem. B* 104 (2000) 8238.
89. T.H. Tran-Thi, C.Desforge, C. Thiec, *J. Phy. Chem.* 93(1989) 1226.
90. Meng-Sheng Liao, Steve Scheiner, *J. Chem. Phys.* 114 (2001) 9780.
91. Zhan Xin-qi, Li Dong-hui, Zheng Hong, Xu Jin-gou, *Anal. Chim. Acta.* 448 (2001) 71.
92. Paul G. Seybold, Martin Gouterman, *J. Mol. Spec.* 31(1) (1969) 1.
93. Benny Joseph, C.S Menon, *E-Journal Chem.* 5 (2008) 86.
94. Pritam borker, A.V. Salkar. *Mat. Sci. Eng. B* 133 (2006) 55.
95. Xiaojing Li, Jerry W. Cabbage, Troy A Tetzlaff, William S. Jenks, *J. Org. Chem.* 64 (1999) 8509.
96. Hogqui Sun, Yuan Bai, Huijing Liu, Wangin Jin, Nanping Xu, *J. Photochem Photobio. A. Chemistry* 201(2009) 15.
97. Susanta K. Mohapatra, Narasimharao Kondamudi, Subarna Banerjee, Mano Misra *Langmuir.* 24 (19) (2008) 11276.
98. Rajesh J. Tayade, Praveen K. Surolia, Manoj A. Lazar, Raksh V Jasra, *Ind. Eng. Chem. Res.* 47 (2008) 7545.
99. J.A. Zazo, J. A. Casas, A. F. Mohedona, M. A. Gilarranz, J. J. Rodriguez, *Environ. Sci. Tech.* 39 (2005) 9295.

100. Susana L.H. Rebelo, Mariette M. Pereira, Paula V. Monsanto, Hugh. D. Burrows, J. Mol. Cat. A Chemical. 297 (2009) 35-43
101. Zhigang Xiong, Yiming Xu, Lizhong Zhu, Jincai Zhao, Langmuir. 21 (2005)10602.
102. Gai Kel, Dong Yanjie, Plasma Sources Sci. Technol. 14 (2005) 589.
103. Hong Liu, H.K. Shon, Xuan Sun, S. Vigneswaran, Hao Nan, Appl. Surf. Sci. 257 (2011) 5813.
104. Chouhaid Nasr, K. Vinodgopal, Luke Fisher, Surat Hotchandani, A. K. Chattopadhyay, Prashant V. Kamat, J. Phys. Chem. 100(1996) 8436.
105. Ammar Houas, Hinda Lachheb, Mohamed Ksibi, Elimame Elaloui, Chantal Guillard, Jean-Marie Herrmann, Appl. Catal. B: Environ. 31(2) (2001) 145.
106. Hinda Lachheb, Eric Puzenat, Ammar Houas, Mohamed Ksibi, Elimame Elaloui, Chantal Guillard, Jean-Marie Herrmann, Appl. Catal. B: Environ. 39(1) (2002) 75.
107. Rajesh J. Tayade, Thillai Sivakumar Natarajan, Hari C. Bajaj, Ind. Eng. Chem. Res. 48 (23) (2009) 10262.
108. Nanping Xu, Zaifeng Shi, Yiqun Fan, Junhang Dong, Jun Shi, Michael. Hu, Ind. Eng. Chem. Res. 38 (2) (1999) 373.
109. Jun Yao, Chaoxia Wang, Inter. J Photo. (2010), Article ID 643182, 6 pages  
doi:10.1155/2010/643182
110. Shiyong Zhang, Zhenhua Chen, Yunlong Li, Qun Wang, Long Wan, Catal. Comm. 9(6) (2008) 1178.
111. Antonio E. H.Machado, Marcela D. Franc, Valdemir Velani, Gabriel A.Magnino, Hosana M.M, Velani, F avio, S. Freitas, Paulo S. Muller Jr., Christian Sattler, Martin Schmucker, Inter. J Photo (2008) Article ID 482373, 12 pages

doi:10.1155/2008/482373

112. Kavita Kabra, Rubina Cheudhary, Rameshwar L. Sawhney, *Ind Eng. Chem. Res.* 43 (2004) 7683.
113. Michael R. Hoffmann, Scot T. Martin, Wonyong Choi, Detlef W. Bahnemannt, *Chem. Rev.* 95 (1995) 69.
114. Nthapo Sehlotho, Tebello Nyokong, *J. Mol. Catal. A: Chemical.* 209 (2004) 51.
115. A. Valente, C. Palma, I. M. Fonseca, A.M. Ramos, J. Vital, *Carbon.* 41 (2003) 2793.
116. Celine Perollier, Alexander B. Sorokin, *Chem. Commun.* (2002) 1548.
117. Amina Amine Khodja, Tahar Sehili, Jean Francois Pilichowski, Pierre Boule, *J. Photochem Photobio. A. Chemistry.* 141 (2001) 231-239.
118. Sanjay R. Thakare, N.S. Bhave, *Ind. J. Chem.* 44 (2005) 2262.
119. Cang Li, Morton Z Hoffman, *J. Phys. Chem. A.* 104 (2000) 5998.
120. Evgeny V. Kudrik, Sergei V. Makarov, Achim Zahi, Rudi Van Eldik, *Inorg. Chem.* 42(2) (2003) 618.
121. F. Shirini, M.A. Zolfigol, M.R. Azadbar, *Russ. J. Org. Chem.* 37(11) (2011) 1600.
122. Roy J. Gritter, Thomas J. Wallace, *J. Org. Chem.* 24(8) (1959) 1051.
123. Ji-Dong Lou, Zhi-Nan Xu, *Tetrahedron Lett.* 43(35) (2002) 6149.
124. Steven A Jymonko, Bryce A. Nattier, Ram S. Mohan, *Tetrahedron Lett.* 40 (1999) 7657.
125. Hindeyuki Kuno, Kyoko Takahashi, Makoto Shibagaki, Kazuko Shimazaki, Hajimi Matsushita, *Bull Chem. Soc. Jpn.* 63 (1990) 1943.
126. a) Karl. P. Peterson and Richard C. Larock. *J. Org. chem.* 63 (1998) 3185.  
b) Takahiro. Nishimura, Tomoaki Onoue, Kouichi. Ohe, Sakae Uemuca, *J. Org. Chem.* 64(18) (1999) 6750.

127. Majid Moghadam, Shahram Tangestaninejad, Valiollah Mirkhani, Iraj Mohammadpur-Baltork, Hadi Kargar, *Bioorg. Med. Chem.* 13 (2005) 2901.
128. Alex G. Griesbeck, Anna bartoschek, *Chem. Commun.* (2002) 1594.
129. Vishal B. Sharma, Suman L.Jain, Bri Sain, *Tetrahedron Lett.* 44 (2003) 383.
130. Suman L.Jain, Bri Sain, *J Mol. Catal. A: Chemical.* 176 (2001) 101.
131. Konstantinos Skobridis, Vassiliki Theodorou, Edwin Weber, *Arkivoc.* (2006) 102.
132. Istvan E. Marko, Arnaud Gautier, Isabelle Chelle-Regnaut, Paul. R. Giles, Masao. Tsukazaki, Christopher J. Urch, Stephen M. Brown, *J. Org. Chem.* 63 (1998) 7576.
133. Mirvin Weiss, Mildred Appel, *J. Am. Chem. Soc.* 70 (11) (1948) 3666.
134. Alexander Mc Killop, Brian P. Swann, Michael E. Ford, Edward C. Taylor, *J. Am. Chem. Soc.* 30 (1973) 3641.
135. William W. Paudler, H.L.Blewitt, *J. Org.Chem.* 30 (1965) 4081
136. Hans Wynberg, H.J.Kooreman, *J. Am. Chem. Soc.* 20 (1965) 1739.
137. Kenn E. Harding, Leslie M. May, Kevin F. Dick, *J. Org. Chem.* 40(11) (1975) 1664.
138. Saul Soloway, Angelo Santoro. *Anal. Chem.* 27(5) (1955) 798.
139. S.S. Kim, H.C. Jung, *Synthesis*, (2003) 2135-2137
140. Didier Villemin, Mohamed Hammadi, Messaoud Hachemi, *Synth. Commun.* 32(10) (2002) 1501.
141. Martine De Min, Sylvei Croux, Cecile Tournaire, Michel Hocquaux, Bernard Jackquet, Esther Oliveros, Marie-Therese Maurette, *Tetrahedron.* 48(10) (1992) 1869.
142. Rashda Ali, Syed Asad Sayeed, *ACS Symposium Series.* 662 (1997) 223.
143. P. Dinesh Babu, R.S. Subhasree. *Acad. J. Plant. Sci.* 2(4) (2009) 231.
144. Sanjay Gaikwad, Charushila Gaikwad, *J. Chem. Pharm. Res.* 2(4) (2010) 106.

145. Christopher Wright, Giliyar V. Ullas, *J. Label compd Radiopharm.* 45 (2002) 1265.
146. Yan Yan, Feng-Shou Nao, Guodong Zheng, Kaiji Zhen, Chiguang Fung, *J. Mol. Catalysis A: Chemical.* 157 (2000) 65.
147. Yan Yan, En-Hua Kang, Ke-Er Yang, Shan-Ling tong, Chi-Guang Fang, Si-Jie Liu, Feng-Shau Xiao, *Catal. Comm.* 5 (2004) 387.
148. Elodie Haggiage, Emma E. Coyle, Kieran Joyce, Michael Oelgemoller, *Green Chem.* 11 (2009) 318.
149. Krystyna Osowska-pacewicka, Howard Alper, *J. Org. Chem.* 53 (1988) 808.
150. Spyros Spyroudis, *Molecules.* 5 (2000) 1291.
151. Tong-Shuang Li, Hui Yun Duan, Bao-Zhi Li, Brij B Tewari, Sheng- Hui Li, *J. Che. Soc. Perkin Trans. 1* (1999) 291.
152. M. Lakshimi Kantam, B. Kavita, F. Figueras, *Catal. Lett.* 51 (1998) 113.
153. Olga V. Zalomaeva, Oxana A. Kholdeera, Alexander B. Sorokin, *C. R. Chimie.* 10 (2007) 598.
154. Alexander B. Sorokin, Aloun Tuel, *Catal. Today.* 57 (2000) 45.
155. Vijay Nair, P.M Treesa, Davis Maliakal, Nigam P. Rath, *Tetrahedron* 57 (2001) 7705.
156. S.Y. Rane, S.D. Gawali, A.S. Kumbhar, S.B. Padhye, P.P. Bakare, *J Therm. Anal. Cal.* 55 (1999) 246.
157. H.H. Krause, S.L. Cosgrove, C.M. Allen, *J. Chem. Eng. Data.* 6 (1) (1961) 112.
158. U.S. Tewari, S.K. Sharma, *Tribology International.* 22 (4) (1989) 253.
159. US Patent US 4,950,413
160. US Patent US 4,769,163

161. Daniela A. Geroldo, Chamunorwa A. Togo, Janice Limson, Tebello Nyokong, *Electro Chemica. Acta.* 53 (2008) 8051.
162. S. M. S. Chauhan, Anil Kumar, K. A. Srinivas, *Chem. Commun.* (2003) 2348.
163. Giovanni Palmisano, Maria concepcion Gutierrez, Maria Luisa Ferrer, Maria Dolores Gil-Luna, Vincenzo Augugliaro, sedat Yurdakal, Mario Pagliaro, *J. Phys. Chem.* 112 (2008) 2667.
164. Toshio Nakamura, Chilharu Hayashi, Jetsushi Ogawara, *Bull. Chem. Soc Jpn* 69 (1996) 1555.
165. Huang Jun, LiMingtian, Tang Yan, Fang Hua, Ding Liyun, *J. Wuhan Univ. Tech. Matt.* 23(5) (2008) 606.
166. R. Fogel, P. Mashazi, T. Nyokong, J. Limson, *Biosensors and Bioelec.* 23(2007) 95.
167. Cleone das Dores, C. Conceicao, Ronaldo Censi Faria, Orlando Fatibello-Filho, Auro Atsushi Tanaka, *Anal. Lett.* 41 (2008) 1010.
168. Ja-Ryong Koo, Young-Kwan Kim, Jung-Soo Kim, *Mol. Cryst. Liq. Cryst.* 316 (1998) 385.
169. Tadashi Nagasawa, Kenji Murakami, Kenzo Watanabe, *Mol. Cryst. Liq. Cryst.* 316 (1998) 389.
170. a) S. Radhakrishnan, S.D. Deshpande, *Sensors.* 2 (2002) 185.  
b) Shu, J.H, Wikle, H.C, Chin, B.A, *Sensors.* 11 (2010) 56.
171. A. Arshak, S. Zleetni, K. Arshak, *Sensors.* 2 (2002) 174.
172. Georgij L. Pakhomov, Lev G. Pakhomov, Vlad V. Travkin, Mikhail V. Abanin, Pavlo Y. Stakhira, Vladyslav V. Cherpak, *J. Mater Sci.* 45 (2010) 1854.
173. Svetlana V. Kudrevich, Hasrat Ali, Johan E. Van Lier, *J. Chem. Soc. Perkin Trans.*



- (1994) 2767.
174. Abimbola Ogunsipe, Ji-Yao Chen, Tebello Nyokong. *New. J. Chem.* 28 (2004) 822.
  175. Mahmut Durmus, Tebello Nyokong, *Photochem. Photobiol. Sci.* 6 (2007) 659.
  176. Mei-Rong Ke, Jian-Dong Huang, Sheng-Mei Weng, *J. Photochem. Photobiol. A. Chemistry.* 201 (2009) 23.
  177. Jiri Cerny, Marie Karaskova, Jan Rakusan, Stanislav Nes Pu Rek, *J. Photochem Photobiol. A. Chemistry.* 210 (2010) 82.
  178. Andrei N. Vzorov, Luigi G. Marzilli, Richard W. Compansa, Dabney W. Dixon, *Antiviral Research.* 59 (2003) 99.
  179. Tanya Stuchinskaya, Miguel Moreno, Michael J. Cook, Dylan R. Edwards, David A. Russell, *Photochem. Photobiol. Sci.* 10 (2011) 822.
  180. W.Y. Tong, H.Y. Chen, A.B. Djurisic, A.M.C. Ng, H.Wang S. Gwo, W.K. Chan. *Optical materials* 32(2010) 924-927
  181. Chuan-Hui Cheng, Zhao-Qi Fan, Shu-Kun Yu, wen-Hai Jiang, and Xu Wang, *Appl. Phys. Lett.* 88(21) (2006) 3505.
  182. R. Koeppel. *Fullerenes, Nanotubes, Carb. Nano. Struc.* 14 (2006) 441.
  183. A.V. Ziminov, Y.U.A. Plevaya, T. A. Jourre, S. M. Ramsh, M.M. Mezdrogina, N.K. Poletaev, *Semiconductors.* 44(8) (2010) 1070.
  184. Youichi Sakakibara, Raghu N. Bera, Toshiyuki Mizutani, Kohtaro Ishida, Madoka Tokumoto, Toshiro Tani, *J. Phys. Chem B.* 105 (2001) 1547.
  185. T. Uemura, M. Furumoto, T. Nakano, M. Akai-Kasaya, A. Saito, M. Aono, Y. Kuwahara. *Chem. Phy. Lett.* 448 (2007) 232.
  186. Shen Yue, Xia Yi-Ben, Chen Jing-Wei, Gu Feng Jiao Feng-Hua, Zhang Jian-Cheng.

- Chin. Phys. Lett, 22(9) (2004) 1717.
187. Youichi Sakahibara, Martin Vacha, Toshirotane, Mol. Cryst. Liq. Cryst. 314 (1998) 71.
188. Donghong Gu, Qiyang Chen, Xiaodong Tang, Fuxi Gan, Shuyin Shen, Kai Liu, Huijun Xu, Optics Comm. 121 (1995) 125.
189. Tim Maisch, Lasers Med. Sci. 22 (2007) 83.
190. Winslow S. Caughey, Suzette A. Priola, David A. Kocisko, Lynne D. Raymond, Anne Ward, Byron Caughey, Antimicrob. Agents. Chemo. (2007) 3887.
191. Barbara Cosimelli, Gabrio Roncucci, Donata Dei, Lia Fantetti, Fiammetta Ferroni, Micaela Riccio, Domenico Spinelli, Tetrahedron 59 (2003) 10025.
192. Asiye Nas, Elif Çelenk Kaya, Halit Kantekin, , Atalay Sökmen, Volkan Çakır J. Organomet. Chem. 696 (2011) 1659.
193. Joseph T. Parisi Microbiological Reviews, 49(2) (1985) 126.
194. Mlynarczyk A, Mlynarczyk G, Pupek J, Transplant Proc. Nov 39(9) (2007) 2879.
195. Sunenshine RH, Tan ET, Terashita DM, Clin Infect Dis. 45(5) (2007) 527.
196. Vet. Res. 36 (2005) 493. © INRA, EDP Sciences, DOI: 10.1051/vetres:2005011
197. Carlo Leifert, Stephen Woodward. Plant Cell, Tissue and Organ Culture. 52 (1998) 83.
198. Pitt TL, Sparrow M, Warner M, Stefanidou M, Thorax. 58 (2003) 794.
199. Vogel Test book of practical Organic Chemistry (1991) fifth edition. 1065
200. Young J. G, Onyebuagu W, J. Org. Chem. 55 (1990) 2155.
201. Cooper KE, Nature. 176 (1955) 510.
202. Cooper KE, Woodman D, J. Pathol. Bacteriol. 58 (1946) 75.

## APPENDIX - I

### PUBLICATIONS

- 1. Photoluminescence and photocatalytic degradation studies on some metallophthalocyanines**  
P. A. Pavaskar, S. Chodankar, A. V. Salker  
Eur. J. Chem. 2 (3), (2011), 416-419
- 2. Synthesis and antimicrobial activity on Manganese tetra (n-carboxylacrylic) aminophthalocyanine**  
P. A. Pavaskar, S.S. Patil , I. Furtado and A.V. Salker  
Biointerface Res. ~~Chem. Appl.~~ 2(4), (2012) 374-379
- 3. Selective catalytic oxidation of naphthol to lawsone on Copper Phthalocyanine**  
P. A. Pavaskar, A. V. Salker  
Current Catal. Accepted (in press)
- 4. Synthesis and evaluation of antibacterial activity of water soluble copper, nickel and zinc tetra (n-carboxylacrylic) aminophthalocyanines**  
P. A. Pavaskar, S.S. Patil , I. Furtado and A.V. Salker  
Med. Chem. Res. (2012) (Under review)

## CONFERENCE PUBLICATIONS

**1. Synthesis and Characterizations of nano size tetraamino metal phthalocyanine.**

P. A. Pavaskar, A. V. Salker

National Seminar on Advances in nanomaterials and drug delivery.

NIO, Dona Paula-Goa, Feb. 22-23, 2008.

**2. Synthesis and magnetic studies on nano size tetraamino metal phthalocyanine.**

P. A. Pavaskar, A. V. Salker

National Symposium MR-08 at IIT-Bombay May 16-17, 2008

**3. Synthesis and Catalytic study of metal phthalocyanine on aromatic alcohols**

P. A. Pavaskar, A. V. Salker

International Conference on supramolecular chemistry and nanomaterials, ICSN-2011,

University of Mumbai, Feb. 14-16, 2011